University of Florida
Civil and Coastal Engineering

University of Florida
Civil and Coastal Engineering

Final Report **December 2011**

Hillsboro Canal Bridge Monitoring

Principal investigator:
H. R. Hamilton

Research assistants:
James L. McCall
Xinlai Peng
Abhay P. Singh

Department of Civil and Coastal Engineering
University of Florida
P.O. Box 116580
Gainesville, Florida 32611

Sponsor:
Florida Department of Transportation (FDOT)
Stephen Eudy – Project Manager

Contract:
UF Project No. 00079095
FDOT Contract No. BDK75 977-16

Disclaimer

The opinions, findings, and conclusions expressed in this publication are those of the authors and not necessarily those of the State of Florida Department of Transportation.

Technical Report Documentation Page

1. Report No.	2. Government Accession No.	3. Recipient's Catalog No.

4. Title and Subtitle	5. Report Date
Hillsboro Canal Bridge Monitoring	December 2011
	6. Performing Organization Code
7. Author(s)	8. Performing Organization Report No.
J.L. McCall, X. Peng, A. P. Singh and H. R. Hamilton	
9. Performing Organization Name and Address	10. Work Unit No. (TRAIS)
University of Florida Department of Civil & Coastal Engineering P.O. Box 116580 Gainesville, FL 32611-6580	11. Contract or Grant No. BDK75 977-16
12. Sponsoring Agency Name and Address	13. Type of Report and Period Covered
Florida Department of Transportation Research Management Center 605 Suwannee Street, MS 30 Tallahassee, FL 32399-0450	Final Report Oct. 2009-Nov. 2011
	14. Sponsoring Agency Code

15. Supplementary Notes

16. Abstract

This report describes the implementation of a testing and monitoring program for bridge 930338 in Belle Glade. Glass-fiber reinforced polymer (GFRP) deck panels and plates were installed over an existing steel superstructure using grouted steel studs. This was done to evaluate the use of GFRP decking as a substitute for steel grid decking.

Strain gages and displacement gages were installed on the GFRP deck and the steel superstructure. Bridge tests were conducted in October 2009 and 2010 using a Florida Department of Transportation (FDOT) test truck. Four different load levels were used in each of five different travel paths. Global positioning system (GPS) monitoring enabled the creation of influence lines for each strain gage. The GPS data were also used to confirm that the truck followed the designated travel line and evaluate the sensitivity of the strain readings to load proximity. Shear and flexural distribution factors were obtained from these influence lines.

Increases in strain recorded in the right lane between the two bridge tests are attributed to a combination of the cracked and spalled grout leveling layer and a loss of rigidity in the shear stud connections and not necessarily a loss of stiffness of the deck system. Flexural distribution factors were unchanged after one year of service. There was no appreciable composite action detected between the GFRP bottom panel and top plate.

Monitoring occurred between October 2009 and April 2011. Steel girder strain gages confirmed that the majority of the heavy traffic traveled in the right lane. Thermocouples confirmed that a thermal gradient developed within the GFRP deck each day and dissipated at night.

G17. Key Word	18. Distribution Statement
glass, fiber, reinforced, polymer, bridge, deck, monitor, instrumentation	No restrictions. This document is available to the public through the National Technical Information Service, Springfield, VA, 22161

19. Security Classif. (of this report)	20. Security Classif. (of this page)	21. No. of Pages	22. Price
Unclassified	Unclassified	239	

Form DOT F 1700.7 (8-72) Reproduction of completed page authorized

SI* (MODERN METRIC) CONVERSION FACTORS

*APPROXIMATE CONVERSIONS **TO** SI UNITS*

SYMBOL	WHEN YOU KNOW	MULTIPLY BY	TO FIND	SYMBOL
LENGTH				
in	inches	25.4	millimeters	mm
ft	feet	0.305	meters	m
yd	yards	0.914	meters	m
mi	miles	1.61	kilometers	km
AREA				
in^2	square inches	645.2	square millimeters	mm^2
ft^2	square feet	0.093	square meters	m^2
yd^2	square yard	0.836	square meters	m^2
ac	acres	0.405	hectares	ha
mi^2	square miles	2.59	square kilometers	km^2
VOLUME				
fl oz	fluid ounces	29.57	milliliters	mL
gal	gallons	3.785	liters	L
ft^3	cubic feet	0.028	cubic meters	m^3
yd^3	cubic yards	0.765	cubic meters	m^3
NOTE: volumes greater than 1000 L shall be shown in m^3				
MASS				
oz	ounces	28.35	grams	g
lb	pounds	0.454	kilograms	kg
T	short tons (2000 lb)	0.907	Megagrams	Mg (or "t")
TEMPERATURE (exact degrees)				
^oF	Fahrenheit	5(F-32)/9 or (F-32)/1.8	Celsius	^oC
ILLUMINATION				
fc	foot-candles	10.76	lux	lx
fl	foot-Lamberts	3.426	candela/m^2	cd/m^2
FORCE and PRESSURE or STRESS				
kip	1000 pound force	4.45	Kilonewtons	kN
lbf	pound force	4.45	newtons	N
lbf/in^2	pound force per square	6.89	kilopascals	kPa

*SI is the symbol for the International System of Units. Appropriate rounding should be made to comply with Section 4 of ASTM E380.

SI* (MODERN METRIC) CONVERSION FACTORS

*APPROXIMATE CONVERSIONS **FROM** SI UNITS*

SYMBOL	WHEN YOU KNOW	MULTIPLY BY	TO FIND	SYMBOL
LENGTH				
mm	millimeters	0.039	inches	in
m	meters	3.28	feet	ft
m	meters	1.09	yards	yd
km	kilometers	0.621	miles	mi
AREA				
mm^2	square millimeters	0.0016	square inches	in^2
m^2	square meters	10.764	square feet	ft^2
m^2	square meters	1.195	square yards	yd^2
ha	hectares	2.47	acres	ac
km^2	square kilometers	0.386	square miles	mi^2
VOLUME				
mL	milliliters	0.034	fluid ounces	fl oz
L	liters	0.264	gallons	gal
m^3	cubic meters	35.314	cubic feet	ft^3
m^3	cubic meters	1.307	cubic yards	yd^3
MASS				
g	grams	0.035	ounces	oz
kg	kilograms	2.202	pounds	lb
Mg (or "t")	megagrams (or "metric	1.103	short tons (2000 lb)	T
TEMPERATURE (exact degrees)				
^oC	Celsius	1.8C+32	Fahrenheit	^oF
ILLUMINATION				
lx	lux	0.0929	foot-candles	fc
cd/m^2	candela/m^2	0.2919	foot-Lamberts	fl
FORCE and PRESSURE or STRESS				
kN	Kilonewtons	0.225	1000 pound force	kip
N	newtons	0.225	pound force	lbf
kPa	kilopascals	0.145	pound force per square inch	lbf/in^2

*SI is the symbol for the International System of Units. Appropriate rounding should be made to comply with Section 4 of ASTM E380.

Acknowledgements

The authors would like to acknowledge and thank the Florida Department of Transportation (FDOT) for providing funding for this project. We also extend thanks to the staff of the FDOT Marcus H. Ansley Structures Research Center for their outstanding efforts during the 2009 and 2010 bridge tests and for their work on the bridge monitoring system. In particular, we would like to thank David Allen, Stephen Eudy, Sam Fallaha, Tony Hobbs, Seth Murphy, Kyle Ramsdell, Paul Tighe, David Wagner, and Chris Weigly.

We would also like to acknowledge and thank FDOT District Four for their support during instrumentation and bridge testing. In particular, we would like to thank John Danielsen, P.E., District Structures Maintenance Engineer, and Alberto O. Sardinas, Manager, Special Projects, Structures Maintenance.

Stephen B. Stokes, Target Engineering Group, has our gratitude for his help with the data acquisition system during remote monitoring.

We are pleased to acknowledge the technical advice and support provided by Mr. Dan Richards of Zellcomp, Inc., of Durham, NC.

Ronald Rice, sugarcane, rice, and sod agent at Palm Beach County Cooperative Extension, is thanked for information pertaining to sugarcane harvest practices.

Executive Summary

This study evaluated the performance of glass-fiber reinforced polymer (GFRP) deck panels that were used to replace the steel grid deck of bridge no. 930338 in Belle Glade, FL. This evaluation consisted of two bridge tests using FDOT test trucks and remote monitoring of strain, displacement, and temperature under normal traffic conditions. The bridge tests were conducted in October of 2009 and 2010. The monitoring period lasted 18 months, from October 2009 through April 2011.

The bridge was constructed with a two-part GFRP deck placed upon a steel frame superstructure. The bottom GFRP panels featured integral webs to resist flexure and were attached to the steel girders with grout pockets containing steel studs welded to the girders. A thin layer of grout was placed between the GFRP panels and the steel stringers to provide leveling. GFRP top plates were attached to the bottom GFRP panels using mechanical fasteners. A layer of polymer concrete was placed on the top of the deck to provide a wearing surface.

Instrumentation was applied to the deck before and after installation, which occurred in August 2009. Instrumentation included: foil strain gages placed on the soffit of the GFRP panels to record flexural strain; rosette gages placed on lower panel webs to record GFRP shear strain; displacement gages to record GFRP deck displacement; thermocouples to study temperature gradients within the GFRP panels; and full bridge strain gages to record strain in the steel superstructure. The instrumentation was placed in the northbound lanes to capture the effect of sugarcane-laden trucks crossing the bridge.

Two bridge tests were conducted, one in October 2009 and a second in October 2010. These tests were conducted to evaluate changes in the performance of the bridge after one year of service and to correlate strains recorded during monitoring with applied wheel loads. Static tests were performed during which the test trucks were pulled into selected positions and readings were taken. Rolling tests were conducted where the truck traveled at approximately 1 mph while sensor readings were recorded and truck positions were determined using a GPS (global positioning system) antenna mounted to the truck. Finally, a 35 mph test was conducted during the 2010 bridge test to study dynamic load effects and to compare them with American Association of State Highway and Transportation Officials (AASHTO) impact factors.

The bridge was monitored for 18 months as part of this study. Deck and girder strains were monitored to determine the number and magnitude of loading events. Rainflow counting was used to determine the number and magnitude of load and stress cycles based upon strain measurements. Temperatures at selected depths of the deck panel were monitored and the formation of thermal gradients was analyzed.

GFRP deck strains were found to be sensitive to wheel position measured parallel to the direction of travel along the right of way. For example, flexural strain deceased by 60% when the test truck wheel had moved only 1 ft away from the strain gages. This sensitivity to wheel position makes it difficult to maximize strain at specific strain gages by static truck positioning because positioning tolerance is so low.

The GPS tracking capability of the FDOT test truck was crucial for locating where maximum strains occurred in the GFRP deck. The ability to track the truck position resulted in strain influence lines, which were used to determine distribution factors for the GFRP deck. Influence line plots confirmed that the GPS tracking was accurate to a one-inch resolution. The GPS data were also used to confirm that the truck followed the designated travel line and evaluate the sensitivity of the strain gages to load proximity.

Table of Contents

List of Figures

List of Tables

1 Introduction

Florida has the largest inventory of moveable bridges in the nation, with a total of 148, of which 91% are bascule, 7% are swing and 2% are lift bridges. Most employ open grid steel decks as a riding surface for part of their span (National Bridge Inventory 2008). Compared to solid bridge decks, steel grid decks have several advantages: they can be assembled in the factory, they are lightweight, and they are easy to install. Unfortunately, worn steel grid decks have high maintenance costs and provide poor skid resistance, especially in rain. Furthermore, they provide poor riding comfort and produce high noise levels when traffic travels across the bridge.

The Florida Department of Transportation (FDOT) is investigating the possibility of using glass-fiber reinforced polymer (GFRP) decks to replace worn steel grids. GFRP decks have the potential to provide a solid riding surface, addressing the noise and stopping distance concerns of worn steel grids. GFRP deck panels can be designed and manufactured to meet weight and dimensional requirements of a bridge, allowing direct replacement of steel grid decks.

GFRP bridge decks are relatively new to the bridge industry. The first public U.S. all-composite (GFRP) vehicular bridge was placed in service in December 1996 on No - Name Creek in Russell, Kansas (MDA 2000). It is a 27-ft wide, two-lane bridge. The bridge has a clear span of 21 ft - 3 in. and was constructed of three fiberglass sandwich panels measuring 23 ft-3 in. long and 9 ft wide. The entire installation required one and a half days from start to finish, demonstrating the simplicity of this type of construction (Plunkett 1997).

There has been continuous research on the use of GFRP bridge decks since their inception, but there are neither well-adapted design guidelines nor structural analysis procedures. A primary concern for GFRP deck systems is their durability and field performance.

To investigate the performance of this deck type, Innovative Bridge Research and Construction (IBRC) funding was used by the FDOT to install a GFRP deck on bridge number 930338 over the Hillsboro canal in Belle Glade, Florida. The canal crossing superstructure was originally constructed of steel stringers with a steel grid riding surface and was intended to be moveable. The objective of the IBRC study was to investigate the short- and long-term field performance of the relatively new GFRP deck system technology. This was accomplished with a

combination of long-term monitoring and two bridge load tests. The load tests provided information on the behavior of the deck installation under truck loading. Bridge test data combined with the monitoring data allowed estimates of truck frequency and the weight carried by the GFRP deck during the monitoring period. The selected bridge is on a main route from sugarcane fields to processing plants and carries a significant amount of truck loads during the harvest season. This report presents the instrumentation, procedures, and results of the bridge tests conducted in October 2009 and October 2010, as well as an analysis of monitoring data collected intermittently from October 2009 through April 2011.

2 Objectives

The objective of this study was to investigate the initial performance of a GFRP bridge deck installed on bridge number 930338 over Hillsboro canal in Belle Glade, Florida. This was accomplished with the combination of long-term monitoring and two bridge tests.

The instrumentation and data acquisition detailed in this report was installed by FDOT Structures Research Center personnel with assistance from UF personnel in summer 2009. One bridge test was conducted in October 2009 immediately after GFRP deck installation to calibrate the instrumentation to the test truck axle loads. This allowed strain measurements taken over time to be used to estimate the frequency and magnitude of truck loading that the GFRP deck experienced during the monitoring period. An additional bridge test was conducted in October 2010 after 12-14 months of service to check calibration of the instrumentation and to determine if the GFRP deck system had degraded with service use.

Instrumentation was designed in spring 2009 and installed on the deck panels in summer 2009. The deck was installed in August 2009. The first bridge test was conducted in October 2009. Long-term monitoring was started immediately after first bridge test. The second bridge test was conducted in October 2010. Monitoring was terminated April 2011.

3 Literature Review

3.1 Background of GFRP Bridge Decks

GFRP decks are lightweight and have sufficient strength and stiffness to be used to replace conventional bridge decks. Decks made with GFRP are suitable for bridge replacement projects. These decks are manufactured in appropriate lengths and can be shipped to a job site with minimal transportation and handling effort. Installation times for GFRP bridge decks are generally shorter than those of conventional decks.

Alampalli and Kunin (2003) reported that nearly one third of the nation's bridges are structurally deficient. Structural deficiency does not imply that a bridge is unsafe or likely to collapse but that it requires additional monitoring, inspection, and maintenance. More than 29,000 of these bridges are classified as structurally deficient because of poor deck conditions and lack of load ratings. New materials, methods, and technologies to cost-effectively replace old bridge decks and improve load ratings are needed. Glass-fiber reinforced polymer (GFRP) composite systems are one such alternative under consideration. Glass-fiber reinforced polymers are gaining popularity in the bridge industry. These materials have high strength-to-weight ratios and excellent durability.

Fu et al. (2007) reported that there are several manufacturing methods used for GFRP decks: (1) pultrusion, (2) vacuum-assisted-resin-transfer-molding (VARTM), and (3) open mold and hand lay-up.

Connecting GFRP deck panels to steel girders was the subject of research by Moon et al. (2002). All three tested connections displayed significant structural ductility and satisfied fatigue and structural limit state requirements. The connections had substantial inelastic deformations prior to failure and showed little variation in response from one cycle to the next. Approximately 60-70% of the capacity of a longitudinal connection in a concrete deck was achieved. It was concluded that the connection strength for this type of composite structure must be analyzed on a case-by-case basis, with the bearing strength of the GFRP panel providing a lower bound and the shear strength of the steel studs providing an upper bound.

Alagusundaramoorthy et al. (2006) presented a comparison of GFRP deck sections made by several manufacturers, including Creative Pultrusion, Composite Deck Solutions, Hardcore Composites, and Infrastructure Composites International. Figure 1 shows the GFRP deck

sections made by different manufacturers. The shear, deflection, and flexural performance of the different GFRP panels were determined and compared with each other, with the Ohio Department of Transportation specifications, and with comparable concrete decks. The flexural and shear rigidities of the GFRP panels were also determined.

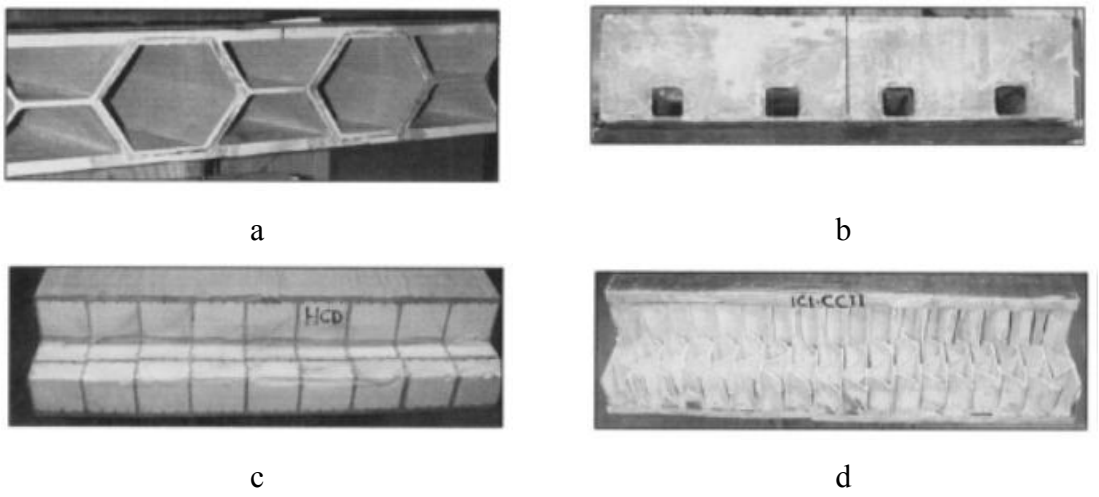

a b

c d

Figure 1 – FRP deck sections manufactured by (a) Creative Pultrusions (b) Composite Deck Solutions (c) Hardcore Composites (d) Infrastructure Composites International

3.2 GFRP Bridge Deck Experimental Studies

Camata and Shing (2010) performed static and fatigue load tests on honeycomb GFRP deck panels. These panels had a sandwich configuration consisting of two stiff E-glass face shells separated by a light-weight honeycomb core. Vinyl ester resin was used as a bonding material for the deck construction. The core was made up of corrugated plates with a sinusoidal wave configuration as shown in Figure 2. Deck panels were connected together using a tongue-and-groove connection.

A full-scale model deck having the same panel design as an actual bridge was tested in a two-span continuous configuration with a concentrated load applied at each midspan location. The loads were applied with 305-mm × 305-mm × 25.4-mm (12 × 12 × 1 in.) steel plates and 19-mm (¾-in.) thick rubber pads between the plates and the deck. The deck was first subjected to a static test to obtain its elastic stiffness and bending behavior. It was then subjected to fatigue load cycles with different load amplitudes. Finally, the deck was loaded statically one span at a time to failure. Strain gages and Linear Variable Differential Transformers (LVDTs) were used for the measurement of test data.

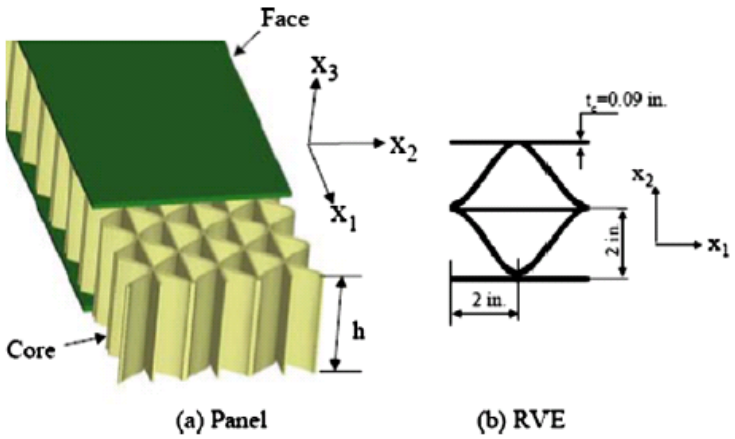

Figure 2 – Configuration of the core and faces of the GFRP panel and representative volume element (RVE)

During the static load test, midspan deflections under the design wheel loads of 116 kN (26 kip), corresponding to an American Association of State Highway and Transportation Officials (AASHTO) HS 25-44 truck, were 1.22 mm (0.048 in.) and 1.19 mm (0.047 in.) for Spans 1 and 2, respectively. The span of the bridge was 4 ft. After the static test, the panel was subjected to alternating cyclic loads at the middle of the spans to evaluate its fatigue endurance. The test had 1.5 million load cycles applied in three phases: 0–15,200 cycles, 15,200–370,200 cycles, and 370,200–1,500,000 cycles. In the first phase, the applied load varied between 9 and 175 kN (2 and 39 kip); in the second phase, the load varied between 9 and 97 kN (2 and 22 kip); and in the third phase, the load varied between 9 and 138 kN (2 and 31 kip). Bottom face delamination was observed during the third phase of the loading.

After the fatigue test was completed, the two spans were loaded one at a time up to 445 kN (100 kip). A crack formed in one of the spans in the top face of the panel near the loading plate at a load of 267 kN (60 kip) and propagated gradually. The top face delaminated, accompanied by a strong noise emission, a load drop, and stiffness reduction. Despite this, the panel did not collapse and was able to carry load up to 445 kN (100 kip).

A detailed finite element model was developed to study the failure behavior of the test deck using the cohesive interface model in ABAQUS Version 6–6.1 (SIMULIA). Effective width in bending was calculated for the deck design, both experimentally and numerically. The effective bending width calculated from finite element analysis under the wheel load of an

AASHTO HS 25-44 truck was 873 mm (34.4 in.), less than two times the width of the wheel load.

Lee et al. (2007) conducted an experimental study on pultruded GFRP bridge decks used for light-weight vehicles. The GFRP deck used in this study was a rectangular dual-cell profile that was formed through a pultrusion process with E-glass fiber embedded in a polyester resin as shown in Figure 3.

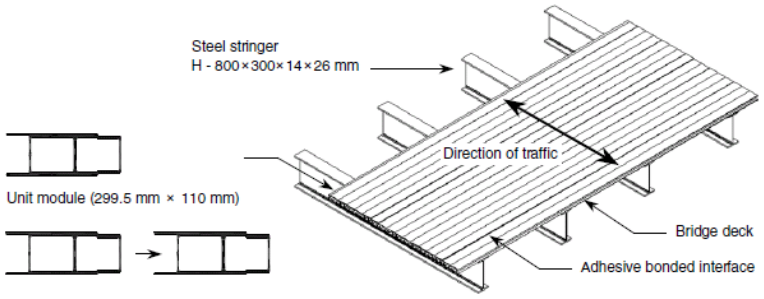

Figure 3 – Schematic of GFRP deck on steel stringers

Four-point bending tests were performed in the lab to test the unit and double module assembly, with the finite element model calibrated using test data. The behavior of all specimens tested was nearly linearly elastic and showed brittle fracture in bending. The failure load of the LT-series deck was found to be 187.8 kN (42.2 kip), which was almost seven times higher than the design wheel load of 26.5 kN (6.0 kip).

Alagusundaramoorthy et al. (2006) conducted load tests on 16 FRP deck panels and 4 concrete decks. These FRP deck panels were made by four different manufacturers, with 12 single spans and four double spans. This study evaluated the force-deformation responses of FRP composite bridge deck panels under AASHTO MS 22.5 (HS25) truck wheel load and up to failure. The test results of the FRP composite deck panels were compared with the flexural, shear, and deflection performance criteria per Ohio Department of Transportation specifications and with the test results of reinforced concrete deck panels. Static load tests were performed for design wheel loads of 26 kip (wheel load + 30% for impact) as per the AASHTO LRFD standard MS 22.5 (HS 25) truck wheel load. Decks were tested for cyclic loading under a service load of 12 kip (4 kip/ft) with a load cycle from 0 to 12 kip and back to zero, which was repeated five times. One more cyclic loading was performed for the design wheel load of 26 kip with load

cycle from 0 to 26 kip and back to zero, which was also repeated five times. After the cyclic loading, decks were tested to failure. This study also presented failure loads, modes of failure and safety factors. The flexural and shear rigidities of the FRP decks were calculated using first order shear deformation beam equations. The safety factor against failure of the FRP bridge deck panels varied from 3 to 8.

Cousins et al. (2009) performed load tests on Zellcomp GFRP panels identical to those utilized in the deck installation of Belle Glade bridge 930338. The objectives of this study were to (1) investigate connection behavior under simulated pseudo-static service load; (2) examine flexural strength and failure mode of connections and deck; (3) explore fatigue behavior during simulated cyclic wheel loading and residual strength after fatigue loading; and (4) investigate viability of transition connections. Two test sections were constructed that included sections of the deck attached to supporting steel stringers. The first was flat, 11 ft by 8 ft in plan, and subjected to static and simulated truck loadings. The second included a transition connection and was 17 ft by 8 ft in plan. Static and cyclic behavior of deck connections was tested; these included top plate to bottom panel, panel to panel, and panel to supporting stringers. The flat deck test specimen had a 1.4 safety factor against sustaining permanent damage and a 2.4 safety factor against failure when subjected to an HL-93 wheel load of 22 kip. There was no measurable composite action between the top plate and supporting T-section.

The flat specimen generally performed well during the fatigue test but with some indication of deterioration of the lap joint connections at 1 million cycles of load and a loss of stiffness at about 2.5 million cycles of load. Numerous top plate screw connections in the sloped deck specimen loosened during the first 600,000 cycles of load, with several completely fracturing. The damage to the deck increased over the following 400,000 cycles.

Alampalli and Kunin (2003) conducted a field test on a newly constructed GFRP bridge deck. The bridge was a simply supported single span truss bridge with a skew angle of 27 deg. Two lanes of traffic were carried by the 42.67-m (140-ft) long by 7.3-m (24-ft) wide bridge. Steel wide-flange beams and girders supported GFRP composite panels made by Hardcore Composites Operations, LLC. The GFRP deck consisted of top and bottom face skins with a web core and was fabricated using E-glass fibers and vinyl ester resin using a patented vacuum assisted resin infusion process.

A field load test was conducted on this bridge using two dump trucks. Each fully loaded truck closely resembled an M-18 (H-20) AASHTO live-loading. No composite action was measured between the floor beams and the deck since the neutral axis of the deck/ floor beam system was observed to coincide with the neutral axis of the floor beam. The maximum strain experienced by the floor beam was about 95 με and occurred when both of the test trucks were on the bridge. This loading caused a corresponding longitudinal FRP strain of 159 με. The maximum transverse FRP strain was 90 με, which occurred when only one truck was on the bridge.

Chiewanichakorn et al. (2007) conducted an analytical study to evaluate the dynamic and fatigue performance of the same FRP bridge deck studied by Alampalli and Kunin (2003). For the validation of the finite element model, data from Alampali and Kunin (2003) were utilized. For comparison, a reinforced concrete deck was also modeled. Significant improvement in the predicted fatigue life resulted from the replacement of concrete deck by FRP deck. The fatigue life of the FRP deck system was almost double that of the reinforced concrete deck system.

Jeong et al. (2007) conducted field and laboratory tests on a GFRP bridge deck which was fabricated using a pultrusion process with E-glass fiber embedded in a vinyl ester resin. The GFRP deck (8 m /26.2 ft long, 3 m / 9.8 ft wide, 200 mm /7.9 in. deep) was composed of an assembly of nine modules with a sand-blasted wearing surface on the top flange. Modules were connected with an adhesive applied over an 80 mm (3.2 in.) lap length. Static and fatigue tests were performed on the deck. A loading pad of 230 mm × 580 mm (9.1 in. x 22.8 in.) that simulates the area of the design wheel load was used. Fatigue tests were also conducted on the specimen used for the static load test. Load ranged between a maximum of 117.6 kN (26.4 kip) and a minimum of 19.6 kN (4.4 kip). Two million cycles were imposed at a rate of 1 Hz. The static failure load was 431.2 kN (96.9 kip) with a strain at the center of the deck of 3013 με.

A field load test was conducted on a bridge with the same GFRP deck in place using a three-axle dump truck. The field test results showed that the mid span deflection of the GFRP deck was 1.74 mm (0.07 in.), satisfying the deflection limit of 2.5 mm (L/800). The maximum strain was about 400 με, which was 13% of the ultimate strain (3013 με).

3.3 Bridge Monitoring Techniques

One of the approaches in non-destructive bridge testing is the use of diagnostic load testing and instrumented health monitoring. This technique provides insight into the response of the structure to applied loads. Instrumentation placed on the structure is composed of static sensors, including strain gages, displacement gages, and thermocouples. The test duration can vary from seconds to years (continuous monitoring). Applied loads may be experimental loads (test trucks), environmental loads (wind loads, thermal gradients, etc.), traffic loads, and seismic loads. It is possible to compute the effective load or stress range for bridge design by using this technique with extensive instrumentation to measure the critical aspects of bridge load response.

Wang et al. (2010) carried out a five-year long monitoring program on the Ruyang Cable-stayed Bridge in China from May 2005 to September 2010. This monitoring system used accelerometers, strain gauges, temperature sensors, displacement transducers, GPS receivers, and weigh-in-motion sensors permanently installed on the bridge along with data acquisition and processing systems. Stress distributions in the box-shaped girders were analyzed from recorded strain histories. Based on these distributions, a computer algorithm was developed to evaluate the fatigue damage that was assumed to occur in increments according to a lognormal distribution.

Previous work by Chakraborty and DeWolf (2006) described the implementation and evaluation of a long-term strain monitoring system on a three-span, multi-steel girder composite bridge located within the interstate system. The bridge had been analyzed using standard AASHTO specifications and the analytical predictions were compared to field monitoring results. The study included an evaluation of the load distribution to different girders caused by large trucks and the location of the girder neutral axes. A finite-element analysis of the bridge was performed to study the distribution of live load stresses within the steel girders and to study how continuity of the slabs at the interior joints would influence overall behavior of the bridge. Results of the continuous data collection were used to evaluate the influence of truck traffic on the bridge and to establish a baseline for long-term monitoring.

Sartor et al. (1999) reported on tests of four bridges that were experiencing different types of problems. The first was an aged bascule bridge that required a review of the counterweight hanger because age, corrosion, and the condition of the bearings made analytical assessments impossible. A second bridge developed cracks between a girder and a filler plate,

and an investigation was required to determine whether the cracks were due to fabrication errors or degradation. Monitoring was performed on a third bridge to determine the effective live load strain range, which would determine whether girder cracks would propagate and cause a brittle failure under live loads. A fourth bridge required a revised load rating produced from traffic monitoring because an analytical approach indicated that the live load capacity of the bridge was too low for a planned deck overlay. The investigators used multiple strain gauges at each bridge and a portable data acquisition system for their investigation. Monitoring occurred while the bridges were open to traffic. In each case, dozens of strain time histories were captured and post processed to gather the information needed. This study includes examples of how field data was used to save time and money and eliminate unnecessary repairs.

Howell and Shenton (2006) developed an in-service bridge monitoring system (ISBMS) to provide near real-time web-based monitoring of live load strains. This is a second generation ISBMS using an integrated single board computer/data logger with a cellular modem and a single strain transducer. This transducer may be either a single bridge foil gage or a full bridge transducer. The ISBMS unit is portable and may be installed on any component of a bridge for monitoring up to three weeks. A web interface allows access to the unit from any computer. Time history, peak response, and rainflow histograms are all available as data output options. The ISBMS was load tested in a laboratory and then field tested on a highway bridge with a high average daily truck traffic count. This system is intended to be used during biannual bridge inspections to provide additional data for management of bridge inventory. Assessments of bridge deterioration are improved, ensuring that necessary repairs take place.

An innovative, probabilistic approach for the assessment of bridge structure condition was proposed by Sun and Sun (2011). This approach involved the long-term strain monitoring of a steel girder in a cable-stayed bridge. First, the methodology of damage detection in the vicinity of monitoring points using strain-based indices was investigated. Then, the strain response of bridge components under operational loads was analyzed. The influence of temperature and wind on strains was eliminated and strain fluctuation under vehicle loads was obtained. Finally, damage evolution assessment was carried out based on the statistical characteristics of rain-flow cycles derived from the strain fluctuation under vehicle loads.

4 Main Street Bridge, Belle Glade

The bridge selected for GFRP deck replacement is located in Belle Glade, Florida (Figure 4). Bridge no. 930338 is located on North Main Street and crosses over the Hillsboro Canal (Figure 5) carrying five lanes of traffic. There are two northbound and two southbound lanes with a northbound left-turn lane and sidewalks on each side. North- and southbound lanes are separated by a raised median. Intersections with traffic signals are located at each end of the bridge; N. Main Street and E. Lake Road intersect at the north end, and N. Main Street and E. Canal Street South intersect at the south end.

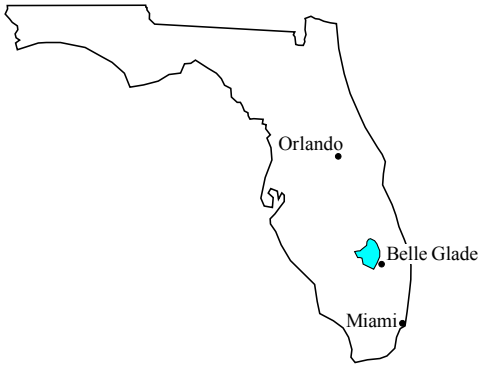

Figure 4 – Bridge location.

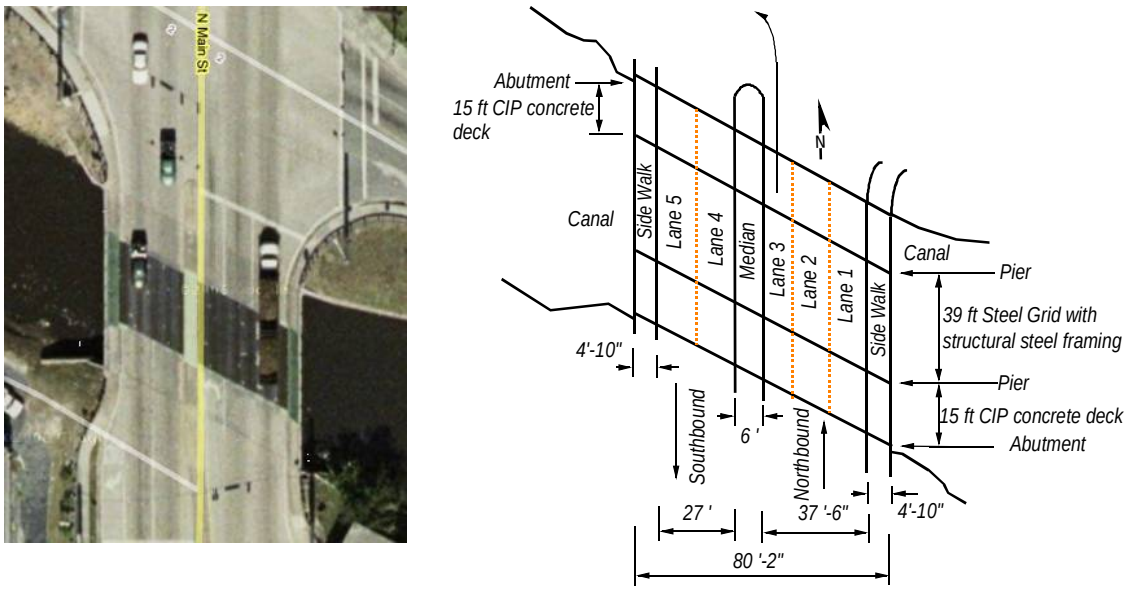

(a) (b)

Figure 5 – Bridge site plan (a) aerial photo (b) detailed site plan

The superstructure crosses the canal with three short spans. Cast-in-place flat concrete slabs span 15 ft from the abutments to the pile bents (Figure 6). The middle span was a steel grid deck supported by structural steel framing.

Figure 6 – Elevation view of main span

Heavy traffic occurs during the sugarcane harvesting season (from late October through mid-April). Sugarcane-laden trucks haves been observed traveling in the two northbound lanes, noted as lane one and lane two in Figure 5. Figure 7 shows the local damage sustained by the steel grid deck and associated repairs using steel plates. This grid deck was replaced by the GFRP deck which is the focus of this study.

Figure 7 – Damaged and repaired existing steel grid deck

The bridge was constructed in 1976 and was intended to allow passage of marine traffic through the canal by using cranes to lift out sections of the steel framing and grid deck to provide clearance. Figure 8 shows the steel superstructure framing plan. W24x68 steel girders provide the main superstructure support and are spaced at approximately 4 ft center-to-center. Frames were assembled using intermediate and end diaphragms fully welded to the girders. Three girders compose the outside (easternmost) frame; four girders compose the other frames studied in this project. These frames are rigid enough that they can be lifted off of the substructure as individual units to allow passage of marine traffic. Traffic and pedestrian barriers are supported by transverse members that are integrated with the girders under the sidewalks.

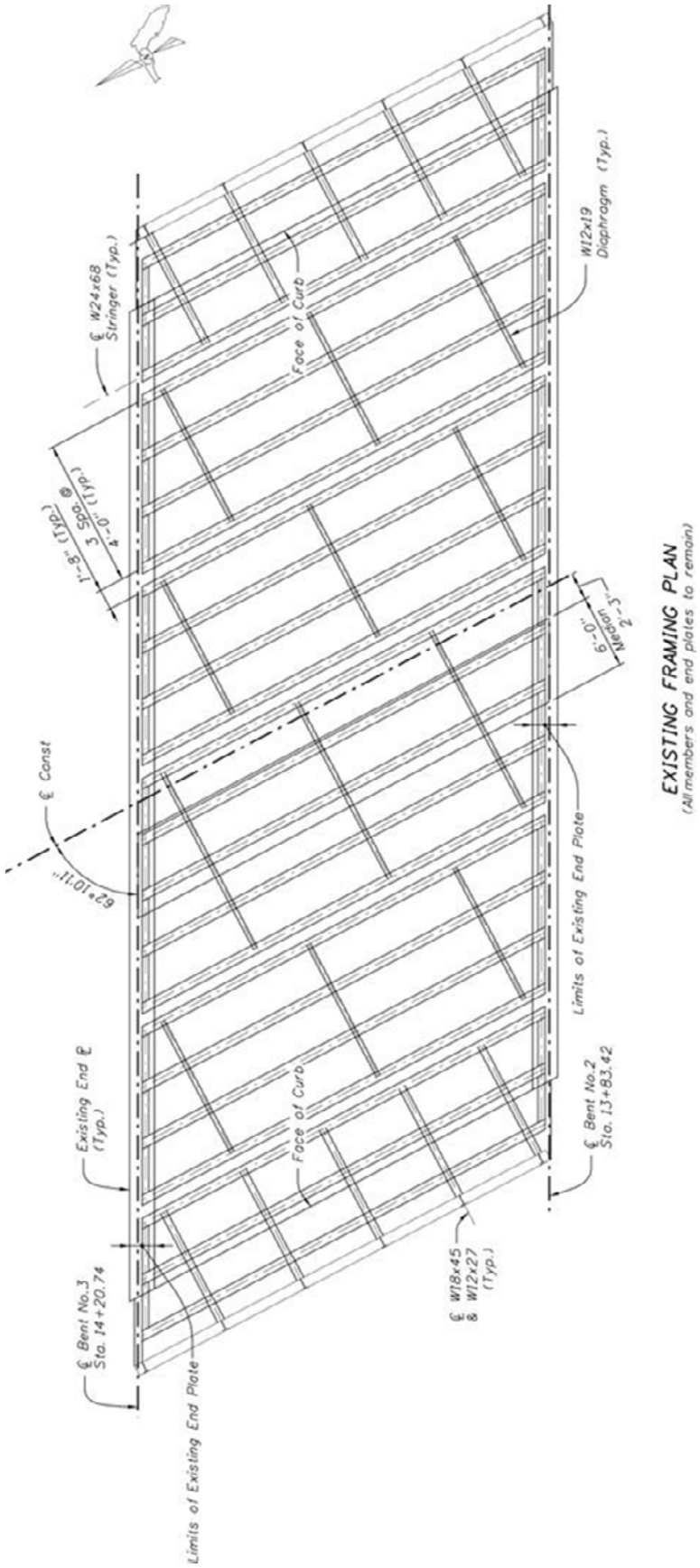

Figure 8 – Existing framing plan for lift out span

5 GFRP Deck System

5.1 Deck Design

Figure 9 shows the deck system used to replace the existing steel grid deck. The deck system is a pultruded GFRP composite deck composed of a bottom panel and top plate. E - glass fibers and isopolyester resin were used to fabricate the section; fiber lay-up and resin properties are proprietary. Bottom panels were manufactured in widths of approximately 2.5 ft and were composed of a 0.5-in. thick bottom plate pultruded integrally with four I-shaped webs. Bottom plates were thickened locally near each web to match the thickness of the top flange. To form the wearing surface, pultruded 0.5-in. thick GFRP plates were fastened to the top flanges of the bottom section using 1.75-in. long mechanical fasteners. Top plates were generally 35 in. to 48 in. wide and were placed perpendicular to the direction of the bottom panels. Pultrusion fabricated continuous sections were cut to fit the bridge. Adjacent bottom panels were joined by fastening the protruding portion to that of the adjacent panel with mechanical fasteners.

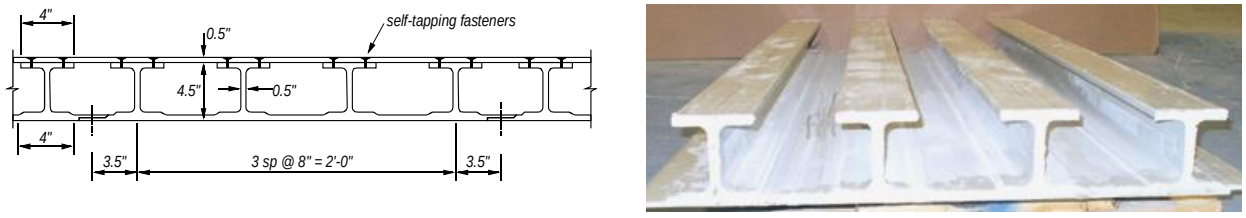

(a) (b)

Figure 9 – GFRP deck configuration (a) typical section (b) single bottom panel section shown without top plate

5.2 Deck Installation

Deck replacement was carried out under a construction contract with FDOT District 4, which included roadway resurfacing in addition to the deck replacement. To accommodate the deck replacement, traffic was routed around the bridge to an adjacent bridge.

The existing steel grid (Figure 10) was removed from the superstructure. A layer of leveling grout was placed between the top flange of the steel girders and the soffit of the GFRP deck to ensure that the finished wearing surface of the new deck aligned with the remainder of the bridge deck. Grout pads were poured using the formwork system shown in Figure 11.

Formwork was placed such that it created a nominal 0.5-in. gap for the grout to fill. This gap varied as needed to accommodate construction tolerances.

Figure 10 – Existing steel grid deck

Figure 11 – Formwork for grout pads

Installation of the deck began with placement of bottom panels on the leveling formwork (Figure 12) perpendicular to the existing steel beams. Bottom panels had already been manufactured and cut to length and were stored on site. Each panel was custom fitted to a particular location within the bridge deck. As bottom panels were placed, they were mechanically interconnected using the protruding bottom deck flange.

Figure 12 – Installation of bottom GFRP panels

Figure 13 shows the details of the transition between the GFRP deck and the concrete deck on the approach spans. To accommodate this transition, cast-in-place concrete was placed over the end of the structural steel girder frames (visible in Figure 13b). The edge GFRP panel was used as a stay-in-place form for the concrete by removing the top flanges of the three outside

panel webs. Reinforcement for the pour was threaded through holes drilled in the webs and was welded to the existing end plate on the abutment.

(a) (b)

Figure 13 – Transition between GFRP deck and concrete deck (a) reinforcement for cast-in-place concrete (b) installation of welded headed stud

The GFRP deck was connected to the existing steel stringers with welded headed studs. Holes were drilled through the bottom GFRP deck panels to accommodate the steel studs. The studs were then welded to the top flange of the existing girder through the holes in the GFRP deck (Figure 13b). Foam dams were placed adjacent to the studs to retain the grout. Grout (Figure 14) was then poured into the pockets. At first, the grout flowed through the hole and filled the space between the deck and the top flange of the steel girders. When this space was full, additional grout was placed to surround the stud. These grout pockets provided fixed connections between the GFRP deck and the steel girder superstructure.

Figure 14 – Grout pockets being poured at each stud

Longer studs also were welded to the existing steel beams to anchor the median to the bridge deck (Figure 15). Figure 16 shows top plate installation; they were cut to length, stored on site, and attached using mechanical fasteners.

Figure 15 – Median anchors

Figure 16 – Top GFRP plates

After top plate installation, the existing median was reattached using the median anchors. After the installation of the median, a 0.5-in. thick overlay of polymer concrete (Figure 17) was placed on the top plates to create the wearing surface. Figure 18 shows the completed deck system open to traffic.

Figure 17 – Placement of polymer concrete wearing surface

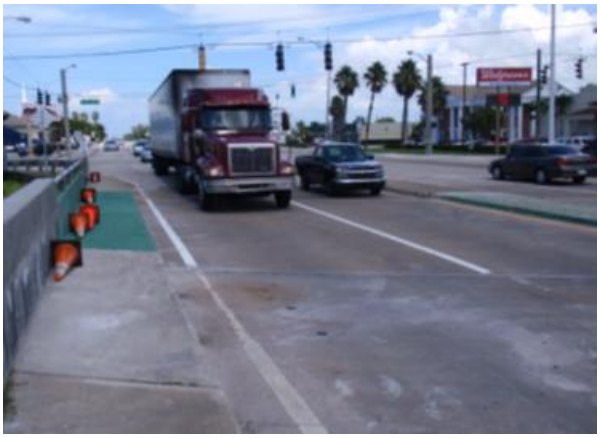

Figure 18 – Completed deck

6 Instrumentation and Data Acquisition

The instrumentation installed on the bridge was intended to serve two purposes. One was to acquire data during the two bridge tests. The other was to monitor the performance of the bridge deck under actual traffic conditions. Instrumentation for both bridge tests and monitoring was placed on the superstructure only; the substructure behavior would not significantly affect the behavior of the bridge under either bridge tests or actual traffic loads.

6.1 Approach

Visual observation of the traffic and inspection of the steel grid repairs (Figure 19) indicated that the two northbound lanes were the most heavily used. Consequently, these lanes were chosen to receive the instrumentation for monitoring and bridge testing.

The bottom panel webs were instrumented with strain rosettes to measure shear strain. Uniaxial strain gages were applied to the bottom panel soffit to measure flexural strains parallel to the webs; these gages were placed directly under a web. Thermocouples were mounted on the GFRP deck in strategic locations to measure the temperature gradient throughout the deck thickness. Displacement gages were used to measure the deck panel deflection and the relative deflections of the steel girders during the bridge test. Full-bridge strain (FBS) transducers were mounted on top of the bottom flange at the midspan of four structural steel girders.

Web gages (strain rosettes) and thermocouples were installed prior to deck installation due to a lack of access to the bottom panel webs after the top plate had been fastened in place. Soffit and FBS gages were installed after deck installation and just prior to the bridge test. FDOT District 4 supplied a barge to facilitate installation of instrumentation and wiring.

Table 1 summarizes the instrumentation used for the 2009 bridge test, while Table 2 summarizes the instrumentation used for the 2010 bridge test. Table 3 summarizes the instrumentation used for long-term monitoring. With the exception of the thermocouples, instruments were located at the midspan of the steel girders. Surface temperature measuring thermocouples were installed on deck panel B8, which was located closer to the data acquisition system (DAQ). Thermocouples were also installed at the traffic box containing the data acquisition system used for monitoring. Wires were routed from the instruments to the east side of the north abutment where the DAQ was housed.

Figure 19 – Two northbound lanes showing truck traffic marks on the road surface.

Table 1 – Summary of instrumentation for 2009 bridge test

Gage	Location	No. of gages	Installed
Full bridge strain gage	Steel beams	4	After the construction of the deck
Bonded quarter bridge foil strain gage	FRP deck panels	8	After the construction of the deck
Deflection gage	Steel beams and FRP deck	3	After the construction of the deck
Bonded quarter bridge foil strain rosette (0-45-90)	FRP deck	8 x 3	Before the construction of the deck
Surface temp. measuring Thermocouple	FRP deck	4	Before the construction of the deck
Ambient temp. measuring Thermocouple	Traffic box	1	After the construction of the deck

Table 2 – Summary of instrumentation for 2010 bridge test

Gage	Location	No. of gages	Installed
Full bridge strain gage	Steel beams	4	After the construction of the deck
Bonded quarter bridge foil strain gage	FRP deck panels, steel beams	20	After the construction of the deck
Deflection gage	Steel beams and FRP deck	4	After the construction of the deck
Surface temp. measuring Thermocouple	FRP deck	4	Before the construction of the deck
Ambient temp. measuring Thermocouple	Traffic box	1	After the construction of the deck

Table 3 – Summary of instrumentation for monitoring

Gage	Location	No. of gages	Installed
Full bridge strain gage	Steel beams	4	After the construction of the deck
Bonded quarter bridge foil strain gage	FRP deck panels	8	After the construction of the deck
Deflection gage	FRP deck	1	After the construction of the deck
Surface temp. measuring Thermocouple	FRP deck	4	Before the construction of the deck
Ambient temp. measuring Thermocouple	Traffic box	1	After the construction of the deck

6.2 Strain Gages

Figure 20 shows the location of the four FBS gages that were attached to the steel girders. These transducers (BDI-ST350 by Bridge Diagnostics Inc.) were bonded to the top of the steel girder bottom flange. Girders 3, 5, 6, and 9 were each instrumented with FBS gages to measure tensile strain. The FBS gages on Girders 3 and 5 were expected to show significant strain when traffic was in lane one. Similarly, Girders 6 and 9 were expected to show significant strain when traffic was in lane two. All FBS gages were located at the mid-span of the girders and were used for bridge testing and monitoring.

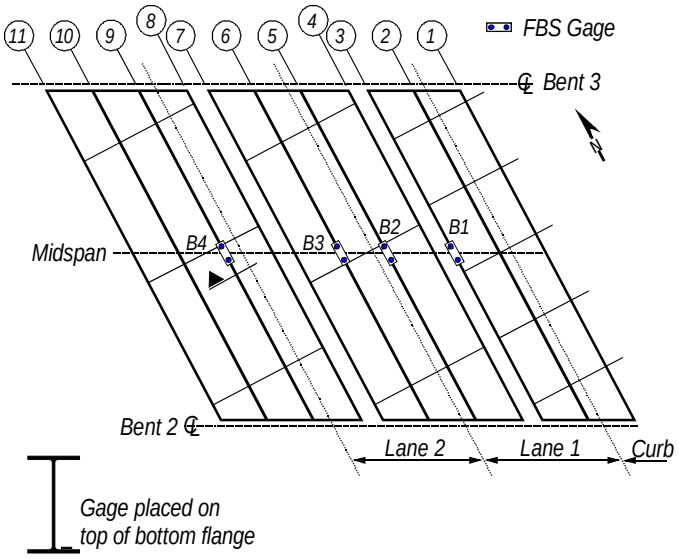

Figure 20 – FBS gages mounted on steel girders.

Figure 21 shows the mounting tabs and tab jig used for the installation of the FBS gages. Mounting tabs were adhered to the top of the bottom flange of the girder using a two part epoxy. Surfaces of the steel girders were cleaned using a hand grinder, sand paper and denatured alcohol. A 2-part epoxy was then applied on the steel girders to attach the transducer tab.

Mounting tabs and a tab jig (Figure 21 a) were used to install the FBS gage to the steel girders. First, the mounting tabs were placed in the tab jig slot. Slots in the tab jig were perpendicular to the axis of the FBS gage and served to align the tabs properly. The FBS gage was placed on and bolted to the through tabs. After this, the gage and tabs were removed from the tab jig and placed onto the epoxy. Figure 22 shows an installed FBS gage on the top of the girder bottom flange.

(a)

(b)

Figure 21 – FBS gage (a) Mounting tabs and tab jig (b) gage

Figure 22 – Installed FBS gage on the steel girder

The GFRP deck was oriented to span parallel to the abutment and piers, which placed them at a skewed angle to the girders (Figure 23). Panels were cut to length before shipment to the site and were custom fabricated for specific locations within the bridge deck. Panel numbering for the pieces is shown in Figure 23. Panels B9 and B10 were selected to be instrumented due to their proximity to midspan and to the FBS gages on the steel girders.

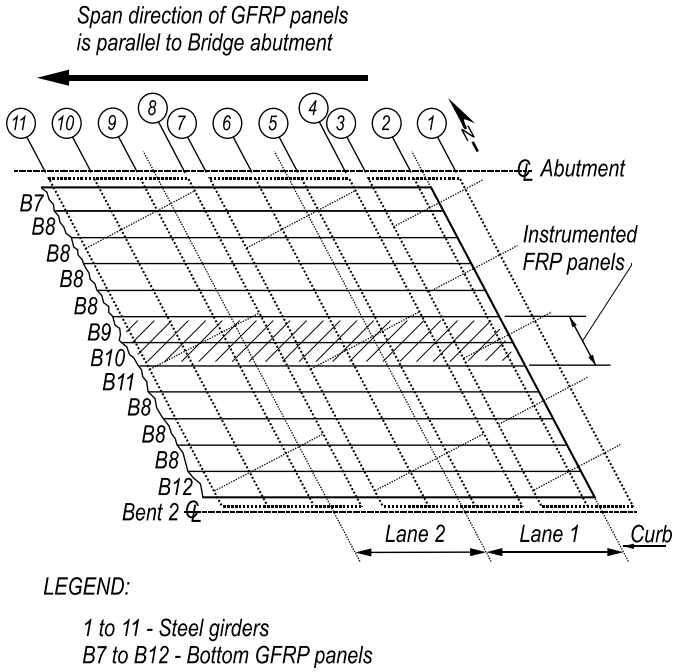

Figure 23 – Location of instrumented panels (B9 and B10)

Four 5-mm (UFLA-5-350-11-5-LT) long bonded quarter bridge foil strain gages from TML Tokyo Sokki Kenkyujo Co., Ltd. (TML) were mounted on the soffit of each of the two instrumented panels (Figure 24). Gages were oriented to read strain parallel to the GFRP webs. Four strain rosettes (0-45-90) (UFRA-5-350-11-5LT) from TML were installed on the webs of each instrumented panel with the zero direction gage oriented along the longitudinal axis of the web. While rosettes were used for the first bridge test only, soffit gages were used for both of the bridge tests and monitoring. Figure 25 shows a bonded gage installed on the soffit of the GFRP deck while Figure 26 shows a bonded strain rosette installed on a GFRP deck web.

Gages S1, S2, S5 and S6 were intended for vehicles traveling in lane one and gages S3, S4, S7 and S8 for vehicles traveling in lane two. During the 2009 bridge test, it was observed that gages S3 and S8 were not working properly. The DAQ recording these two gages indicated large strains compared to other soffit gages, suggesting faulty installation or wire routing through the conduit leading to the DAQ.

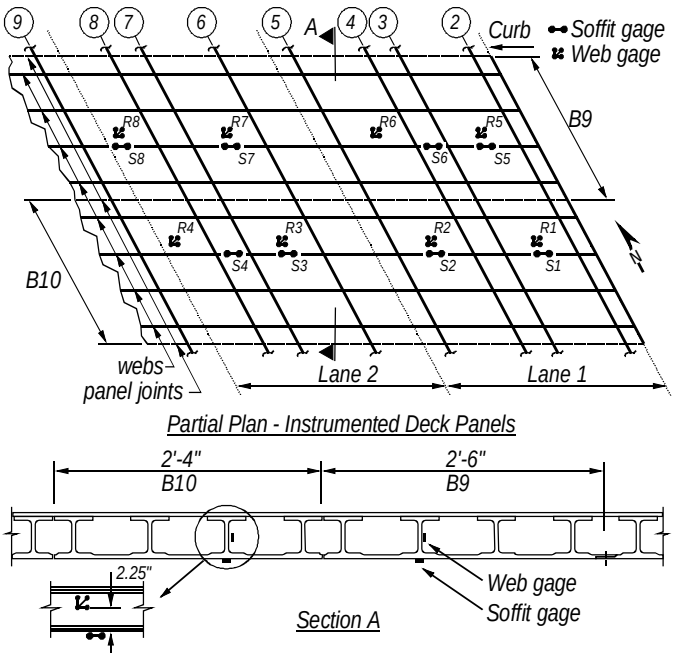

Figure 24 – Position of bonded strain gages and rosettes on GFRP deck

Figure 25 – Bonded strain gage

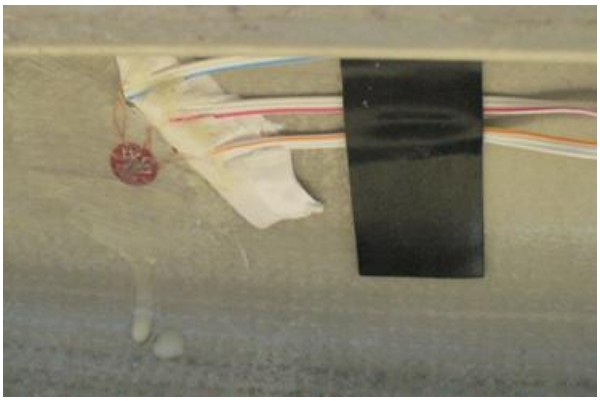

Figure 26 – Bonded strain rosette

6.3 Thermocouples

Figure 27 shows the location of the four general purpose type K thermocouples used to measure GFRP surface temperature. The thermocouples were arranged to provide continuous readings of the thermal gradient that develops during heating and cooling of the bridge deck.

Thermocouples were applied to the GFRP bottom panel before deck installation due to restricted access to the interior of the bridge deck. Panel B8 was chosen to receive thermocouples due to its nearness to the DAQ (Figure 28). To obtain the temperature gradient over the height of the GFRP deck section, thermocouples were evenly spaced over the height. Thermocouples (SA2F-K-K120-SMPW-CC) were installed at the top, mid-height, and bottom of the selected web. One additional thermocouple (SA2C-K-K120-SMPW-CC) was installed at the junction of the web and the top flange. The thermocouple used in this position was designed to be placed on curved surfaces. All thermocouples were purchased from Omega Engineering Inc.

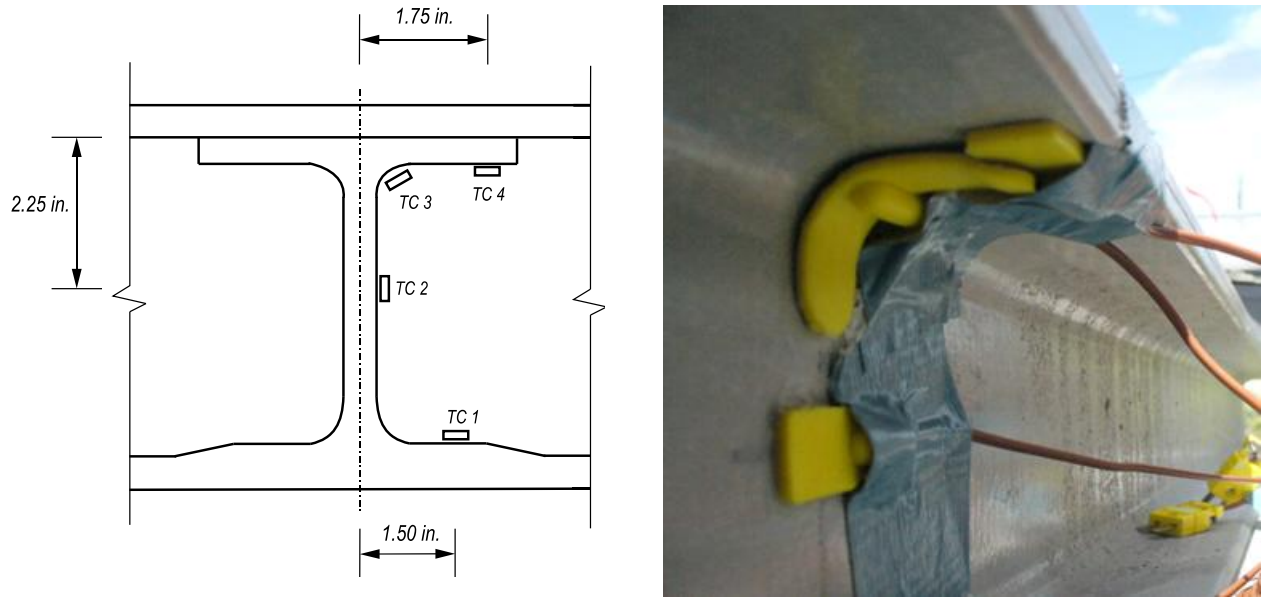

Figure 27 – Surface-temperature-measuring thermocouples on panel B8

One thermocouple (NB4-CAXL-14U02) was installed in the shade under the data acquisition box to measure ambient site temperature.

6.4 Displacement Gages

GFRP deck displacement was measured during the bridge tests and during long-term monitoring. The relative girder displacements were also measured during the 2009 bridge test. The location of the displacement gages is given in Figure 28. Relative girder displacements in two locations were measured using the fixture shown in Figure 29. The frame is attached rigidly to one of the girders with the displacement gage plunger contacting the adjacent girder. Relative displacements were measured between girders 3-4 and 7-8.

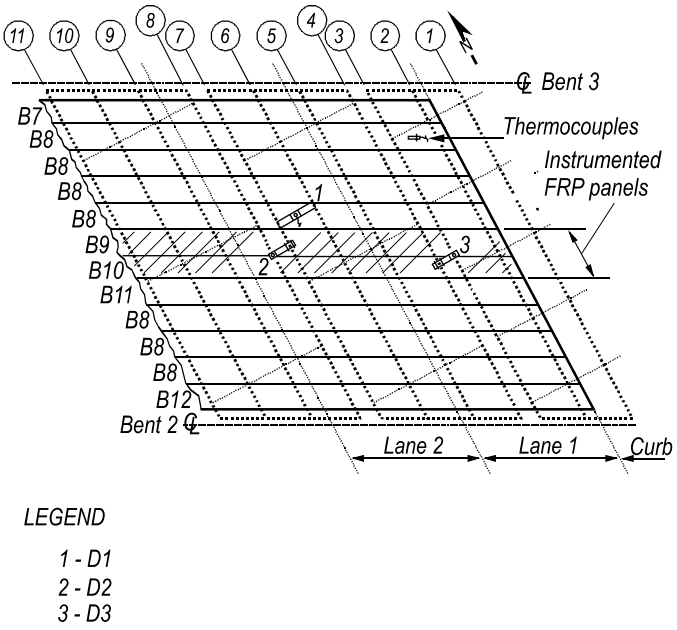

Figure 28 – Location of thermocouples and displacement gages.

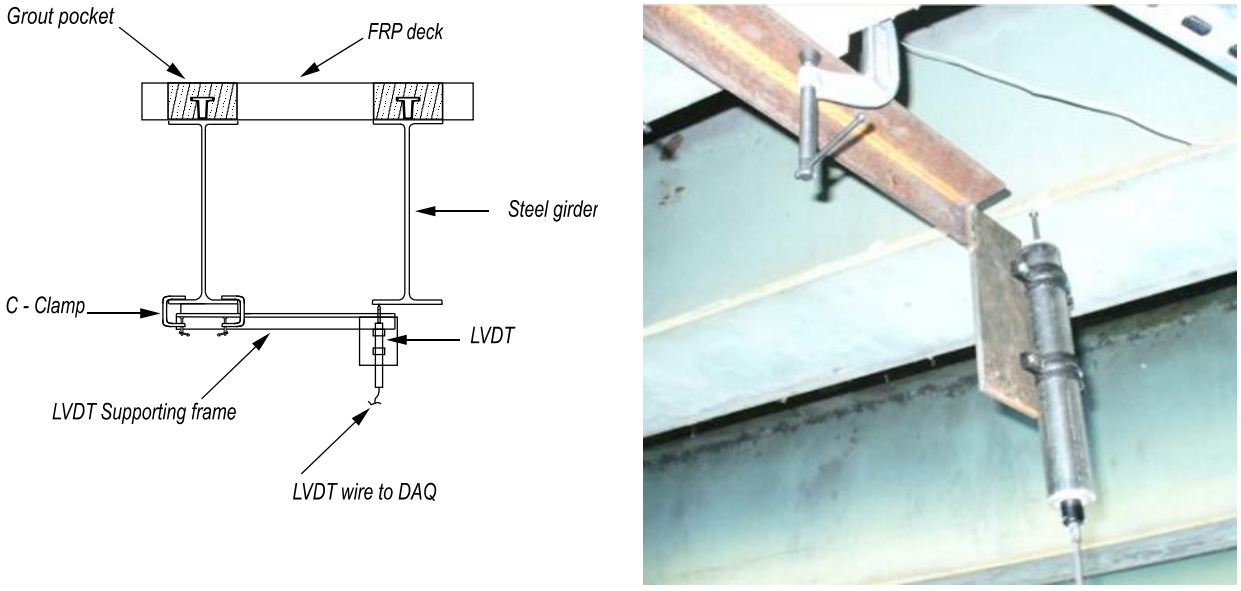

Figure 29 – Deflection gage on steel girder

GFRP deck displacement relative to the structural steel girders was measured both during the bridge test and during the monitoring period. The displacement gage was located in lane two between girders 6 and 7. Figure 30 shows the displacement gage and its support frame, which is c-clamped to the bottom flange of the adjacent steel girders. The displacement gage was

mounted in the center of the frame to provide midspan deflections for the GFRP deck. Two additional displacement gages (Figure 30b) were used during the bridge test for the Acoustic Emission (AE) calibration and were removed following the bridge test. The displacement gage used for monitoring was model LD-620 manufactured by Omega Engineering Inc. and has a guided core with removable spring plunger with a range of ± 1 in.

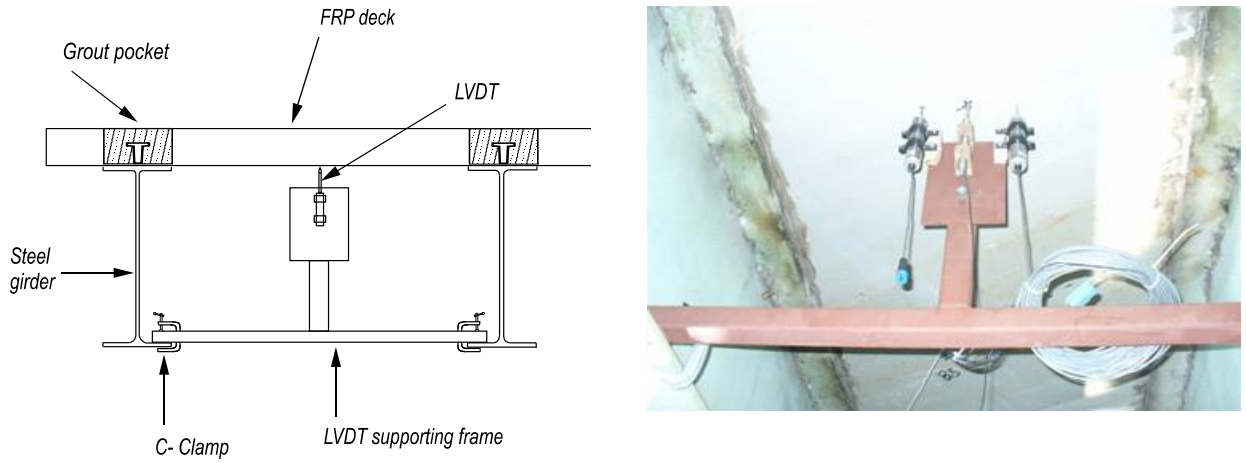

Figure 30 – Displacement measurement instrument and supporting frame (a) schematic (b) photo during bridge test

6.5 Instrument Positions

Truck positions were tracked with GPS during the rolling bridge tests. To enable analysis of the instrument data with respect to the truck position, it was necessary to know the coordinate position of each gage. For the purposes of this report, the coordinate position of both truck and instruments were recorded with respect to the coordinate axes shown in Figure 31. The intersection of the expansion joint (between GFRP deck span and in-situ concrete approach span) and the curb on the southeast side of the bridge was designated the origin.

Instrument positions are shown in Table 4. Girder 2 is 11 in. away from the face of the curb.

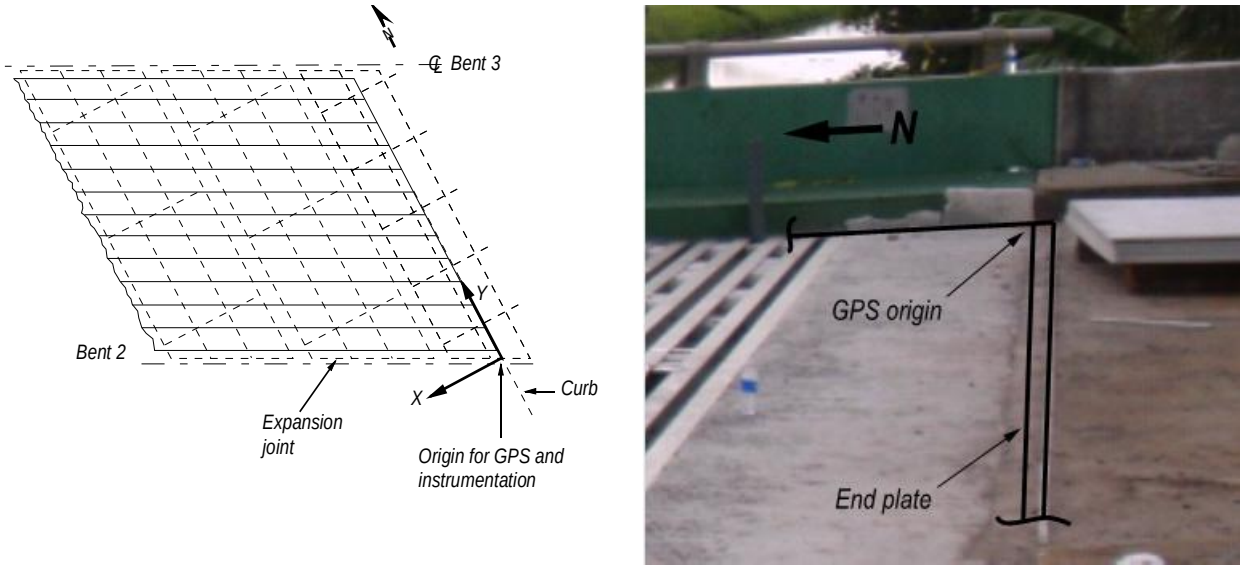

Figure 31 – Coordinate axes used for relative positioning of truck and gages

Table 4 – Coordinate position of gages

Gage	Location	Coordinates	
		x (in.)	y (in.)
B1	Stringer 3	59	240
B2	Stringer 5	128.6	277
B3	Stringer 6	176.6	302
B4	Stringer 9	294.2	364
D1	B8	155	278
D2	Stringer 8	246.2	364
D3	Stringer 3	59	240
S1	B10	35	225
S2	B10	104.6	266
S3	B10	200.6	317
S4	B10	235.4	335
S5	B9	35	256
S6	B9	69.8	273
S7	B9	200.6	342
S8	B9	270.2	379
R1	B10	37	229
R2	B10	105	265
R3	B10	201	316
R4	B10	269	352
R5	B9	37	255
R6	B9	105	291
R7	B9	201	342
R8	B9	269	377

6.6 Sampling Rate

The short spans and relative flexibility of the GFRP deck were expected to cause negligible strain or displacement readings unless the wheel was in close proximity to the gage. This localized effect of the wheel load made the selection of the sampling rate for both the bridge tests and long-term monitoring important considerations.

The use of the GPS system during the bridge test allowed the truck to be rolled across the bridge at a rate of 0.75-1 mph rather than typical practice of positioning it statically. The data acquisition system recorded both truck position and associated instrument readings at regular intervals. The sampling rate chosen for the bridge test was 5 Hz. At the rolling rate used for the test, the truck wheel took approximately 1.76 sec to traverse a single GFRP panel. At a sampling rate of 5 Hz, approximately 9 scans were collected as the wheel traversed the panel, which was deemed sufficient to capture the deck behavior.

Long-term monitoring of vehicular traffic required a higher sampling rate due to the traffic speed. The local speed limit is 35 mph. Traveling at this rate, it takes only half of a second to traverse the GFRP deck. Moreover, the time to traverse a single 31-in. wide GFRP panel is approximately 0.05 sec. To ensure that the peak strain and deflection in the GFRP panel is captured, a higher sampling rate was required. The criterion established for the bridge test of a minimum of 9 data points for a single panel was used to establish the sampling rate for traffic monitoring. A sampling rate of 200 Hz was selected to ensure that at least 10 data points were recorded on any single GFRP panel. Table 5 shows the calculation of traverse time for the traffic traveling at the allowable speed limit

Table 5 – Sampling rate calculations

Span	35 ft
Average instrumented panel width	31 in.
Allowable speed on the bridge	35 mph (51 ft/sec)
Time taken to cross the bridge	0.68 sec
Time taken to cross the instrumented panel	0.05 sec

6.7 Data Acquisition System

In October 2009, an initial bridge test was conducted. Following the bridge test, the monitoring data acquisition system was activated. The instrumentation for both the bridge test and monitoring was installed immediately prior to the October 2009 load test. For the bridge test, the FDOT Structures Research Center's data acquisition system (FDOT DAQ) was used for

collecting data from the instrumentation during the bridge test. This required that the instruments be wired temporarily to the FDOT DAQ.

Following the bridge test, the wiring was then connected to the DAQ used for monitoring traffic. A CompactRio (cRIO 9104, 8 slot 3 M gate reconfigurable chassis) data acquisition system (cRIO DAQ) from National Instruments, Inc. was used for this purpose. The system was fitted with a quarter bridge module (NI 9236) capable of handling 8 channels, a full bridge module (NI 9237) capable of handling 4 channels, an analog voltage input module (NI 9215) capable of handling 4 channels and two thermocouple modules (NI 9211) each capable of handling 4 channels. Figure 32 shows the cRIO and various input modules.

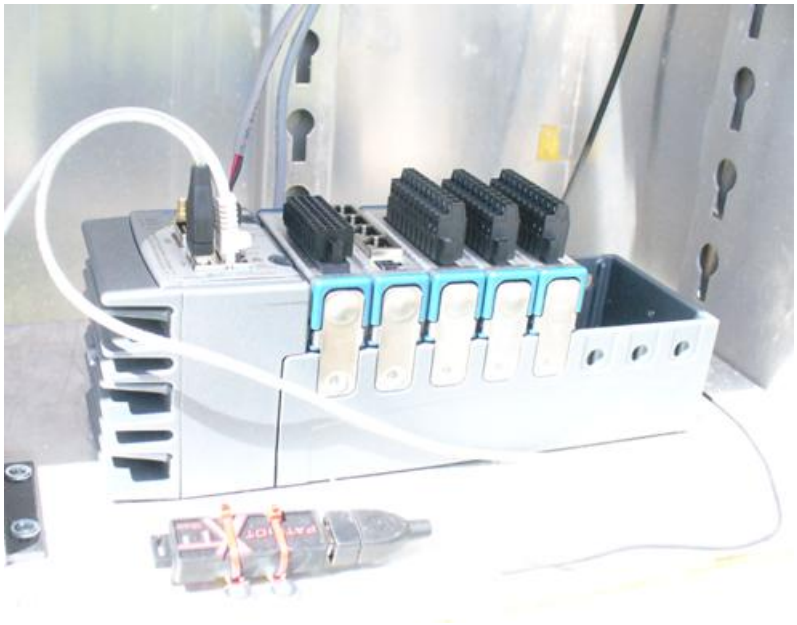

Figure 32 – cRIO and various input modules

Figure 33 shows the wiring diagram for the long-term monitoring system. Instrument wires were collected into a single bundle inside a unistrut tray that extended to the sidewalk. At the sidewalk, the bundle exited the unistrut tray, and entered a protective sleeve, turned north, and followed a steel girder to the pier. The bundle entered a flexible conduit at the pier, which followed the slab bridge span to the abutment and eventually terminated at the traffic box on the bank. C-clamps were used to attach the flexible sleeve to the steel girder. The rigid conduit was attached to the concrete slab of the sidewalk. A solar panel (Figure 35) was used to power the DAQ and was installed next to the traffic box.

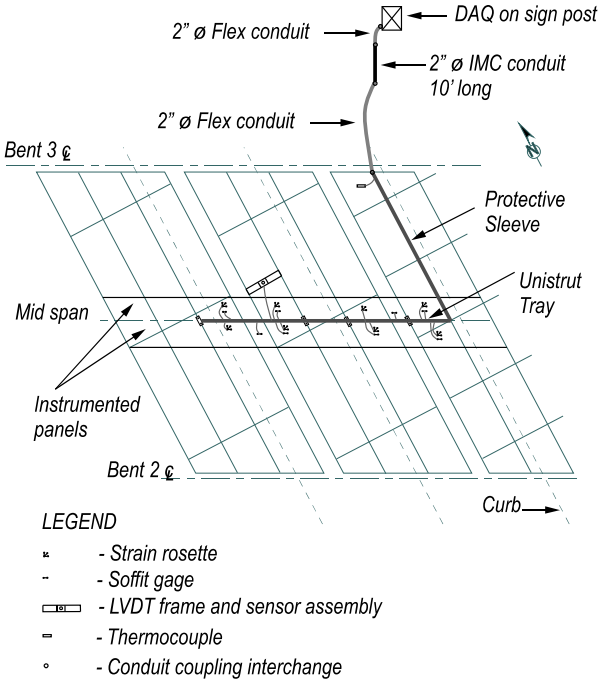

Figure 33 – Instrumentation wiring

Figure 34 – Traffic box mounted on a sign post

Figure 35 – Solar panel

Data were continually collected from all the sensors and stored in an external USB drive acting as a remote server on site. Data collected before the 2010 bridge test were transferred remotely to the FDOT Structures lab Tallahassee using a cellular modem (RAVEN X from Sierra Wireless) with a Verizon wireless data plan. Data collected after the 2010 bridge test were retrieved semimonthly from the USB flash drive.

6.8 2010 Bridge Test

Instrumentation was almost identical to that used in the October 2009 bridge test. Existing foil gages and wiring were replaced. New foil gages were installed by FDOT that were adjacent to the existing foil and BDI gages. The rosette strain gages were inoperative by October 2010. Installation of new rosette gages was not feasible due to a lack of access to the gage location.

6.8.1 Repair and Replacement

Soffit mounted strain gages originally installed for monitoring and the October 2009 bridge test were replaced prior to the October 2010 bridge test. The gage resistance was checked for each strain gage prior to replacement. Gages S1, S2, and S5 had malfunctioned while gages S3 and S8 had never functioned. Replacing all eight soffit gages was done to prevent errors due to variations in gage conditions. All new gages were covered with waterproof mastic tape for protection during long-term monitoring. New wire was used to connect the gages to the monitoring equipment.

Visual inspection was performed on the four FBS gages by removing the PVC cover. Gage B1 had water intrusion that rusted the contact surface. B1 was removed from the beam surface, the surface was cleaned using a grinder, acetone and rag paper, and the gage was reattached at the same location using Loctite adhesive and an accelerator. Gage B2 had a strong bond to the monitored girder with no rust present. New wire was used to connect B2 to the monitoring equipment. Gages B3 and B4 likewise had strong bonds with no rust present. The wiring connection was redone at the gage end for B3 and at the monitored end for all FBS gages.

Functionality of the gages was established by monitoring continuous traffic on the bridge. The soffit strain gages, FBS gages, and the LVDT recorded data through the DAQ successfully.

6.8.2 New Installation

Prior to the 2010 bridge test, four new foil gages were installed on the girders at the top of the bottom flanges adjacent to the BDI gages. Eight new foil strain gages were attached adjacent to the existing soffit gages. These twelve new gages were connected to the FDOT DAQ while the existing gages were left attached to the cRIO DAQ during the bridge test. A separate LVDT was placed adjacent to the D1 gage. These redundant instruments were used to ensure that the cRIO monitoring data was calibrated with the FDOT bridge test data. Considerable time was saved during setup, since the existing gages did not have to be rewired from the FDOT DAQ back to the cRIO DAQ after the bridge test. As a result, the FDOT DAQ recorded data from different gage locations in 2009 than in 2010. This is discussed later in the report.

7 Bridge Test Procedure

7.1 Overview

This chapter presents the procedures used to conduct the bridge tests on the Belle Glade bridge on October 14, 2009 and October 7, 2010. Initially a static bridge test was conducted using two load trucks positioned individually and then in tandem over the instrumented GFRP panels. Based on this initial testing, it was found that a single truck could be used for the remainder of the bridge test. The remainder of the testing was conducted with a single truck by rolling it slowly over the bridge while recording instrument and truck position data. Utilizing strain and truck position (GPS data), influence lines were created for the soffit gages and full bridge gages. Load distribution between the webs of GFRP deck was calculated using the influence lines. Deflection gage data are presented in load-displacement plots for the GFRP deck. Response of the steel girders is presented in terms of strain and deflection. Composite behaviors between top and bottom GFRP sections were calculated analytically and determined experimentally. Load-strain calibration plots are presented for all of the soffit gages. A comparison between lab and field testing is also presented. A high speed test conducted during the 2010 bridge test provided impact factors that were compared with factors recommended in AASHTO LRFD Bridge Design Specifications, 4th Edition, 2007 (AASHTO).

7.2 Objectives

The purpose of the bridge tests was to classify the load levels experienced by the bridge under varying traffic conditions and establish a base line of strains and deflection for future monitoring. Distributions factors for wheel loads on the GFRP panel webs were also obtained. Composite action between existing steel girders and GFRP deck and between bottom GFRP deck panel and top GFRP plate were also investigated.

7.3 Truck Positions and Load Levels

FDOT Structures Research Center load trucks were used during the bridge tests (Figure 36). The truck trailer is designed to impose known wheel and axle loads to the bridge as a function of the number of blocks stacked on the trailer. Table 6 shows the axle loads associated with the number of blocks stacked on the trailer.

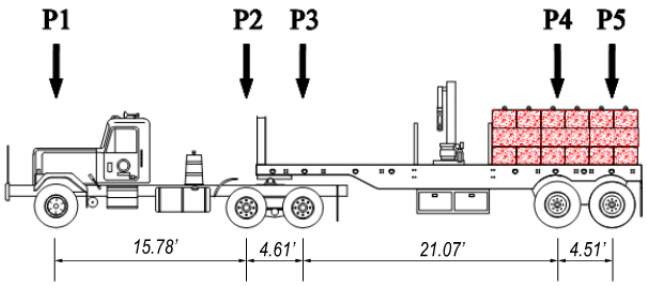

Figure 36 – FDOT utility truck used for bridge tests

Table 6 – Test truck axle loads (kip)

No. of Blocks	Front Axle P1 (kip)	Front Tandem		Rear Tandem	
		P2 (kip)	P3 (kip)	P4 (kip)	P5 (kip)
12	11.3	10.8	10.8	19.0	19.0
18	11.6	10.0	10.0	25.5	25.5
24	11.2	11.0	11.0	30.6	30.6
30	11.4	12.0	12.0	35.5	35.5

Five truck positions (TP1 through TP5) were used to maximize the bending and shear effects in the strain gages mounted on the GFRP panels and to cover most combinations of transverse traffic movement in the two instrumented northbound lanes. All truck positions were marked parallel to the curb by measuring the distance from the face of the curb to the intended position of the tires on the west side of the truck.

TP1 through TP5 are shown graphically in Figure 37 through Figure 41. Figure 42 provides the distance from the face of the curb to the outside of the wheel on the driver's side. Lines were marked from 1 through 5 for the five truck positions on the deck. The face of the curb was located 1.5-ft away from the inside of the first lane mark.

TP1 and TP4 corresponded approximately to the tire marks in each lane and are considered to be the path that trucks will typically take when traversing the bridge in lanes one and two, respectively.

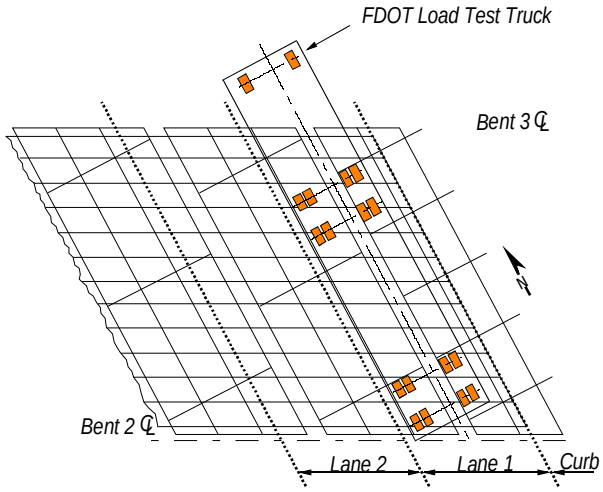

Figure 37 – Truck in position TP1

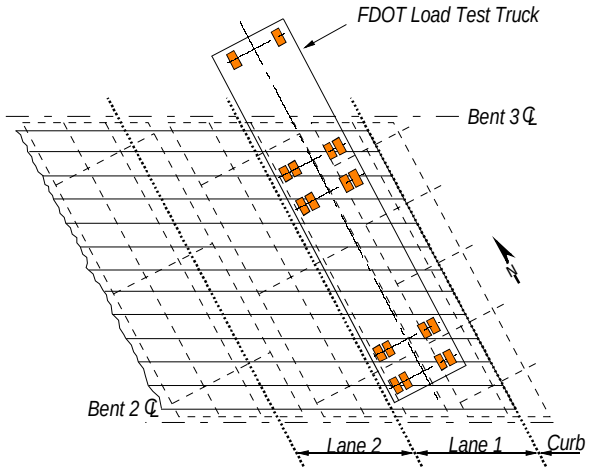

Figure 38 – Truck in position TP2

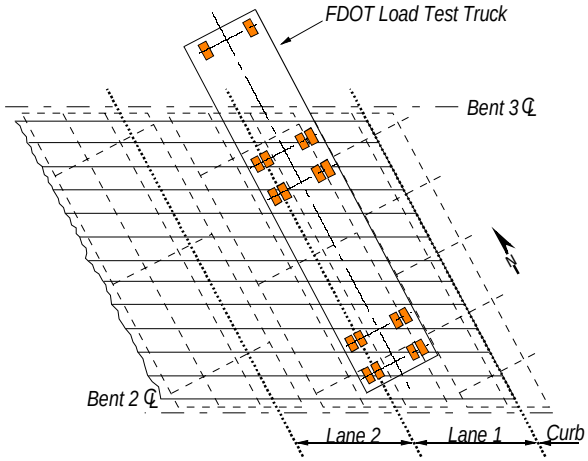

Figure 39 – Truck in position TP3

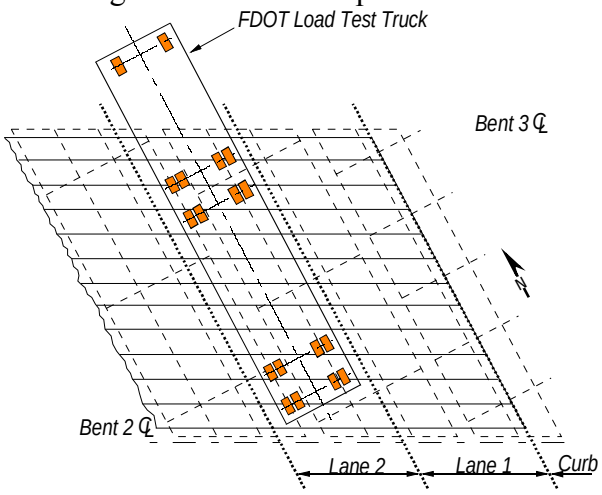

Figure 40 – Truck in position TP4

Table 6 shows the four load steps used for the bridge test. Maximum axle load applied at load step four was 35.5 kip, which results in a wheel load of approximately 18 kip. Tandem tires ensure that the wheel load is spread over two tire widths on the rear trailer axle. This load was chosen to ensure that the AASHTO design service wheel load of 16 kip was reached. AASHTO LRFD (2007) section 3.6.1.2 specifies an unfactored design wheel load of 21.3 kip (16 kip x 1.33 (IM)). As noted in the table, the test started with 12 blocks on the trailer and went up to 30 blocks in 6 blocks increments.

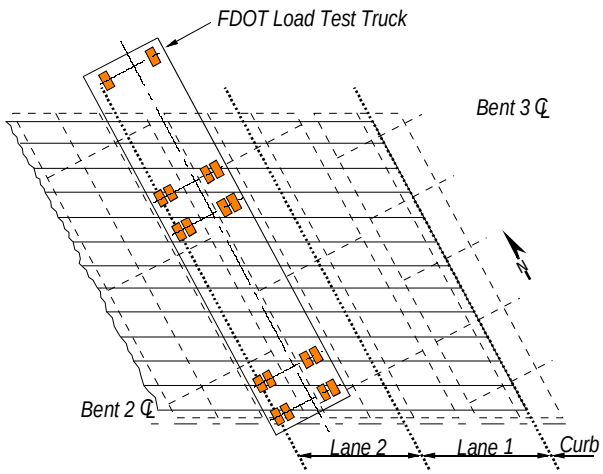

Figure 41 – Truck in position TP5

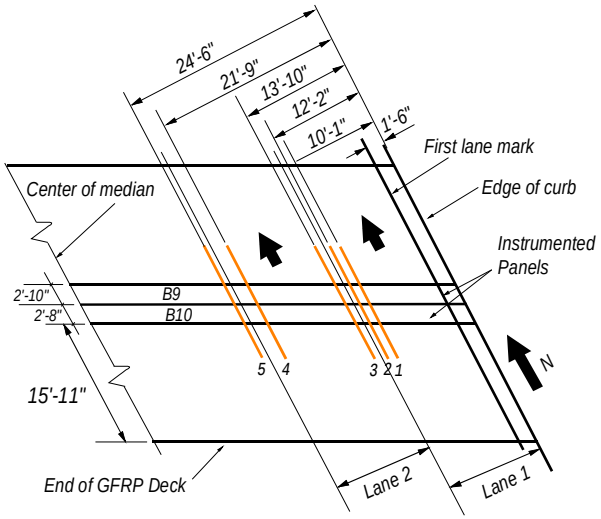

Figure 42 – Truck positions for bridge test. Lines indicate outside edge of tires on west side of truck

7.4 Test Setup

The instrumentation needed for the bridge test and monitoring were installed during the two days prior to the bridge tests. The 2009 bridge test was performed at night from 9pm to 5am while the 2010 bridge test was performed from 9pm to 2am to avoid causing traffic delays. The FDOT DAQ and AE systems were placed on the east sidewalk of the bridge during the test. Truck position reference marks were painted on the bridge deck (Figure 43).

Figure 43 – Truck position reference marks on the bridge deck

GPS was used during the bridge tests to record the position of the truck along with each data scan of the instruments. Figure 44 shows the position of the GPS dome with respect to the truck axles. Prior to the bridge tests the GPS dome was used to take position readings of several reference points, including the origin for GPS and instrumentation, the edges of the truck positions, and ends of the marked instrumented panels on the bridge.

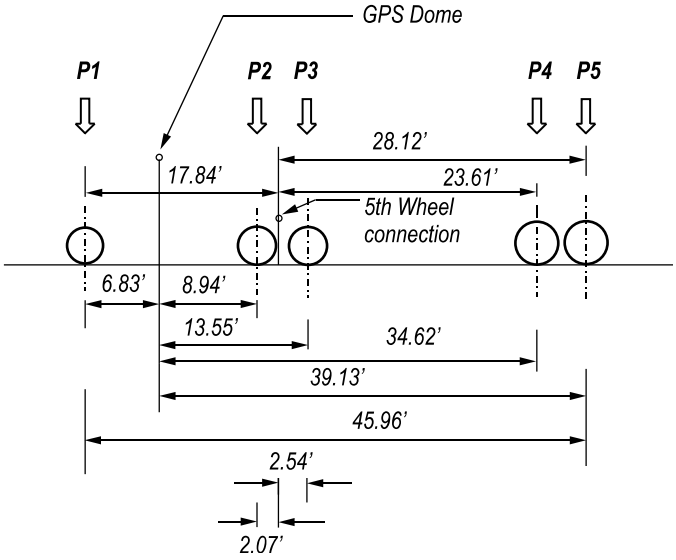

Figure 44 – Location of the GPS dome

7.5 2009 Procedures

7.5.1 Static Test

This test was performed by statically positioning (non-rolling) the two trucks to determine if it was necessary to use both trucks for the entire load test or if one truck would be sufficient to capture the behavior of the bridge deck. The test was started by positioning the truck in lane one at TP2 (Figure 38) with the rear axle over the instrumented panel B9. It was necessary to adjust the truck position slightly to maximize the strain in soffit gage S5. Strain and deflection were recorded when truck was in this position. Leaving the first truck in lane one, the second truck was positioned in lane two at TP5 (Figure 41) with the rear axle over the instrumented panel B9. Strain and deflection were recorded. Leaving the second truck in lane two, the first truck was removed from lane one. Strain and deflection were recorded and the static test was terminated.

7.5.2 Rolling Test

A single truck was rolled slowly (0.75 – 1 mph) across the bridge in all five truck positions as shown in Figure 42. For each load step, the truck was rolled through all five truck positions before moving on to the next load step. To allow correction for residual strain, zero readings were recorded prior to every load step. Figure 45 shows a flowchart for the procedure used during the rolling test.

During the test, strain and deflection from selected gages were plotted and monitored for linearity to avoid damaging the bridge.

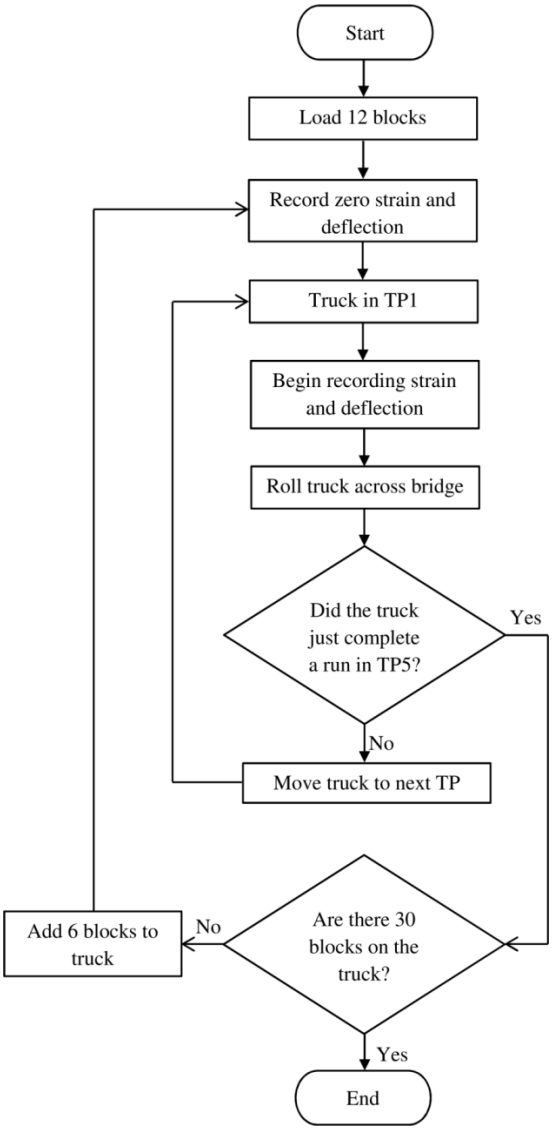

Figure 45 – Flowchart for bridge tests

7.6 2010 Procedures

7.6.1 Static Test

This test was performed by statically positioning (non-rolling) the two trucks to determine if it was necessary to use both trucks for the entire load test or if one truck would be sufficient to capture the behavior of the bridge deck. The test was started by positioning the truck in lane one at TP2 (Figure 38) with the rear axle over the instrumented panel B9. It was necessary to adjust the truck position slightly to maximize the strain in soffit gage S5. Strain and deflection were recorded when truck was in this position. The truck in lane one was removed and the second truck was positioned in lane two at TP5 (Figure 41) with the rear axle over panel B9. Strain and deflection were recorded. The first truck was then repositioned in lane one at TP2 (Figure 38) with the rear axle over panel B9 with the second truck remaining in position. Strain and deflection were recorded and the static test was terminated.

7.6.2 Rolling Test

A single truck was rolled slowly (0.75 – 1 mph) across the bridge in all five truck positions as shown in Figure 42. For each load step, the truck was rolled through all five truck positions before moving on to the next load step. To allow correction for residual strain, zero readings were recorded prior to every load step. The procedure followed here was identical to that followed in the October 2009 test. Figure 45 shows a flowchart of the bridge test.

During the test, strain and deflection from selected gages were plotted and monitored for linearity to avoid damaging the bridge.

7.6.3 35 MPH Test

35 mph tests were conducted to determine the dynamic response of the bridge. The high speed tests began with placing 12 blocks on the FDOT test truck. This was equal to the lowest weight level used during the rolling test. The truck was backed up to gain space to accelerate. It was not possible for the truck to precisely follow the designated truck positions. Consequently, on the first run, the truck traversed the bridge in lane one and on the second run, the truck traversed in lane two. The truck accelerated to 35 mph before reaching the bridge. This simulated a tractor-trailer driving across the bridge at the speed limit. Upon exiting the far side of the bridge, the truck came to a stop. The truck was backed up across the bridge, again

reaching a point from which it could accelerate to 35 mph before reaching the bridge. During both runs, strain and displacement were measured by the FDOT DAQ at 200 Hz.

8 Bridge Test Results – Static Truck

To determine the effect of a truck positioned in an adjacent lane, three static truck load cases were tested using 12 blocks on each trailer. Zero load reference readings were taken immediately prior to truck loading. In the 2009 test, initial readings were taken with a single truck positioned in lane one at TP2 (Figure 38) and a second truck in lane two at TP5 (Figure 41). A second set of readings was taken with a truck in TP2 but no truck in lane two. A third set of readings were taken with a truck in TP5 but no truck in lane one. In the 2010 test, the second and third sets of readings were taken in reverse order. For each static load case, the trucks were maneuvered into position with the rear trailer axle over the instrumented panels until the data acquisition indicated a maximum strain was reached at strain gage S5 for the truck in lane one and strain gage S7 for the truck in lane two. The FDOT DAQ continued recording strains and deflections at these truck positions for 25 – 30 sec. at a sampling rate of 5 Hz.

Soffit gage strains were calculated from the static load test data. The analysis consisted of correcting the processed strain values for appropriate zero load reference readings and plotting the strain-time history. An average of the maximum corrected strains was calculated for three static load cases and presented in Table 7 and Table 8.

Table 7 – Maximum static strain values (October 2009 test)

Instrumentation	One truck in lane one (TP2)	One truck in lane two (TP5)	Two trucks (TP2+TP5)
S1	48.0	0.3	26.7
S2	5.4	-0.4	-3.0
S4	-21.2	20.7	-5.6
S5	84.3	-4.8	58.1
S6	106.8	-16.4	184.2
S7	-6.4	442.3	417.8
B1	147.5	9.4	148.2
B2	118.7	41.8	160.2
B3	66.5	81.3	146.1
B4	8.0	102.7	105.4

Table 7 and Table 8 show that the maximum strains were recorded by soffit gage S7. From the 2009 test, the recorded strain was 442 με when loaded with one truck (TP5) and was 418με when loaded with two trucks (TP2+TP5). From the 2010 test, the recorded strain was 359

με when loaded with one truck (TP5) and was 347 με when loaded with two trucks (TP2+TP5). This indicates that the effect of wheel loads was localized and that the maximum difference in strain caused by an adjacent truck was about 5%. The local wheel load response of the bridge and linear-elastic material behavior allowed superimposing the wheel load effect from other lanes. Similar behavior is not necessarily true for the steel girders, but the focus of this study was the GFRP deck.

Table 8 – Maximum static strain values (October 2010 test)

Instrumentation	One truck in lane one (TP2)	One truck in lane two (TP5)	Two trucks (TP2+TP5)
S1	107.3	-3.0	61.5
S2	-1.8	-7.0	2.5
S3	-4.4	81.8	76.8
S4	-25.0	-47.1	-71.8
S5	46.5	-3.2	42.0
S6	70.8	-30.5	47.3
S7	-8.9	358.5	347.6
S8	-25.0	7.3	0.5
B1	156.2	7.4	154.8
B2	75.5	53.8	129.4
B3	106.0	172.6	227.2
B4	3.6	80.9	86.1

The static load test strain data indicate that a direct comparison of the 2009 and 2010 static tests is difficult. No consistent pattern emerged regarding which strain gage locations showed a loss of stiffness. The procedure for the static test made consistency difficult. The truck was moved as slowly as possible, which was about 1 fps. The observer watching the strain gage output had to communicate the correct stopping position to the truck driver. With a person relaying this information between the test monitors and the truck driver, a delay was inevitable. Positioning the truck within 1 ft of the position that maximizes strain was not feasible. As indicated in this report, the deflections in the GFRP panels are localized; a wheel that misses the coordinate measured parallel to the right-of-way that causes maximum strain by even a foot is going to produce strains that are less than half what a wheel located directly over the gage would produce. This explains why the gage readings from the 2010 bridge test are not always greater in magnitude than the readings from the 2009 bridge test.

The FBS gages on the steel girders indicated that some transfer of stress occurred between girders within a frame. Gage B1 had a nominal increase in strain, but this was small

enough to be within the margin of error. Gage B2 recorded a much smaller strain in the 2010 test, with strain dropping by 19% since the 2009 test. Gage B3, which is a part of the same frame as B2, indicated a 55% increase in strain from the 2009 test to the 2010 test. This suggests that some of the load carrying capacity was transferred from one girder to the other since B2 and B3 are adjacent. Gage B4 recorded an 18% lower strain in the 2010 test versus the 2009 test. Again, this is possibly due to load sharing among the other girders of frame containing the B4 gage.

9 Bridge Test Results – Rolling Truck

Rolling bridge tests were conducted after the static bridge tests. These tests were designed to evaluate the use of GPS in bridge tests, create influence functions of the loading at each strain gage, and to create distribution factors for the GFRP panel webs. A single test truck was rolled over the bridge at 0.75 – 1 mph in TP1 through TP5 for four load levels. Regular moving traffic has some dynamic wheel load effect on the bridge because the speed limit on the bridge was 35 mph. Due to the low velocity of the test truck, dynamic wheel load effects were considered negligible; strains and deflections presented in this section were nearly identical to static values. Influence lines representing strains as functions of truck positioning were produced for the GFRP deck panels and steel girders. Distribution factors were computed from influence lines for the GFRP panels. These distribution factors describe the responsiveness of the GFRP panels as a function of the distance at which load is applied. Distribution factors were determined for the response in the GFRP panels to flexural and shear strains.

9.1 Influence Lines

9.1.1 Deck Soffit

The resulting strain influence lines are shown in Figure 46 through Figure 55. Each graph contains plots that correspond to the four load levels (9.5 kip, 13 kip, 15.5 kip, and 18 kip) used in the bridge test. Graphs on the left are from the 2009 test unless noted otherwise; graphs on the right are from the 2010 test.

The x-axis in each graph reflects the position of axle P5 relative to the strain reading. When x is zero, P5 is directly over the strain gage and is causing a maximum strain. When P5 is approximately 46-ft south of the gage, then the front axle (P1) is directly over the gage. Consequently, the mirrored shape of the truck takes form in the plots with the five peaks representing the five truck axles.

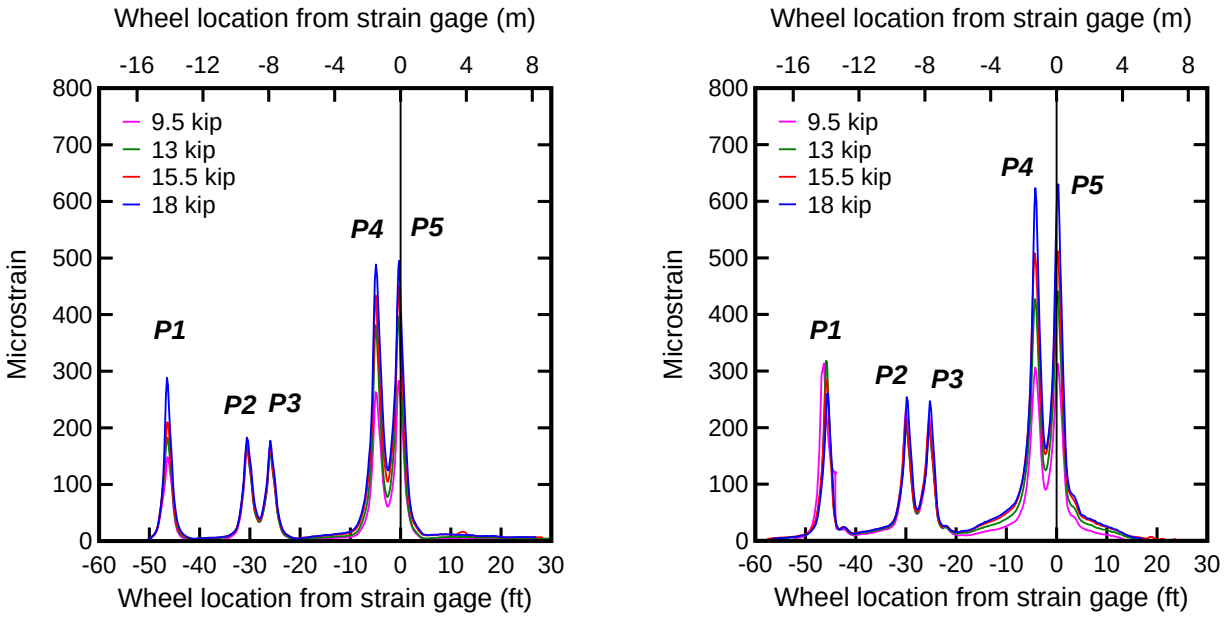

Figure 46 – Influence lines for S1 positive bending (TP1) for (a) 2009 (b) 2010

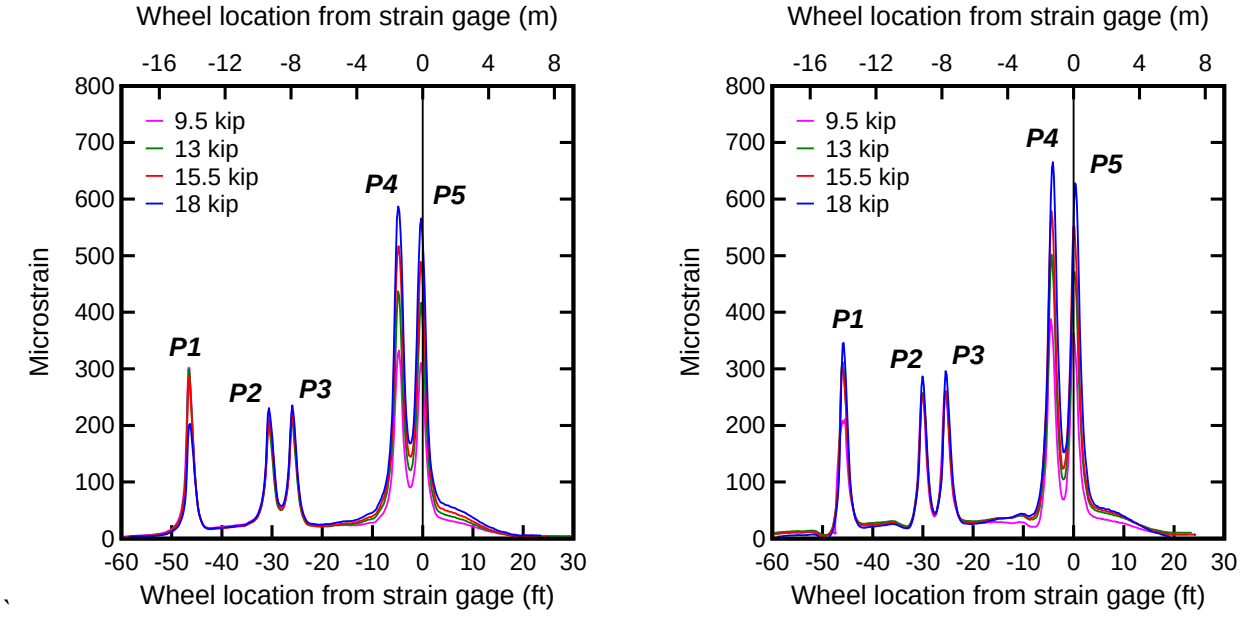

Figure 47 – Influence lines for S2 positive bending (TP1) for (a) 2009 (b) 2010

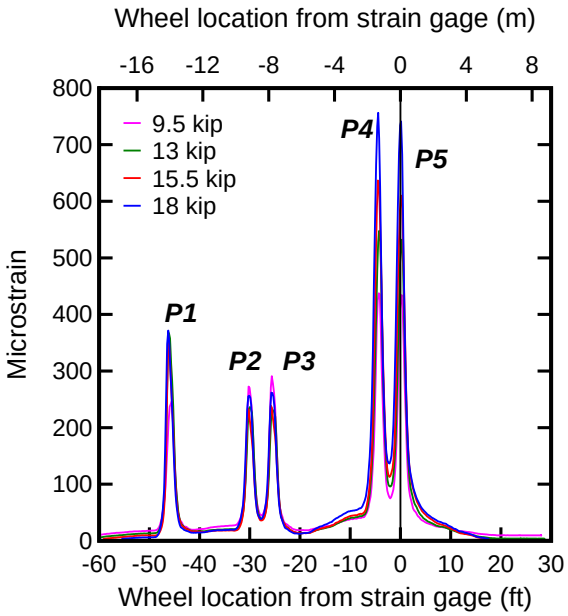

(a)

Figure 48 – Influence lines for S3 positive bending (TP5) for (a) 2010

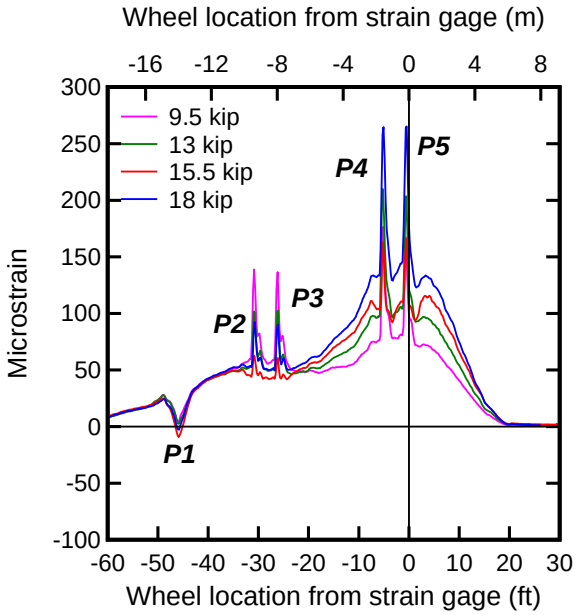

(a)

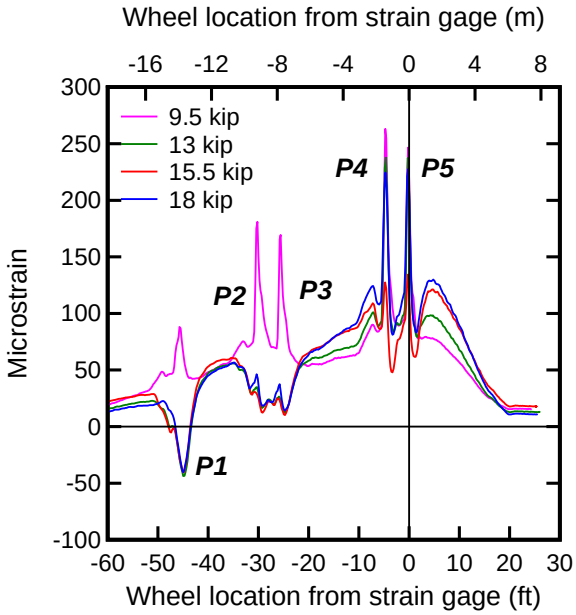

(b)

Figure 49 – Influence lines for S4 positive bending (TP4) for (a) 2009 (b) 2010

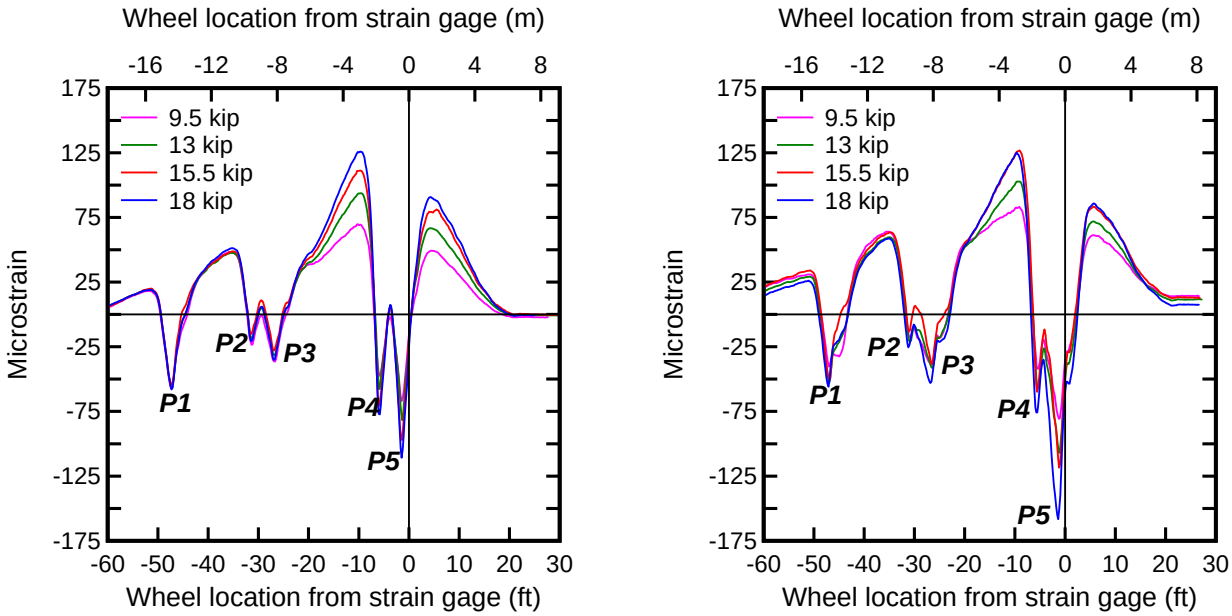

Figure 50 – Influence lines for S4 negative bending (TP5) for (a) 2009 (b) 2010

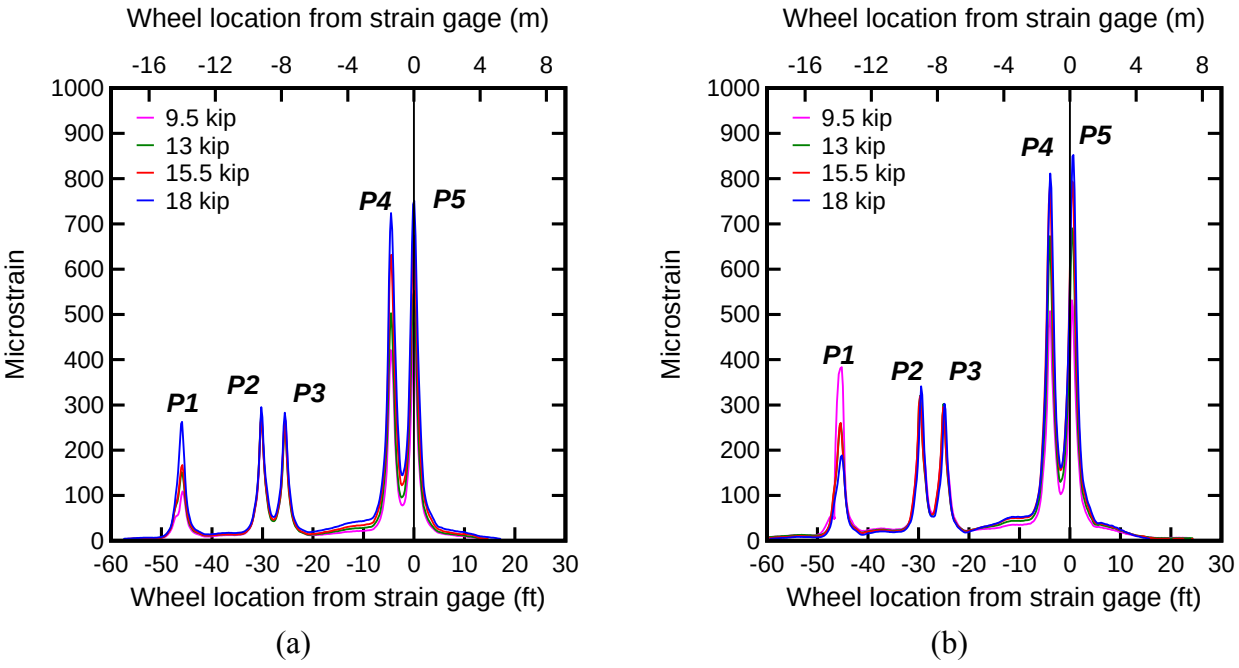

Figure 51 – Influence lines for S5 positive bending (TP1) for (a) 2009 (b) 2010

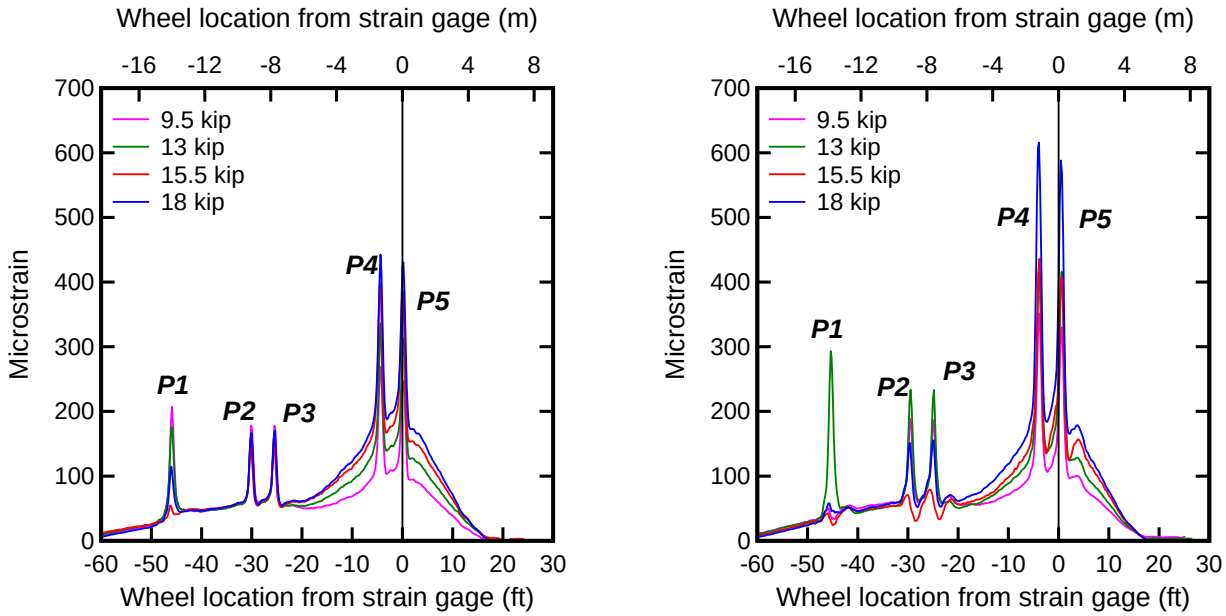

Figure 52 – Influence lines for S6 positive bending (TP3) for (a) 2009 (b) 2010

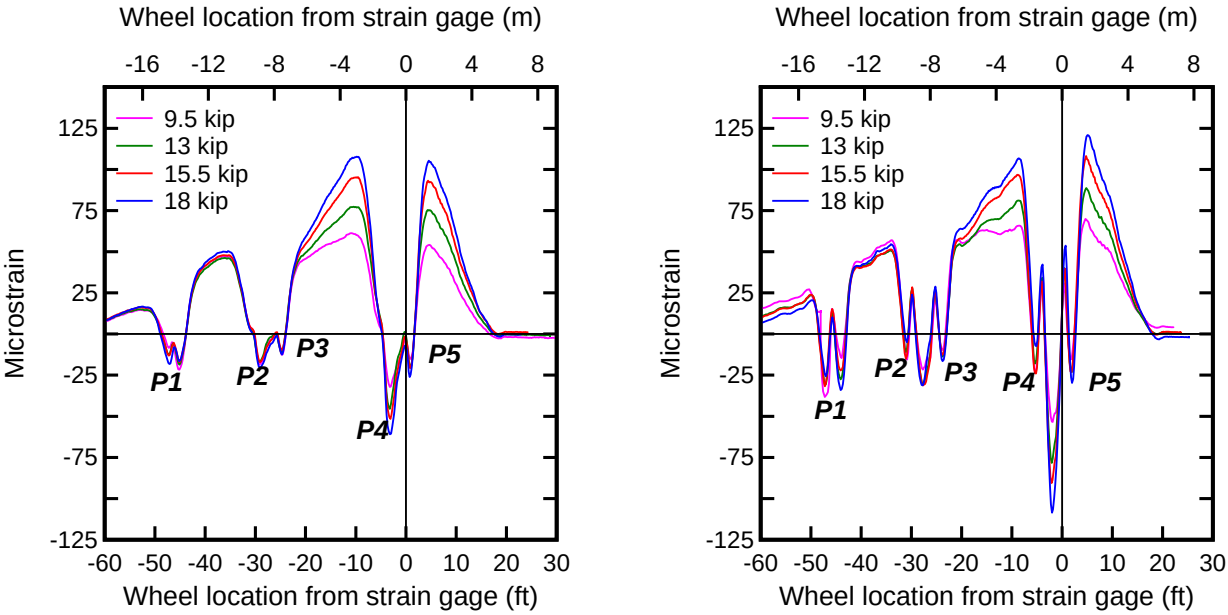

Figure 53 – Influence lines for S6 negative bending (TP1) for (a) 2009 (b) 2010

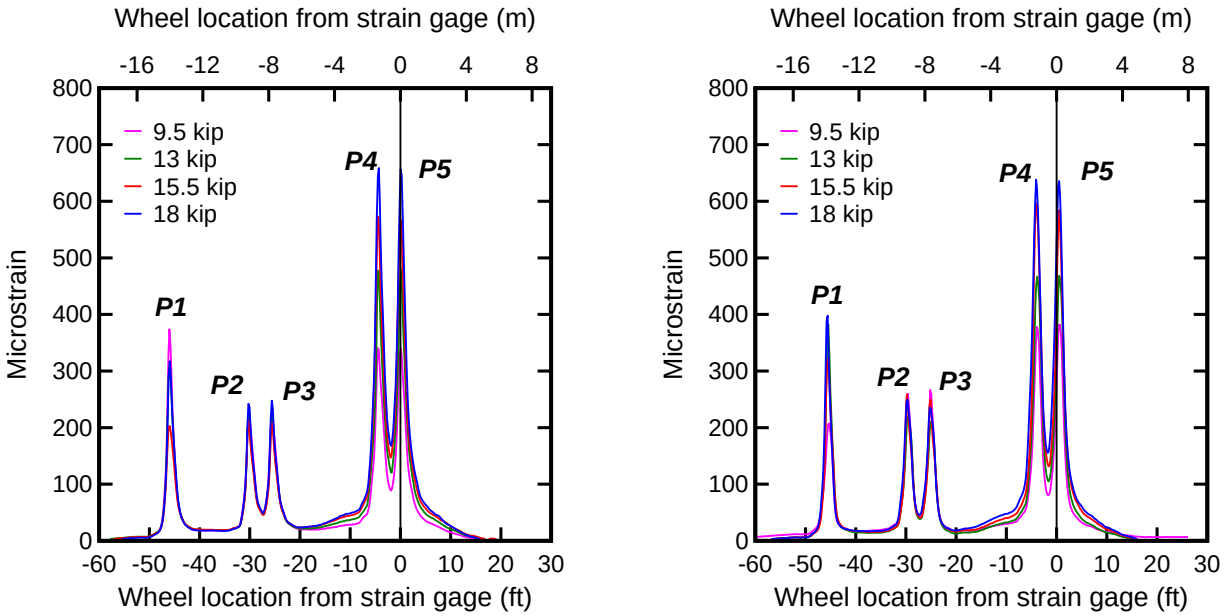

Figure 54 – Influence lines for S7 positive bending (TP5) for (a) 2009 (b) 2010

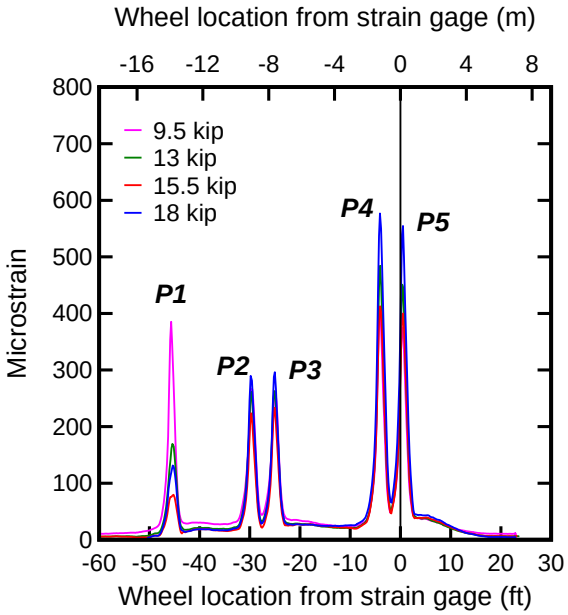

Figure 55 – Influence lines for S8 positive bending (TP5) for (a) 2010

The GPS locations of the peak strain values associated with each of the axles (Figure 56) match well with the dimensions of the truck shown in Figure 57. Maximum error in the measurement of truck position is 2%, which is indicative of the GPS accuracy.

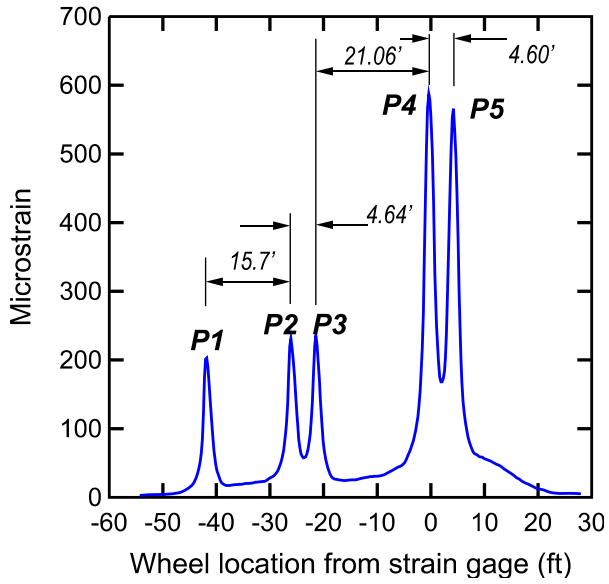

Figure 56 – Distance between the axles of test truck from influence lines for gage S5 (2009)

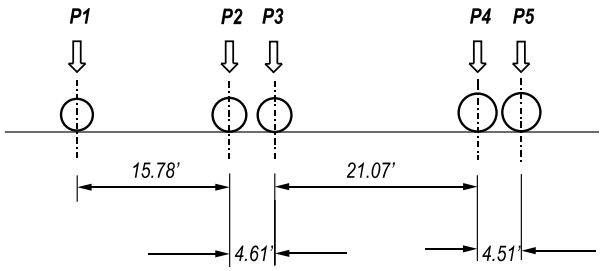

Figure 57 – Actual distance between the axle of test truck

For TP1, gages S1, S2, and S5 show positive strains. This indicates tension (Figure 46, Figure 47, and Figure 51) occurs in the bottom of the GFRP panels due to downward deflection caused by positive bending moment. Figure 37 shows the orientation and wheel path for TP1 in lane one. For TP1, the forward motion of the truck carries the left wheel line over gage S2, which is located at the mid-span of the GFRP panel. At this location, the girders are spaced at 4 ft center to center. As the wheels move over the gage, the resulting moment is positive.

As the wheel continues its northerly motion to the next GFRP panel, a peak negative (compressive) strain is noted in gage S6 (Figure 53), which is positioned in the short span adjacent to the panel over which the wheel passes. This reflects the negative moment generated by the continuity of the panel over the steel girder.

For TP5 (Figure 41), gages S3, S7, and S8 likewise show positive bending moment (Figure 48, Figure 54, and Figure 55) while gage S4 shows negative bending moment (Figure 50). This indicates that the deck panels are exhibiting similar behavior in lane two with the truck in position TP5.

Figure 58 shows the influence lines for gages S5 (positive bending) and S6 (negative bending) for TP1 (Figure 37). Figure 59 shows the relative location of the positive and negative gages. From these influence lines, it can be observed that depending on the wheel path, strain changes sign. Change of sign indicates that the deck transitions from positive to negative bending. Maximum positive strain (S5) is 751 με while maximum negative strain (S6) is 61 με for the same load and same truck path (TP1). This shows that negative bending is not that significant (about 10 % of the positive bending) but the deck goes through the cycle of positive to negative bending. Similar behavior is evident from gages S3 and S4 (Figure 60 and Figure 61) for TP5 (Figure 41). These results indicate that the deck panels behave with continuity in the direction perpendicular to the direction of travel because the influence of applied loads is transmitted through the panels across steel girders.

The maximum strain measured during the 2009 bridge test (751 με) was recorded by gage S5 and corresponded to the maximum wheel load (18 kip) used during the test. During the 2010 bridge test, the maximum strain measured was 852 με, which was also recorded by gage S5. This represents an increase of 13%.

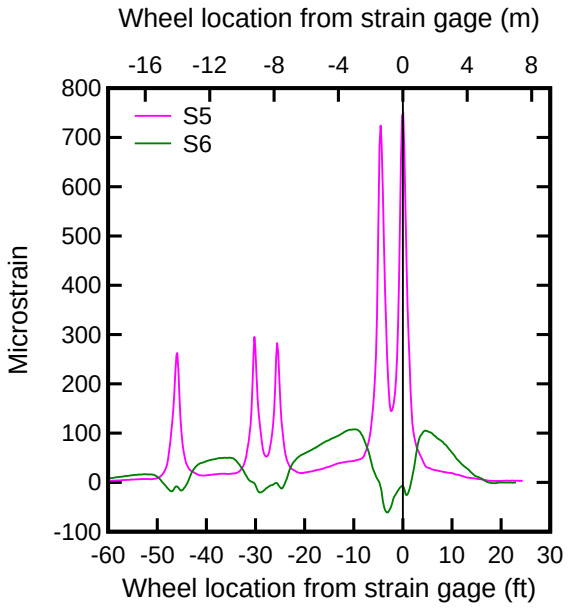

Figure 58 – Influence lines for gage S5 and S6 for TP1 (2009)

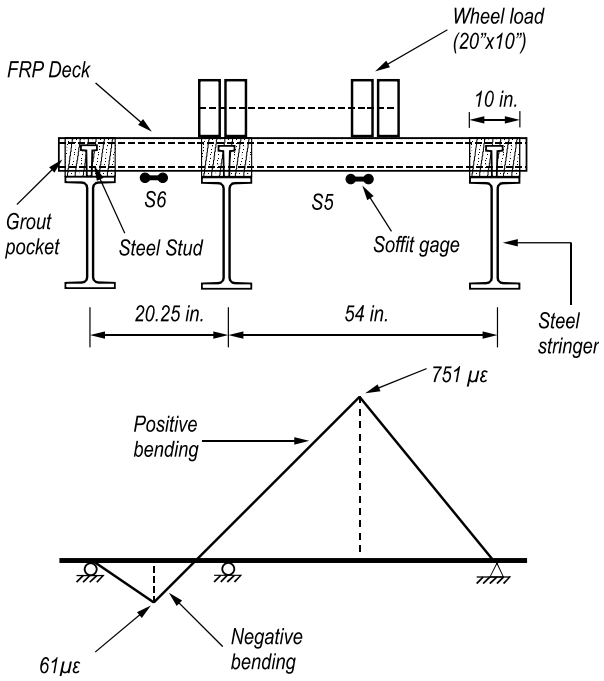

Figure 59 – Relative location of gages S5 and S6 and maximum strain

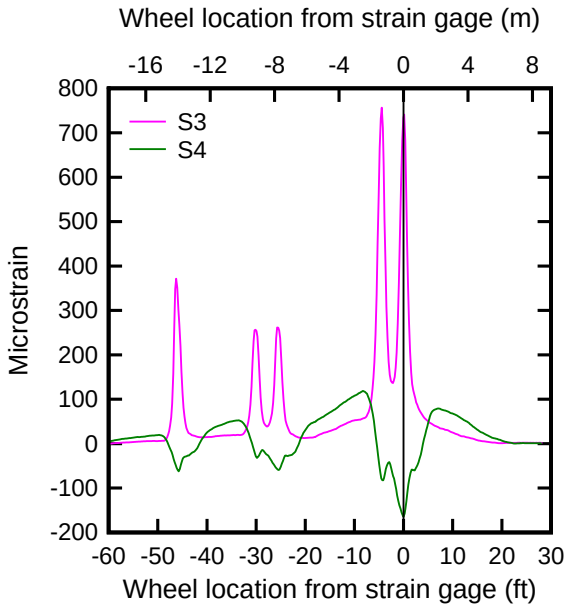

Figure 60 – Influence lines for gage S3 and S4 for TP5 (2010)

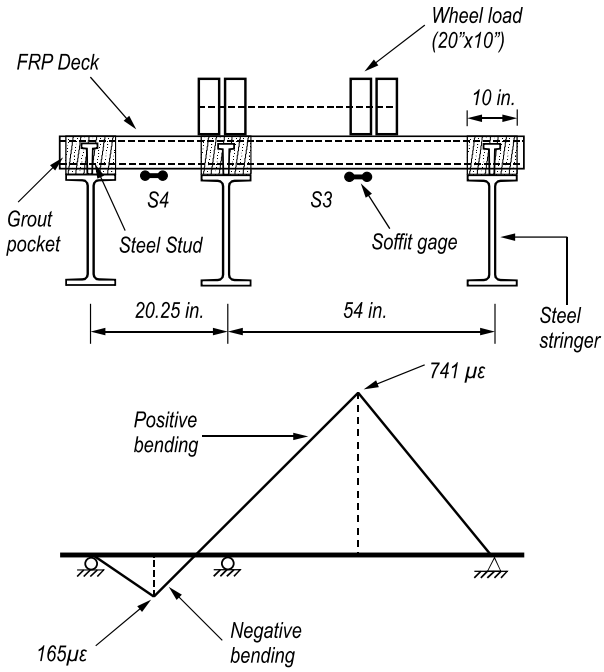

Figure 61 – Relative location of gages S3 and S4 and maximum strain

The influence lines also indicate that the effect of the wheel load on panel strain is localized. Figure 62 shows the influence line produced by gage S7 at axle P5. Strain decreased rapidly as the tire moved away from the gage. For example, strain decreased to half of the peak strain when P5 had moved to the adjacent web, which was 8 in. away. When the wheel moved to the next web (at 16 in.) the strain dropped to 27% of the peak strain. Strain dropped to 10% of its maximum value when the wheel moved to 32 in. from the strain gage. Similar behavior was noted in strain data from bonded gages recording positive bending.

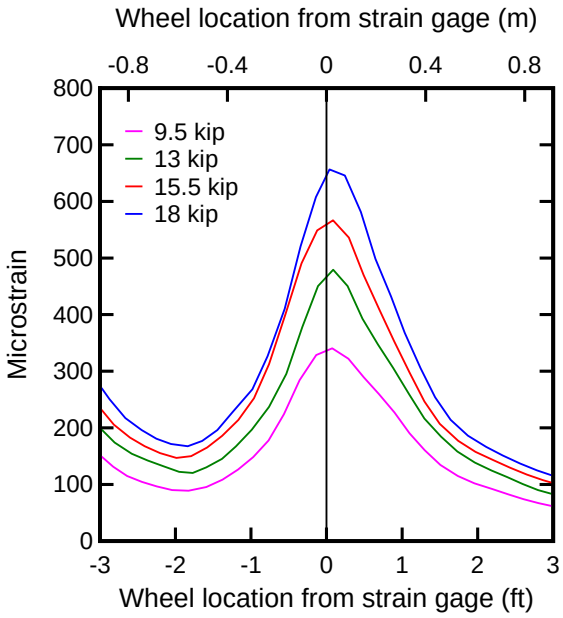

Figure 62 – Partial influence lines for soffit gage S7 at axle P5 (2009)

9.1.2 Deck Webs

Shear strain influence line plots were produced from the rosette strain data. Rosettes used for the bridge test were 0-45-90 degree rosettes as shown in Figure 63.

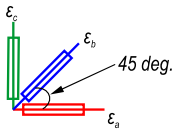

Figure 63 – 0-45-90 degree rosette used for bridge test

Four web gages (R1, R2, R5 and R7) were chosen corresponding to soffit gages S1, S2, S5 and S7 for the purpose of comparison. Rosettes R1, R2 and R5 were located in lane one while R7 was located in lane two. Plots of shear strain versus truck position were created using GPS data and calculated shear strains. Shear strains were calculated for selected rosettes using the Mohr's circle formula given in Equation 1.

$$\gamma_{xy} = 2 * \varepsilon_b - (\varepsilon_a + \varepsilon_c) \qquad \text{Equation 1}$$

The combined GPS and shear strain data were used to create shear strain influence lines (Figure 64). GPS coordinate data were transformed so that each reading reflected the north-south distance from the strain gage of interest to axle P5 on the test truck; this is shown on the x-axis. Axle P5 was selected as the reference axle because the strain was generally at a maximum at this location. The y-axis represents shear strain calculated from the uniaxial strain data from the strain gage rosette.

Influence lines were created for rosettes R1, R2, R5 and R7 as shown in Figure 64. In this figure, the four plots correspond to the four load levels used during the bridge test. Strains used in the figures for R1, R2, and R5 were taken from when the truck was in TP1 while those used in the figure for R7 was taken from when the truck was in TP5.

In conjunction with flexural strain peaking, shear strain changed sign as the tire passed over the rosette (Figure 65). As the tire traveled toward the rosette, the right leading corner (relative to the direction of travel) of the tire passed over the gaged web first (Figure 66a), causing most of the tire load to be transferred to the web on the right side of the rosette (Figure 66b). As the tire passed overhead of the rosette, the shear strain changed sign signifying the location of the peak moment. As the tire traveled past the rosette, the left trailing corner of the tire loaded the web on the left side of the rosette (Figure 66c and d). It is likely that torsional rotation of the web contributed to the sign change as well.

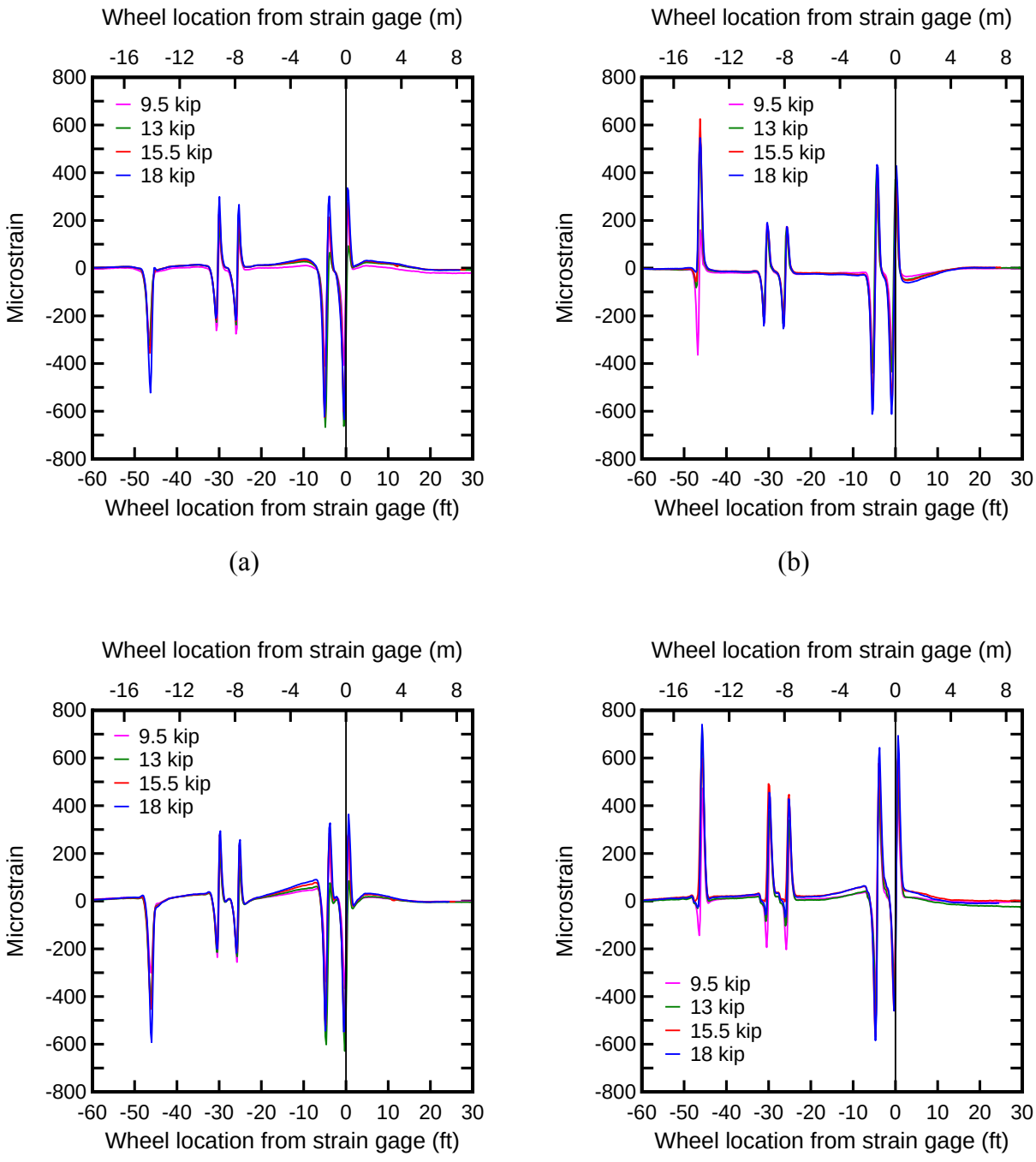

Figure 64 – Influence lines for rosette (a) R1 (b) R2 (c) R5 (d) R7

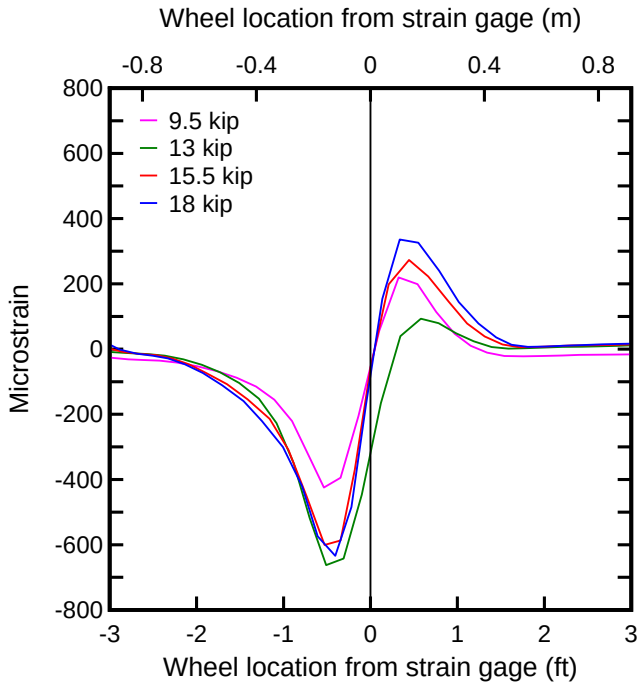

Figure 65 – Partial influence lines for web gage R1 at axle P5

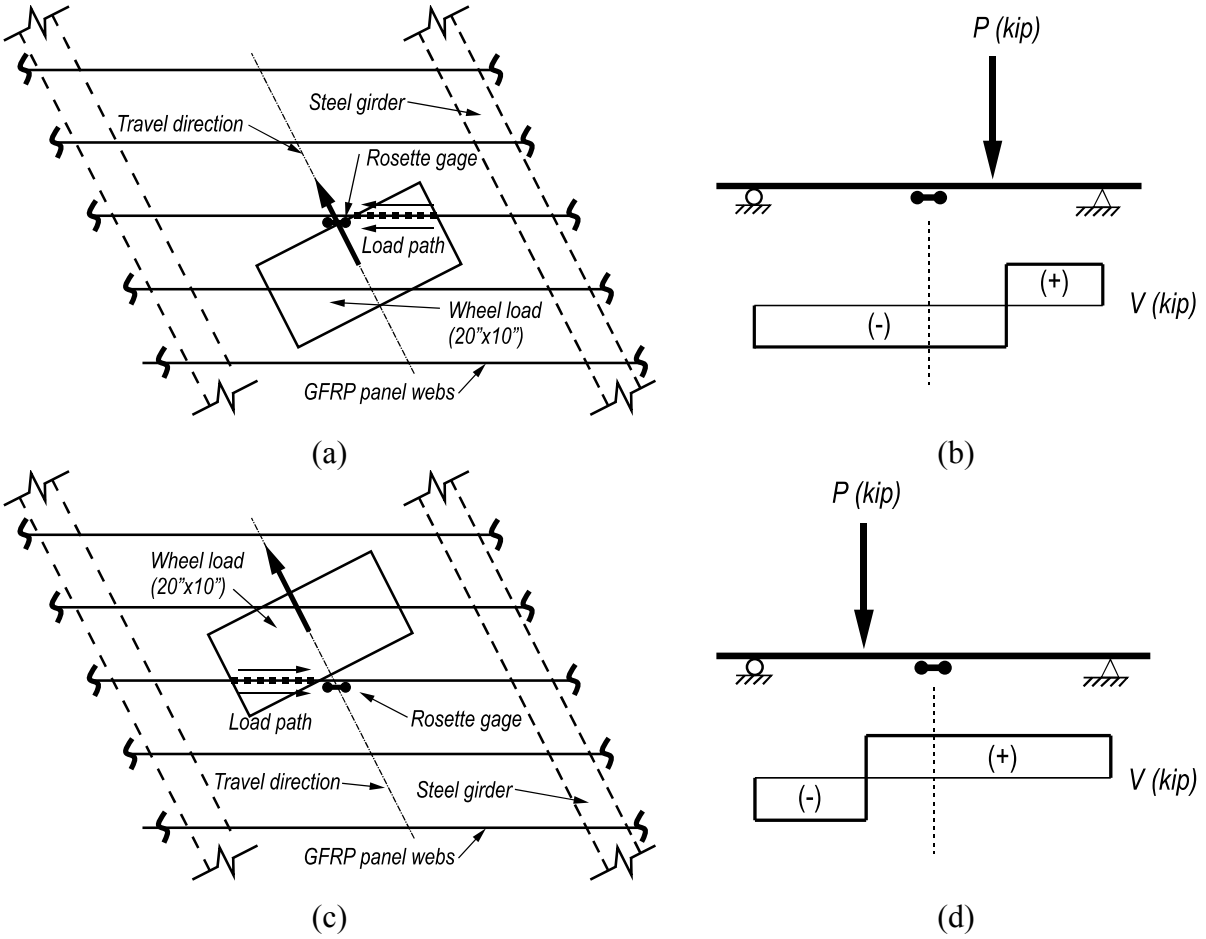

Figure 66 – Effect of wheel position on sign of shear strain (a) wheel position causing negative strain (b) shear diagram before wheel crosses gage (c) change in wheel position causing change is strain sign (d) shear diagram after wheel crosses gage.

9.1.3 Steel Girders

Steel girders were instrumented by full bridge strain (FBS) gages to evaluate the performance of the existing steel superstructure. This instrumentation was used for both of the bridge tests and long-term monitoring. Additional steel girder strain data were recorded with foil gages during the 2010 bridge test. Strain data from these gages combined with GPS data were used to create steel girder flexural strain influence line plots that are presented in this section.

All steel girder gages were located at the girder mid-span and were installed on the top surface (rather than the bottom surface) of the bottom flange to protect them from vandalism. Strains measured at the top of the bottom flange were thought to be adequate because the primary focus of this study was the performance of the GFRP deck and the steel strain readings were used for relative comparison. Additionally the steel girders were assumed to have

negligible composite action with the GFRP deck. This simplification allows direct comparison of steel strains among girders since a precise analysis of composite behavior between the GFRP deck and steel girders is impossible. Figure 67 illustrates the placement of the BDI gages and the relationship between the measured strain and the maximum strain.

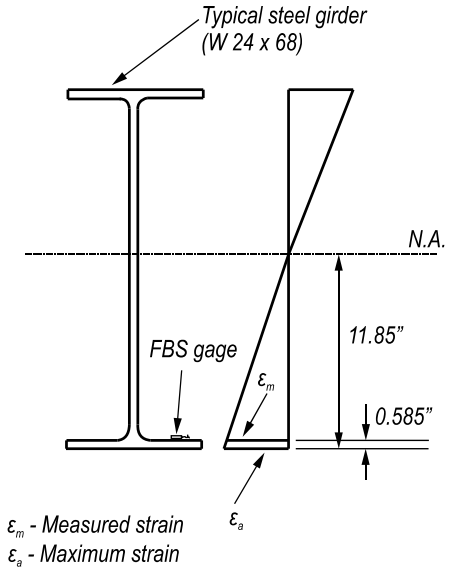

Figure 67 – Strain in bottom of steel girder

Influence lines were constructed similar to those constructed for the deck. GPS coordinate data were transformed so that each reading reflected the north-south distance from the full bridge gage of interest to axle P5 on the test truck. Axle P5 was selected as the reference axle because the strain was generally at a maximum at this location. Negative x values indicate that P5 was south of the gage and positive values indicate that P5 was north of the gage. The truck traveled from south to north during loading. Figure 68 through Figure 69 show the resulting influence lines. The four plots in each graph correspond to one of the four load levels (19 kip, 26 kip, 31 kip, and 36 kip) used during the bridge test.

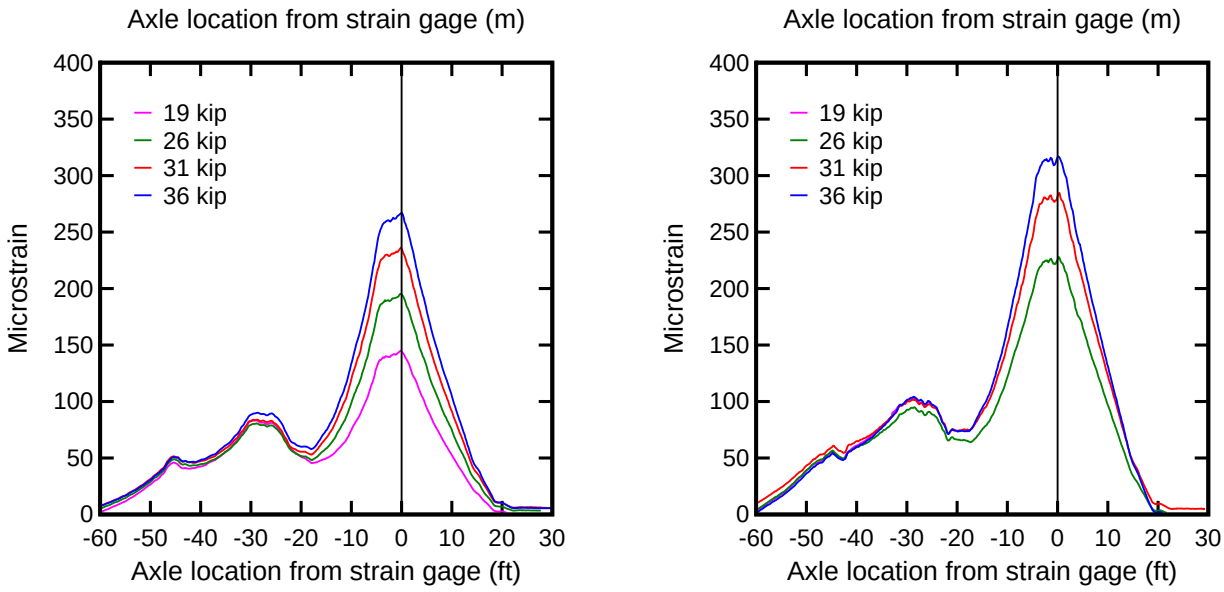

Figure 68 – Influence lines for B1 (TP2) for (a) 2009 (b) 2010

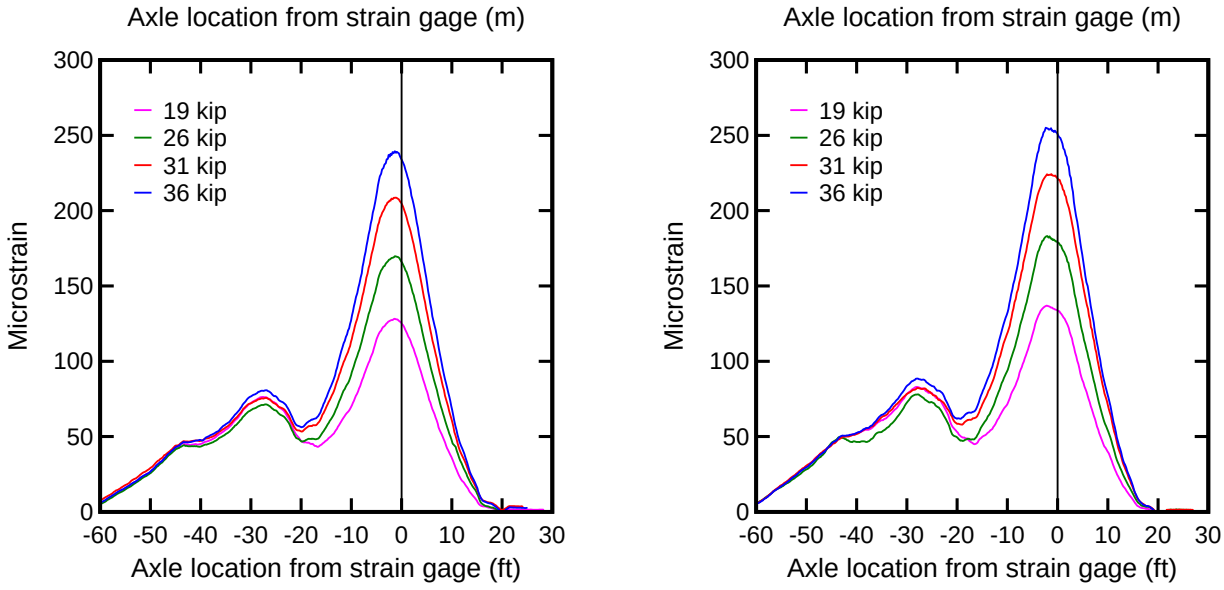

Figure 69 – Influence lines for B2 (TP3) for (a) 2009 (b) 2010

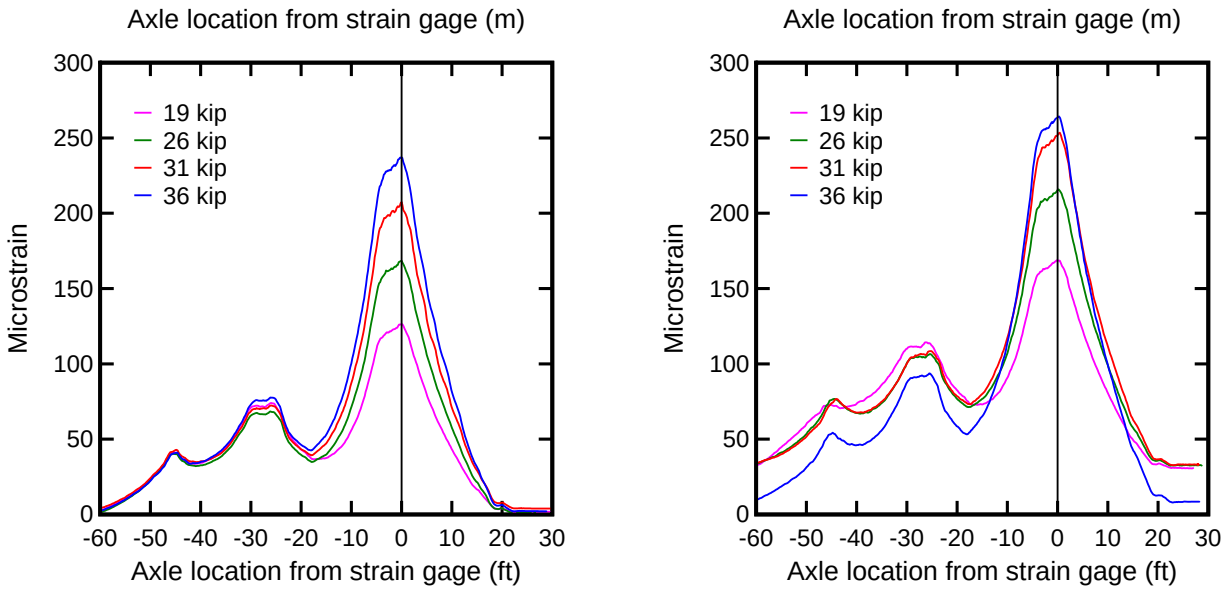

Figure 70 – Influence lines for B3 (TP4) for (a) 2009 (b) 2010

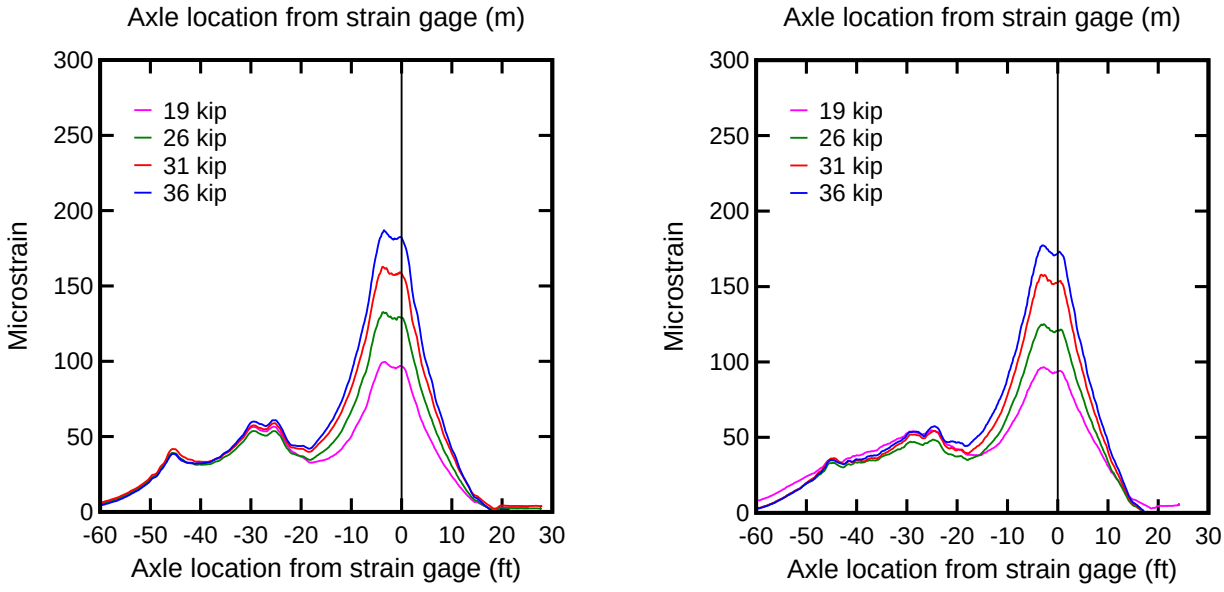

Figure 71 – Influence lines for B4 (TP5) for (a) 2009 (b) 2010

9.2 Distribution Factors

9.2.1 Deck Soffit

Distribution factors for the webs of the GFRP deck panels were calculated using soffit gage strain influence lines. Truck positions were chosen to maximize strains in the soffit gages in these influence lines. The soffit gages were located at the extreme bottom fiber of the GFRP deck panels directly underneath the panel webs, recording the maximum flexural strain experienced by the panel.

Influence lines for gages S1, S2, S3, S5, S7, and S8 are presented in Figure 46 through Figure 55. In these figures there are four plots corresponding to the four load levels used during the 2009 and 2010 bridge tests. For the distribution factor calculations, only the plots corresponding to the maximum load level (wheel load of 18 kip) were used. Influence lines were corrected for the shift between the peak and the zero location (gage location), ensuring that each peak aligns with zero. These corrected influence lines are plotted in Figure 72 through Figure 77. In each case, the influence line was analyzed from zero to 135 in., which encompassed 16 webs including the web at the gage location. This distance was chosen since strain drops to 5% of its peak value once the wheel load is 16 webs away from the instrumented web. Although the webs of the GFRP deck were 8 in. apart, a 9 in. distance between the webs was considered for calculating distribution factors due to the skew of the bridge. A mirror image of the influence line was created on the negative side of the x-axis on the assumption that the same influence line continues on both sides of the gage. This was done to filter out the significant influence that the adjacent axle (P4) had on the rear axle (P5). For example, the influence line in Figure 46 was used to create the corrected distribution factor shown in Figure 72. Distribution functions were not formulated for the front axle because they were less consistent. For example, the maximum strain caused by the front axle occurred under 9 kip of truck load in 2009 but occurred under 18 kip in 2010 at gage S7 (Figure 54).

Figure 78 shows the relationship between a typical influence line and the web locations within the instrumented panels. Distribution factors of the instrumented web above each soffit gage were obtained by dividing the value of strain at this web by the sum of strains at the webs on the either side of the instrumented web and the strain at the instrumented web. These strains were obtained from the influence lines. Fifteen webs were considered on either side of the instrumented web for this purpose. Strain dropped to less than 5% of its peak value once the

wheel load was fifteen webs away from the instrumented web. Table 9 presents the distribution factors calculated for wheel loads in lanes one (S1, S2, and S5) and two (S3, S7, and S8). The average wheel load distribution factor was 0.24 for both the 2009 and 2010 tests. This suggests that the panels did not become less stiff during the time between the 2009 and 2010 bridge tests. A loss in panel stiffness would probably lead to an increase in the distribution factor because load would be distributed less evenly between the instrumented web and nearby webs. The coefficient of variation was 0.12 for both the 2009 and 2010 tests, indicating that the precision of the measurements was consistent.

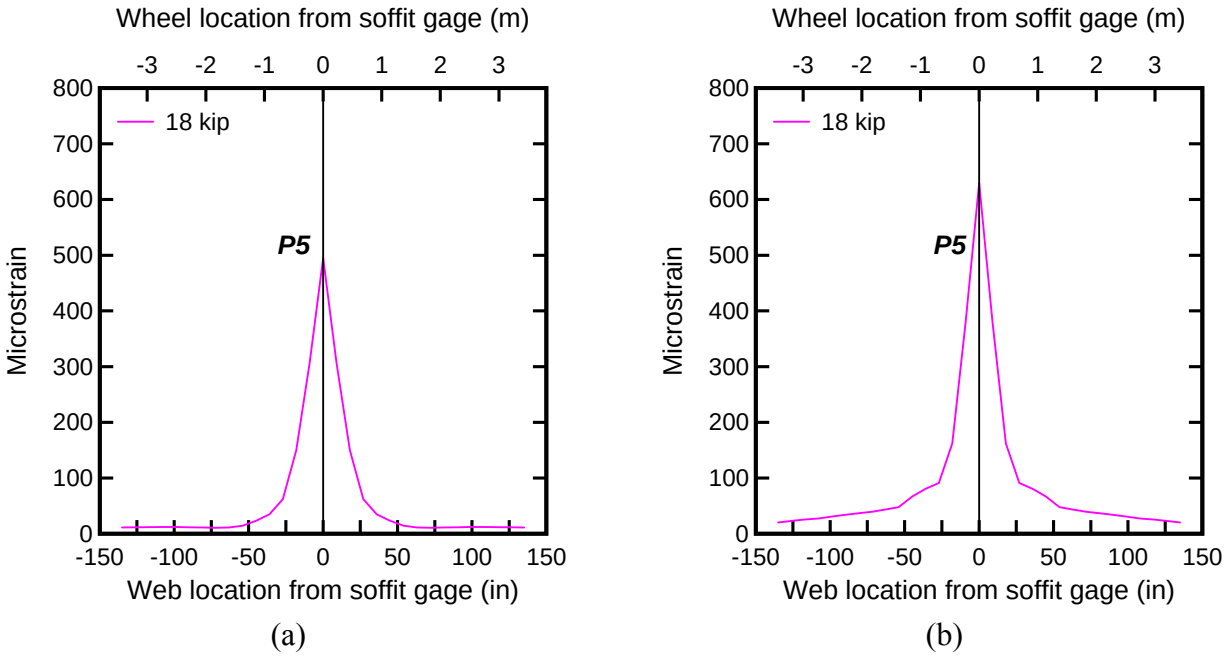

Figure 72 – Modified S1 influence lines used in distribution factor calculations for (a) 2009 (b) 2010

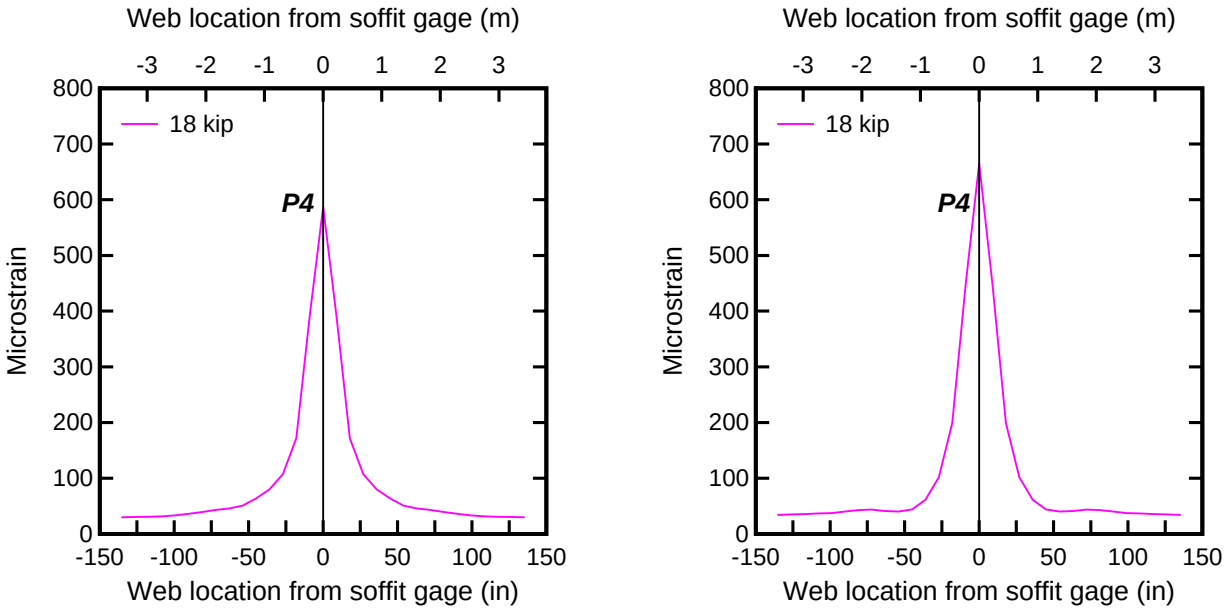

Figure 73 – Modified S2 influence lines used in distribution factor calculations for (a) 2009 (b) 2010

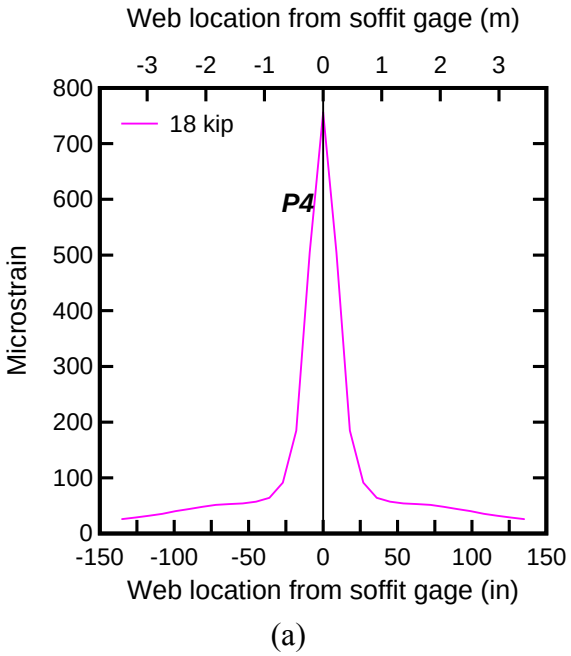

Figure 74 – Modified S3 influence lines used in distribution factor calculations for (a) 2010

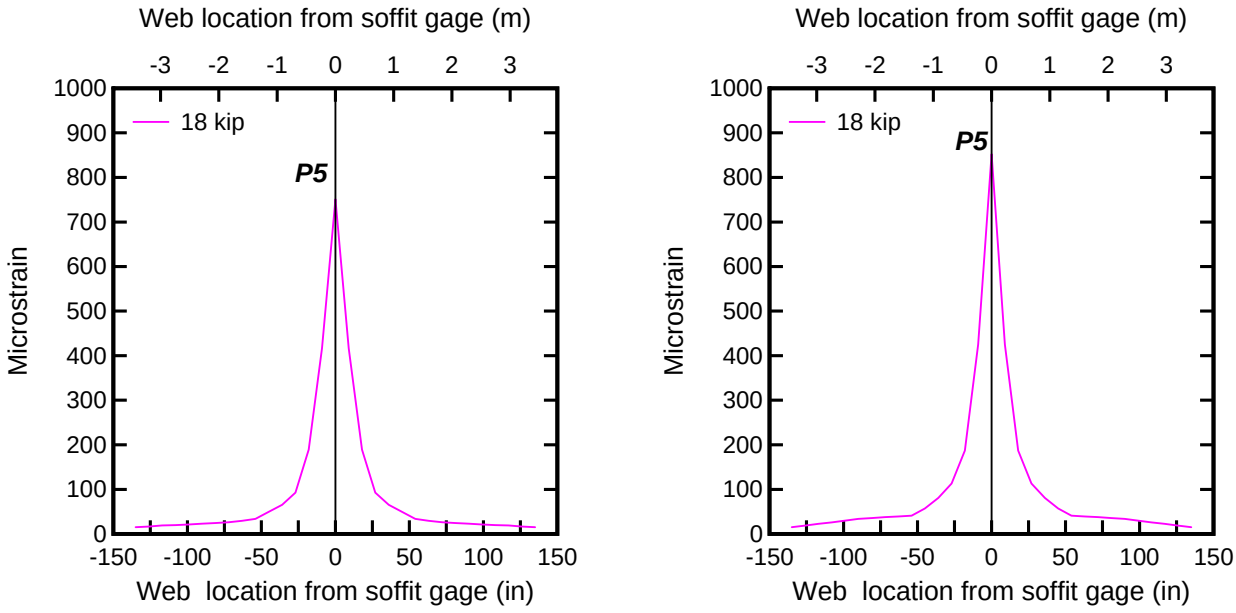

Figure 75 – Modified S5 influence lines used in distribution factor calculations for (a) 2009 (b) 2010

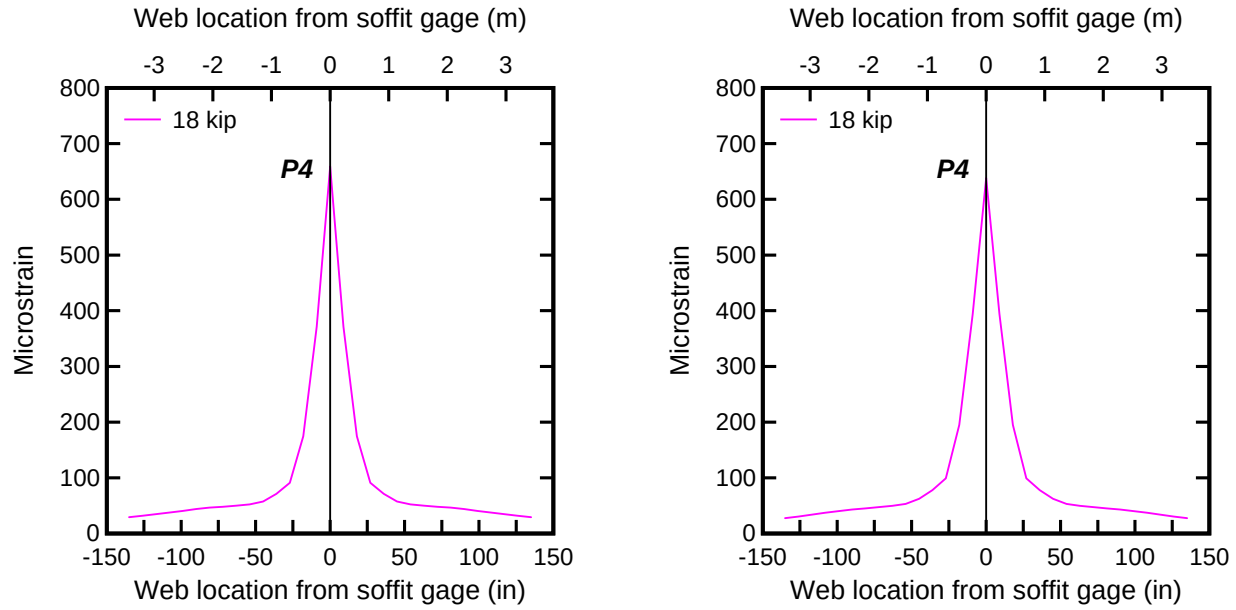

Figure 76 – Modified S7 influence lines used in distribution factor calculations for (a) 2009 (b) 2010

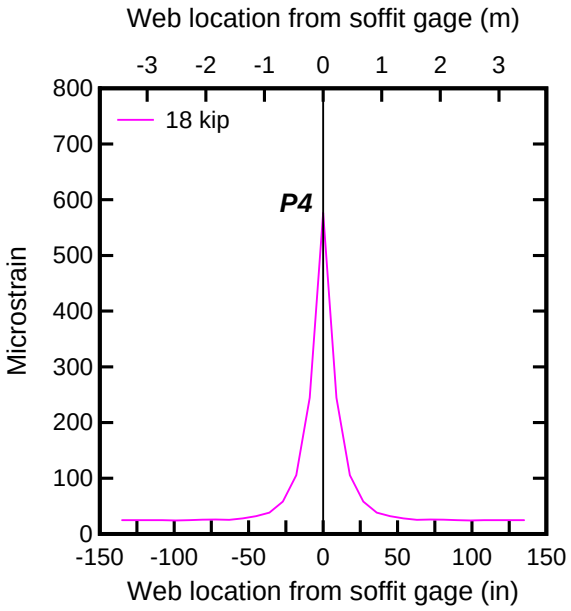

(a)

Figure 77 – Modified S8 influence lines used in distribution factor calculations for (a) 2010

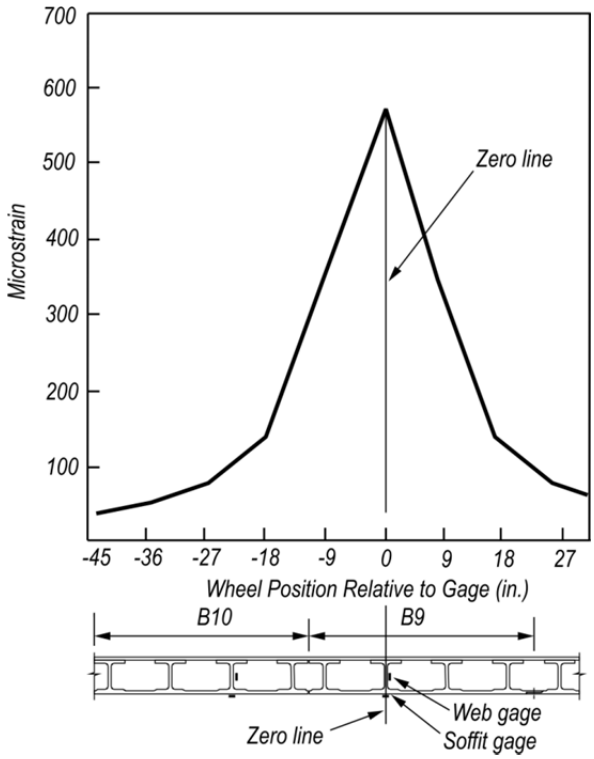

Figure 78 – Typical influence line illustrating calculation of distribution factor

Table 9 – Wheel distribution factors from soffit gages

Strain gage	Distribution Factor (2009)	Distribution Factor (2010)
S1	0.26	0.22
S2	0.20	0.21
S3	NA	0.22
S5	0.27	0.27
S7	0.22	0.21
S8	NA	0.28

9.2.2 Deck Webs

Distribution factors were also calculated using web strain gage data from the 2009 bridge test. Distribution factors were based on the shear strains calculated from the measured strains in the rosette gages on the web. Distribution factors at the maximum load level (18 kip wheel load) were determined in a manner similar to the soffit influence lines. Once corrected, the influence lines were plotted in Figure 79 and used for determining distribution factors. Distribution factors of the instrumented webs were obtained by dividing the value of strain at this web and the sum of strains at the webs on the either side of the instrumented web and the strain at the instrumented web. These strains were obtained from the influence lines. Three webs were considered on either side of the instrumented web for this purpose. Strain dropped to less than 2% of its peak value once the wheel load was three webs away from the instrumented web. Table 10 presents the distribution factors calculated for the wheel loads in lane one (R1, R2, and R5) and lane two (R7). The average wheel distribution factor was 0.38 with a coefficient of variation of about 14 percent.

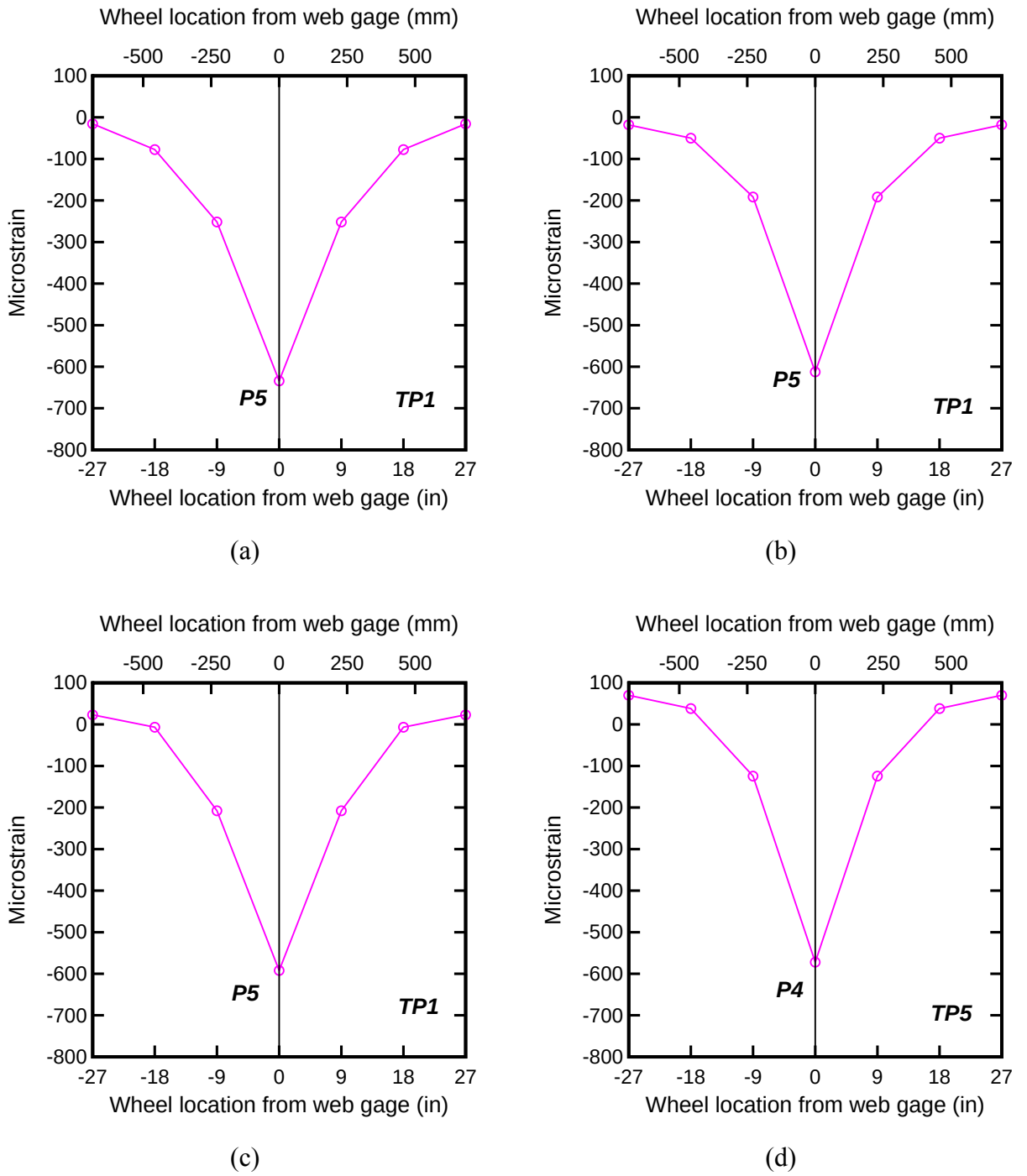

Figure 79 – Modified influence lines for distribution factor calculations for 18 kip of wheel load for (a) R1 (b) R2 (c) R5 (d) R7

Table 10 – Wheel distribution factors from web gages

Web gages	Distribution Factor
R1	0.33
R2	0.35
R5	0.37
R7	0.46

9.3 Deck Displacement

The load vs. displacement (Figure 80) for the GFRP deck was plotted for the deflection gage (D1), which was located in lane two. It can be observed from the load displacement plots that significant deflection was produced in TP5 only. This reaffirms that load effects upon the GFRP deck are local as indicated by the sharp peaks of the GFRP panel flexural influence line plots (Figure 46 through Figure 55) and distribution factors determined from the bridge tests (Table 10). The maximum relative deflection produced during the bridge test was 0.09 in. for an 18 kip load. This maximum deflection occurred during the 2009 test. Deflection measured by D1 decreased from 0.09 in. to 0.06 in. between the 2009 and 2010 tests. The cause of this decrease is unknown; the apparent increase in measured stiffness is also contrary to other visual evidence and strain data. The load – displacement plot is linear indicating that the GFRP deck material never goes into non-linear range of its material behavior. Similar linear behavior was also observed from the load – strain calibration curve.

AASHTO Section 2.5.2.6.2 specifies a service limit for deflection as span/800 for steel, aluminum, and or concrete, which is 0.06 in. for the deck span of 4 ft. Maximum deflection measured during the 2009 bridge test was 50% more than the service limit, but equal to the service limit in the 2010 bridge test measurements.

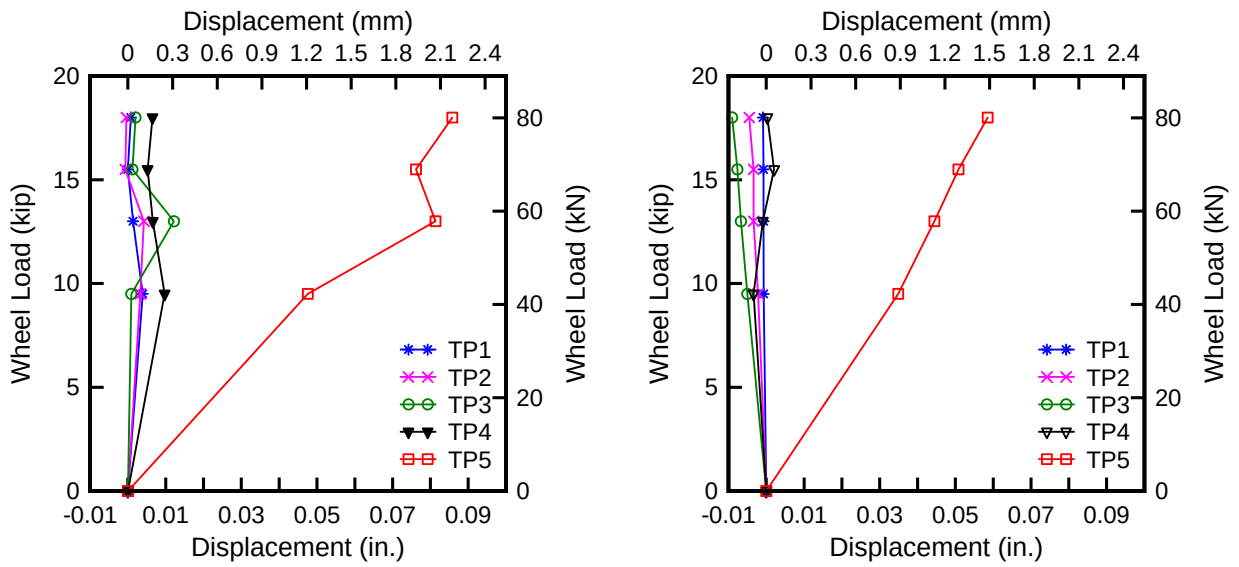

Figure 80 – Load – displacement for the bridge deck from (a) 2009 (b) 2010

During the 2009 bridge test, relative deflections of the steel girders in adjacent frames were also measured and are presented in Figure 81 and Figure 82 as displacement – time history plots for gages D2 and D3 under the maximum wheel load (18 kip) used during the test. Downward displacement is shown as positive. Gages D2 and D3 were located at the mid-span of the bridge, each installed on the outer girders of adjacent frames. D2 was located in lane two and D3 in lane one. As indicated by Figure 81, when the truck was in lane one, a maximum relative deflection of 0.03 in was recorded at D3 and a small relative deflection of 0.007 in. was recorded at D2. Figure 82 indicates that the situation is reversed when the truck is in lane two, with D2 indicating a relative deflection of 0.05 in. and D3 indicating a relative deflection of 0.003 in. A maximum relative deflection of 0.03 in. for TP1 and 0.05 in. for TP5 was recorded. The maximum relative deflection of the steel girders was about half (55 %) of the maximum GFRP deflection recorded for the 18 kip wheel load. This indicates that the girder frames have a much higher stiffness than the GFRP deck.

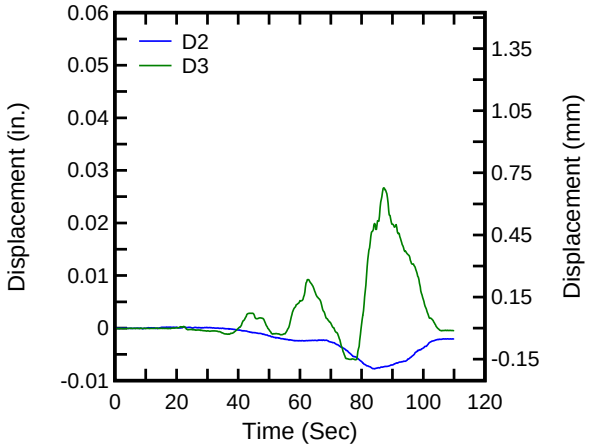

Figure 81 – Displacement time history of steel girders at TP1

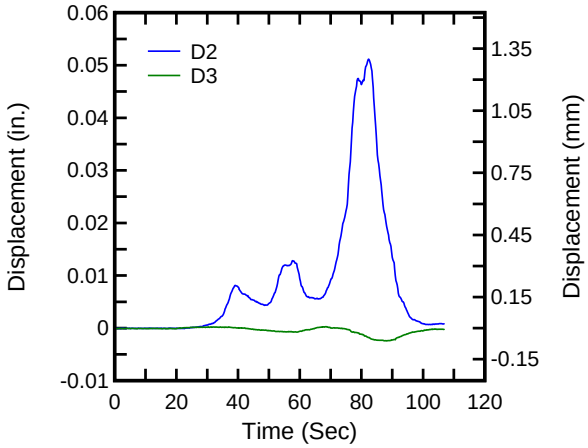

Figure 82 – Displacement time history of steel girders at TP5

9.4 Truck Course Deviation

Five truck paths (TP1 through TP5) were used for the bridge tests. While the paths were intended to be parallel to the curb, rolling the truck over the bridge with no transverse deviation was not possible. Consequently, this transverse deviation of the truck from its intended path was investigated using the GPS position data to determine how much difference in strain readings might be expected to occur between the 2009 and 2010 bridge tests. Influence lines for the maximum load case of the 2009 and 2010 bridge tests are presented in Figure 83 for gages S5 and S7. In addition, the truck path deviation is plotted; this deviation was determined using the GPS position data from both the 2009 and 2010 bridge tests. For comparison purposes, truck paths recorded during the 2009 bridge test are considered the reference paths. The plot shows the truck path deviation, which is the deviation of the 2010 truck paths from the 2009 reference paths. Positive deviation indicates that the truck passed closer to the gage of interest in 2010 than in 2009, leading to the possibility that any increase in strain could be an artifact of the truck position and not indicative of a loss of stiffness.

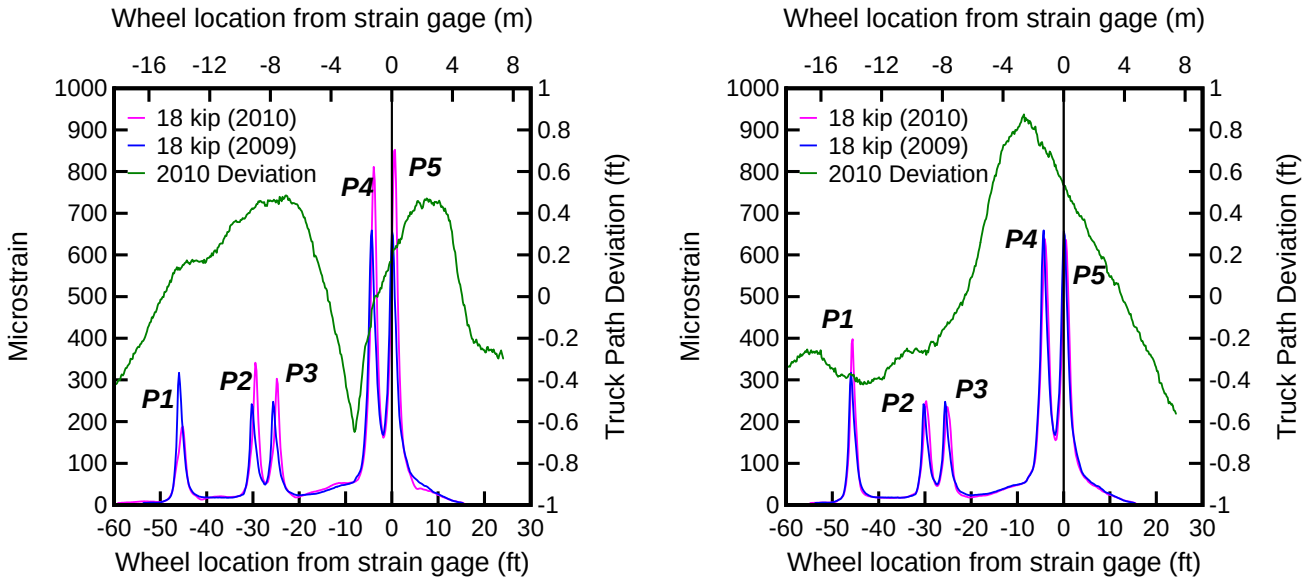

Figure 83 – Influence line and truck deviation for (a) gage S5 and (b) gage S7

Figure 83a shows that P5 was closer to the correct position in 2010 by about 2 in. than it was in 2009 when crossing strain gage S5. P1, P2, and P3 also show an increase in strain and up to a 5 in. increase in deviation between tests. P4, however, was in almost the same position relative to S5 for both tests (less than 1 in. difference), yet showed an increase of almost 100 με between 2009 and 2010. This indicates that the change in strain from 2009 to 2010 is not the result of truck path deviation.

Figure 83b also supports the conclusion that the truck positioning is not a significant factor in strain readings. P1 was farther away from S7 in 2010 than in 2009, yet the gage recorded an increase in strain. P2 and P3 show no significant strain changes despite the patches being as much as 3 in. farther away in 2010 than 2009. P4 and P5 also show no significant increase in strain despite the tire patches passing over S7 at least 6 in. farther away in 2010 than 2009. This indicates that the two influence lines (2009 and 2010) are nearly identical since no bridge component was likely to have gained stiffness between the two tests. The magnitude of transverse deviation had no discernible effect on the recorded strain. Consequently, the transverse position of the truck relative to the bridge centerline is much less important than the longitudinal position along the right-of-way for influencing the strain in the GFRP panels. This is logical since the tire patch of the test truck was 2-ft wide. With such a wide area to distribute

load, the tire patch crossed over the soffit strain gage of interest even if the truck deviated by a foot from the path that was designed to take the center of the tire patch over the soffit gage. In addition to the tire patch size, the span along the right-of-way is 9 in. while the transverse span is about 4 ft. The longer span would be less sensitive to truck positioning since the ratio of deviation to span would be less, thus producing less difference in recorded strain.

10 Deck Composite Behavior

One goal of this project was to determine the extent to which the top plate and bottom panels of the GFRP deck behave as a composite element. Composite action between top plate and bottom panel was calculated by comparing the measured and calculated elastic neutral axes. Each calculated neutral axis was determined using a transformed section having a single modulus of elasticity. This was accomplished by transforming the various moduli of elasticity of different parts of the sections into one section having a single modulus of elasticity by multiplying appropriate modular ratio (Ratio of moduli of elasticity). Figure 84 shows the elastic modulus map used for the calculation of the transformed section properties. The modulus map was provided by the deck manufacturer.

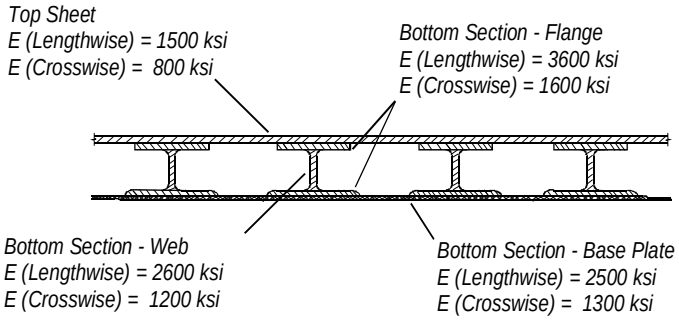

Figure 84 – GFRP deck Modulus map

Three different neutral axes position were calculated; one including the top plate, a second ignoring the top plate, and a third ignoring the top plate and assuming a uniform modulus of elasticity throughout the bottom section. To determine the measured neutral axis position, the soffit gage and corresponding rosette data were utilized. The zero degree strain gage from the 0-45-90 rosettes was used for this purpose; this gage was aligned with the axis of the web and thus in the same direction as the soffit gages.

Soffit gages S1, S2, S5, S7 and corresponding rosettes R1, R2, R5 and R7 were analyzed. Soffit gages S1, S2, S5 and rosettes R1, R2 and R5 were located in lane one and gave the largest output for TP1 (Figure 37). TP5 (Figure 41) activated soffit gage S7 and rosette R7. For the plots in Figure 85, rosette strain was obtained at the same time that the corresponding soffit strain was peaking. For the plots in Figure 86, the soffit strain was obtained at the same time that the corresponding rosette was at a minimum. In each of these two plot types, the strain was

plotted as a function of the depth of the section. The neutral axis of the section is located at the depth where flexural strains are zero, which is indicated by a reference line placed at zero strain. Figure 85 and Figure 86 present the measured neutral axis plotted for the four selected soffit gages and rosettes.

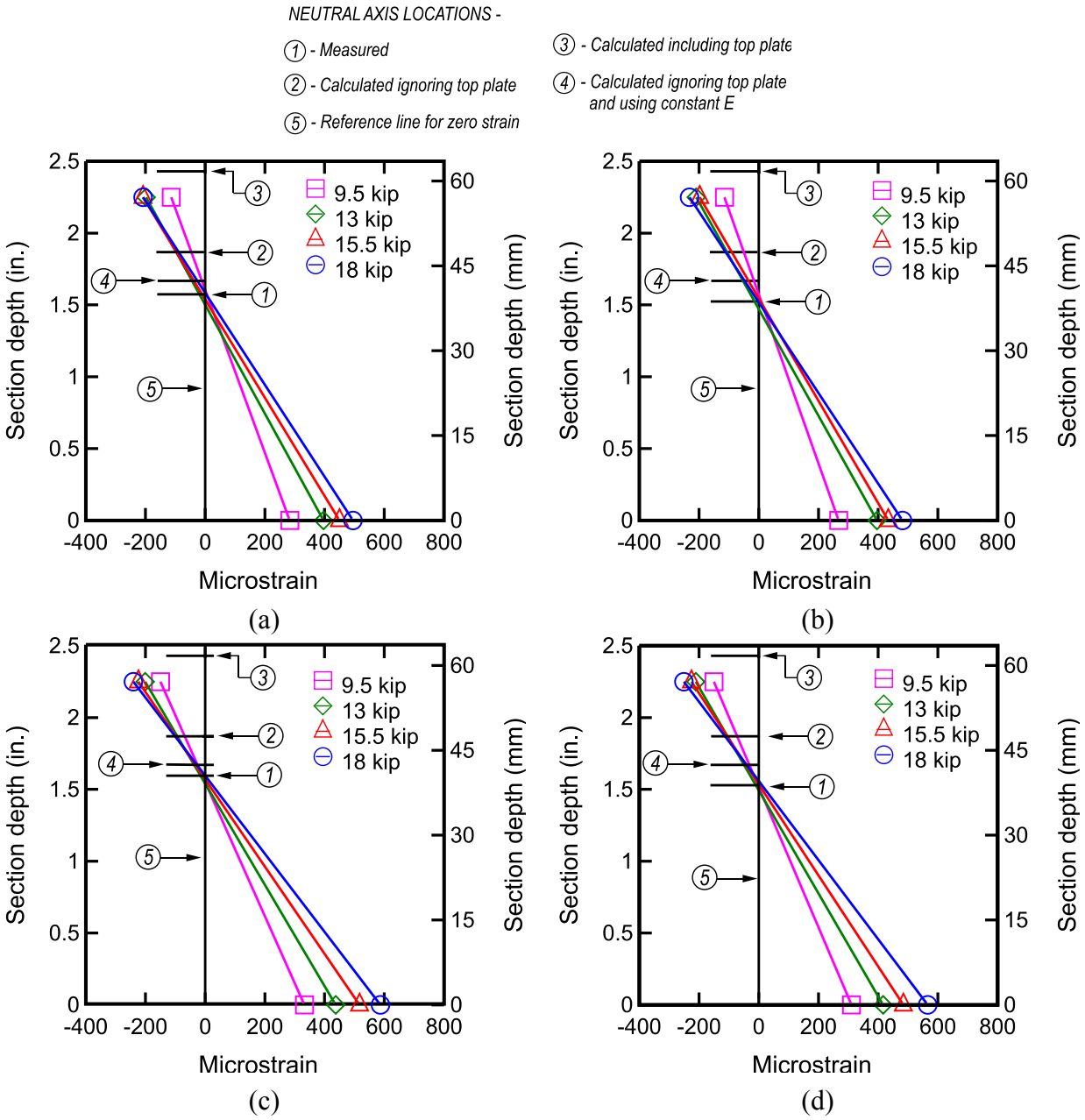

Figure 85 – Composite behavior (2009) demonstrated by (a) Maximum strain in S1 and corresponding strain in R1 (b) Minimum strain in R1 and corresponding strain in S1 (c) Maximum strain in S2 and corresponding strain in R2 (d) Minimum strain in R2 and corresponding strain in S2

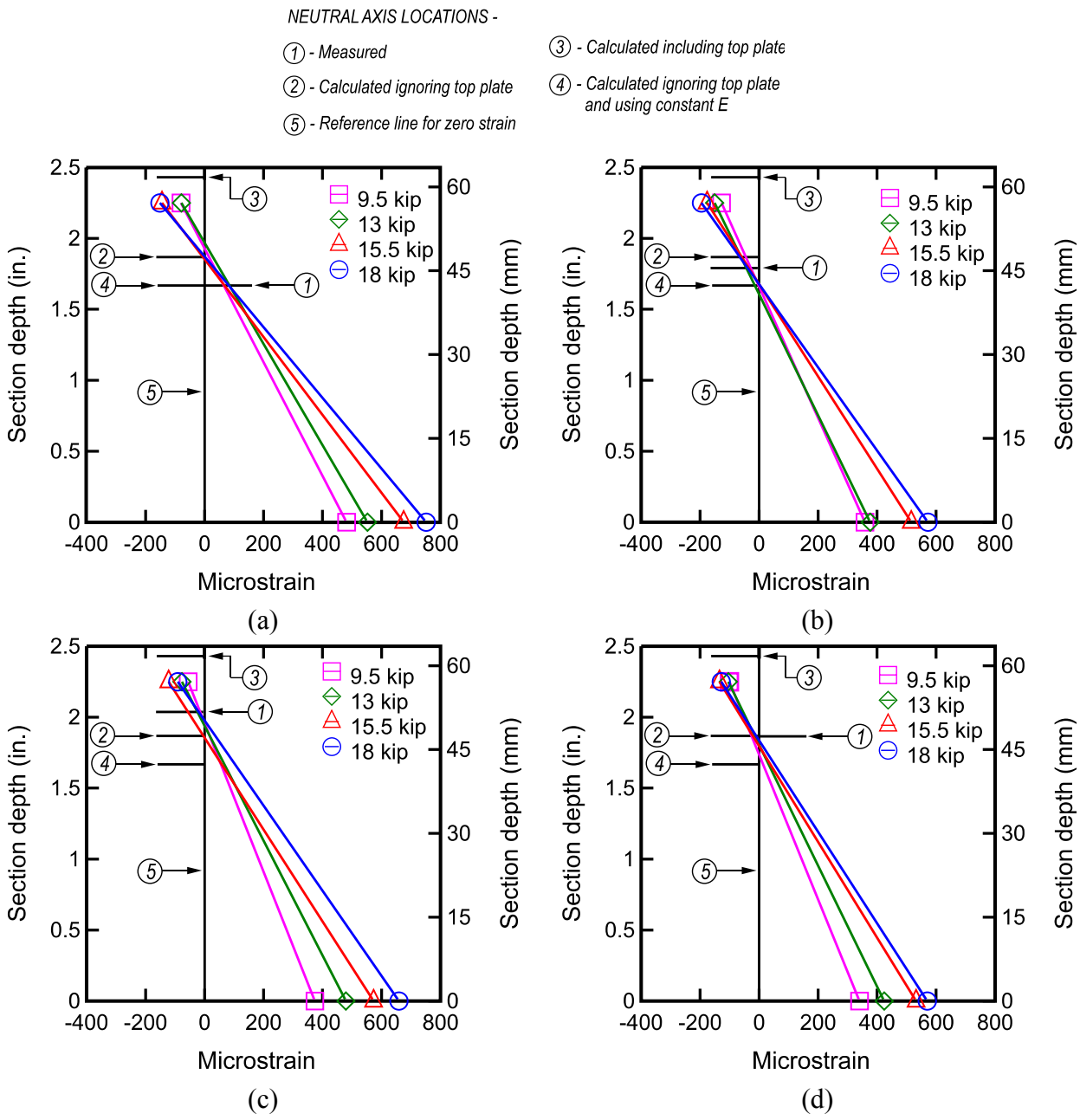

Figure 86 – Composite behavior (2009) demonstrated by (a) Maximum strain in S5 and corresponding strain in R5 (b) Minimum strain in R5 and corresponding strain in S5 (c) Maximum strain in S7 and corresponding strain in R7 (d) Minimum strain in R7 and corresponding strain in S7

Figure 85 and Figure 86 show that the location of the measured neutral axis remained at nearly the same location for all four load levels. The consistent nature of these plots indicates that for all the load levels tested the GFRP deck material behavior remained in the linear-elastic range. Figure 87 indicates that the measured neutral axis was consistently located 0.7 in. below

the calculated neutral axis for the entire section with top plate but was located close (0.2 in.) to the calculated neutral axis ignoring the top plate. The measured neutral axis aligns with the calculated neutral axis for the section without the top plate and with a uniform elastic modulus throughout the section.

Figure 87 presents a summary of the measured neutral axes plotted for selected gages. The average of the neutral axes was calculated for all four gages and plotted in this figure. The figure shows that the measured neutral axis coincides with the calculated neutral axis for the section ignoring the top plate and assuming a constant elastic modulus throughout the section. Therefore, it is concluded that the contribution of top plate in the flexural response of the deck is insignificant.

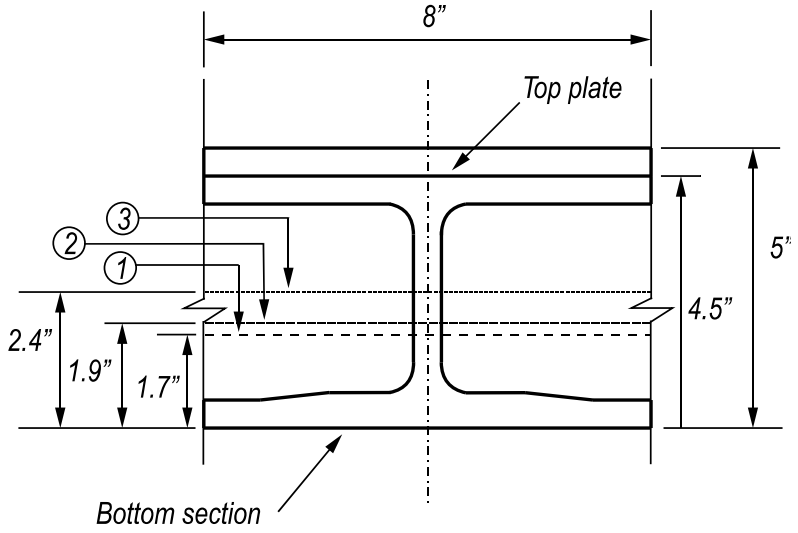

LEGEND

1 - Average of measured N.A. location and N.A. ignoring top plate, constant E

2 - Ignoring top plate

3- Including top plate

Figure 87 – Location of measured and calculated elastic N.A.

11 Comparison of 2009 and 2010 Results

11.1 Deck Soffit Strains

The GFRP deck displayed evidence of a reduction in stiffness during the time between the bridge tests conducted in October 2009 and October 2010. This reduction was much more pronounced in lane one, presumably because heavily loaded trucks usually travel in the far right lane. Both the soffit and steel girder gages showed this pattern. It is suspected that the increase in strain in the GFRP panels was due to the increase in the panel effective span caused by the loss of the grout underlayment observed prior to the 2010 bridge test (Figure 88). A total loss in grout underlayment increases the effective span from 45 in. to 53 in. From basic mechanics, this would lead to an increase in strain of 38% over the original strain. Even if the span increase was only 4 in., the strain increase would be 17%. Another possible reason for the increase in strain in the GFRP panels is a reduction in stiffness of the grout pocket-shear stud connection at the steel girders. Although visually unconfirmed, grout degradation similar to that noted above would increase flexibility at the support, which would result higher strains by allowing more rotation of the GFRP panels to occur.

Table 11 shows a comparison of key strain data from the two bridge tests. Maximum strain measured by gage S1 (Figure 46) increased by 27% from 495 με to 630 με. Measured strains for gages S2 (Figure 47) and S5 (Figure 51) also increased about 13%. These three gages measure strains in lane one (Figure 24). Gage S7 (Figure 54) measured strain in lane two and indicated that there was no appreciable change in deck stiffness.

Table 11 – Maximum strains recorded by soffit gages during 2009 and 2010 bridge tests

Instrumentation	2009 strain (με)	2010 strain (με)	Difference (με)	Ratio 2010/2009
S1	495.1	629.8	134.8	1.27
S2	587.1	665.3	78.2	1.13
S3	NA	771.2	NA	NA
S5	751.2	852.5	101.3	1.13
S7	658.8	638.3	-20.6	0.97
S8	NA	574.2	NA	NA

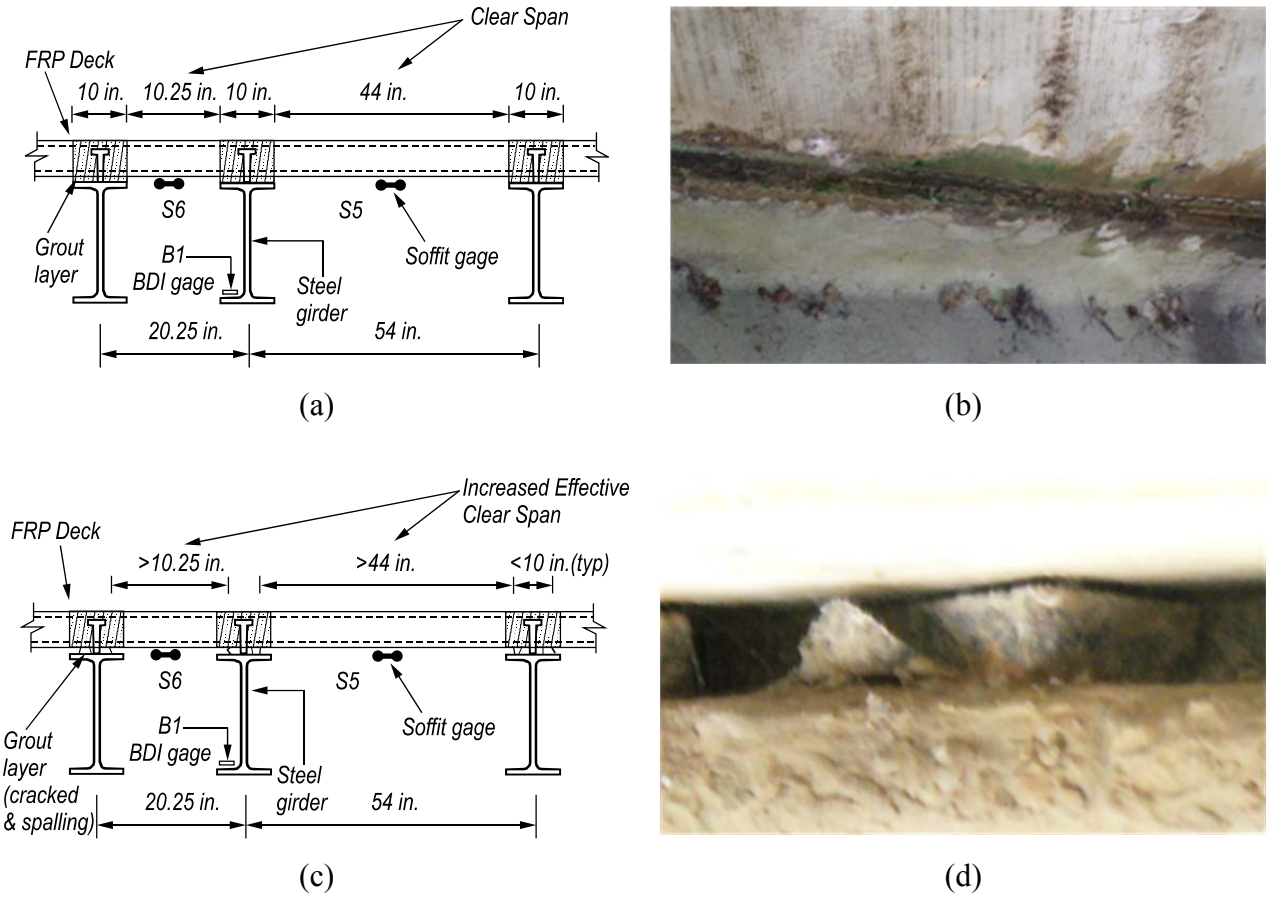

Figure 88 – Sections of bridge superstructure showing (a) initial and (c) degraded grout conditions and pictures of (b) intact and (d) degraded grout

11.2 Deck Distribution Factors

The GFRP soffit gage distribution factor analysis indicates that the GFRP panels (not considering composite action) did not experience a loss of stiffness during the year separating the two bridge tests. From Table 9 it is apparent that the distribution factors for the deck panels did not change between the 2009 and 2010 bridge tests. The distribution factor average is unchanged in 2010 from 2009; both are 0.24. This suggests that the sensitivity of the GFRP panels to the proximity of concentrated loads was unchanged from one year to the next.

11.3 Steel Girders

Comparison of deck strain data from the two bridge tests indicated a general decrease in stiffness in lane one but not in lane two, which is attributed to the cracked and loose grout observed during the 2010 bridge test (Figure 88). Although composite action between GFRP deck panels and steel girders is typically discounted, the grout pad and pockets undoubtedly

contributed some to composite behavior. Consequently, the grout cracking may impair the girder-deck composite action, which would be evident in the strain data. The steel girder strain data from the 2009 and 2010 bridge tests were examined to determine if these differences were notable.

Table 12 compares the maximum strains recorded by the strain gages mounted to the steel girders during the 2009 and 2010 bridge tests. Gages B1 through B3 show a decrease in stiffness (strain increase) while B4 shows a slight increase. B1 was mounted on a girder in the outermost frame and is located near the center of lane one (Figure 20); an increase in strain of 19% was measured. B2 and B3 were mounted to girders in the adjacent frame and carried traffic in both lanes one and two. The decrease in stiffness was not as large for B2 and B3, with an increase in strain of approximately 7% and 12%, respectively. This frame would have only supported about half of the load of trucks in lane one, explaining the lower loss of composite behavior relative to that of the outer frame (location of B1). Gage B4 was in a frame located under the turning lane (lane 3). This frame carried only partial loads from lane two; no notable change in strain was observed.

Table 12 – Maximum girder strain measured during 2009 and 2010 bridge tests

Instrumentation	2009 (με)	2010 (με)	2010/2009	Gage position*
B1	267	317	1.19	Lane one – middle
B2	240	257	1.07	Lane one – left side
B3	237	264	1.12	Lane two – right side
B4	187	177	0.95	Lane two – left side

*See Figure 20 for exact location.

12 Bridge Test Results – 35 mph Truck

The 35 mph bridge test was conducted without GPS monitoring of the truck position. In addition, it was not possible for the truck to follow any of the designated truck positions precisely. Consequently, the driver was instructed to travel through each lane in a normal manner at 35 mph without attempting to follow the designated truck positions.

Figure 89 compares the 35 mph and rolling test results for steel girder gages B1 and B3. Although the truck position was not tracked during the 35 mph test, the relative truck speeds were used to coordinate the truck position for comparative plotting. The figure shows that the high speed bridge test produced a strain pattern that was similar to that produced by the rolling bridge test. Strain peak locations were consistent between the two tests, with the magnitude of the strains at the peaks higher in the 35 mph test than the rolling test.

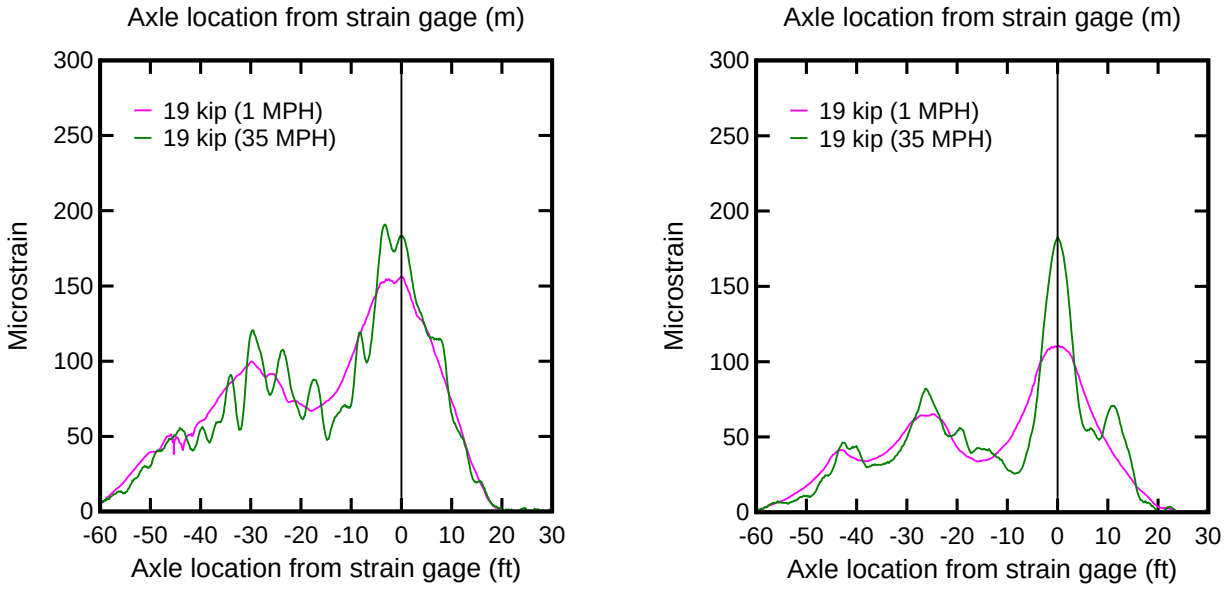

Figure 89 – Comparison of rolling and high speed bridge test data for (a) B1 (b) B3

Figure 89b also indicates that the truck dynamically excited the bridge as it crossed as indicated by the periodic shape of the strain curve. This was likely caused by the flexibility of the GFRP deck in combination with the stiff truck suspension. As the truck wheels traveled across the deck spanning from one girder to the next, the flexing of the deck caused the wheel to impact the opposite girder. Resonance may have developed in both the truck and the bridge

because the truck, maintaining a constant speed, drove over the GFRP panel webs at uniform intervals.

Figure 90a is a comparison of the 35 mph test in TP5 to the rolling test in TP5 for gage S3. This figure shows a phenomenon observed during the 35 mph test; the rear axle of each tandem axle caused less strain than the front axle. For example, during the rolling test, axles P4 and P5 produce nearly identical strain readings, as do P2 and P3. During the high speed test, axle P4 produces a higher strain than P5 while P2 produces a higher strain than P3. This is caused by rear axle not completely loading the GFRP panel between the panel webs. The wheels in the front axle of each tandem would launch upwards off the GFRP panel webs, reducing the weight applied at the strain gage by the tires of the rear axle of each tandem.

Figure 90b is a comparison of the 35 mph test in TP1 to the rolling test in TP1 for gage S5. This figure shows that the strain influence lines recorded at gage S5 were much lower for the 35 mph test than for the rolling test. Truck position 1 was designed so that the truck wheel patches would pass directly over strain gage S5. A proper lane alignment during this test would have resulted in higher strains recorded during the high speed test than the rolling test. An example of proper alignment is presented in Figure 90a, which indicates that the high speed test conducted in lane two (TP5) followed the intended path since gage S3 recorded a higher strain during the high speed test than the rolling test. The low magnitude of strain recorded by S5 during the high speed test indicates that the S5 strain gage was not optimally placed to record traffic in lane one. Gages S1 and S2 also failed to produce large strain during the high speed test. The failure of the soffit gages to record lane one traffic effects during this test indicates that the gages failed to properly record traffic strains in lane one. This suggests an explanation for the data recorded by the soffit gages during the traffic monitoring. This data indicated that more truck loads occurred in lane two than lane one, which contradicts data from the steel girder gages and the load test data. The explanation for this discrepancy is that the soffit gages under lane one were not positioned to record traffic strains effectively.

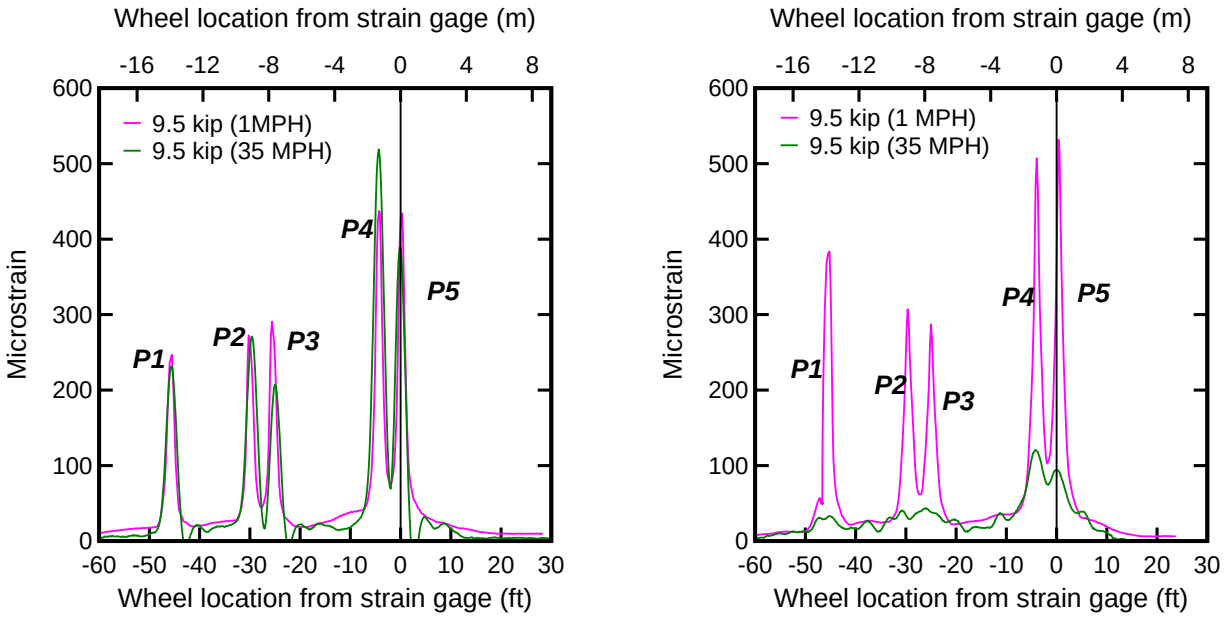

Figure 90 – Comparison of (a) strong strain gage response (gage S3) and (b) weak strain gage response (gage S5)

Table 13 and Table 14 summarize the results of the two 35 mph tests. Impact factors were calculated as the ratio of 35 mph strain to rolling test strain. Impact factors obtained from the gages mounted to the steel girders ranged from 1.11 to 1.44 for lane one and 1.08 to 1.29 for lane two. Impact factors obtained from the soffit gages ranged from 0.24 to 0.63 for lane one. Lane two had an impact factor of 1.15 as measured by the S3 gage.

Table 13 – Impact factors for lane one

Instrumentation	Impact Factors		
	TP 1	TP2	TP3
B1	1.22	1.11	1.44
S5	0.24	0.63	NA

Table 14 – Impact factors for lane two

Instrumentation	Impact Factors	
	TP4	TP5
B3	1.08	1.29
S3	NA	1.15

The impact factors, given in Table 13 and Table 14, are generally close to the AASHTO dynamic load allowances. The impact factors calculated from the steel girder strain data varied from 1.08 to 1.44. This compares with the 1.33 dynamic load allowance from AASHTO for limit states other than fatigue and fracture. Impact factors calculated from the GFRP deck strain data were less consistent due to the difficulty of maintaining the proper lane of travel during this test. Impact factors varied between 0.24 and 0.63.

13 DAQ System Calibration

For the 2010 bridge test, the FDOT DAQ used strain gages that were mounted adjacent to the gages used by the FDOT DAQ during the 2009 test. This was because the gages used in the 2009 test had been connected to the cRIO DAQ for long-term data collection and were not used during the 2010 bridge test except for calibration. Because the FDOT DAQ and cRIO DAQ were both recording data during the 2010 bridge tests, it was possible to compare the results from each machine. This verified that comparing the strains recorded by the FDOT DAQ in 2009 to strains recorded by the FDOT DAQ in 2010 was acceptable despite using different strain gages.

Figure 91 and Table 15 compare the maximum strains obtained by both the FDOT DAQ and cRIO DAQ for each of the positive-moment soffit strain gages. The differences between the two DAQ measurements are small, less than 10%. Gage S5, which showed the largest increase in strain between the 2009 and 2010 tests (Figure 51), had less than a 1% difference between the two DAQ devices.

Table 16 shows the comparison between the maximum strains recorded by the FDOT DAQ and the cRIO DAQ for the strain gages mounted to the steel girders. The cRIO DAQ was recording strain through the BDI full bridge strain gages while the FDOT DAQ was recording strain with bonded foil gages mounted adjacent to the BDI gages. The strains indicated by the two DAQ systems were similar, with a maximum difference of 6%.

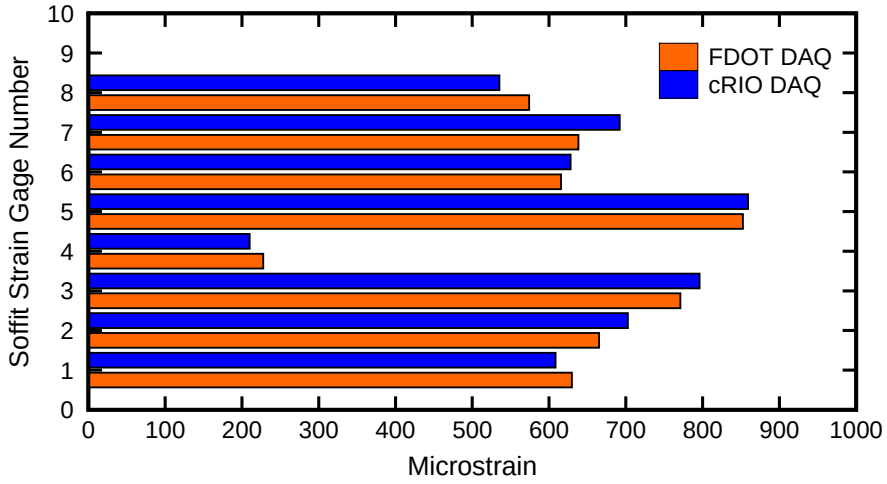

Figure 91 – Comparison of maximum strains recorded at soffit strain gages for 18 kip truck load

Table 15 – Maximum GFRP deck strains for 18 kip truck load

Instrumentation	FDOT DAQ (με)	cRIO DAQ (με)	Ratio cRIO/FDOT
S1	630	609	0.97
S2	665	703	1.06
S3	771	796	1.03
S5	853	859	1.01
S7	638	692	1.08
S8	574	535	0.93

Table 16 – Maximum steel girder strains for 18 kip truck load

Instrumentation	FDOT DAQ (με)	cRIO DAQ (με)	Ratio cRIO/FDOT
B2	255	266	1.04
B4	189	177	0.94

The BDI gage data recorded by the cRIO after the 2010 bridge test were adjusted using the correction factors shown in Table 17. BDI readings were adjusted to match the foil gage data recorded by the FDOT DAQ during the second load test. These factors were obtained by comparing the zero-corrected strain output for the cRIO-BDI and FDOT foil gages for 5 seconds before and after the instant axle P5 was over the gages.

Table 17 – Correction factors for BDI gages

Instrumentation	Correction Factor			
	19 kip	26 kip	31 kip	36 kip
B1	0.732	NA	0.733	0.732
B2	0.823	0.889	0.933	0.958
B3	0.847	0.814	0.793	0.702
B4	1.008	0.891	0.951	0.962

The soffit gage strains measured by the FDOT DAQ and cRIO DAQ were also compared to verify that the 5Hz sampling rate used for the rolling bridge tests was fast enough to capture peak strain in the GFRP deck soffit gages. The cRIO DAQ had a sampling rate of 200Hz, providing forty times as many data points as the FDOT DAQ, graphically illustrated in Figure 92. In Figure 92a, the strains at axle P4 as measured by the cRIO and FDOT DAQs for gage S5 are presented. Both strain gage/DAQ combinations indicate nearly identical strains at the peak. The FDOT DAQ plot has a two points near the peak, with only a slight cutoff at the cRIO peak. It is apparent that there could be no missing data points that would significantly change the peak

strain. Figure 92b also indicates that there were no missing data points that could change the peak strain. The two gage/DAQ combinations recorded slightly different strains (54 με difference from Table 15) but the smoothness of the FDOT DAQ influence line is apparent. There are no indications that a peak data point may have been missed. This confirms that the differences between the peaks measured by the FDOT and cRIO DAQs were not due to the lower sampling rate of the FDOT DAQ.

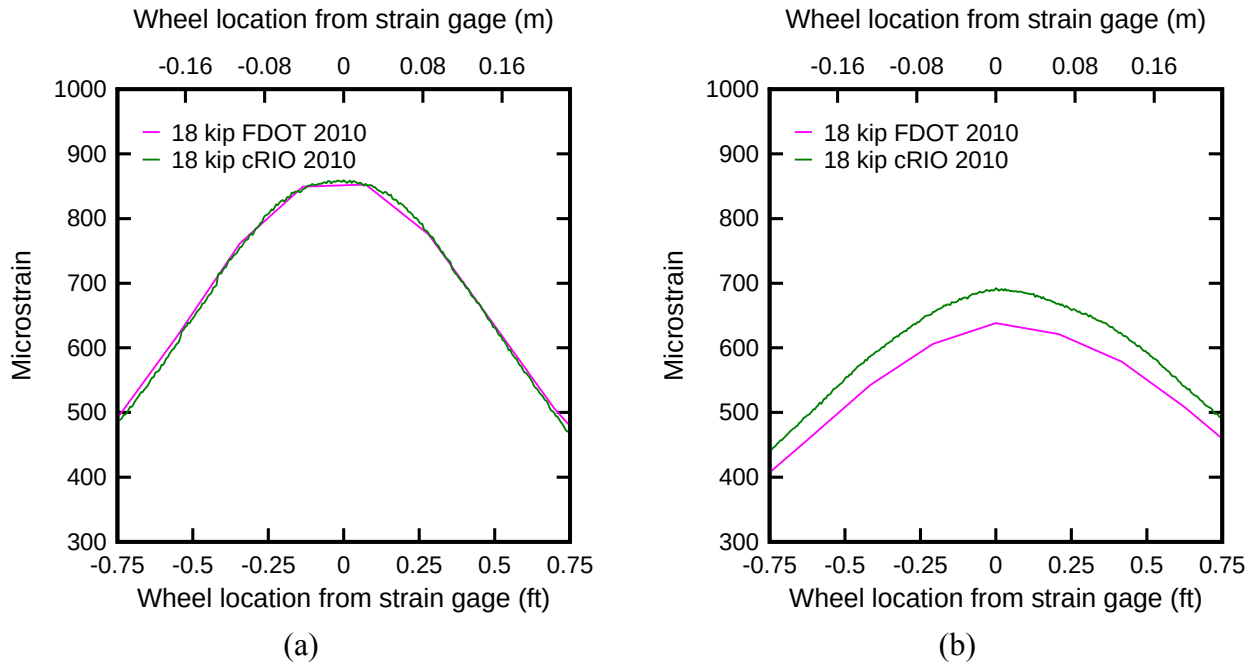

Figure 92 – Comparison of FDOT and cRIO peak strain measurements for (a) S5 (b) S7

14 Load Strain Calibration Curve

Strains generated in the GFRP deck and steel girders were plotted against the wheel load level used during the bridge test. These plots were the indicator of the local wheel load response of the GFRP deck. They also indicated that the behavior of both materials (GFRP and steel) remained in the linear-elastic range. The load – strain calibration curves were used to convert monitored strains into wheel loads. Wheel loads were used instead of axle loads for producing the GFRP deck load-strain calibration since the response of the deck panels to loading is so localized.

The values of strain at P5 from each load case were plotted against the corresponding wheel load to create the load – strain plots (Figure 93 through Figure 100) for the eight soffit gages (six from the 2009 test and eight from the 2010 test). Each graph has five plots for the five truck positions. Plots for each truck position have four points that corresponds to the four load levels used during the bridge test.

The localized behavior of the deck under the wheel load is confirmed by comparing the load – strain plots of different truck positions recorded by each soffit gage. One example of this was the variation in strain at S2 when the truck position changes from TP1 to TP5. The strain recorded for TP1 is nearly six times greater than that recorded for the other truck positions. Similarly, S7 recorded significantly higher strains for TP5 than for any of the other truck positions. A similar effect is present for all soffit gages.

The load – strain calibration curves remain linear for all load levels, indicating that during the test, the GFRP deck material remained elastic. Nonlinear behavior would have been indicative of plastic deformation and would have indicated that the bridge was sustaining damage during the load tests.

These load – strain curves were generated from the rolling load tests and were intended to be used to convert strains recorded during the monitoring period into wheel loads. A linear regression was produced for the plot of the truck position that produced the highest strain. This regression was not forced through the origin because the slope of the regression line (wheel load divided by microstrain) was the important aspect of the analysis. Multiplication of the regression slope by the strain recorded during monitoring yielded the wheel load. This method did not account for dynamic effects.

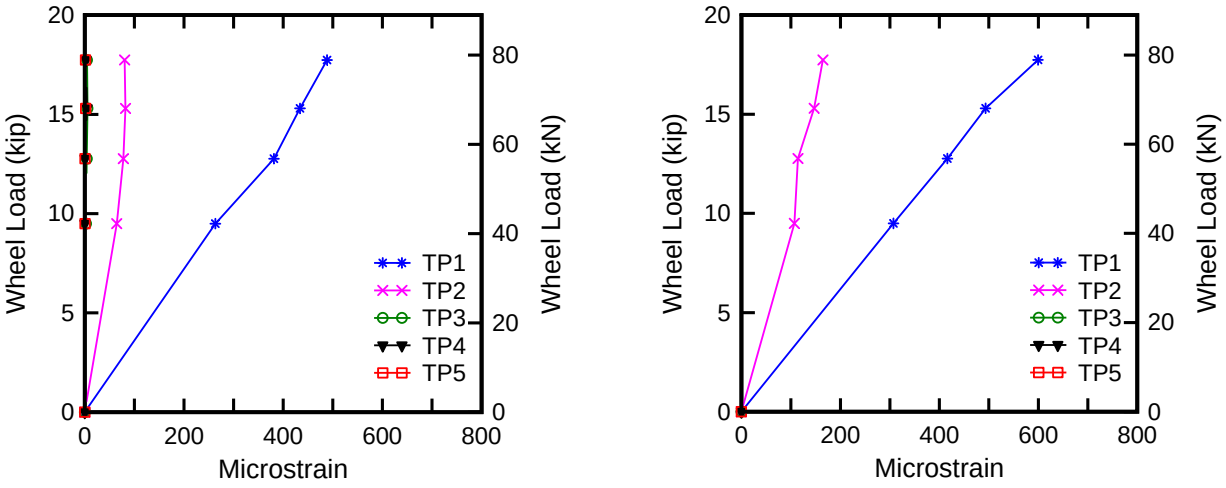

(a) (b)

Figure 93 – Gage S1 load-strain calibration curve for (a) 2009 (b) 2010

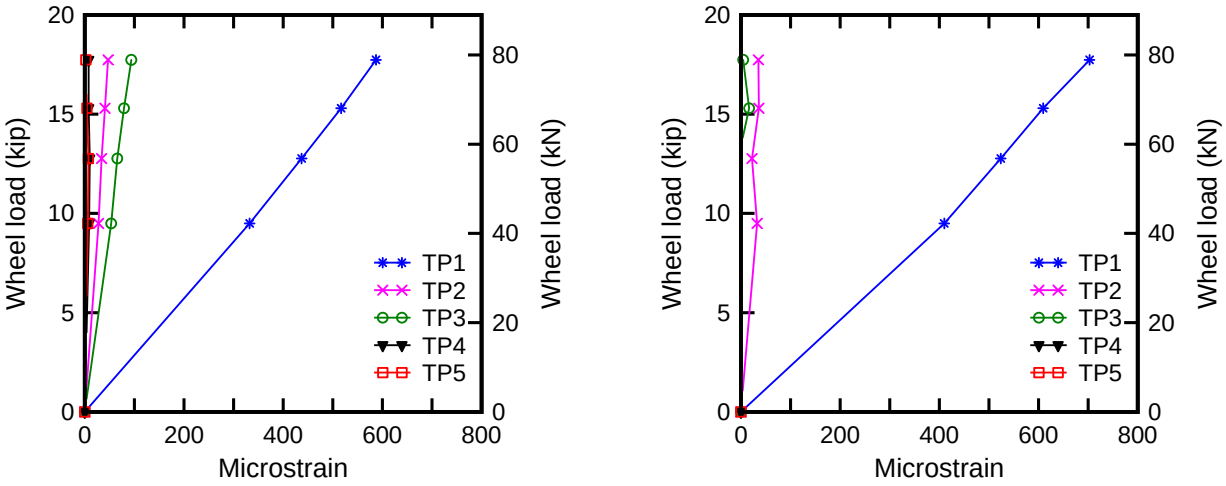

(a) (b)

Figure 94 – Gage S2 load-strain calibration curve for (a) 2009 (b) 2010

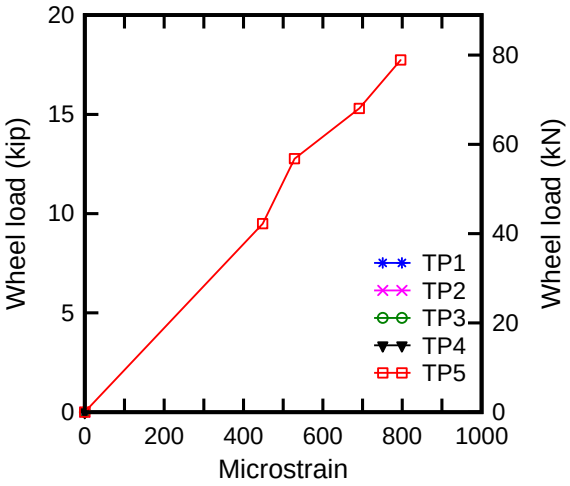

(a)

Figure 95 – Gage S3 load-strain calibration curve for (a) 2010

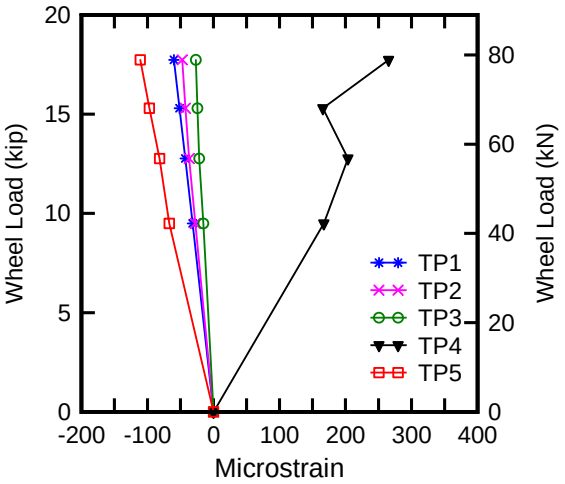

(a)

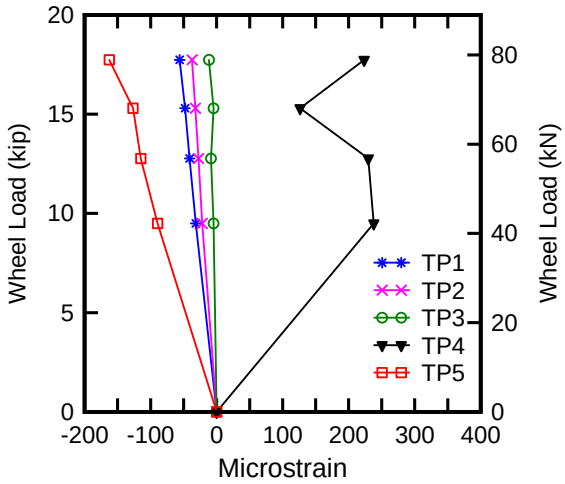

(b)

Figure 96 – Gage S4 load-strain calibration curve for (a) 2009 (b) 2010

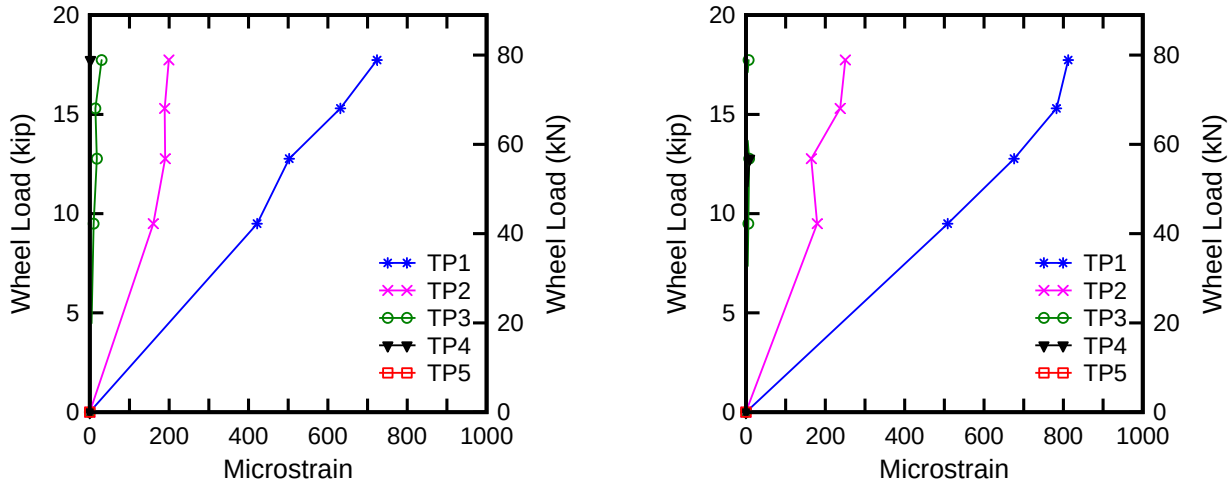

(a) (b)

Figure 97 – Gage S5 load-strain calibration curve for (a) 2009 (b) 2010

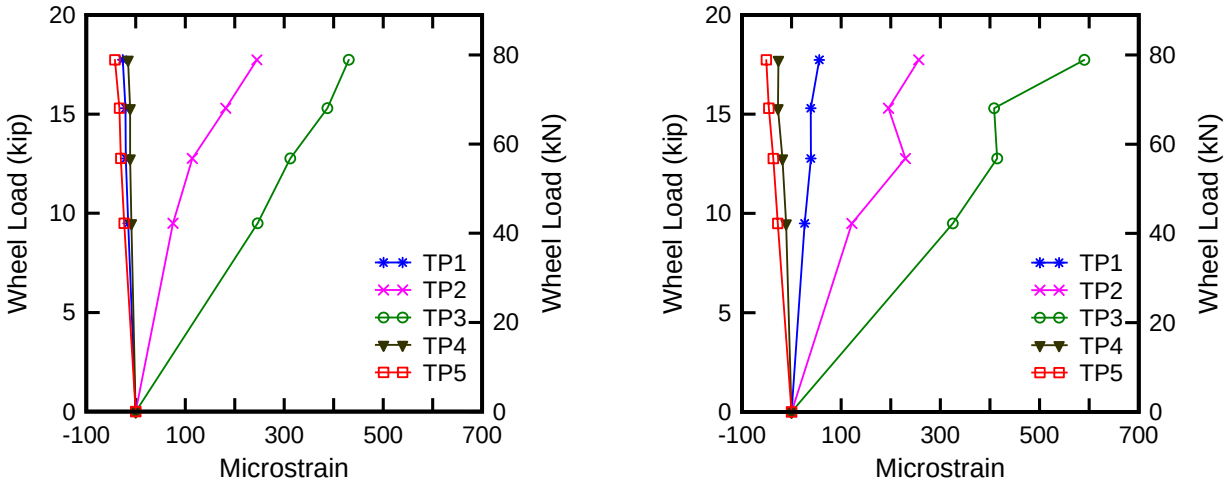

(a) (b)

Figure 98 – Gage S6 load-strain calibration curve for (a) 2009 (b) 2010

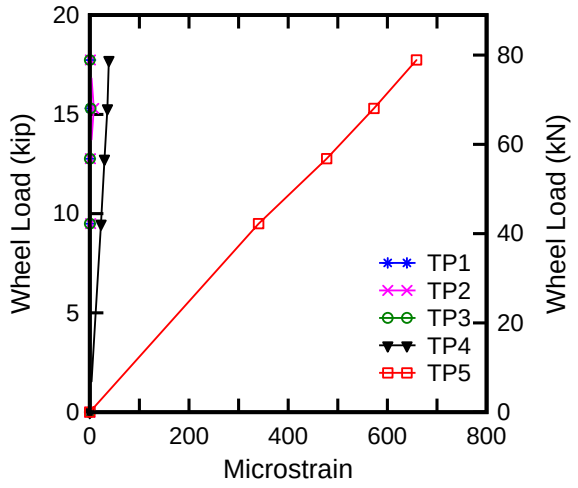

(a)

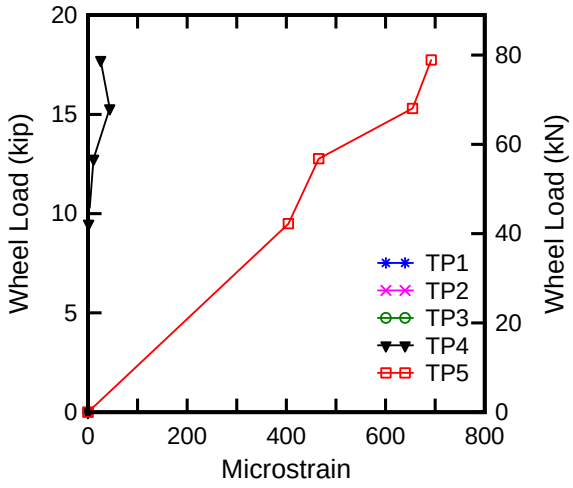

(b)

Figure 99 – Gage S7 load-strain calibration curve for (a) 2009 (b) 2010

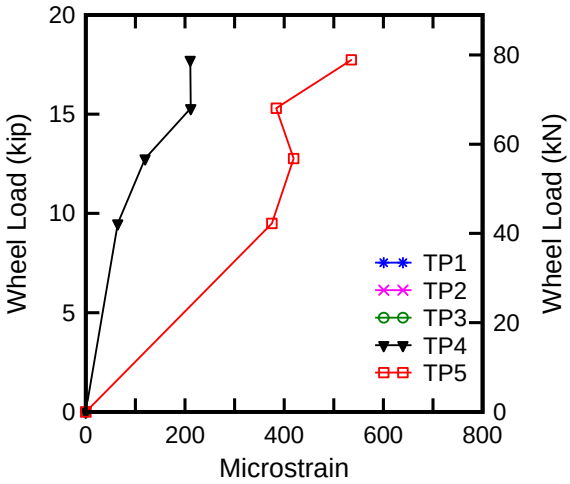

(a)

Figure 100 – Gage S8 load-strain calibration curve for (a) 2010

Figure 101 through Figure 104 show the load – strain plots for the gages installed on the steel girders. These plots were formulated similar to the soffit gage plots. The only differences were that the combined weight of axles P4 and P5 was used instead of wheel load on the y-axis and the strain on the x-axis was recorded at the top of the girder bottom flange and not the extreme tensile fiber. The influence lines (Figure 68 through Figure 71) indicate that the steel girders were not sensitive to individual wheel loads. Therefore the total weights of the two back axles P4 and P5 (Figure 36) were used instead of the wheel loads for the steel girder load – strain

plots. Maximum strain in the steel girder was produced when the two rear axles were at mid span. This occurred when the other axles were off the span supported by the steel girders. All plots remain linear at all load levels, indicating that the behavior of the steel in the girders remained linear-elastic.

From Figure 101, the maximum strain in the BDI gages was produced at gage B1 when truck is in the middle of lane one (TP2). Maximum strain was 320 με for 71 kip of the axle load (P4+P5), which occurred in the 2010 test.

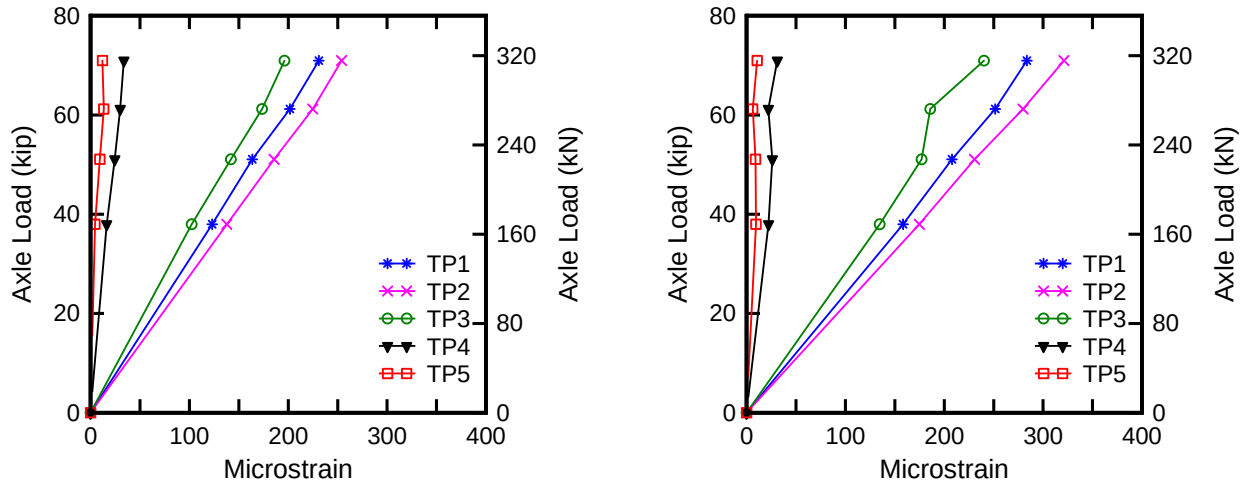

Figure 101 – Gage B1 load-strain calibration curve for (a) 2009 (b) 2010

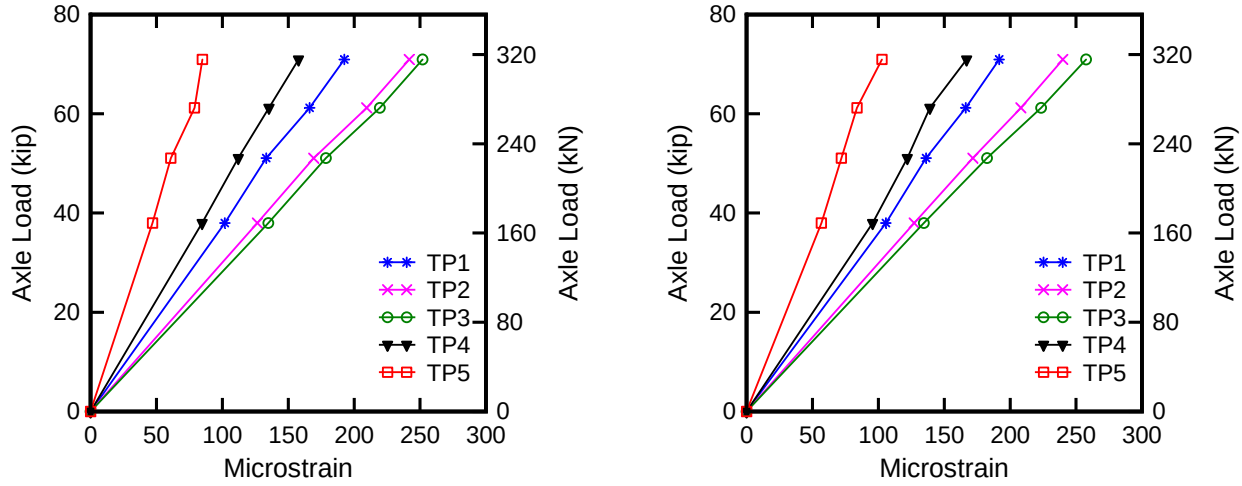

Figure 102 – Gage B2 load-strain calibration curve for (a) 2009 (b) 2010

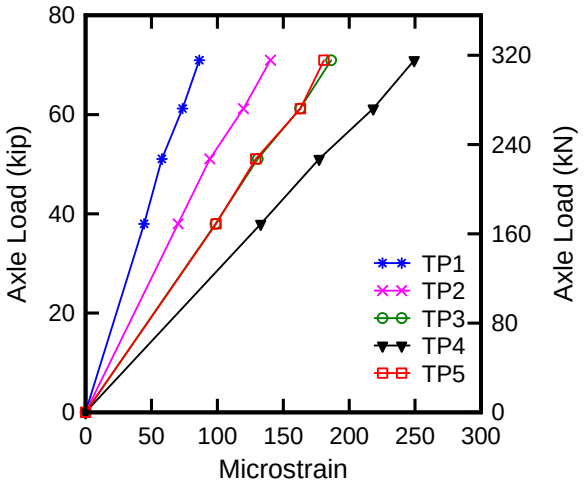

(a)

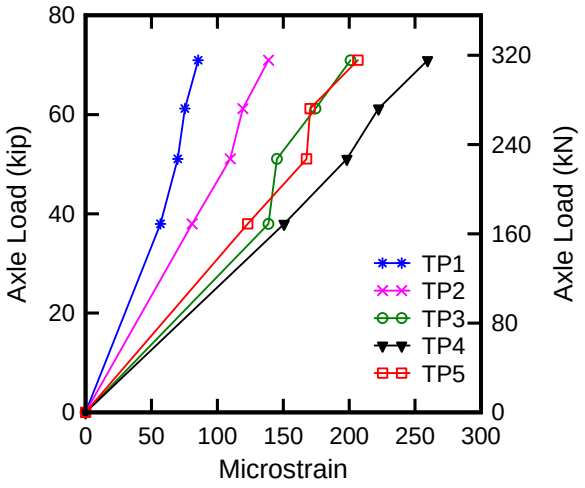

(b)

Figure 103 – Gage B3 load-strain calibration curve for (a) 2009 (b) 2010

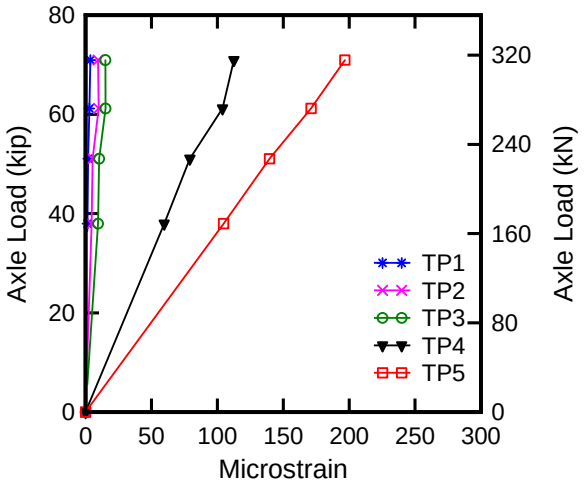

(a)

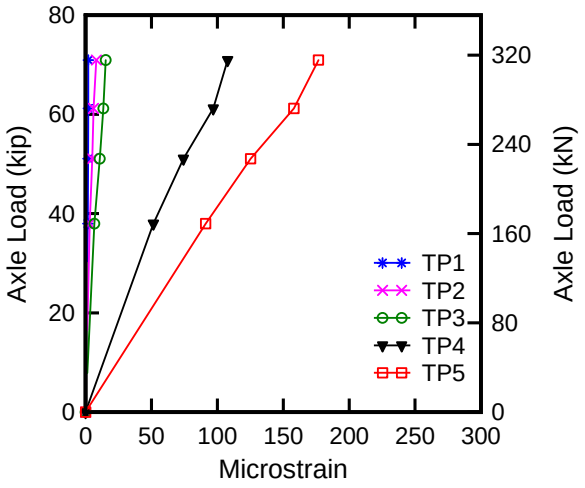

(b)

Figure 104 – Gage B4 load-strain calibration curve for (a) 2009 (b) 2010

15 Predictions of Deck Performance

15.1 Bridge Test vs. Lab Test

This section presents a comparison between laboratory tests conducted on the same type of GFRP deck that was installed on the Belle Glade bridge. Vyas et al. (2009) performed static and fatigue testing on the GFRP deck using the test setup shown in Figure 105. The specimen was supported in three locations and was continuous over the center support. The 4 ft spacing used for the supports was similar to that of the bridge. Load was applied over a 10 in. x 20 in. bearing pad; these are the same dimensions as the tire patch loading area specified in AASHTO Section 3.6.1.2.5.

Figure 105 – Structural test of GFRP deck used in Belle Glade bridge (Vyas et al. [2009])

The maximum strain observed was 751με for gage S5 with the truck in TP1 (lane one) and 660 με for gage S7 with the truck in TP5 (lane two) during the 2009 field test. During the 2010 test a maximum strain of 852 με was observed in gage S5 with the truck in TP1 and 636 με for gage S7 with the truck in TP5. These strains were recorded with the trucks loaded with 30 blocks, which translates to a rear wheel load of 18 kip (80 kN). Truck velocity during these tests was 1 mph or lower, eliminating dynamic impact effects. Vyas et al. (2009) measured service level strains of 700 με under a load of 20 kip (90 kN) during the laboratory test. Failure strain measured during the lab test was between 4000-6000 με. AASHTO Section 3.6.1.2 specifies a design wheel load of 16 kip (72 kN) x 1.33 dynamic load allowance = 21.3 kip (94.7 kN). The minimum GFRP panel failure strain during the laboratory tests was 4.7 times as large as the

maximum strain encountered during the bridge load tests. This indicates that the strain level in the GFRP panels installed on the Belle Glade bridge is far below that required to cause failure and that a substantial safety factor against flexural failure exists.

15.2 Theoretical Deck Analysis

An analysis of the bridge deck using a frame element model was conducted before the bridge test. This analysis was carried out to ensure that axle loads used during the bridge test would not overload and damage the bridge. Axle loads were chosen such that both materials (GFRP and steel) remain in the linear – elastic behavior range. The truck axle load was simulated by using two patch loads equivalent to the wheel load.

A continuous beam of the same length as the instrumented panel (panel B9) was modeled using transformed section properties based on the varying moduli as shown in Figure 106. A reference modulus of elasticity of 2500 ksi (bottom panel) was chosen for the calculation of the transformed section properties. The maximum value of the modulus of elasticity (3600 ksi) occurs at the flanges of the bottom panel. Table 18 presents the transformed section properties calculated for use in the panel analysis.

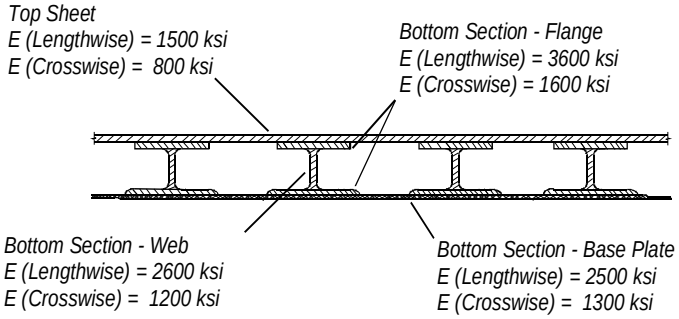

Figure 106 – GFRP deck Modulus map

Table 18 – Transformed Section Properties

Transformed Section Prop.	Including top plate	Ignoring top plate
Moment of Inertia (in.4)	183.6	121.4
Cross sectional area (in.2)	47.5	38.2

Steel girders were modeled as spring supports. The stiffness of these springs was calculated by analyzing a simply-supported beam spanning the same length as the length of the steel girders. This beam had similar section and material properties to those of the steel girders.

A unit kip load was applied on the beam at the location of the center of the instrumented panel B9 for the calculation of the beam stiffness. The steel girders have a skew of 28.73 degrees and the center of panel B9 was located 16.75 ft from the south end of the steel girder. By definition, the deflection corresponding to the unit kip load was the stiffness (32 kip/in.) of the beam. This stiffness was used to model the spring supports for panel B9.

Figure 107 presents the model of panel B9 as a continuous beam. A truck wheel load was applied as a patch load on the beam. Two patch loads simulate the two tires of the back axle of the test truck. A tire contact area of 20 in. x 10 in., consistent with AASHTO 3.6.1.2.5, was used to represent the FDOT test truck loading. For the purpose of this analysis an 18 kip wheel load was considered. Three truck positions were analyzed by placing the two patch loads at different distances from the edge of the curb. Three different truck positions were chosen to simulate various combinations of traffic movement on the bridge in transverse direction.

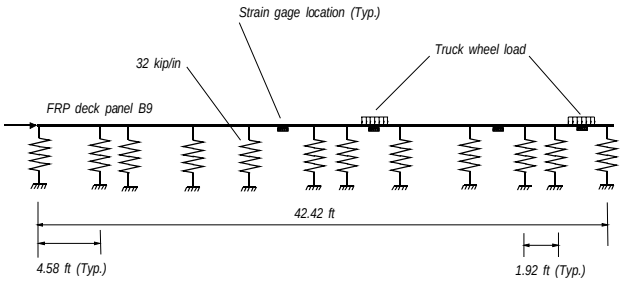

Figure 107 – GFRP bridge deck analysis

To bound the problem, linear-elastic analyses were conducted both with and without the stiffness contribution of the top plates. The maximum moment was observed in the center of the extreme right span. Strain was calculated using classical beam theory. Table 19 presents a comparison of the strain calculated from the simplified deck analysis and the measured strain during the bridge tests. Analytical strain values presented in Table 19 were calculated both including and not including the top plate in determining the stiffness of the GFRP panel. The analytical model of the GFRP deck overestimated the strain produced by the wheel load. This was probably because the actual span between the girders was less than the 54.25 in. used in the analysis since the girders were modeled as point springs. The actual span, prior to grout degradation, was 45 in.

Table 19 – Comparison of strain (με) for maximum wheel load (18 kip)

Material	Analytical – with top plate	Analytical – without top plate	Bridge test – 2009	Bridge test - 2010
GFRP deck	927	1050	751	852

16 Traffic Monitoring: Daily Load Spectra Analysis

Bridge monitoring started in the middle of October 2009 and continued, with several interruptions, through April 2011. Strain data from traffic loading were collected at a sampling frequency of 200 Hz; each scan included eight GFRP strain gages, four steel strain gages, and one displacement gage. Data were recorded continuously for 16 to 17 hours per day and data acquisition was terminated for the remainder of the day to perform data transmission. Depending on the wireless bandwidth available at the bridge site, data recording could be stopped for 6 –7 hours per day, which created daily gaps in the data record.

Data were recorded and transmitted in binary format. Binary data were then converted into TDMS (Technical Data Management Streaming) using a TDMS converter utility written in LABVIEW. TDMS files were converted into the more useful ASCII (.CSV) format using a LABVIEW routine. Both converters (Binary to TDMS and TDMS to ASCII) were capable of batch operation. After data were converted into CSV files, monthly time-history plots were produced to observe trends in strain over time, gaps in data recording, and assess the functionality of the different sensors. Data were downsampled to 5 Hz by plotting every 40th data points to avoid computing issues and were plotted using MATLAB (Appendix E and F).

Rainflow counting was used to determine the number and magnitude of the load cycles applied to the bridge during the monitoring period. This algorithm is taken from ASTM E1049 – 85 Standard Practices for Cycle Counting in Fatigue Analysis. To perform this analysis, the data were analyzed to determine the peaks and troughs from the strain gage output. Peaks and troughs are paired up until none remain. Each pair represents a half-cycle of the strain-time function. The magnitude of the difference in strain between peak and trough in a given pair determines the strain magnitude of the half-cycle corresponding to that pair. The quantity of half-cycles of each strain magnitude may then be used to determine the equivalent strain that would produce an equivalent amount of fatigue when applied in the same number of cycles as measured by the strain gages.

Typically, fatigue damage is defined to be cumulative and irreversible. The Palmgren-Miner Rule is used to account for this damage accumulation. The linear damage rule proposed by Palmgren in 1924 was further investigated by Miner in 1945 (Fisher et al. 1997). It assumes that damage fraction at any particular stress range level is a linear function of the corresponding

number of cycles. For a structural detail, the total damage can be expressed as the sum of damage occurrences that have taken place at individual stress range levels (i.e., Miner's Rule). The equation known as Miner's Rule is given as Equation 2.

$$D = \sum \frac{n_i}{N_i} \qquad \text{Equation 2}$$

where n_i is the number of cycles at stress range level i and N_i is the number of cycles to failure at stress range level i. Theoretically, the fatigue damage ratio, D, is equal to 1.0 at failure, practically it may be less than 1.0 due to various uncertainties.

Typically, fatigue details in bridge structures are subjected to variable amplitude stress ranges rather than constant amplitude fatigue when they are exposed to fatigue loading. For useful estimation of fatigue life, variable amplitude stress ranges can be converted into an equivalent constant amplitude stress range by using Miner's Rule (Miner 1945). The estimated S_{re} assists equivalent estimation of fatigue damage with respect to that estimated from variable amplitude stress ranges. S_{re} can be computed directly from the stress-range bin histogram and Miner's Rule (Fisher et al. 1997, Miner 1945). The equation is given as Equation 3.

$$S_{re} = \left[\sum \frac{n_i}{N_{total}} * S_{ri}^m\right]^{1/m} \qquad \text{Equation 3}$$

where n_i is the number of observations in the predefined stress-range bin (S_{ri}), N_{total} is the total number of number of stress cycles during the monitoring period (T), and m is a material constant representing the slope of the S-N curve determined by laboratory testing and was taken as three for this analysis.

16.1 GFRP Deck Histograms

Figure 108 shows an example of the histograms produced by using the rainflow counting method. Strains recorded by the strain gages were converted into wheel loads by using the load-strain calibration performed during the 2010 load test. Wheel loads were divided into nine bins of 4 kip. Electronic noise and small loads, such as those produced by cars and light trucks, represented the overwhelming percentage of the cycles recorded. Consequently, the first histogram bin was ignored. Histogram plots were created for each of the six soffit gages that had

been placed to measure positive flexural strains. Similar plots were also generated for the four steel girder gages, with the number of occurrences of different stress ranges plotted. The stresses in these plots were obtained by multiplying the measured strain by the modulus of elasticity of steel.

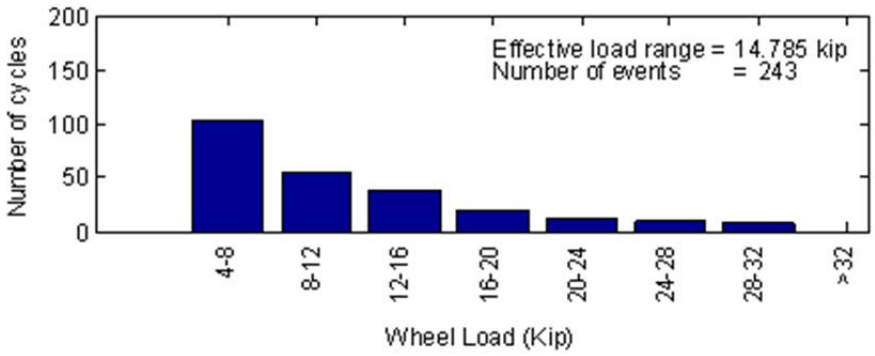

Figure 108 – Example histogram showing load occurrence distribution measured by a soffit gage between 7am and 6pm during one day

Continuous data recording was not feasible as the DAQ had to write data to the flash drive from memory. The only period when continuous data were recorded was between December 3rd and 20th, 2010. Substantially more data were available on days where recording did not include all 24 hours. December 14, 2010 was selected to assess the percentage of truck traffic crossing the bridge between 7am and 6pm due to the high number of occurrences on this day. The large volume of heavy truck traffic shown in Figure 110 was caused by a surge in sugarcane harvesting following a hard freeze (discussed in 16.3). Trucks were expected to predominantly operate during these hours since sugarcane is harvested during daylight and most businesses do not receive shipments outside these hours. Figure 109 through Figure 111 compare daylight hours to earlier morning and late evening hours for S2 gage (lane one) and S3 gage (lane two). For lane one, about 9% of the occurrences were outside of daylight hours while for lane two about 17% of the occurrences were outside of daylight hours.

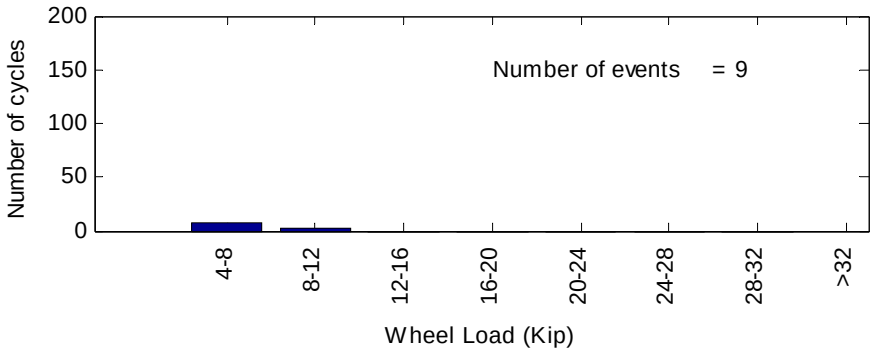

(a)

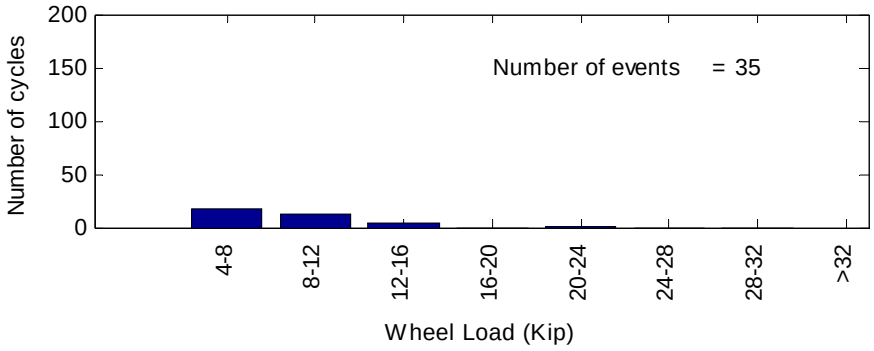

(b)

Figure 109 – Strains recorded by soffit gages (a) S2 and (b) S3 between 12am and 7am on December 14, 2010

Approximately 102 days during the monitoring period from October 2009 through April 2011 had full data records for the hours between 7am and 6pm for the soffit gages. For these days, the average equivalent load range and daily number of load occurrences within each load range were computed from the histogram data using Miner's Rule (Equation 3).The results are presented in Table 20 for soffit gages used to measure positive flexure. The average equivalent load range is consistent between the six strain gages and between the two lanes of travel. The equivalent load range varied between 7.8 kip and 9.6 kip. Lane two had a slightly higher equivalent load range than lane one. This result indicates that the "average load" applied in lane two was slightly higher than in lane one. As indicated by Figure 112 the average number of daily occurrences also indicates that more loads at each load level are recorded by soffit gages in lane two than in lane one. For example, soffit gages under lane two (S3, S7, and S8) recorded an average of 34.6 daily occurrences of load ranges of at least 8 kip, which is 2.66 times as great as the number of similar load ranges recorded by gages under lane one (S1, S2, and S5).

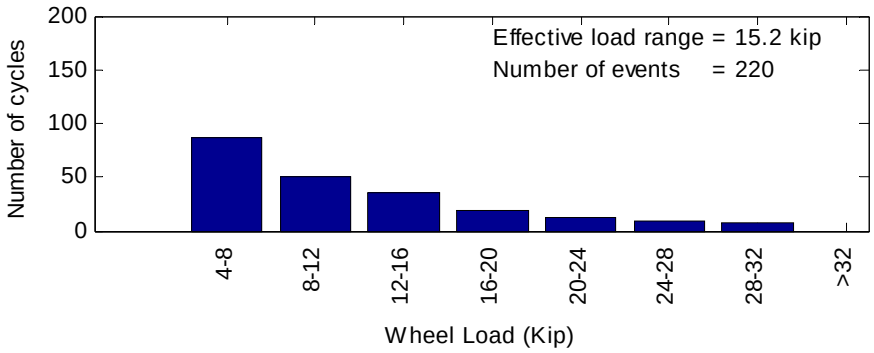

(a)

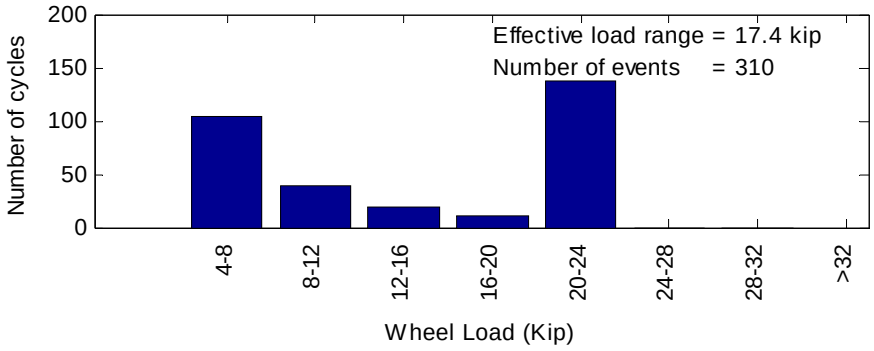

(b)

Figure 110 – Strains recorded by soffit gages (a) S2 and (b) S3 between 7am and 6pm on December 14, 2010

It is unclear why these data show that lane two is more heavily loaded than lane one. One possibility is that that soffit gages in lane one were not in a location that was activated by the typical traffic path in lane one. This is supported by the 35 mph test in which the truck was driven over lane one and lane two; gages in lane two recorded more strain that those in lane one. Data from the bridge tests indicate that lane one experienced a greater loss of stiffness than lane two, as shown by the increase in strain recorded during the rolling test during 2010 compared with 2009. Anecdotal evidence, in the form of grout cracking and spalling observed under lane one, indicates heavier loading under lane one than two also.

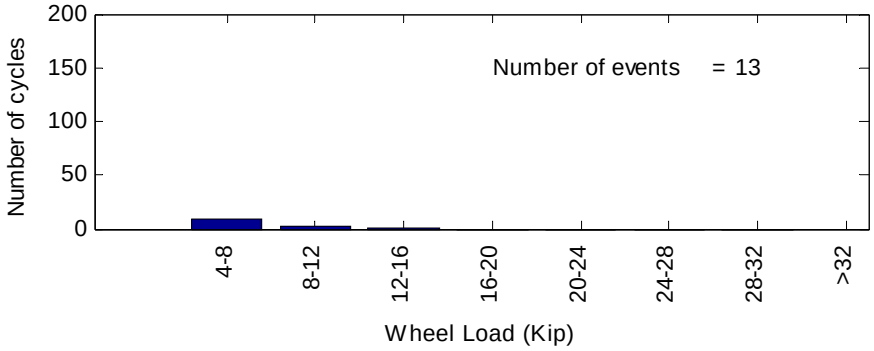

(a)

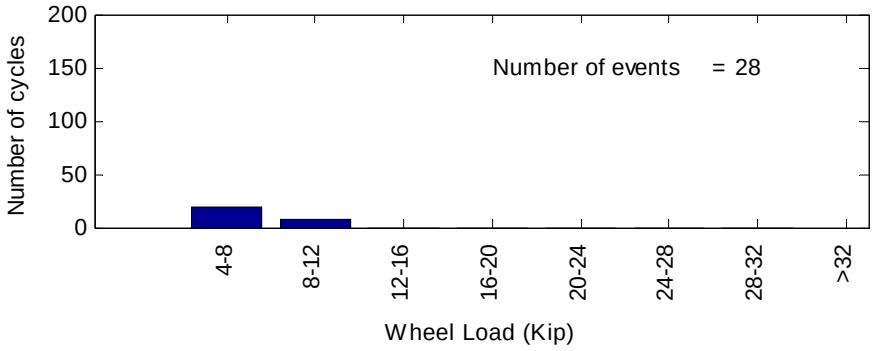

(b)

Figure 111 – Strains recorded by soffit gages (a) S2 and (b) S3 between 6pm and 12am on December 14, 2010

Table 20 – Average equivalent load range and number of daily occurrences (7am through 6pm) for different load levels for soffit strain gages

Instrumentation	Average Equivalent Load Range (kip)	Average Number of Daily Occurrences			
		> 8 kip	> 12 kip	> 16 kip	> 20 kip
S1	8.9	15.1	8.2	5.5	0.0
S2	7.8	10.9	4.2	2.1	1.3
S3	9.2	41.6	20.5	14.6	12.3
S5	8.0	13.0	5.3	2.8	1.3
S7	8.2	38.0	13.0	5.3	2.5
S8	7.8	24.3	8.3	4.6	2.6

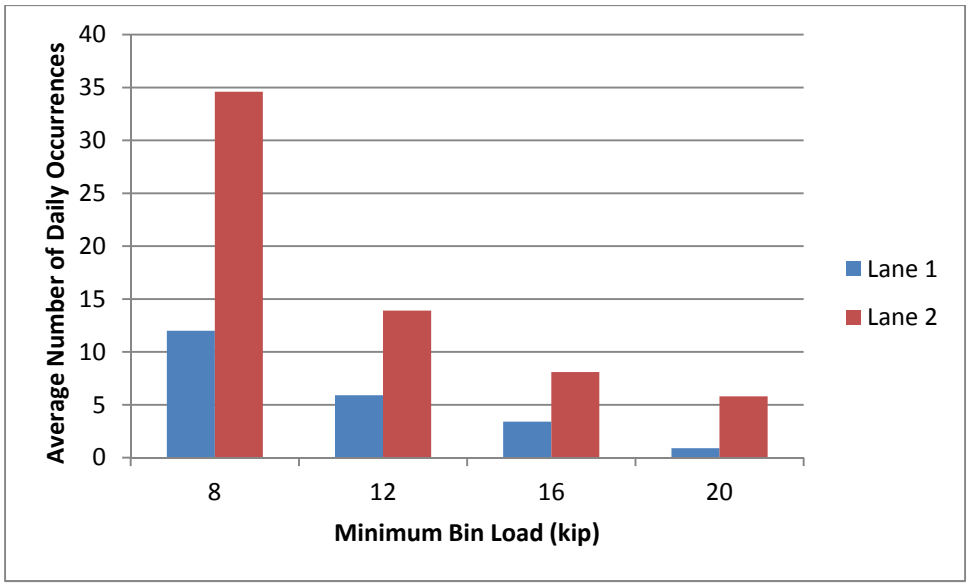

Figure 112 – Average number of occurrences of different load ranges measured by soffit gages S1, S2, S3, S5, S7, and S8

16.2 Steel Girder Histograms

Approximately 102 days during the monitoring period from October 2009 through April 2011 had full data records for the hours between 7am and 6pm for the steel gages. Table 21 shows the equivalent stress range and daily number occurrences (between 7am and 6pm) within each stress range as measured by the steel girder gages. The average equivalent stress ranges were similar for the first three gages B1, B2, and B3. Gage B4 recorded a lower average equivalent stress range than the other three, at 1.9 ksi vs. 2.3 ksi, indicating that there were fewer occurrences of heavy loading at gage B4 than at the other gages. Gage B4 was located between the left-turn lane (which did not carry through traffic) and lane two. Gage B3 was located to detect traffic in lane two while gages B1 and B2 were located to detect traffic in lane one. The girders monitored by B2 and B3 were part of the same frame. This frame supported portions of both lanes one and two. The frame containing the girder monitored by B1 supported lane one only (Figure 20).

The average number of daily occurrences was higher at all stress ranges for lane one than lane two, as indicated by Figure 113. Lane one experienced an average of 98.5 occurrences of stress greater than 2 ksi per day, compared with 49.8 such occurrences in lane two. This supports the hypothesis that lane one experienced more high load events than lane two due to trucks traveling in the right lane. The preponderance of high loads in the right lane would

explain other evidence, including influence lines and observations of grout deterioration, which indicated that the superstructure and GFRP panels experienced a greater loss of stiffness in lane one than lane two.

Table 21 – Average equivalent stress range and number of daily occurrences (7am through 6pm) for different load levels for girder strain gages

Instrumentation	Average Equivalent Stress Range (ksi)	Average Number of Daily Occurrences				
		> 2 ksi	>3 ksi	>4 ksi	>5 ksi	>6 ksi
B1	2.2	123.2	49.6	19.0	4.0	1.2
B2	2.5	73.7	40.9	11.5	2.1	0.5
B3	2.1	87.8	26.5	7.6	2.2	0.7
B4	1.7	11.8	2.9	0.8	0.1	0.0

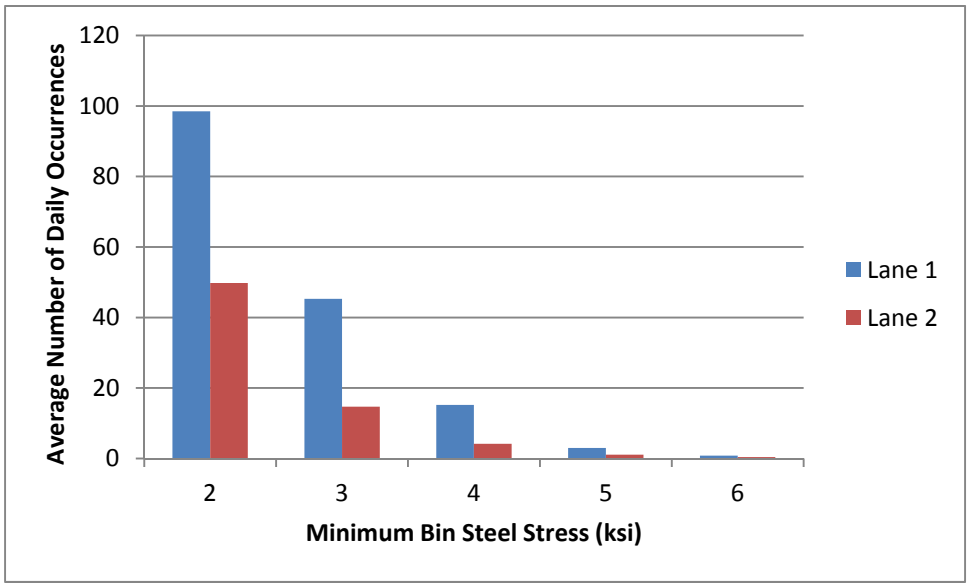

Figure 113 – Average number of occurrences of different stress ranges measured by steel gages B1, B2, B3, and B4

16.3 Effect of Weather on Truck Traffic

During December 2010, the sugar producing area surrounding Belle Glade experienced record-breaking cold weather that severely damaged the sugarcane crop (wunderground.com). Table 22 gives the minimum temperature during the period for which continuous monitoring data was available. Temperature data from two weather stations is given; the station at West Palm Beach International Airport is the closest station that is part of the National Weather

Service while the station at South Bay 15 S is a nearby station operated by the Okeelanta Corporation. The South Bay 15 station is isolated from the moderating influences of Lake Okeechobee and the Atlantic Ocean, providing the minimum temperature experienced by the sugarcane crop. Daily minimums are taken midnight-to-midnight at West Palm Beach International Airport and at 7 AM at South Bay. Table 22 indicates that a freeze occurred on December 14, with cold temperatures lingering through December 16.

News reports indicated that the freeze of December 14th was catastrophic for the sugarcane crop and prompted an emergency partial harvest. One news account by Salisbury (2011) summarized the damage. Between the 14th and 15th, temperatures dropped below 28 degrees (F) for 12 hours; a period of 4 hours below 28 degrees is sufficient to destroy the terminal bud. According to George Wedgworth, President and CEO of the Sugar Cane Growers Cooperative, "Once the terminal bud freezes, it becomes a race against the clock to get the sugarcane from the field to the processing facility as the cane deteriorates over time." Anticipating the hard freeze, an executive order lifting certain weight limits on agriculture-related trucking was signed on December 10th (Fl. Exec. Order No. 10-262 [Dec. 10, 2010]). These events precipitated a significant increase in truck traffic noted in the monitoring data gathered during that period.

Soffit strain gages confirmed that there was significant increase in wheel loads heavier than 16 kip on December 14, 2010 as illustrated in Figure 114. The sudden increase in heavy traffic on the 14th is striking, indicating that freeze–damaged cane was harvested as rapidly as possible. A second surge occurred on December 16th, after a second freeze event on the 15th. A third surge on the 19th may be the result of additional sugarcane being identified as freeze-damaged in the days following the freeze events.

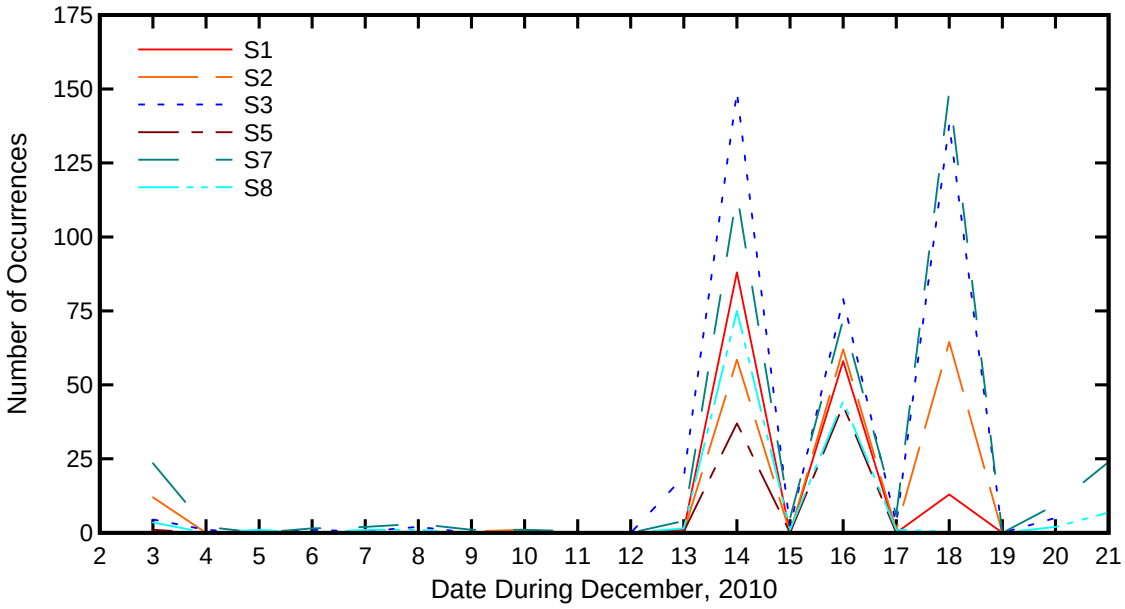

Figure 114 – Number of 16 kip or heavier loads recorded by soffit strain gages between 7am and 6pm daily

Table 22 – Minimum temperatures near Belle Glade during December 2010 freeze

Date (December 2010)	Day	Minimum Temperature at WPB Int'l Apt. (°F)	Minimum Temperature at South Bay 15 S (°F)
12	Sunday	54	50
13	Monday	41	51
14	Tuesday	32	35
15	Wednesday	35	30
16	Thursday	42	38
17	Friday	48	47
18	Saturday	57	52
19	Sunday	55	51
20	Monday	46	58

17 Thermal Response

Temperature was recorded at a 10 Hz sampling rate; readings were taken throughout the monitoring period to quantify the thermal gradient in the GFRP deck. A 10Hz sampling rate was deemed sufficient to capture temperature trends without producing excessive data. Figure 115 through Figure 118 compare the temperature traces for each of four months distributed throughout the year. The temperature trace from a single day during each of these months was selected and plotted to illustrate the time-dependent variation of the thermal gradient within the panel. During the day, the temperature of the top flange of the webs, measured by thermocouple 4, increased more quickly than the bottom of the bottom panel, measured by thermocouple 1. At night, the panels had a uniform temperature nearly identical to the ambient temperature. By early afternoon, the temperature difference between the two locations was up to 30 degrees (F).

The daily plots indicate that the maximum temperature differential between thermocouple 1 and thermocouple 4 was greater in the summer than in the winter. Table 23 shows the maximum differential was 32.2 degrees in June and 19.3 degrees in November. This is logical since less sunlight reaches the deck due to the shorter period of daylight and the shallow angle of the sunlight. The minimum temperature differential between thermocouple 1 and thermocouple 4 had a higher magnitude in the winter than in the summer, although this trend was not quite as pronounced. In June the minimum differential was -1.8 degrees while in February the minimum differential was -4.2 degrees. The negative signs indicate that the top of the bottom panel (measured by thermocouple 4) was colder than the bottom of the panel web.

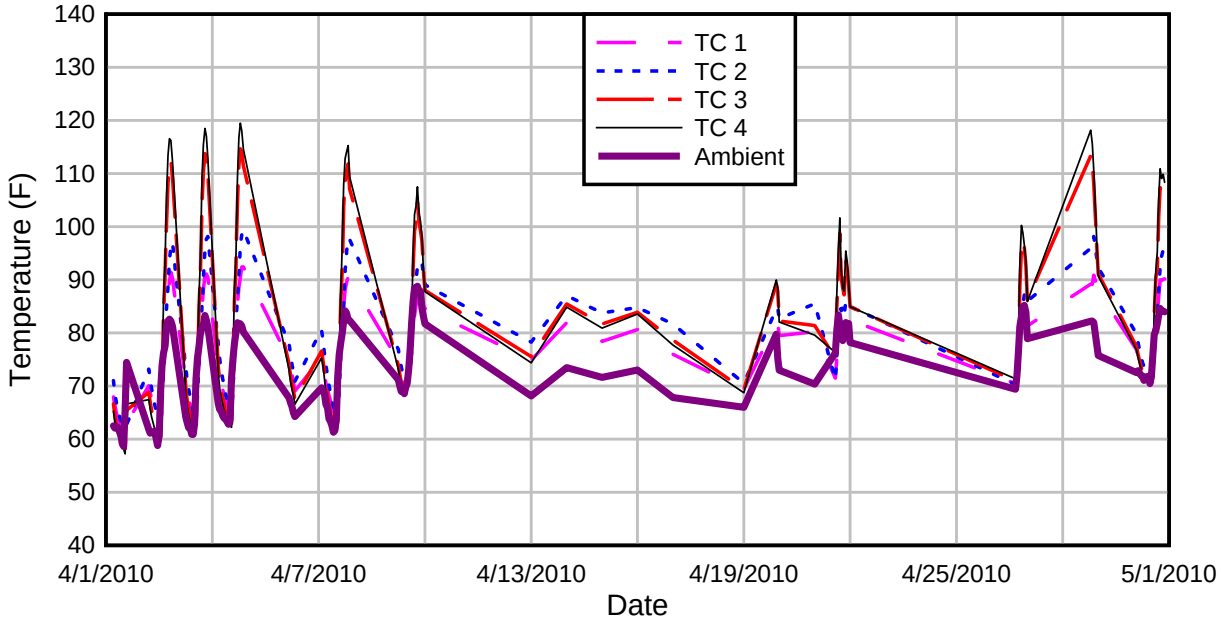

(a)

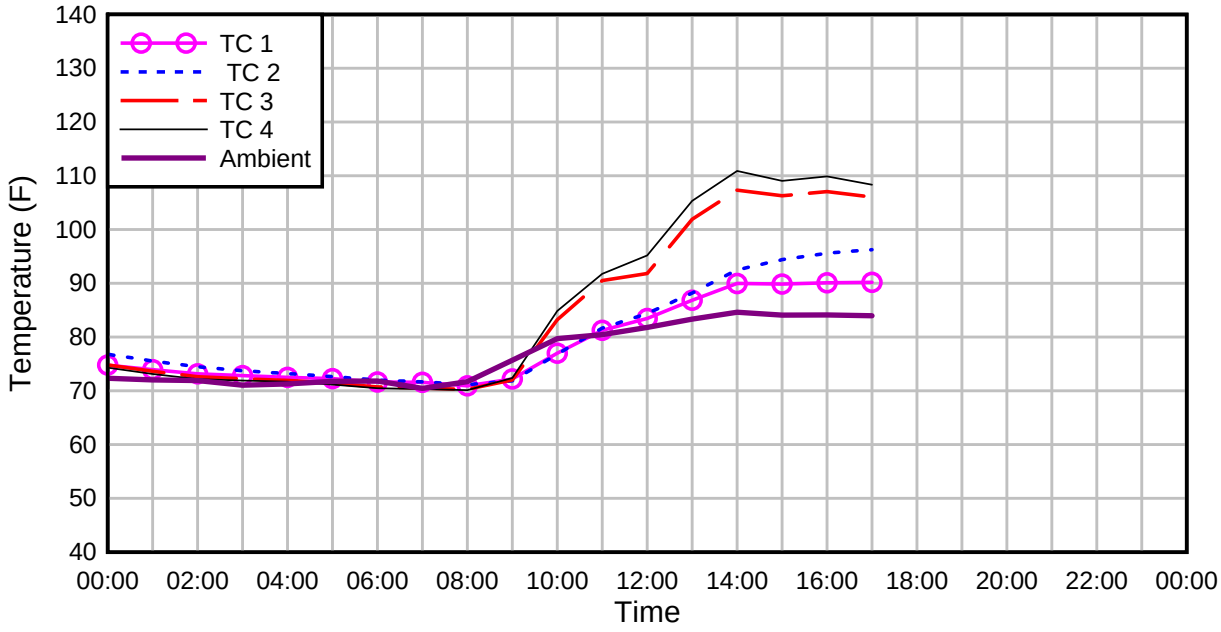

(b)

Figure 115 – Temperature measurements for (a) April, 2010 and (b) April 30, 2010

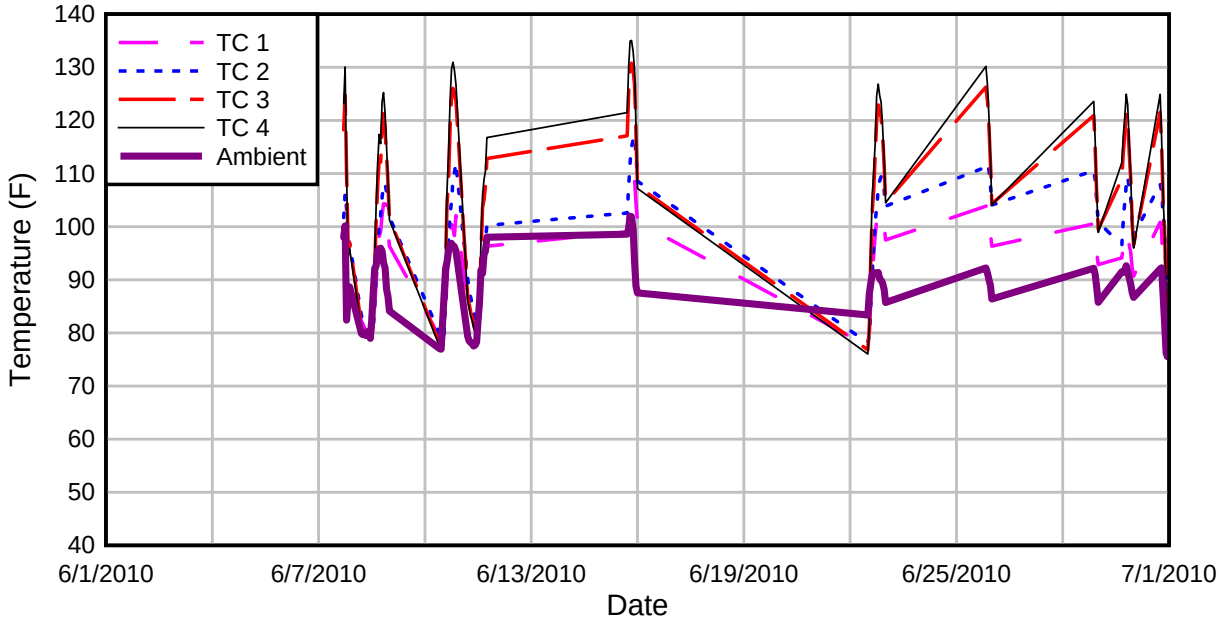

(a)

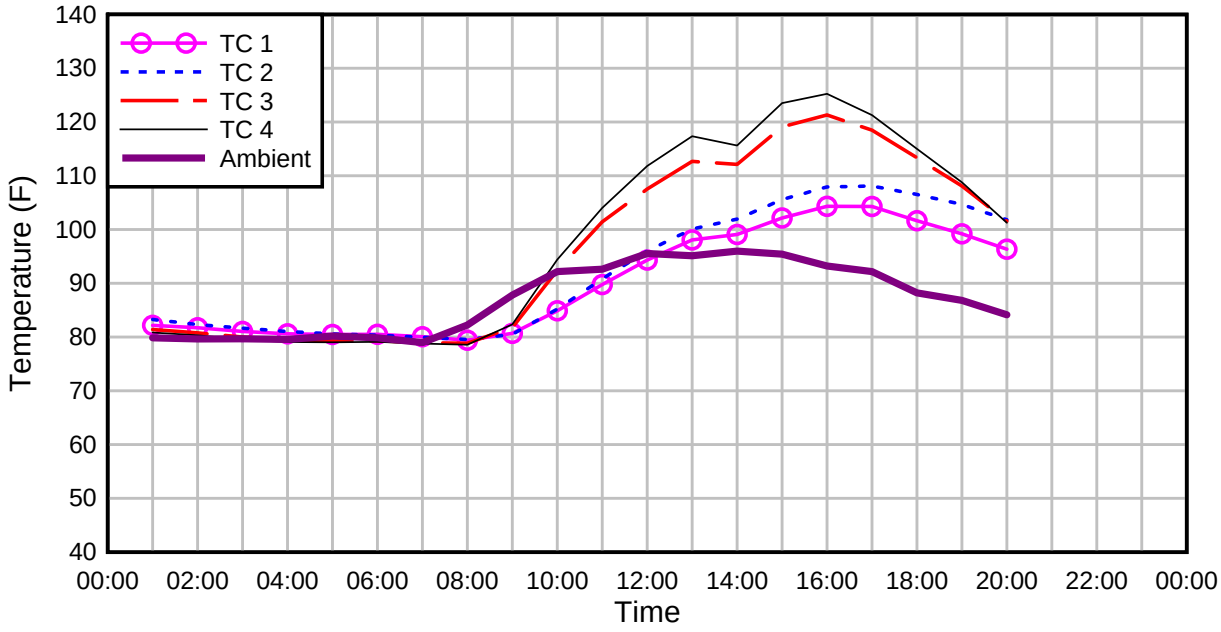

(b)

Figure 116 – Temperature measurements for (a) June, 2010 and (b) June 8, 2010

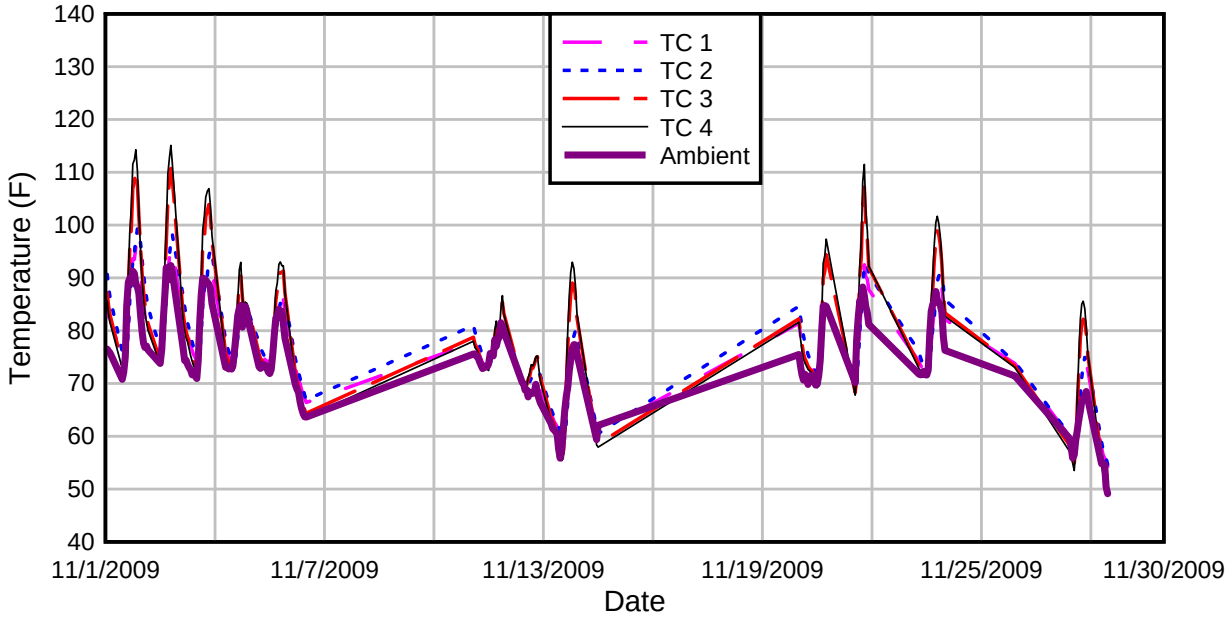

(a)

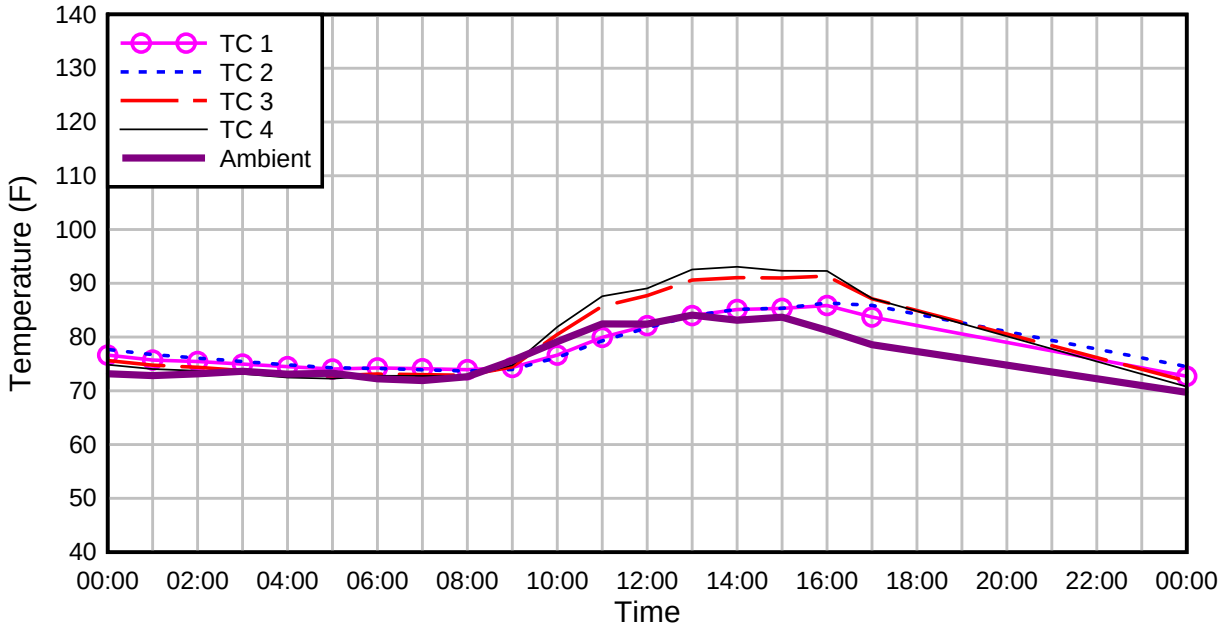

(b)

Figure 117 – Temperature measurements for (a) November, 2009 and (b) November 5, 2009

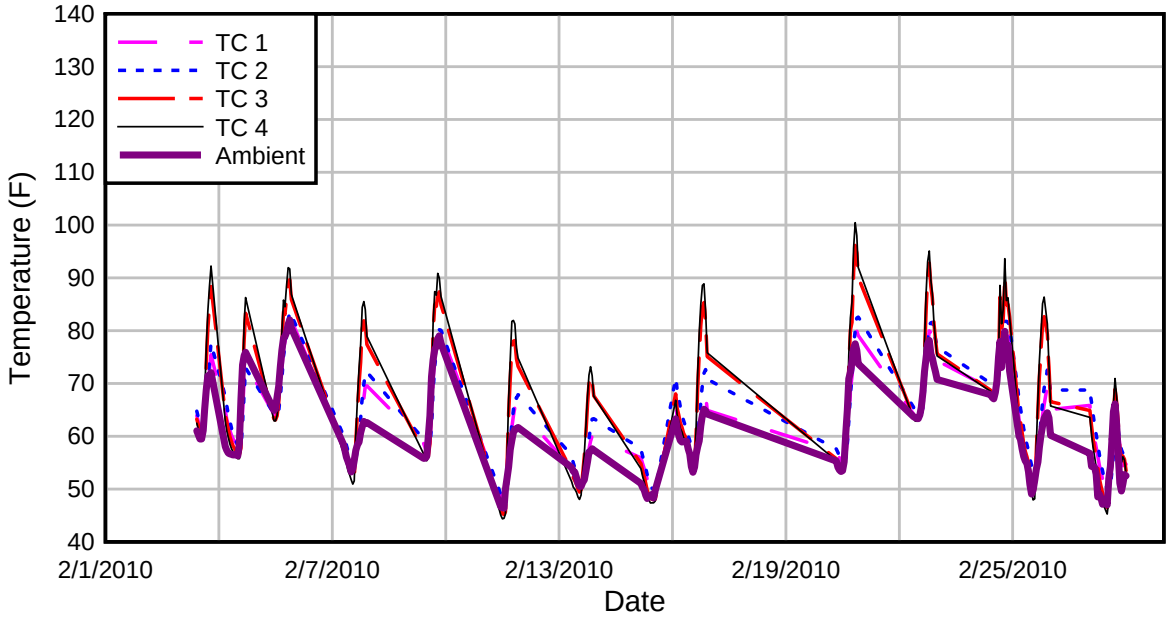

(a)

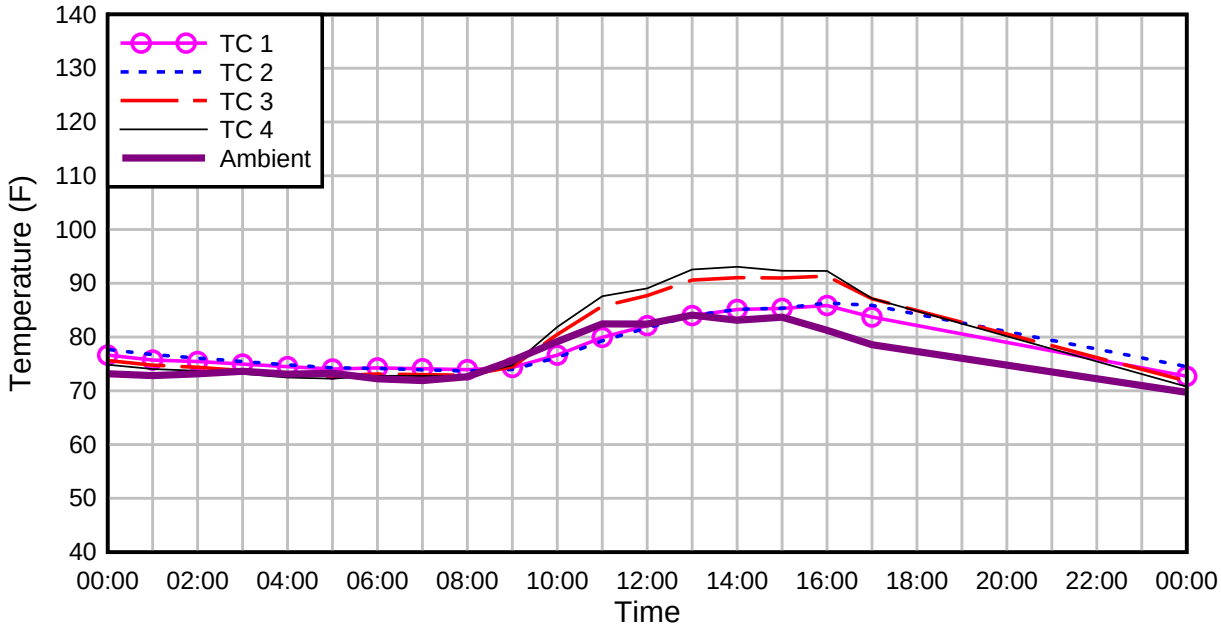

(b)

Figure 118 – Temperature measurements for (a) February, 2010 and (b) February 16, 2010

Table 23 – Temperature extremes (°F)

Month	Maximum temperature differential	Minimum temperature differential	Maximum ambient temperature	Minimum ambient temperature
February 2010	22.2	-4.2	82.0	46.4
March 2010	27.7	-4.2	83.1	46.3
April 2010	29.0	-3.3	88.8	58.6
May 2010	30.4	-2.6	97.5	68.2
June 2010	32.2	-1.8	101.9	75.4
October 2009	21.0	-1.9	94.0	69.1
November 2009	19.3	-3.9	92.4	49.1

It was impractical to apply thermocouples to the top plate, but it may be surmised that the top plate reached a higher temperature than was recorded by thermocouple 4. During heating, this differential would cause the top plate to expand more rapidly than bottom panels, which may work to loosen the screws attaching the top plate to the bottom panel. Stress would be highest at the ends of the top plates in the longitudinal direction due to higher displacement in this direction (equal strain applied over a longer distance). The plates would be expected to expand at the free ends, since there would be no adjacent plate to restrain expansion (Figure 119). Degradation of the wearing surface and the loss of mechanical fasteners were observed at this location (Figure 120), suggesting that temperature effects were significant. Assuming that the panels and plates possessed a similar coefficient of thermal expansion to fiberglass, a relative expansion of 1/16 in. can be expected from a 30 degree (F) temperature differential given a plate length of 17 feet (length of longest top plate).

Figure 119 – Top plate free edge

Figure 120 – Degradation at free edge

Figure 121 shows the thermal gradients recorded at various times of year. In each of these plots, the daylight has raised the temperature of the top plate to its maximum level while the temperature of the center and bottom of the bottom panel lags behind. In all of the plots, the temperature at thermocouples 3 and 4 was substantially higher than that of thermocouples 1 and 2, indicating that the top plate transmitted heat by conduction into the top flange of the bottom panel webs. The mechanical fasteners, composed of metal, may have assisted this process due to higher thermal conductivity. Conversely, the thin webs of the bottom panel acted as effective insulators, with thermocouple 2 registering little temperature increase over thermocouple 1 despite thermocouple 2 being half as far from the warmer top plate as thermocouple 1. This temperature difference was less than three degrees (Fahrenheit) except during the summer months. The change in temperature distributions throughout the panels caused thermal stresses to develop within the deck system. The top GFRP plate was connected to the bottom GFRP panel with metal mechanical fasteners. Since heat was conducted throughout the top plate much more quickly than it can be conducted between the top plate and bottom panel, stresses developed in the panels at the mechanical anchors.

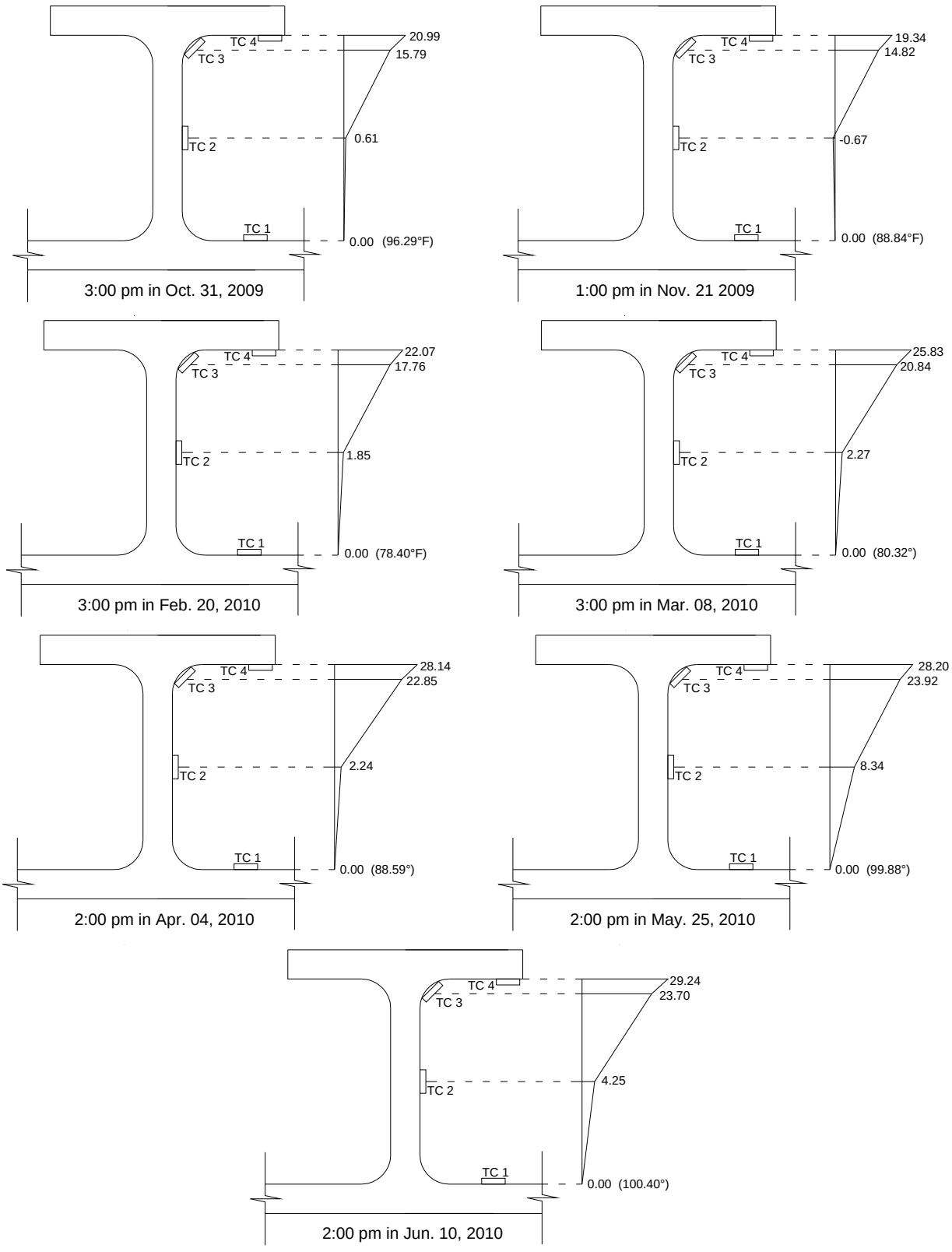

Figure 121 – Maximum thermal gradients throughout the year

18 Accelerated Deterioration

In the months that followed the bridge load tests reported herein, the district continued to monitor the bridge for further deterioration. At the date of the completion of this report, some areas of the bridge deck had deteriorated so severely that repair was necessary (Figure 122, Figure 123, and Figure 124). Several factors are thought to have contributed to the accelerated degradation. Heavy, regular truck traffic combined with deterioration of the grout bearing pad, severe skew, and failed top plate fasteners appear to have contributed to the failure. It is not clear which of these factors, if any, were the primary cause or if other factors may have contributed. Causes of the damage were being evaluated at the time this report was completed. Repair methods were also being developed for the damaged areas.

Figure 122 – Wearing surface damage at panel joints

Figure 123 – Wearing surface damage at intersecting panels

Figure 124 – Severe damage to top plates and webs

19 Summary and Conclusions

This study evaluated the performance of glass-fiber reinforced polymer (GFRP) deck panels that were used to replace the steel grid deck of bridge no. 930338 in Belle Glade, FL. This evaluation consisted of two bridge tests using FDOT test trucks and remote monitoring of strain, displacement, and temperature under normal traffic conditions. The evaluation period lasted 18 months, from October 2009 through April 2011.

The bridge was constructed with a two-part GFRP deck placed upon a steel frame superstructure. The bottom GFRP panels featured integral webs to resist flexure and were attached to the steel girders with grout pockets containing steel studs welded to the girders. A thin layer of grout was placed between the GFRP panels and the deck to provide leveling. GFRP top plates were attached to the bottom GFRP panels using mechanical fasteners. A layer of polymer concrete was placed on the top of the deck to provide the wearing surface.

Instrumentation was applied to the deck before and after installation, which occurred in August 2009. Instrumentation included foil strain gages placed on the soffit of the GFRP panels to record flexural strain; rosette gages placed on lower panel webs to record GFRP shear strain; LVDTs to record GFRP deck displacement; thermocouples to study temperature gradients within the GFRP panels; and full bridge strain gages to record strain in the steel superstructure. The instrumentation was placed in the northbound lanes to capture the effect of loaded sugarcane trucks crossing the bridge.

Two bridge tests were conducted, one in October 2009 and the second in October 2010. These tests were conducted to evaluate changes in the performance of the bridge between the two bridge tests and to correlate strains recorded during monitoring with applied wheel loads. Static tests were performed where the trucks were pulled into selected positions and readings were taken. Rolling tests were conducted where the truck travelled at approximately 1 mph while readings and GPS truck positions were simultaneously taken. Finally, a 35 mph test was conducted during the 2010 bridge test to study dynamic load effects and to compare them with AASHTO impact factors.

Effect of traffic on strain and displacement of the deck and girders was monitored for 18 months; temperature was also monitored. The number and magnitude of load and stress cycles were determined using rainflow counting. Temperatures throughout the depth of the deck panel

were monitored and the formation of thermal gradients was analyzed. The following points highlight the observations and results of this study:

- Static tests indicated that local strains in the deck were unaffected by the presence of a truck in the adjacent lane. Consequently, the bridge tests were conducted using a single truck.
- GFRP deck strains were found to be sensitive to wheel position measured parallel to the direction of travel along the right of way. For example, flexural strain decreased by 60% when the test truck wheel had moved only 1 ft away from the strain gages. This sensitivity to wheel position makes static truck positioning to maximize specific strain gages difficult because the positioning tolerance is so low.
- The GPS tracking capability of the FDOT test truck was crucial for locating the maximum GFRP deck strain. The ability to track the truck position resulted in strain influence lines, which were used to determine distribution factors for the GFRP deck. Influence line plots confirmed that the GPS tracking was accurate to a one inch resolution. The GPS data were used to confirm that the truck followed the designated travel line and evaluate the sensitivity of the strain gages to load proximity.
- Influence lines determined for gages S1, S2, and S5 indicate a significant increase in GFRP deck strain occurred during the year between the two bridge tests. These gages monitored lane one. Gages S2 and S5 indicated that the strain during the 2010 test was 1.13 times the strain during the 2009 test. For gage S1, this ratio is 1.27. This degradation is thought to be the result of the cracking and spalling of the grout leveling layer placed between the GFRP bottom panels and the steel beams and not degradation of the GFRP deck itself. Loss of the grout support at the girders will increase the effective span of the GFRP panels, thus causing an increase in flexural strain as was observed in the two bridge tests. An additional cause for the increase in strain observed in the GFRP deck may have been an increase in the support flexibility due to possible degradation of the grout in the grout pocket containing the shear studs. This would reduce stiffness in the GFRP deck/ steel girder interface and allowed for increased deck rotation and attendant strains in the GFRP deck.

- Influence lines produced for gage S7 indicate that there was no significant increase in flexural strain in the GFRP panels under the left lane (lane two).
- The flexural distribution factors for the GFRP panels remained unchanged at 0.24 for both bridge tests. The shear distribution factors for the GFRP panels averaged 0.38 as measured during the 2009 bridge test.
- The top GFRP plates do not behave compositely with the bottom panels. The neutral axis of the deck system was located using strain gages applied to the bottom and middle of the bottom GFRP panel. The measured neutral axis was consistent with the theoretical neutral axis obtained by assuming that the top plate is not present. This indicates that the increase in GFRP deck strain detected between the two bridge tests was not the result of the failure of the mechanical connections between the top plates and bottom GFRP panels.
- Although not considered in design, some composite action between the GFRP deck and steel girders was detected in the initial bridge test. This is due to the grout and stud connection between the deck and girders. The subsequent bridge test indicated some loss of composite action had occurred in the right lane (lane one). Girder 3 (gage B1) strain was found to have increased approximately 20% in the 2010 test. Gages B2 and B3 indicated less strain increase in girders 5 and 6. Gage B4, situated on girder 7 under lane two, indicated that no strain increase had occurred.
- Measurements of deck displacement were inconclusive. The LVDT used during the bridge tests indicated that the strain in the midspan of a GFRP panel decreased from 0.08 in. to 0.06 in. between the 2009 and 2010 bridge tests.
- Dynamic load factors were difficult to obtain using the soffit gages to measure strains in the GFRP panels. Determining these factors using gages mounted to the steel girders was more reliable. Truck positioning was difficult at 35 mph and GPS was unavailable. Soffit gages in lane one did not record substantial strains during this test, indicating that these gages were not placed optimally to monitor traffic. This is consistent with the data obtained during monitoring. The dynamic load factors obtained using soffit gages in lane

two or using the steel girder gages were comparable to the impact factors specified in AASHTO.

- Substantial thermal gradients developed within the GFRP panels during the early afternoon, especially during the summer. The top of the bridge deck reaches temperatures at least 30 °F hotter than the interior of the deck panels. This cycling, causing a relative expansion of up to 1/16 in. in the top plates relative to the bottom panels, may partially explain the large number of mechanical fasteners that have come loose from the top plate at the end of the bridge.
- The bridge experienced the heaviest loads during the sugarcane harvest season. A hard freeze on December 13, 2010 led to an intense harvesting period. Weight restrictions on agricultural vehicles were lifted to enable rapid harvesting of damaged sugarcane. These factors led a significant increase in heavy loads crossing the bridge.
- Severe deterioration of top plates and webs of portions of the deck were noted by district personnel in the months following the bridge load tests. Causes of the damage were being evaluated at time this report was completed. Repair methods were also being developed for the damaged areas.

20 References

AASHTO, “AASHTO LRFD Bridge Design Specifications,” 4rd Edition, American Association of State and Highway Transportation Officials, Washington, 2007.

Alagusundaramoorthy, P., Harik, I. E., and Choo, C. C. (2006). "Structural behavior of FRP composite bridge deck panels." *Journal of Bridge Engineering*, 11(4), 384-393.

Alampalli, S., and Kunin, J. (2003). "Load testing of an FRP bridge deck on a truss bridge." *Applied Composite Materials*, 10(2), 85-102.

ASTM E1049-85, “Standard Practices for Cycle Counting in Fatigue Analysis,” 2005.

Camata, G., and Shing, P. B. (2010). "Static and fatigue load performance of a GFRP honeycomb bridge deck." *Composites Part B-Engineering*, 41(4), 299-307.

Chakraborty, S., and DeWolf, J. T. (2006). "Development and implementation of a continuous strain monitoring system on a multi-girder composite steel bridge." *Journal of Bridge Engineering*, 11(Compendex), 753-762.

Chiewanichakorn, M., Aref, A. J., and Alampalli, S. (2007). "Dynamic and fatigue response of a truss bridge with fiber reinforced polymer deck." *International Journal of Fatigue*, 29(8), 1475-1489.

Cousins, T. E., Lesko, J. J., Majumdar, P. K., amd Liu, Z. (2009). “Rapid replacement of Tangier Island bridges including lightweight and durable fiber reinforced deck systems.” *Report No*. FHWA/VTRC 10-CR3, Virginia Transportation Research Center, 22 pp.

Fisher, J. W., Kulak, G. L., and Smith, I. F. C. (1997). *A Fatigue Primer for Structural Engineers*, Lehigh University, [Bethlehem, PA].

Fu, C. C., AlAyed, H., Amde, A. M., and Robert, J. (2007). "Field performance of the fiber-reinforced polymer deck of a truss bridge." *Journal of Performance of Constructed Facilities*, 21(1), 53-60.

Howell, D. A., and Shenton III, H. W. (2006). "System for in-service strain monitoring of ordinary bridges." *Journal of Bridge Engineering*, 11(Compendex), 673-680.

Jeong, J., Lee, Y. H., Park, K. T., and Hwang, Y. K. (2007). "Field and laboratory performance of a rectangular shaped glass-fiber reinforced polymer deck." *Composite Structures*, 81(4), 622-628.

Lee, J. H., Kim, Y. B., Jung, J. W., and Kosmatka, J. (2007). "Experimental characterization of a pultruded GFRP bridge deck for light-weight vehicles." *Composite Structures*, 80(1), 141-151.

Market Development Alliance (MDA) of FRP Composite Industry, (2000). *Product Selection Guide: FRP Composite Products for Bridge Applications*. First Edition.

Miner, M. A. (1945). "Cumulative damage in fatigue." *American Society of Mechanical Engineers - Journal of Applied Mechanics*, 12(3), 159-164.

Moon, F. L., Eckel, D. A., and Gillespie, J. W. (2002). "Shear stud connections for the development of composite action between steel girders and fiber-reinforced polymer bridge decks." *Journal of Structural Engineering-ASCE*, 128(6), 762-770.

National Bridge Inventory, (2008). Federal Highway Administration, Washington, D.C.

Plunkett, J.D. (1997). "Fiber-Reinforced Polymer Honeycomb Short Span Bridge for Rapid Installation." IDEA project final report, Contract NCHRP-96-IDO30, IDEA Program. Transportation Research Board, National Research Council.

Salisbury, S. (2011). "Florida sugarcane growers end second shortest season with crop down 20 percent." *Palm Beach Post*. February 22, 2011.

Sartor, R. R., Culmo, M. P., and DeWolf, J. T. (1999). "Short-term strain monitoring of bridge structures." *Journal of Bridge Engineering*, 4(Compendex), 157-164.

Sun, L., and Sun, S. "Bridge condition assessment based on long-term strain monitoring." *Proc., Sensors and Smart Structures Technologies for Civil, Mechanical, and Aerospace Systems 2011, March 7, 2011 - March 10, 2011*, SPIE, The Society of Photo-Optical Instrumentation Engineers (SPIE); American Society of Mechanical Engineers; KAIST; Asian-Pac. Netw. Cent. Res. Smart Struct. Technol. (ANCRiSST).

Vyas, J. S., Lei, Z., Ansley, M. H., and Xia, J. (2009). "Characterization of a low-Profile fiber-reinforced deck system for moveable bridges." Journal of Bridge Engineering, 14(1), 55-65.

Wang, Y., Li, Z. X., and Li, A. Q. (2010). "Combined use of SHMS and finite element strain data for assessing the fatigue reliability index of girder components in long-span cable-stayed bridge." *Theoretical and Applied Fracture Mechanics*, 54(Compendex), 127-136.

Appendix A – 2009 Bridge Test

Soffit gages - maximum strain (με)

Load Case	S1	S2	S3	S4	S5	S6	S7	S8
LC4	283	332	88	2	482	61	1	2695
LC5	64	28	-209	2	160	79	2	5485
LC6	3	53	-294	1	10	269	0	6399
LC7	0	9	-346	177	-6	0	23	8931
LC8	0	6	-108	70	-8	-2	374	8931
LC9	397	437	-225	2	552	77	1	0
LC10	78	34	-1007	1	190	114	1	0
LC11	4	66	-1303	1	18	337	0	0
LC12	1	10	-1543	210	-3	-1	29	0
LC13	0	7	-1245	94	-1	-1	479	0
LC14	450	517	133	2	675	95	1	0
LC15	82	41	-2	3	189	182	8	0
LC16	5	79	-99	4	14	398	1	0
LC17	5	8	58	166	-16	4	36	0
LC18	2	4	398	111	-19	9	573	0
LC19	495	587	-15	2	751	108	2	0
LC20	80	47	-157	3	199	245	1	0
LC21	4	94	-202	5	30	442	0	0
LC22	2	8	-227	265	1	0	38	0
LC23	1	2	289	126	-1	-2	659	0

Soffit gages - minimum strain (με)

Load Case	S1	S2	S3	S4	S5	S6	S7	S8
LC4	-1	0	-369	-32	-1	-32	-15	1269
LC5	1	1	-333	-29	1	-13	-27	3208
LC6	-7	-9	-392	-25	-5	-1	-49	5613
LC7	-4	-12	-420	0	-14	-12	-15	8180
LC8	-2	2	-480	-67	-16	-23	-3	8931
LC9	0	-1	-872	-43	-1	-45	-21	0
LC10	0	-6	-1225	-39	1	-4	-38	0
LC11	-6	-10	-1514	-34	-4	0	-66	0
LC12	-4	-16	-1630	1	-11	-14	-15	0
LC13	-2	2	-1710	-82	-8	-30	-2	0
LC14	0	0	-64	-52	-1	-52	-27	0
LC15	3	-6	-106	-46	-7	1	-48	0
LC16	-5	0	-213	-39	-15	2	-79	0
LC17	-4	-18	-257	-9	-29	-16	-9	0
LC18	-2	-2	-123	-97	-31	-33	-3	0
LC19	0	-1	-114	-60	0	-61	-30	0

Soffit gages - minimum strain (με)

Load Case	S1	S2	S3	S4	S5	S6	S7	S8
LC20	3	-7	-249	-50	3	-1	-58	0
LC21	-6	-6	-291	-43	-2	-3	-93	0
LC22	-5	-27	-314	-3	-12	-19	-22	0
LC23	-3	-5	-304	-111	-13	-42	-4	0

Girder gages – maximum strain (με)

Load Case	B1	B2	B3	B4
LC4	129	97	42	1
LC5	145	120	67	4
LC6	108	128	94	9
LC7	17	80	126	57
LC8	5	45	94	100
LC9	172	127	55	2
LC10	195	161	90	5
LC11	149	170	124	10
LC12	26	107	168	75
LC13	10	58	123	133
LC14	212	158	70	3
LC15	236	199	114	9
LC16	183	209	155	14
LC17	32	129	207	99
LC18	14	75	155	163
LC19	243	183	82	3
LC20	267	230	133	9
LC21	206	239	177	14
LC22	35	150	237	107
LC23	13	81	172	187

Girder gages – minimum strain (με)

Load Case	B1	B2	B3	B4
LC4	-3	-1	-1	0
LC5	-3	-1	-1	0
LC6	-2	0	0	1
LC7	-3	-1	-1	1
LC8	-3	0	-1	1
LC9	-1	-2	-1	-1
LC10	0	-2	-1	-1
LC11	1	-1	-2	-1
LC12	0	-1	-2	0
LC13	0	0	-1	1
LC14	-1	-1	0	0
LC15	3	1	0	0
LC16	3	1	0	1

Girder gages – minimum strain (με)

Load Case	B1	B2	B3	B4
LC17	2	2	1	2
LC18	2	3	2	2
LC19	-1	-2	0	-1
LC20	3	-2	0	-1
LC21	3	0	-1	-1
LC22	0	-1	-1	-1
LC23	-1	0	-1	-1

Web gages – principal strains for LC 20 (με)		
Rosette	emax	emin
R1	217	-227
R2	22	-78
R3	41	-69
R4	10	-10
R5	273	-320
R6	99	-53
R7	27	-29
R8	10	-11

Web gages – maximum principal strains (με)

Load Case	R1	R2	R3	R4	R5	R6	R7	R8
LC4	196	230	11	5	307	236	11	4
LC5	184	32	19	6	240	83	15	5
LC6	73	57	43	9	10	90	33	6
LC7	94	22	26	99	3	38	35	106
LC8	105	15	369	295	1	19	279	289
LC9	217	315	14	6	293	303	23	7
LC10	226	32	26	8	290	105	35	7
LC11	46	74	55	11	15	117	51	9
LC12	17	26	30	136	14	60	73	134
LC13	5687	102	300	329	159	31	770	346
LC14	234	313	19	9	372	353	14	8
LC15	227	19	34	16	282	101	17	9
LC16	57	89	66	18	17	140	81	11
LC17	19	30	27	215	14	72	69	231
LC18	16	28	297	408	8	42	328	397
LC19	262	283	21	7	431	392	14	12
LC20	217	22	41	10	273	99	27	10
LC21	55	106	73	15	20	160	95	12
LC22	19	36	38	197	15	87	89	212
LC23	13	31	369	427	10	48	358	412

Web gages – minimum principal strains (με)

Load Case	R1	R2	R3	R4	R5	R6	R7	R8
LC4	-385	-363	-21	-7	-423	-274	-17	-5
LC5	-177	-73	-32	-7	-295	-59	-24	-6
LC6	-7	-92	-51	-7	-26	-55	-41	-7
LC7	-11	-5	-38	-120	-15	-5	-38	-119
LC8	-14	-3	-519	-360	-17	-4	-358	-334
LC9	-492	-330	-29	-8	-502	-361	-27	-7
LC10	-248	-84	-47	-8	-334	-64	-41	-8
LC11	-5	-120	-72	-9	-23	-70	-68	-9
LC12	3	-8	-55	-162	-5	-2	-68	-152
LC13	-974	-76	-497	-408	-32	-5	-931	-394
LC14	-535	-352	-37	-11	-559	-379	-19	-9
LC15	-247	-77	-57	-14	-335	-57	-22	-10
LC16	-9	-141	-84	-13	-32	-85	-66	-11
LC17	1	-5	-79	-246	-13	-4	-41	-258
LC18	0	-3	-548	-493	-6	-4	-373	-455
LC19	-566	-370	-42	-10	-593	-386	-21	-19
LC20	-227	-78	-69	-10	-320	-53	-29	-11
LC21	-10	-165	-97	-11	-36	-97	-74	-12
LC22	0	-5	-71	-227	-7	-4	-26	-240
LC23	-1	0	-606	-524	-6	0	-431	-484

LVDT – maximum displacement (in.)

Load case	D1	Load case	D1	Load case	D1	Load case	D1
LC4	0.0049	LC9	0.0010	LC14	0.0025	LC19	0.0025
LC5	0.0056	LC10	0.0030	LC15	0.0065	LC20	0.0073
LC6	0.0087	LC11	0.0087	LC16	0.0149	LC21	0.0162
LC7	0.0008	LC12	-0.0013	LC17	0.0028	LC22	0.0046
LC8	-0.0002	LC13	0.0118	LC18	0.0005	LC23	-0.0001

LVDT – minimum displacement (in.)

Load case	D1 (in.)	Load case	D1 (in.)	Load case	D1 (in.)	Load case	D1 (in.)
LC4	-0.0039	LC9	-0.0007	LC14	0.0000	LC19	-0.0008
LC5	-0.0033	LC10	-0.0057	LC15	0.0007	LC20	0.0004
LC6	-0.0009	LC11	-0.0043	LC16	-0.0012	LC21	-0.0020
LC7	-0.0097	LC12	-0.0130	LC17	-0.0052	LC22	-0.0065
LC8	-0.0479	LC13	-0.0852	LC18	-0.0762	LC23	-0.0858

Appendix B – 2010 Bridge Test

Soffit gages - maximum strain (με)

Load Case	S1	S2	S3	S4	S5	S6	S7	S8
LC4	321	383	2	1	529	65	0	1
LC5	111	33	2	2	190	122	0	1
LC6	14	62	9	6	27	347	0	1
LC7	2	6	31	255	5	9	20	71
LC8	4	4	429	75	10	0	376	403
LC9	443	494	11	1	687	87	1	8
LC10	114	38	1	1	174	230	1	1
LC11	18	58	11	5	35	415	8	8
LC12	5	2	62	230	13	2	56	176
LC13	3	4	544	95	6	1	470	482
LC14	513	574	1	2	792	107	1	1
LC15	147	45	8	6	249	205	9	1
LC16	7	182	26	7	27	435	4	9
LC17	0	3	81	126	0	0	65	236
LC18	3	7	637	127	15	0	596	413
LC19	631	665	1	1	852	123	1	0
LC20	165	52	5	2	262	256	1	1
LC21	20	201	24	5	43	618	6	0
LC22	2	1	53	223	2	4	58	229
LC23	3	2	755	121	2	1	640	575

Soffit gages - minimum strain (με)

Load Case	S1	S2	S3	S4	S5	S6	S7	S8
LC4	-2	-1	-9	-32	-1	-58	-15	-7
LC5	1	-11	-17	-27	3	-42	-30	-9
LC6	-14	-6	-40	-23	-2	-3	-54	-10
LC7	-10	-32	-16	2	-2	-17	-23	-4
LC8	-5	-10	-1	-89	-4	-30	-2	0
LC9	-2	-3	-11	-41	-1	-79	-18	-9
LC10	1	-15	-25	-35	2	-23	-43	-12
LC11	-13	-14	-47	-31	-6	0	-68	-13
LC12	-12	-34	-16	-52	-4	-22	-14	0
LC13	-6	-13	-1	-115	-7	-40	-1	0
LC14	-2	-2	-13	-48	-1	-92	-23	-10
LC15	1	-19	-25	-40	0	-2	-46	-14
LC16	-20	-4	-50	-33	-4	0	-80	-17
LC17	-13	-30	-6	-49	-7	-31	-1	0
LC18	-6	-12	-1	-118	-8	-48	-2	3
LC19	-2	-2	-17	-57	-1	-106	-27	-13

LC20	2	-14	-33	-47	0	-8	-57	-17
LC21	-22	-5	-67	-40	-5	0	-98	-21
LC22	-16	-42	-16	-45	-7	-32	-7	-1
LC23	-7	-19	-5	-163	-11	-55	-1	-2

Girder gages – maximum strain (με)

Load Case	B1	B2	B3	B4
LC4	158	106	57	2
LC5	175	127	81	3
LC6	135	137	109	7
LC7	22	96	151	51
LC8	10	57	123	91
LC9	208	136	70	2
LC10	231	172	110	5
LC11	177	183	145	11
LC12	26	122	198	74
LC13	9	72	168	125
LC14	252	166	75	2
LC15	280	208	119	6
LC16	186	223	174	13
LC17	22	139	222	97
LC18	11	85	202	158
LC19	284	192	85	2
LC20	321	240	139	8
LC21	240	258	201	15
LC22	31	167	260	108
LC23	11	103	207	177

Girder gages – minimum strain (με)

Load Case	B1	B2	B3	B4
LC4	-2	-2	5	-1
LC5	-1	-3	9	-1
LC6	5	-2	10	-1
LC7	3	-2	10	-2
LC8	2	-3	11	-2
LC9	-2	-5	1	-1
LC10	0	-4	9	-1
LC11	1	-3	11	-1
LC12	3	-1	13	-2
LC13	1	-4	23	-3
LC14	-3	-6	0	-2
LC15	-1	-2	2	-2
LC16	-2	-6	-1	-1
LC17	-4	-10	0	-3

LC18	3	-8	32	-4
LC19	-3	-3	0	-2
LC20	0	-7	0	-4
LC21	0	-9	-1	-2
LC22	-1	-5	1	-3
LC23	-2	-1	2	-4

LVDT – maximum displacement (in.)

Load case	D1	Load case	D1	Load case	D1	Load case	D1
LC4	0.0011	LC9	0.0013	LC14	0.0014	LC19	0.0016
LC5	0.0022	LC10	0.0034	LC15	0.0034	LC20	0.0045
LC6	0.0050	LC11	0.0067	LC16	0.0076	LC21	0.0091
LC7	0.0034	LC12	0.0030	LC17	0.0017	LC22	0.0028
LC8	0.0000	LC13	0.0001	LC18	0.0000	LC23	0.0000

LVDT – maximum displacement (in.)

Load case	D1	Load case	D1	Load case	D1	Load case	D1
LC4	-0.0039	LC9	-0.0007	LC14	0.0000	LC19	-0.0008
LC5	-0.0033	LC10	-0.0057	LC15	0.0007	LC20	0.0004
LC6	-0.0009	LC11	-0.0043	LC16	-0.0012	LC21	-0.0020
LC7	-0.0097	LC12	-0.0130	LC17	-0.0052	LC22	-0.0065
LC8	-0.0479	LC13	-0.0852	LC18	-0.0762	LC23	-0.0858

Lane one impact factors (strain in με)

	LC 4A	TP1		TP2		TP3	
	Strain	Strain	Impact Factor	Strain	Impact Factor	Strain	Impact Factor
B1	191	156	1.22	172	1.11	132	1.44
B2	130	106	1.23	127	1.02	137	0.95
S5	121	507	0.24	193	0.63	8	14.34
S6	192	31	6.23	126	1.52	330	0.58

Lane two impact factors (strain in με)

	LC8A	TP4		TP5	
	Strain	Strain	Impact Factor	Strain	Impact Factor
D1	0.02 in.	0.00 in.	8.48	0.04 in.	0.70
B2	97	96	1.01	57	1.71
B3	183	169	1.08	141	1.29
B4	98	57	1.73	96	1.02
S3	519	14	36.88	453	1.15
S7	475	-17	-28.59	376	1.26
S8	239	57	4.21	395	0.6

Appendix C – Data Conversion

Bridge monitoring data were collected at 200 Hz (one data point every 5 milliseconds). The subject bridge was instrumented with 17 sensors (8 FRP strain gages, 4 steel strain gages, one displacement gage and 4 thermocouples). Data were recorded continuously at 200 Hz at all strain and deflection gage locations and at least 16 -17 hours per day. Temperature was recorded at a 10 Hz sampling rate. Data could not be recorded and written to the flash drive at the same time, causing the DAQ to stop recording for few hours to write data. Data recording stopped for 6 – 7 hours per day, creating gaps in the data record.

Data were recorded in the form of binary files. Binary data were converted into TDMS (Technical Data Management Streaming) using a TDMS converter utility written in LabVIEW by FDOT programmers. This was done to store the binary data in a more efficient way. To convert the TDMS data into presentable format, TDMS files were converted into the ASCII (.csv) format. A program was written in LABVIEW to perform the conversion from TDMS to .csv. Both converters (Binary to TDMS and TDMS to ASCII) were capable of performing batch operations. After data were converted into .csv files, they were imported into MATLAB to generate the plots.

Monitoring data were arranged in chronological order on monthly basis. Monthly data were processed through TDMS and LabVIEW converter to generate .csv files. Monthly data were imported in MATLAB. To generate the monthly plots, data were downsampled to 5 Hz. The way downsampling was performed in MATLAB was by plotting every 40^{th} data point (downsampling rate of 5 Hz). Bridge monitoring started in the middle of the October 2009 and continued through April 2011.

Raw data collected at the bridge site were in the form of binary files. Each file contained one hour of data for all strain and displacement channels. These binary files were converted to TDMS files utilizing a TDMS converter program capable of performing batch conversions that was written by FDOT personnel. Processing time for monthly data was approximately 2-3 hours per file.

TDMS files were converted to .csv files using the LABVIEW converter. The LABVIEW converter was capable of performing batch operations. This was done by storing the TDMS files

in a single folder and processing with the LABVIEW converter. The time required to convert TDMS files to .csv files was approximately 2 -3 hours per month of a data.

To present the data in the form of the plots, .csv files were imported into MATLAB. The MATLAB routine imported data from the first file into memory, downsampled the data to 5 Hz, plotted the data, cleared the memory and moved to the next file. This sequence was repeated for subsequent files until all files in the folder had been processed. Specific instructions had to be followed during this procedure:

- Create a folder "Month_YY_Binary" and place all of the binary files in this folder to be processed.
- Process the "Month_YY_Binary" folder through the TDMS converter by following the TDMS converter user guide. The TDMS converter provides an option to create a folder where the user wants to keep all TDMS files. At this step create a folder "Month_YY_TDMS" and place the converted TDMS files into this folder (refer to the TDMS converter instructions for a more detail description)
- Process the "Month_YY_TDMS" folder through the LABVIEW converter to produce the .csv files. The LABVIEW converter also provides an option to create a folder where the user wants to keep all .csv files. Otherwise, LABVIEW converter by default will create a folder "Month_YY_TDMS_CSV" and will keep all .csv files in this folder.
- Place the MATLAB routine in the "Month_YY_TDMS_CSV" folder with a text file (belleglade_data.txt) containing the name of all files from a particular month. It is important to have this file in the MATLAB routine folder or the routine will not work.
- Go into the MATLAB routine (Engine_Month_5Hz_all_channels.m) and modify the information inside the "datenum" function with the year, month and date. It can be modified for one channel then copied and pasted for the others.
- Modify the month legend with the desired month and year. This can be done by hitting CTRL + F and replacing the existing month with the desired month.
- Type "dir" in the MATLAB command window, it produces the name of all the files in that folder. Copy and paste all the files in the "belleglade_data.text", delete the extra items and make the text file looks like the example text file.

- Test the code for couple of files.
- Hit the green arrow button in MATLAB and be patient. Approximately 7 hours of processing are required for a month of a data.
- The MATLAB routine processes all the data and saves the figure as .emf (enhanced metafile) and places them in the same directory.
- For reports, import .emf into Word by using the “Insert” command. Select the appropriate “picture” from file.

Appendix D – Time-History Plots

From the plots presented below, the functionality of different sensors can be determined. Monitoring of the bridge was started immediately after the first bridge test conducted in October 2009. The plots are for October 2009 to April 2011; due to some technical problem data were not recorded for the three months period from July 2010 to September 2010. After resolving the technical issues with the Data Acquisition System, monitoring was restarted in October 2010 after the second bridge test.

It can be observed that FRP gages S2, S6, S7 and LVDT worked fine throughout the one year monitoring period except in late April 2010. For later half of April, these gages did function properly for some reasons. However they started working again in May and continued working till June 2010. Strain gages installed on the steel beams started working in the beginning of the monitoring period but afterward it worked intermittently. During the second bridge test in October 2010, it was found that the connections of the instrumentation wires of the Full Bridge gages (Steel gages) to cRIO were loose. This could be a possible reason for these gages did not function as intended.

It can be observed from the plots that rest f the FRP gages (S1, S3, S4, S5 and S8) did not function properly from the beginning. Gage S3 and S8 were declared dead after the first bridge test. Even though gages S1, S4 and S5 worked during the first bridge test but for some reason they did not work throughout the one year monitoring period.

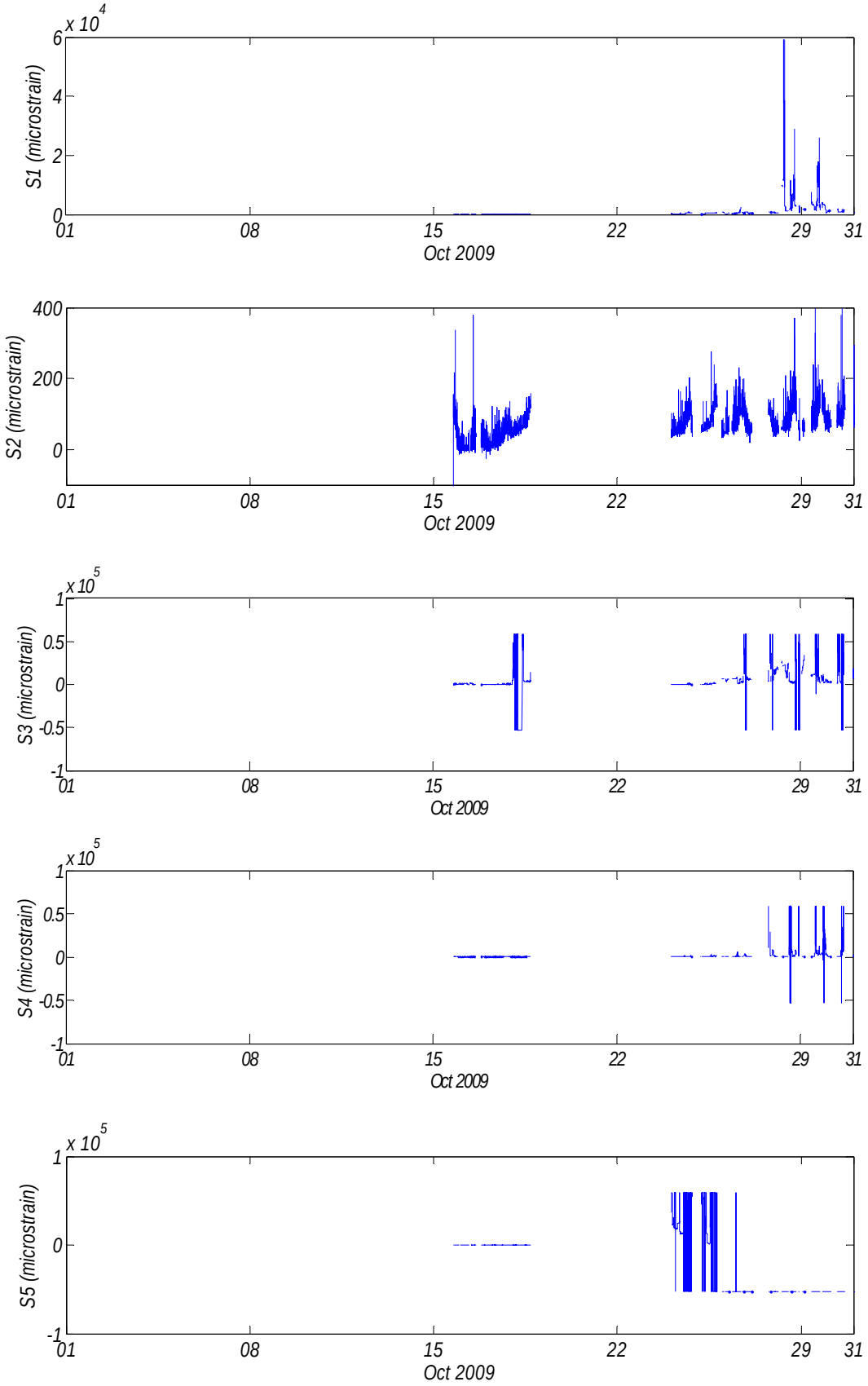
x 10^4
S1 (microstrain)
6
4
2
0
01
08
15
22
29
31
Oct 2009
S2 (microstrain)
400
200
0
Oct 2009
x 10^5
S3 (microstrain)
1
0.5
0
-0.5
-1
Oct 2009
x 10^5
S4 (microstrain)
Oct 2009
x 10^5
S5 (microstrain)
Oct 2009

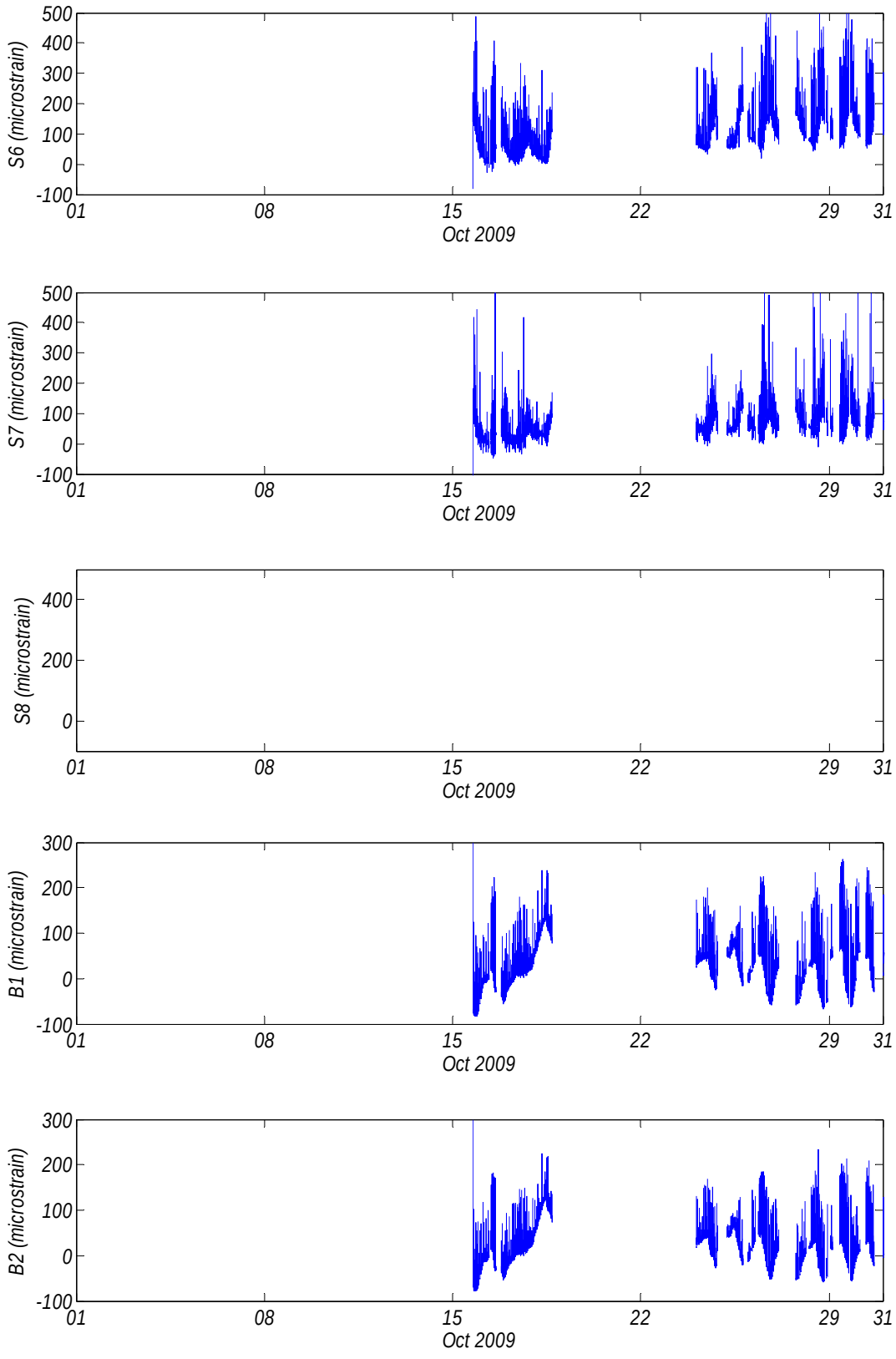
S6 (microstrain)
500
400
300
200
100
0
-100
01
08
15
22
29
31
Oct 2009
S7 (microstrain)
500
400
300
200
100
0
-100
01
08
15
22
29
31
Oct 2009
S8 (microstrain)
400
200
0
01
08
15
22
29
31
Oct 2009
B1 (microstrain)
300
200
100
0
-100
01
08
15
22
29
31
Oct 2009
B2 (microstrain)
300
200
100
0
-100
01
08
15
22
29
31
Oct 2009

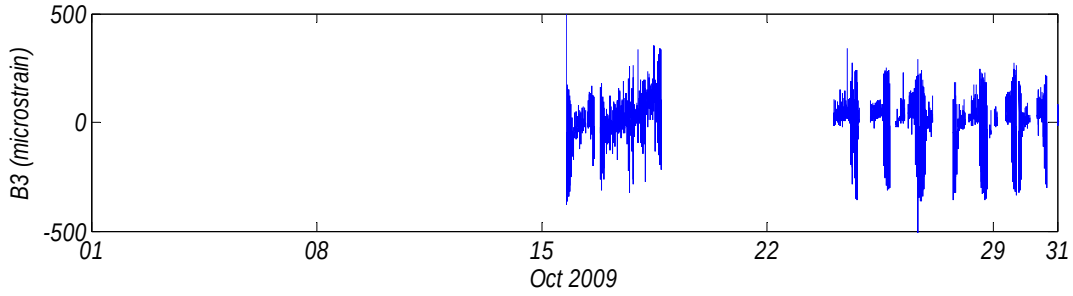
500
0
-500
B3 (microstrain)
01
08
15
22
29
31
Oct 2009

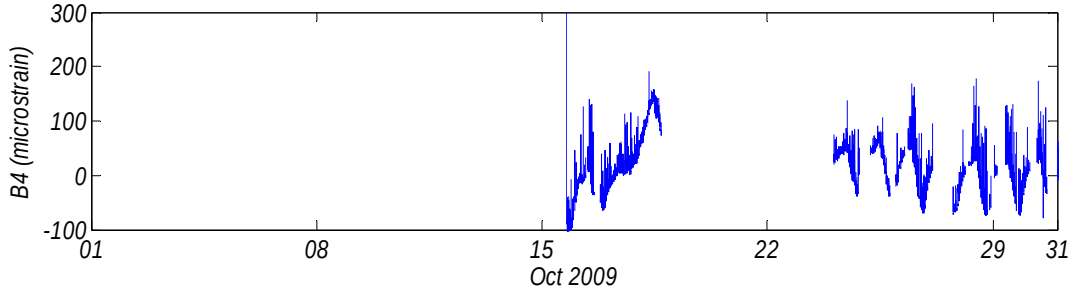
300
200
100
0
-100
B4 (microstrain)
01
08
15
22
29
31
Oct 2009

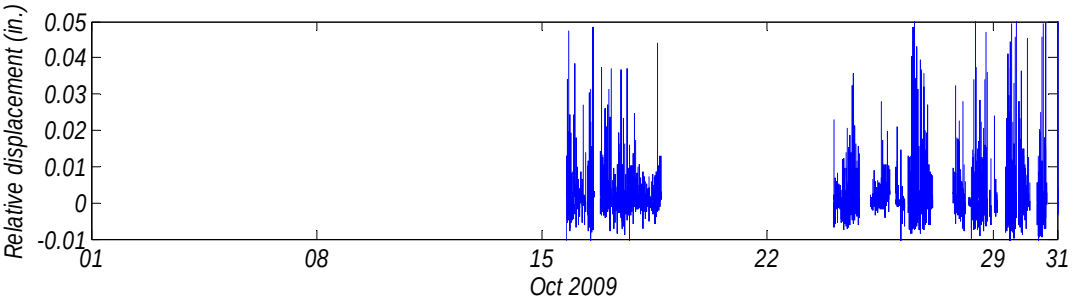
0.05
0.04
0.03
0.02
0.01
0
-0.01
Relative displacement (in.)
01
08
15
22
29
31
Oct 2009

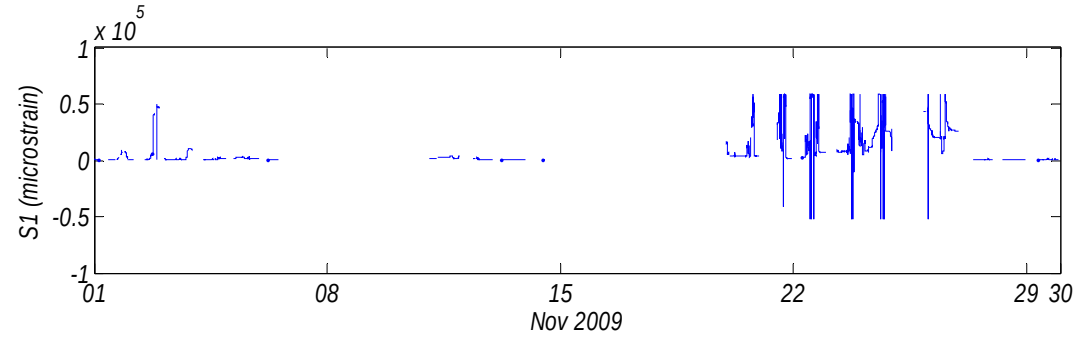
x 10^5
1
0.5
0
-0.5
-1
S1 (microstrain)
01
08
15
22
29 30
Nov 2009

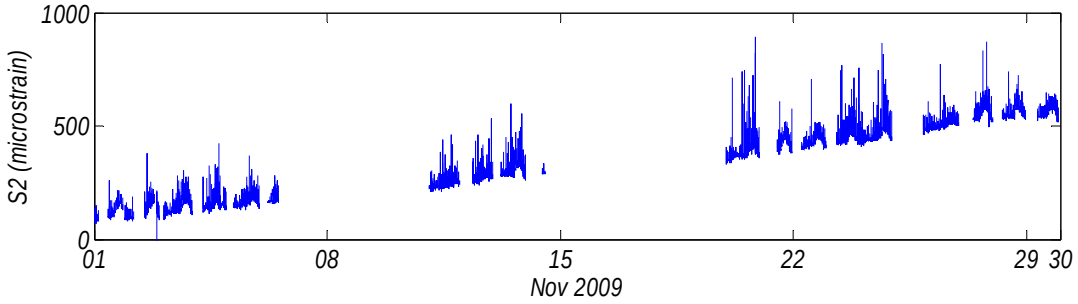
1000
500
0
S2 (microstrain)
01
08
15
22
29 30
Nov 2009

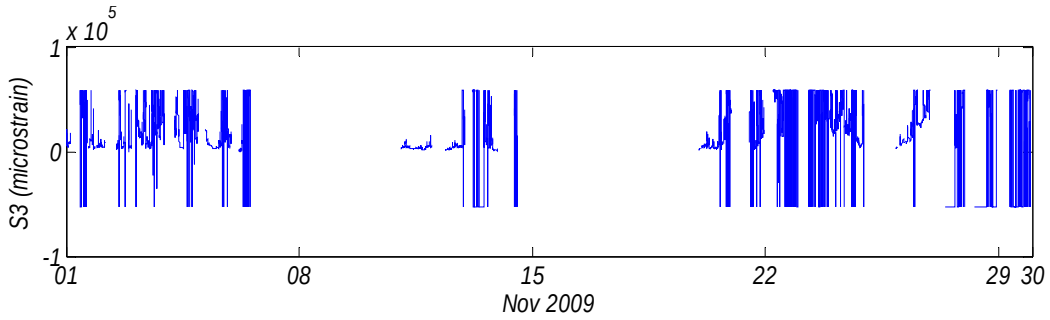
x 10^5
1
0
-1
S3 (microstrain)
01
08
15
22
29 30
Nov 2009

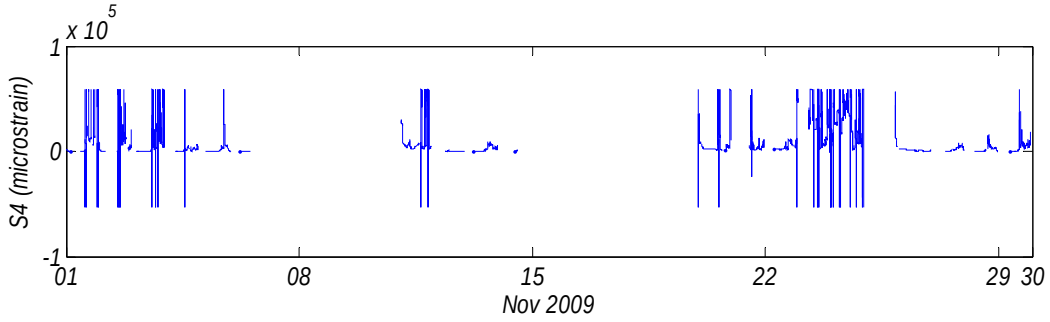
x 10^5
1
0
-1
S4 (microstrain)
01
08
15
22
29 30
Nov 2009

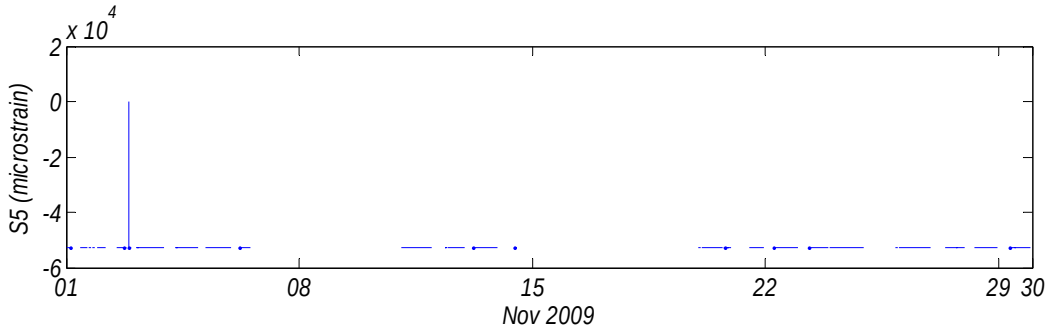
x 10^4
2
0
-2
-4
-6
S5 (microstrain)
01
08
15
22
29 30
Nov 2009

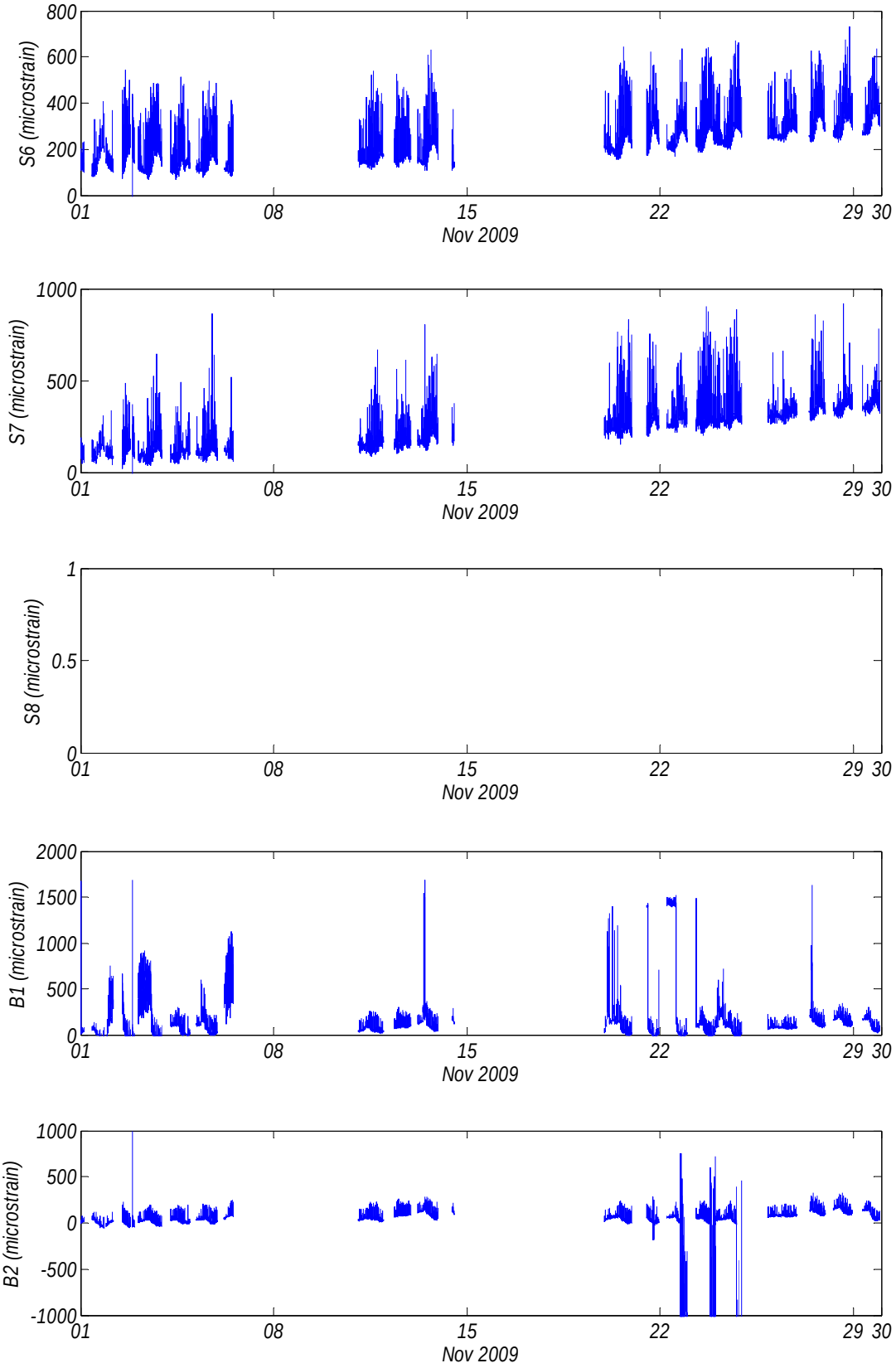
S6 (microstrain)
800
600
400
200
0
01
08
15
22
29
30
Nov 2009
S7 (microstrain)
1000
500
0
01
08
15
22
29
30
Nov 2009
S8 (microstrain)
1
0.5
0
01
08
15
22
29
30
Nov 2009
B1 (microstrain)
2000
1500
1000
500
0
01
08
15
22
29
30
Nov 2009
B2 (microstrain)
1000
500
0
-500
-1000
01
08
15
22
29
30
Nov 2009

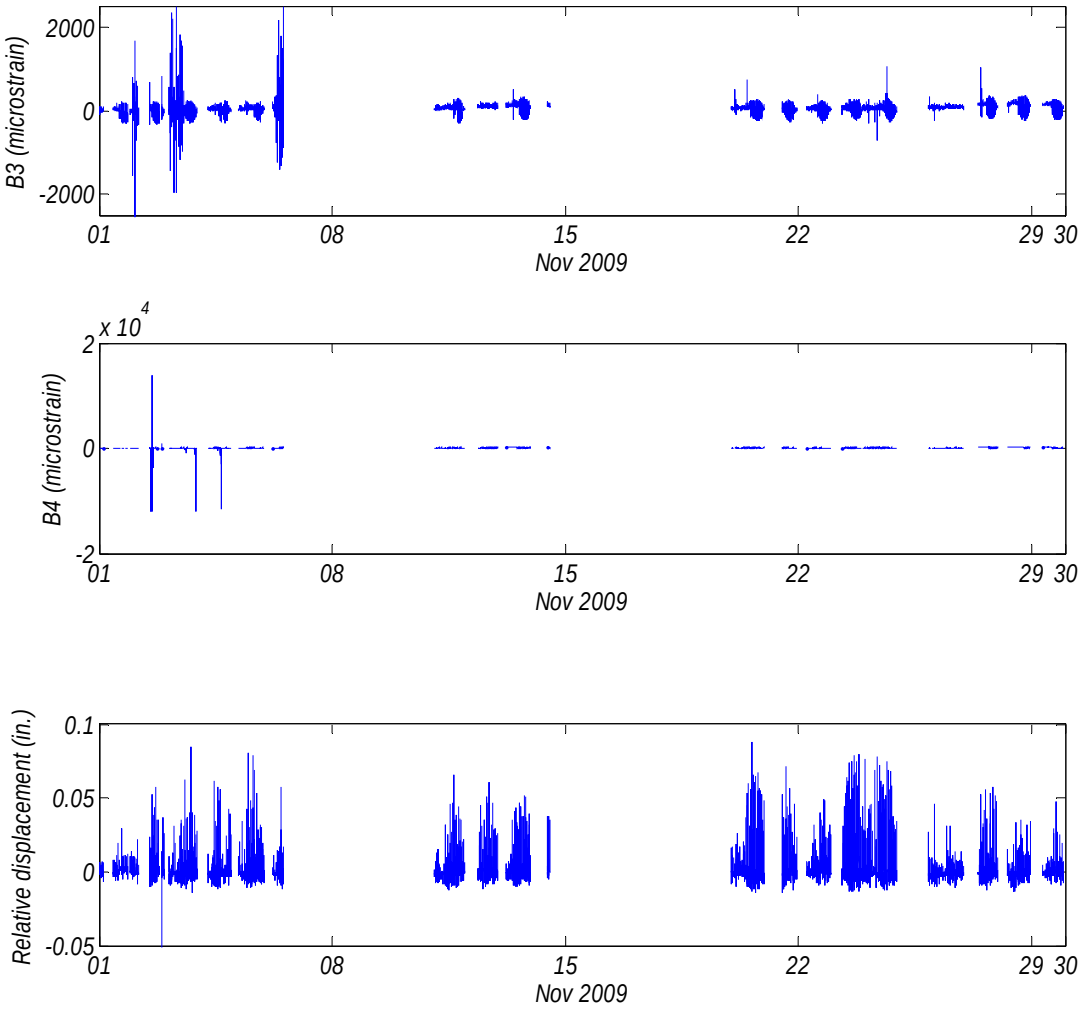
B3 (microstrain)
2000
0
-2000
01
08
15
22
29
30
Nov 2009
x 10^4
B4 (microstrain)
2
0
-2
01
08
15
22
29
30
Nov 2009
Relative displacement (in.)
0.1
0.05
0
-0.05
01
08
15
22
29
30
Nov 2009

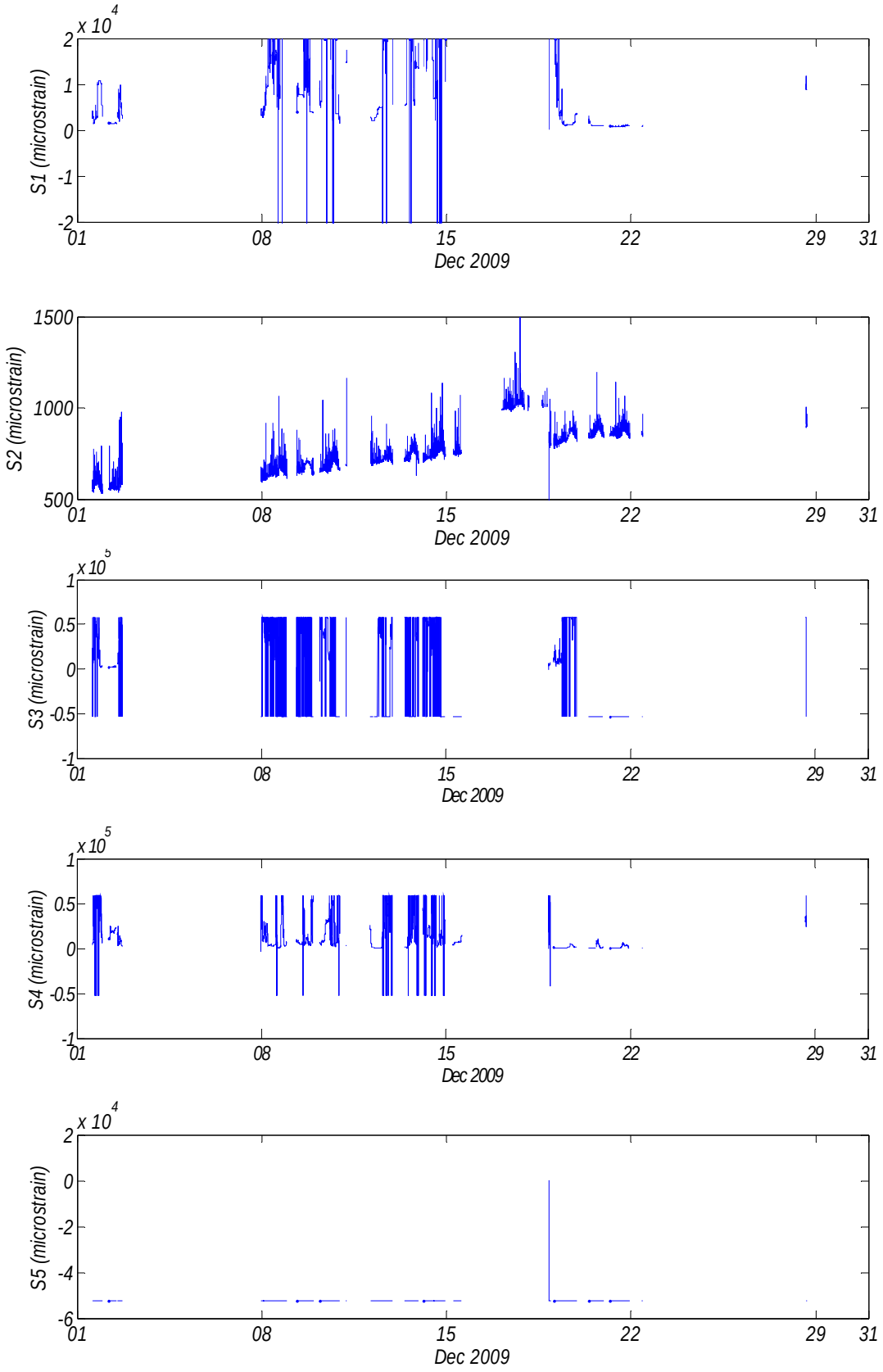
x 10^4
S1 (microstrain)
2
1
0
-1
-2
01
08
15
22
29
31
Dec 2009
S2 (microstrain)
1500
1000
500
Dec 2009
x 10^5
S3 (microstrain)
1
0.5
0
-0.5
-1
Dec 2009
x 10^5
S4 (microstrain)
Dec 2009
x 10^4
S5 (microstrain)
0
-2
-4
-6
Dec 2009

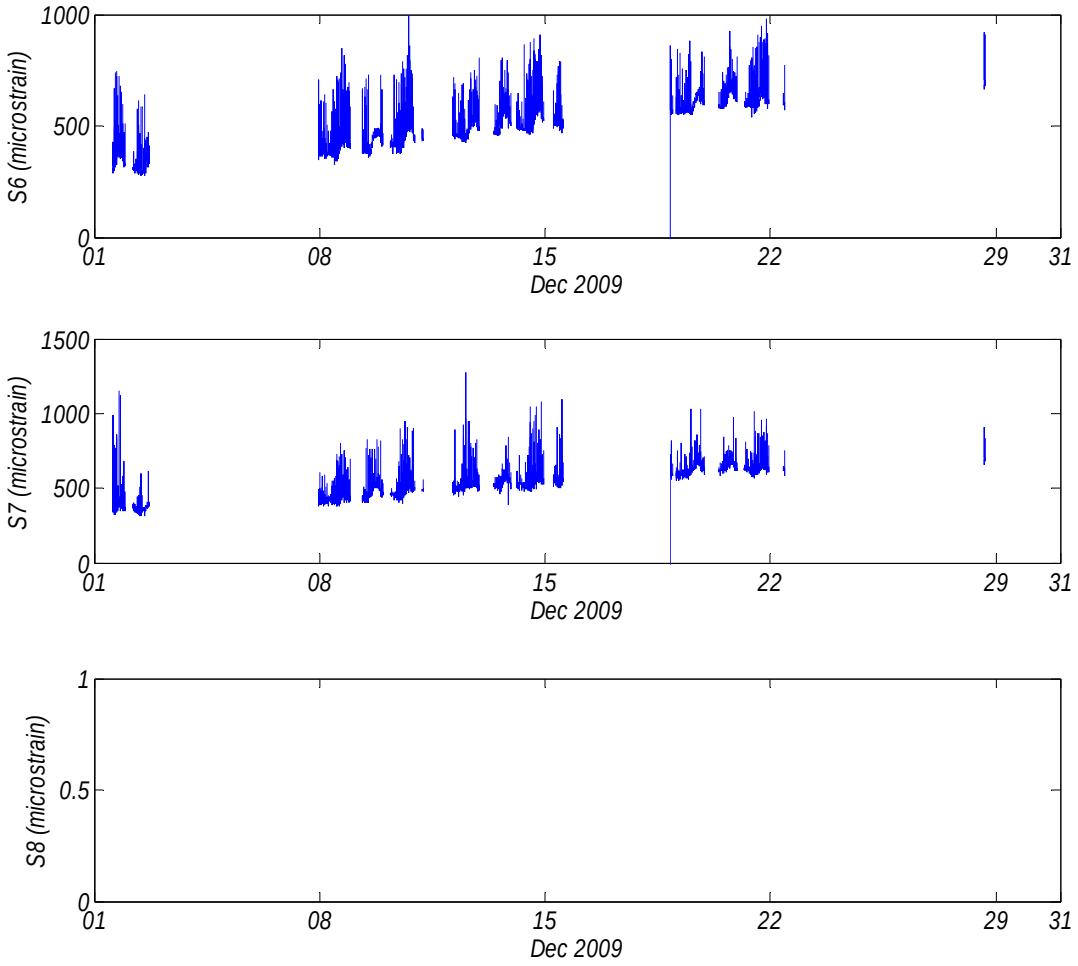
S6 (microstrain)
1000
500
0
01
08
15
22
29
31
Dec 2009
S7 (microstrain)
1500
1000
500
0
01
08
15
22
29
31
Dec 2009
S8 (microstrain)
1
0.5
0
01
08
15
22
29
31
Dec 2009

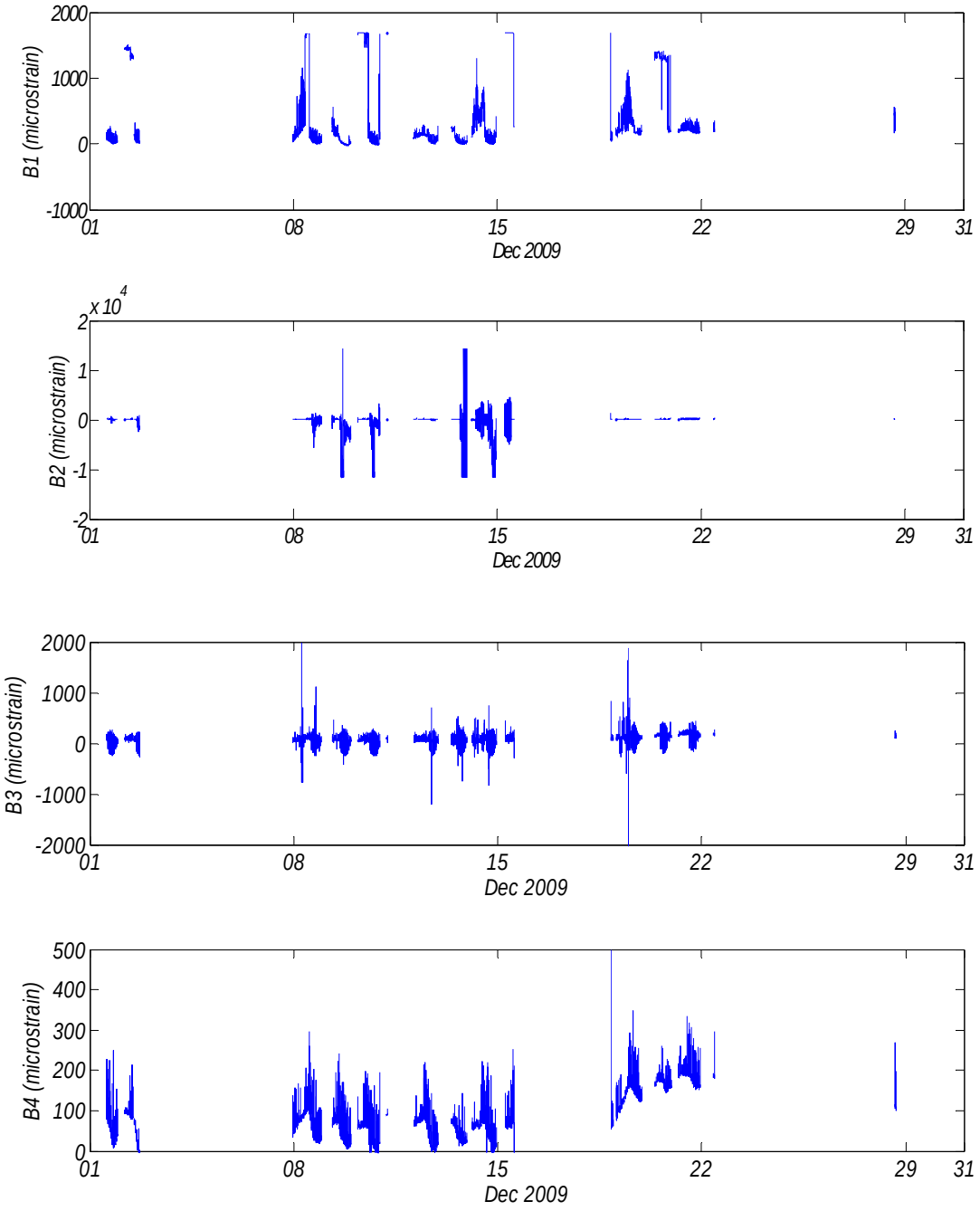
B1 (microstrain)
2000
1000
0
-1000
01
08
15
22
29
31
Dec 2009
x 10^4
B2 (microstrain)
2
1
0
-1
-2
01
08
15
22
29
31
Dec 2009
B3 (microstrain)
2000
1000
0
-1000
-2000
01
08
15
22
29
31
Dec 2009
B4 (microstrain)
500
400
300
200
100
0
01
08
15
22
29
31
Dec 2009

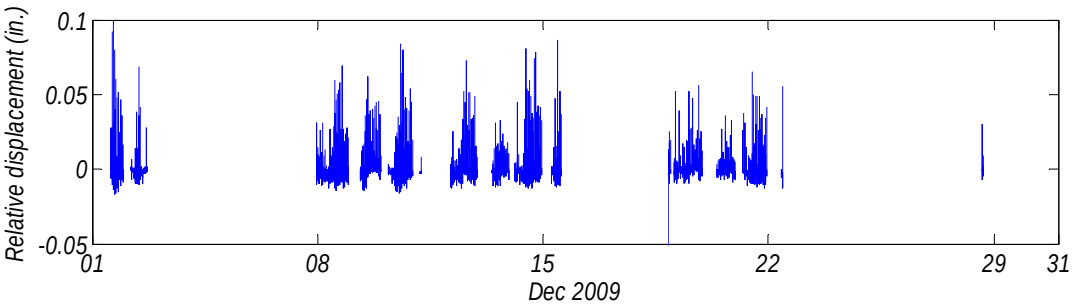
Relative displacement (in.)
0.1
0.05
0
-0.05
01
08
15
22
29
31
Dec 2009

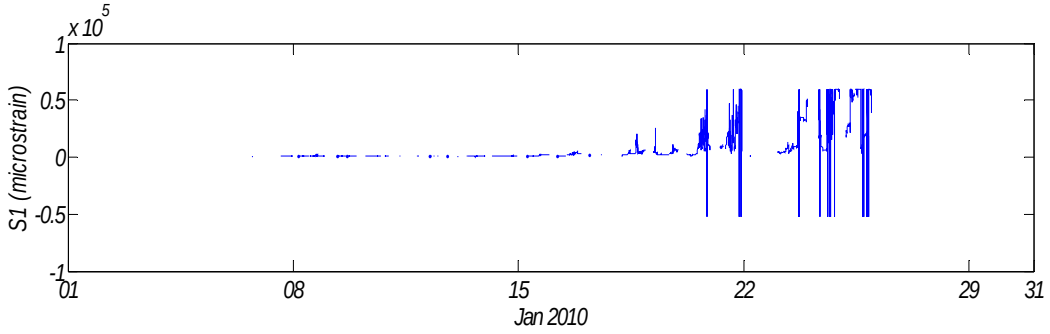
x 10^5
1
0.5
0
-0.5
-1
S1 (microstrain)
01
08
15
22
29
31
Jan 2010

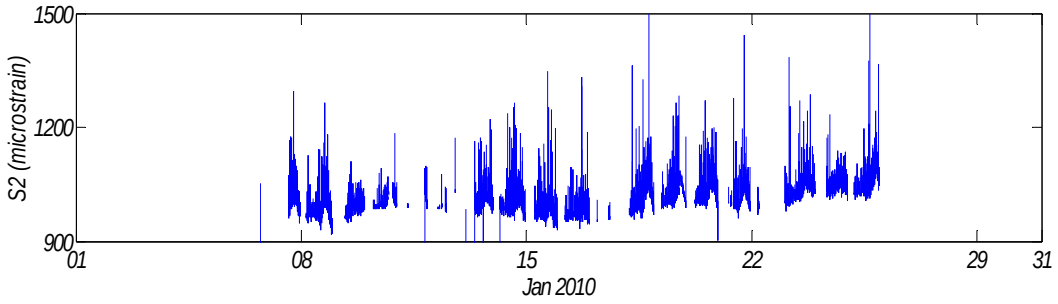
1500
1200
900
S2 (microstrain)
01
08
15
22
29
31
Jan 2010

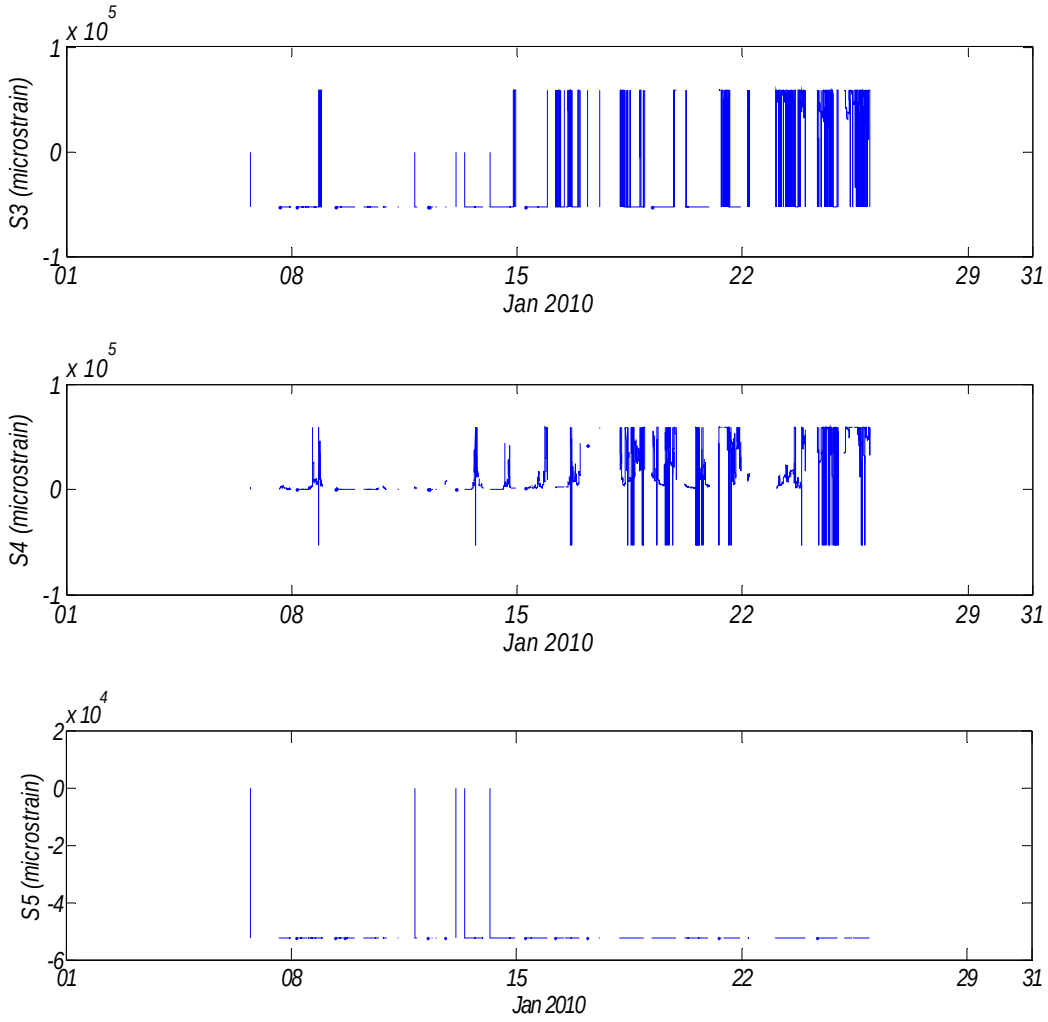
x 10^5
1
0
-1
S3 (microstrain)
01
08
15
22
29
31
Jan 2010
x 10^5
1
0
-1
S4 (microstrain)
01
08
15
22
29
31
Jan 2010
x 10^4
2
0
-2
-4
-6
S5 (microstrain)
01
08
15
22
29
31
Jan 2010

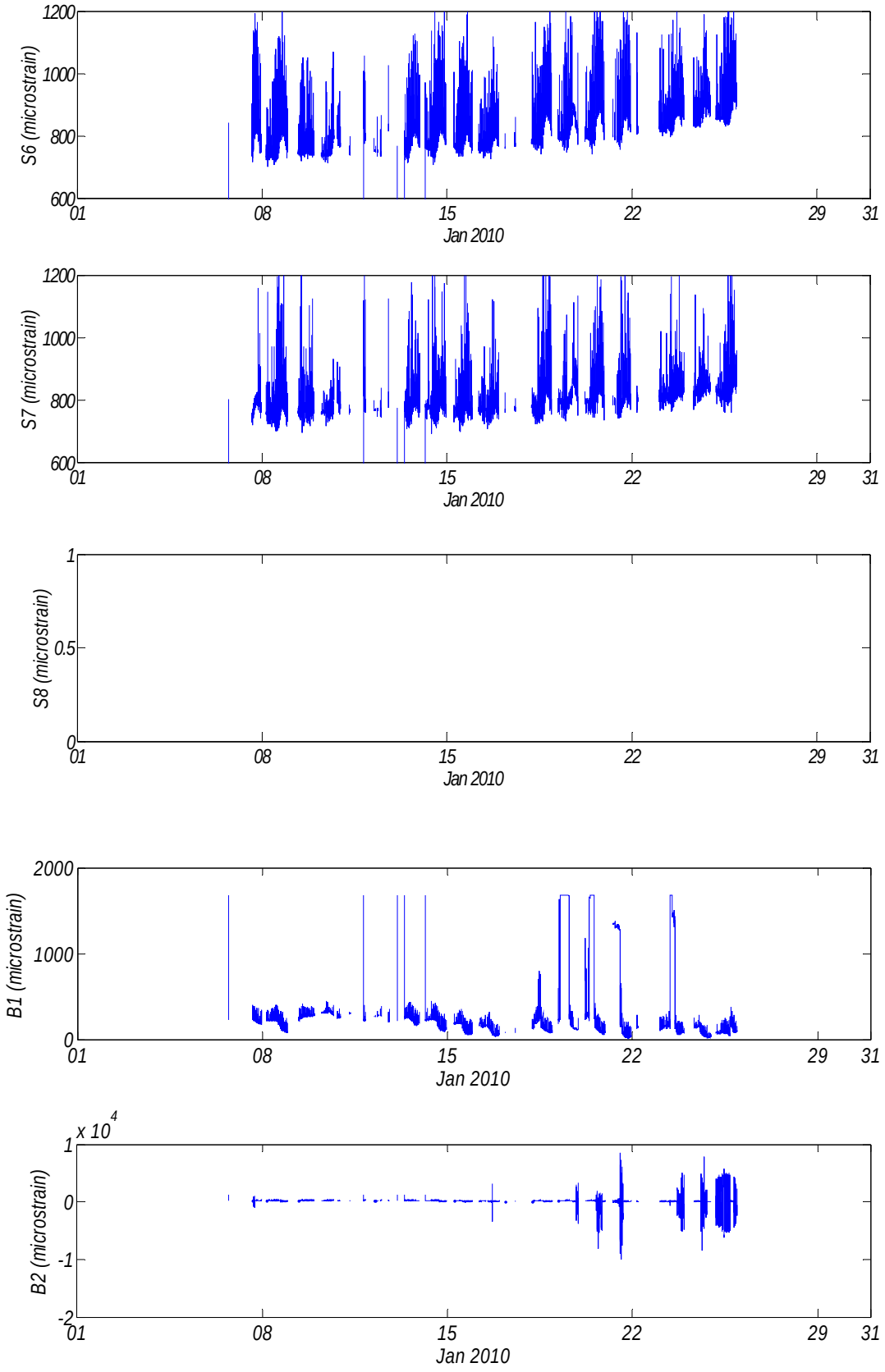
S6 (microstrain)
1200
1000
800
600
01
08
15
22
29
31
Jan 2010
S7 (microstrain)
1200
1000
800
600
01
08
15
22
29
31
Jan 2010
S8 (microstrain)
1
0.5
0
01
08
15
22
29
31
Jan 2010
B1 (microstrain)
2000
1000
0
01
08
15
22
29
31
Jan 2010
x 10^4
B2 (microstrain)
1
0
-1
-2
01
08
15
22
29
31
Jan 2010

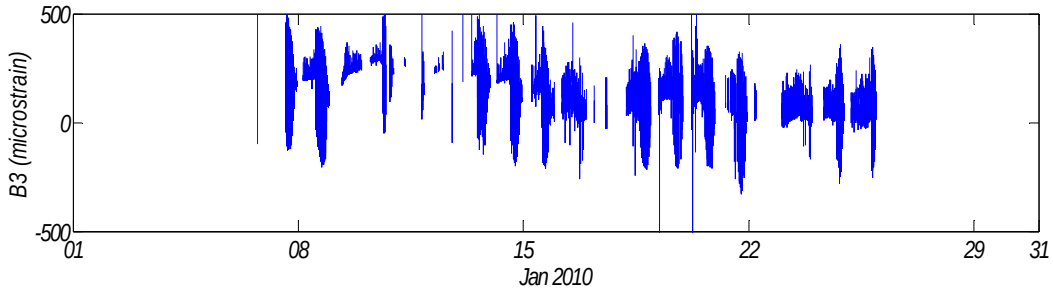
500
0
-500
B3 (microstrain)
01
08
15
22
29
31
Jan 2010

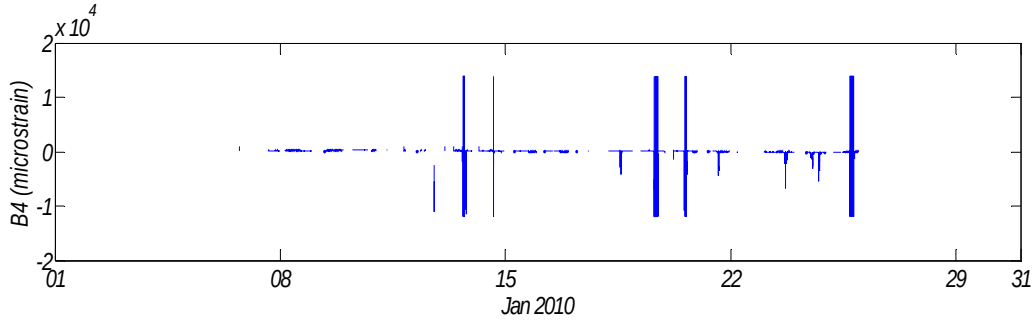
x 10^4
2
1
0
-1
-2
B4 (microstrain)
01
08
15
22
29
31
Jan 2010

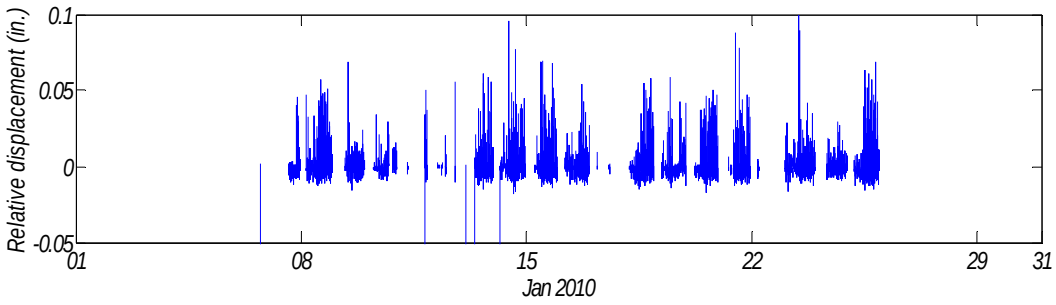
0.1
0.05
0
-0.05
Relative displacement (in.)
01
08
15
22
29
31
Jan 2010

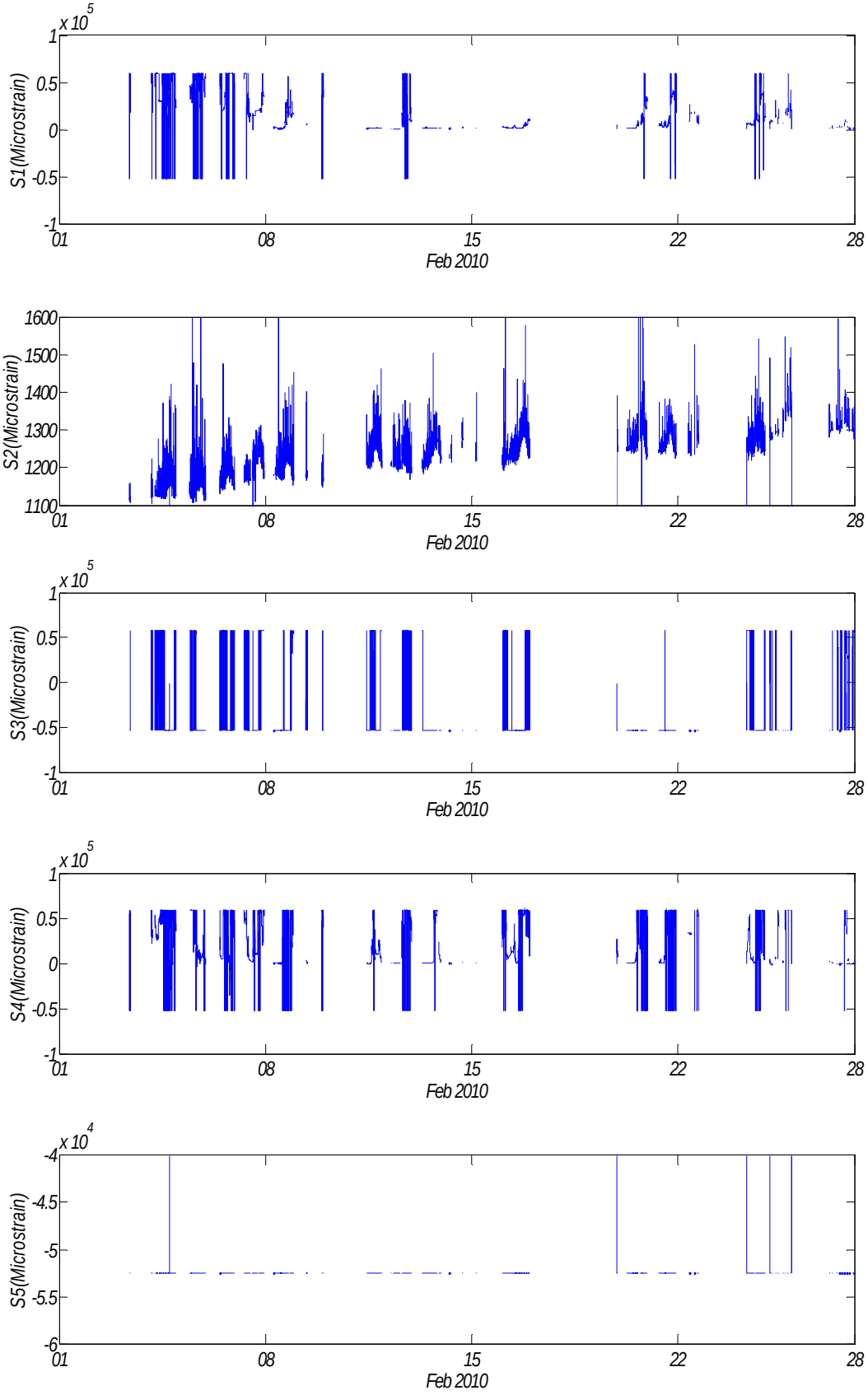
x 10^5
S1(Microstrain)
1
0.5
0
-0.5
-1
01
08
15
22
28
Feb 2010
S2(Microstrain)
1600
1500
1400
1300
1200
1100
Feb 2010
x 10^5
S3(Microstrain)
Feb 2010
x 10^5
S4(Microstrain)
Feb 2010
x 10^4
S5(Microstrain)
-4
-4.5
-5
-5.5
-6
Feb 2010

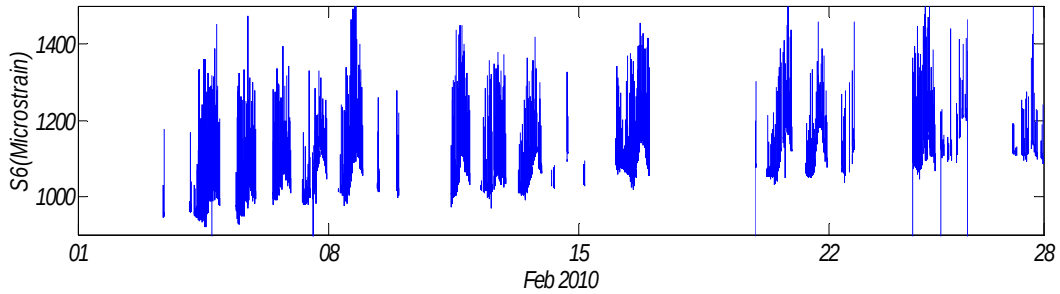
S6(Microstrain)
1400
1200
1000
01
08
15
22
28
Feb 2010

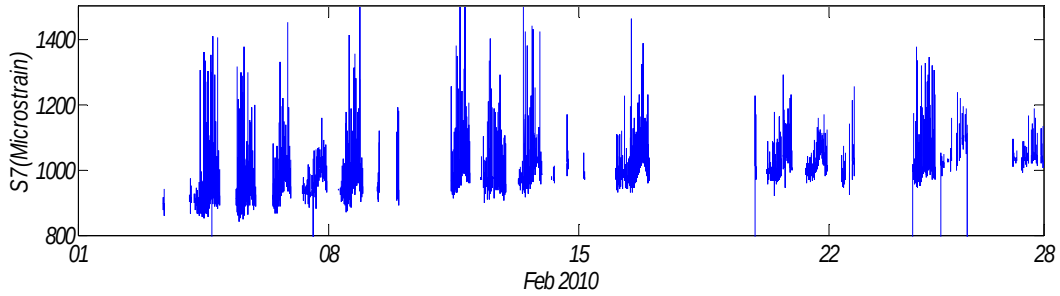
S7(Microstrain)
1400
1200
1000
800
01
08
15
22
28
Feb 2010

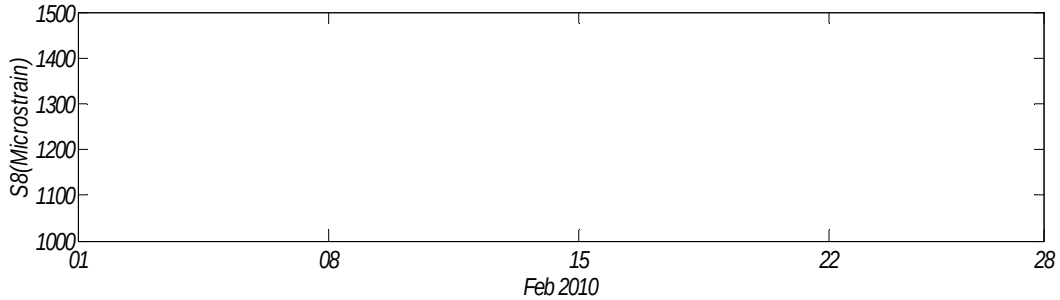
S8(Microstrain)
1500
1400
1300
1200
1100
1000
01
08
15
22
28
Feb 2010

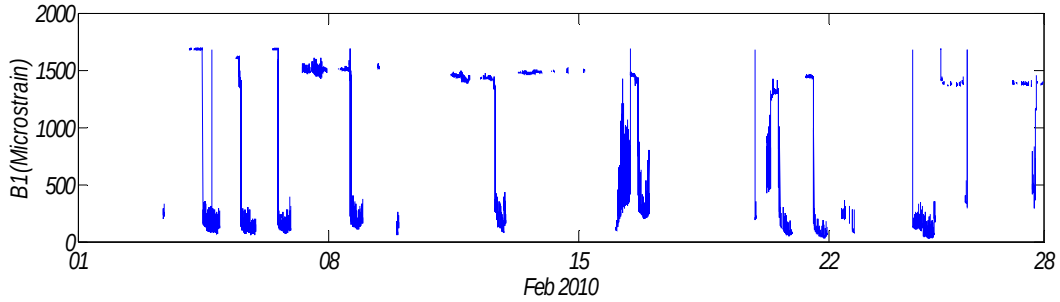
B1(Microstrain)
2000
1500
1000
500
0
01
08
15
22
28
Feb 2010

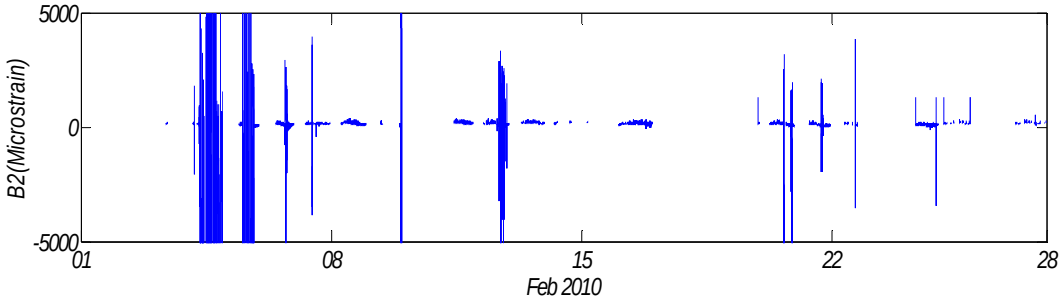
B2(Microstrain)
5000
0
-5000
01
08
15
22
28
Feb 2010

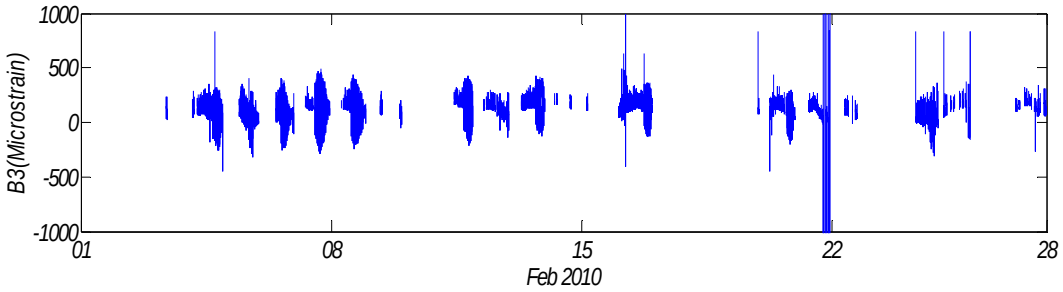
1000
500
0
-500
-1000
B3(Microstrain)
01
08
15
22
28
Feb 2010

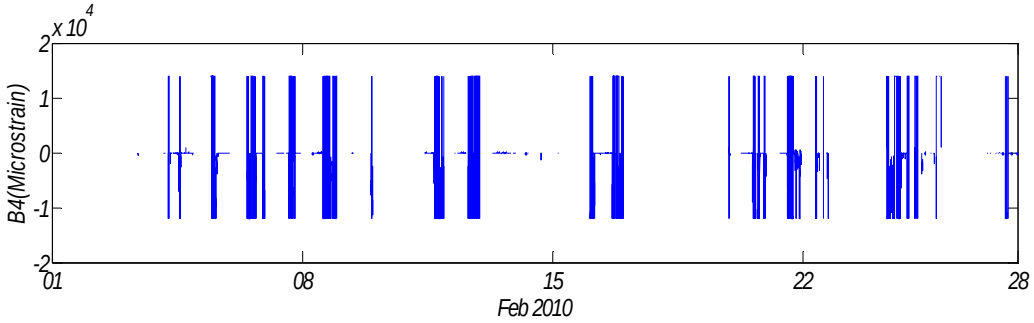
x 10^4
2
1
0
-1
-2
B4(Microstrain)
01
08
15
22
28
Feb 2010

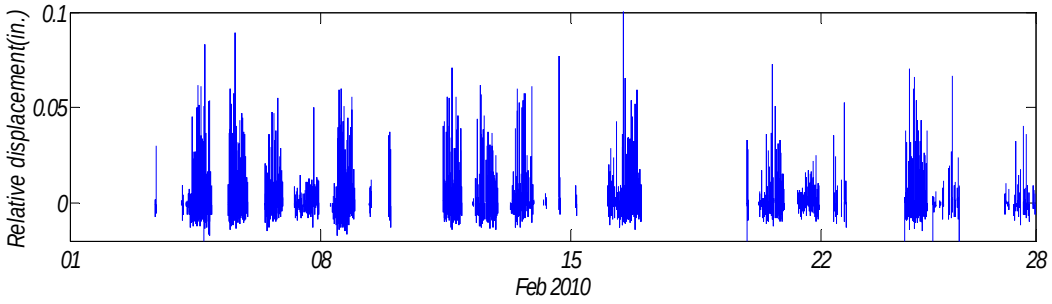
0.1
0.05
0
Relative displacement(in.)
01
08
15
22
28
Feb 2010

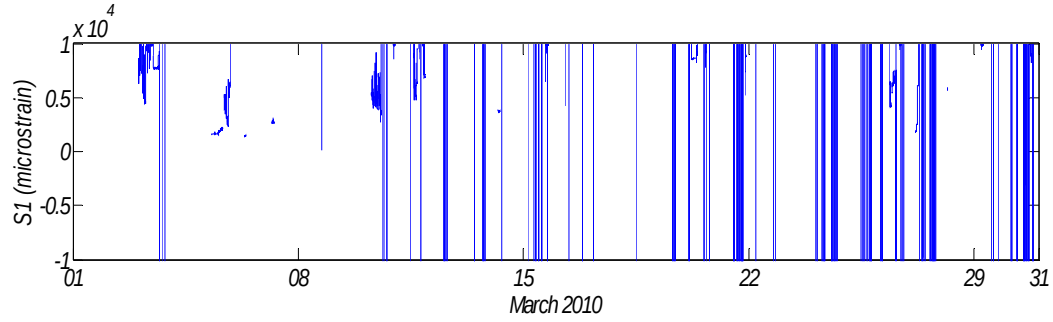
x 10^4
1
0.5
0
-0.5
-1
S1 (microstrain)
01
08
15
22
29
31
March 2010

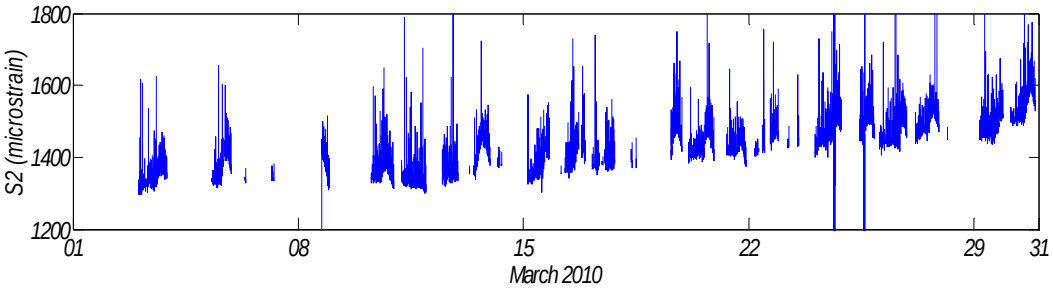
1800
1600
1400
1200
S2 (microstrain)
01
08
15
22
29
31
March 2010

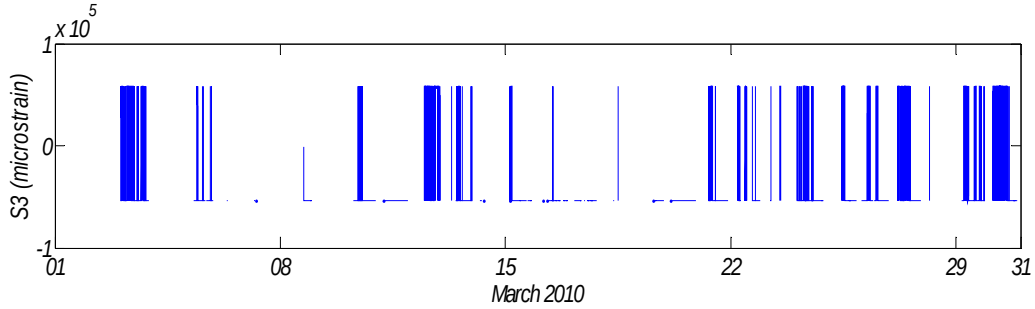
x 10^5
1
0
-1
S3 (microstrain)
01
08
15
22
29
31
March 2010

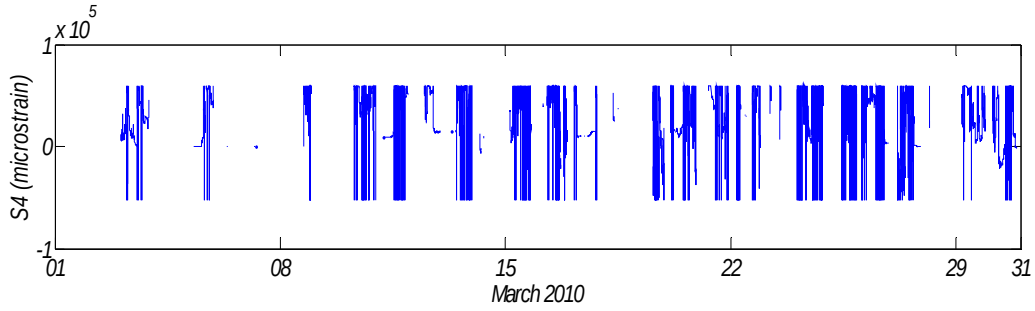
x 10^5
1
0
-1
S4 (microstrain)
01
08
15
22
29
31
March 2010

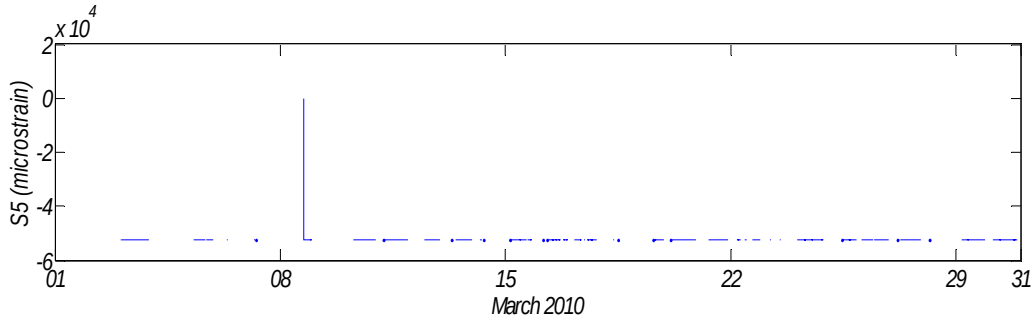
x 10^4
2
0
-2
-4
-6
S5 (microstrain)
01
08
15
22
29
31
March 2010

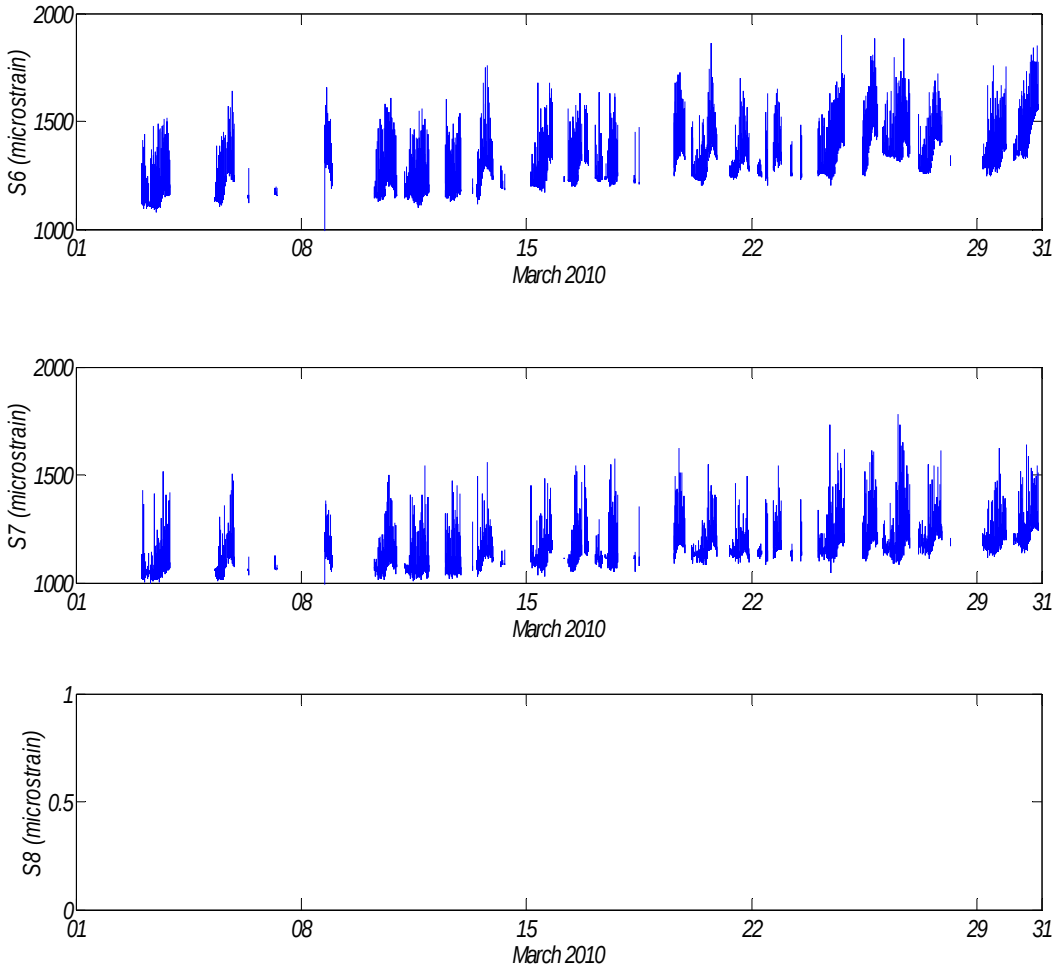
2000
1500
1000
S6 (microstrain)
01
08
15
22
29
31
March 2010
2000
1500
1000
S7 (microstrain)
01
08
15
22
29
31
March 2010
1
0.5
0
S8 (microstrain)
01
08
15
22
29
31
March 2010

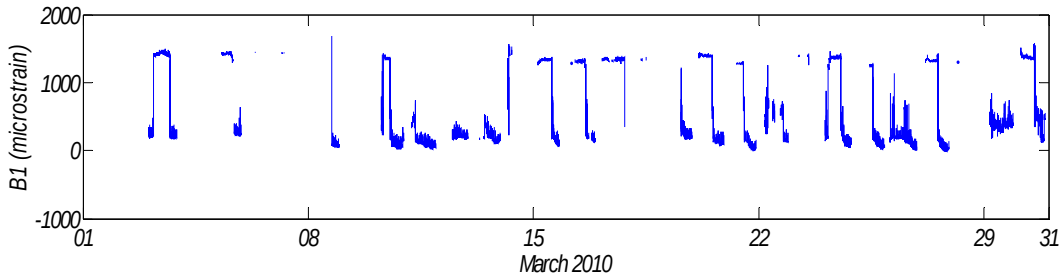
2000
1000
0
-1000
B1 (microstrain)
01
08
15
22
29
31
March 2010

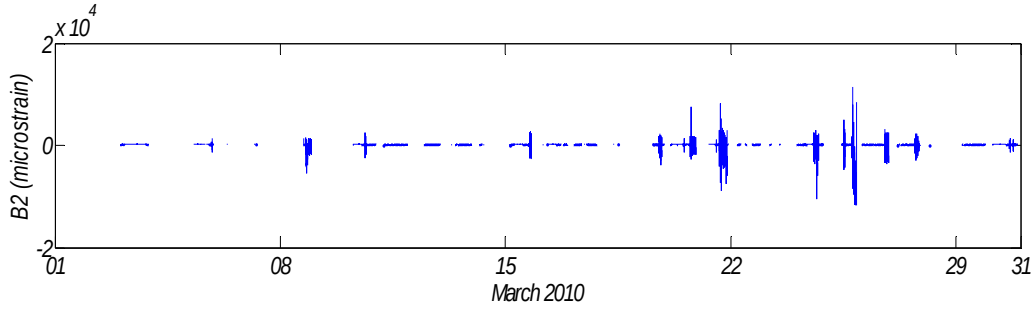
x 10^4
2
0
-2
B2 (microstrain)
01
08
15
22
29
31
March 2010

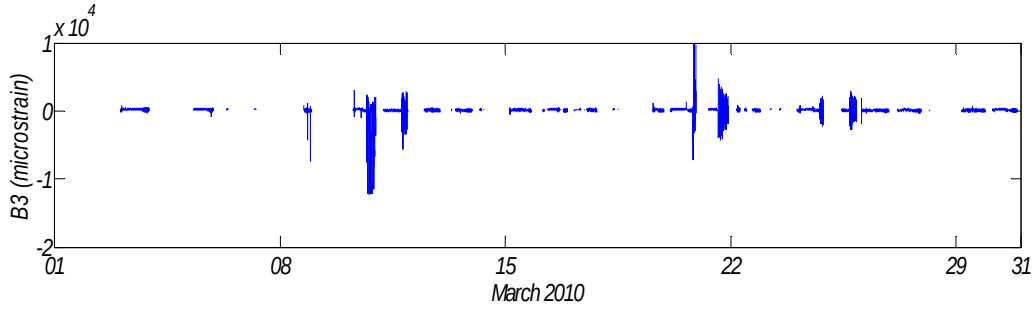
x 10^4
1
0
-1
-2
B3 (microstrain)
01
08
15
22
29
31
March 2010

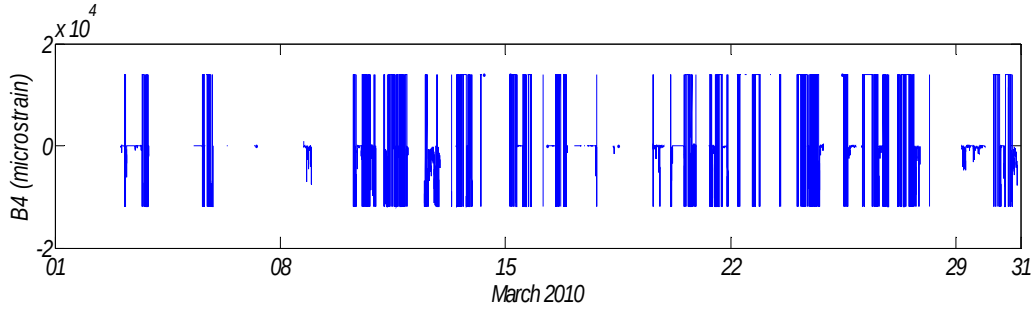
x 10^4
2
0
-2
B4 (microstrain)
01
08
15
22
29
31
March 2010

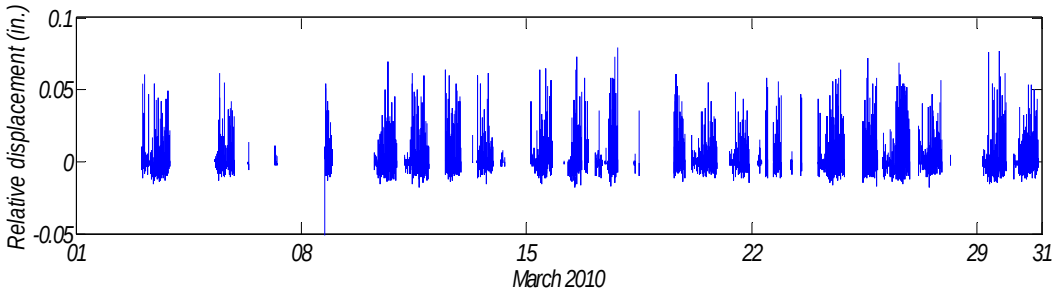
Relative displacement (in.)
0.1
0.05
0
-0.05
01
08
15
22
29
31
March 2010

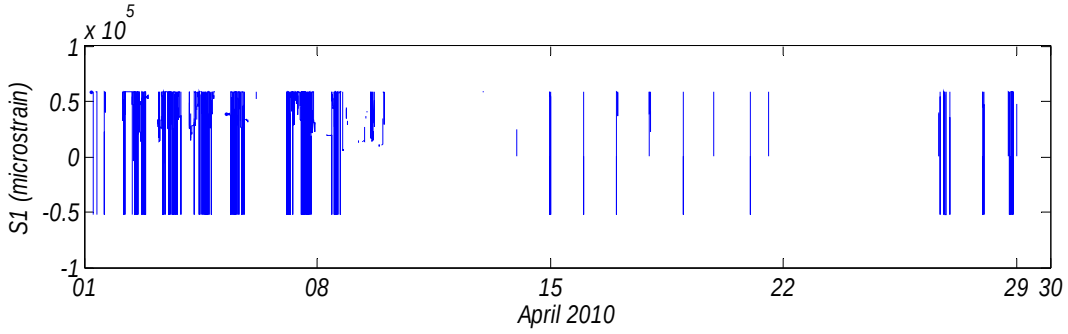
x 10^5
S1 (microstrain)
1
0.5
0
-0.5
-1
01
08
15
22
29
30
April 2010

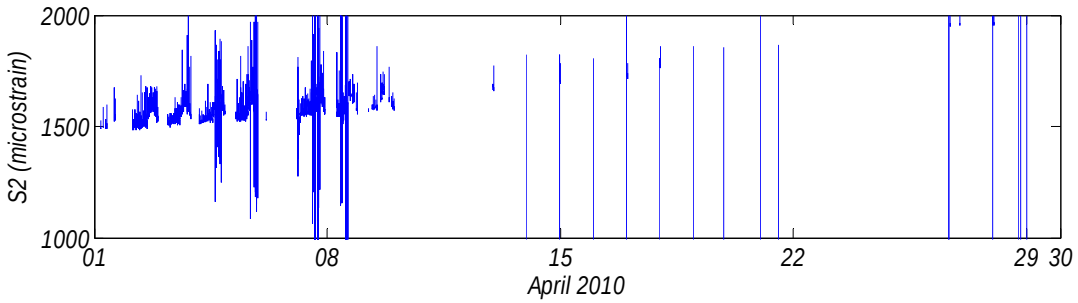
S2 (microstrain)
2000
1500
1000
01
08
15
22
29
30
April 2010

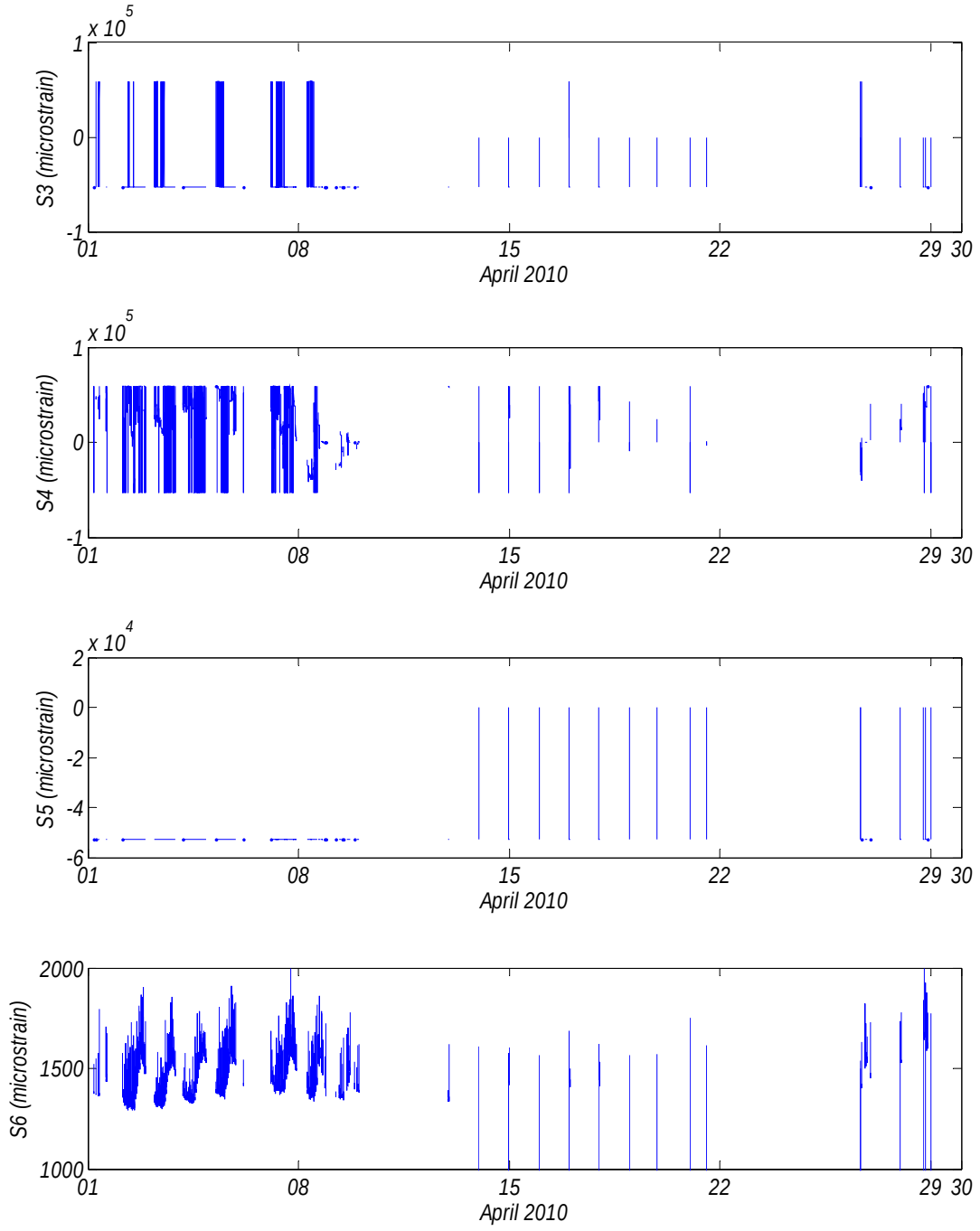
x 10^5
1
0
-1
S3 (microstrain)
01
08
15
22
29
30
April 2010
x 10^5
1
0
-1
S4 (microstrain)
01
08
15
22
29
30
April 2010
x 10^4
2
0
-2
-4
-6
S5 (microstrain)
01
08
15
22
29
30
April 2010
2000
1500
1000
S6 (microstrain)
01
08
15
22
29
30
April 2010

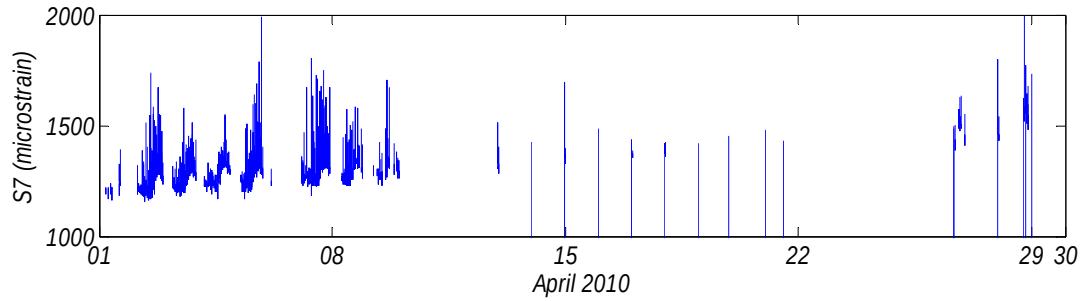
2000
1500
1000
S7 (microstrain)
01
08
15
22
29
30
April 2010

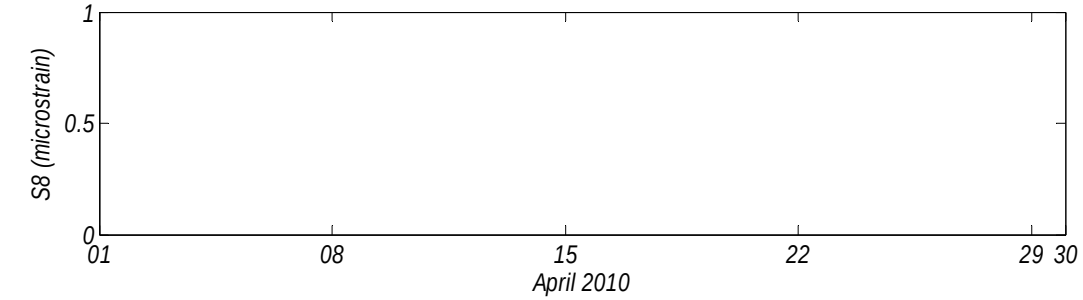
1
0.5
0
S8 (microstrain)
01
08
15
22
29
30
April 2010

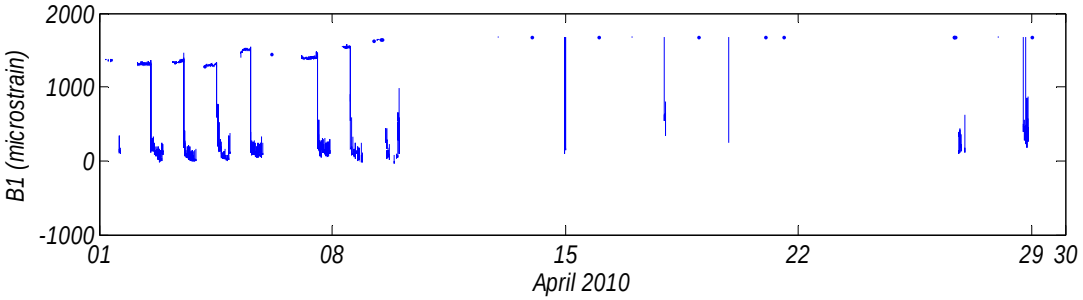
2000
1000
0
-1000
B1 (microstrain)
01
08
15
22
29
30
April 2010

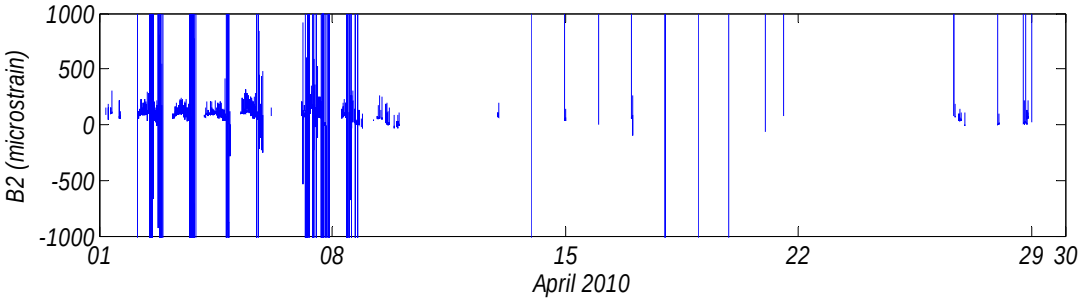
1000
500
0
-500
-1000
B2 (microstrain)
01
08
15
22
29
30
April 2010

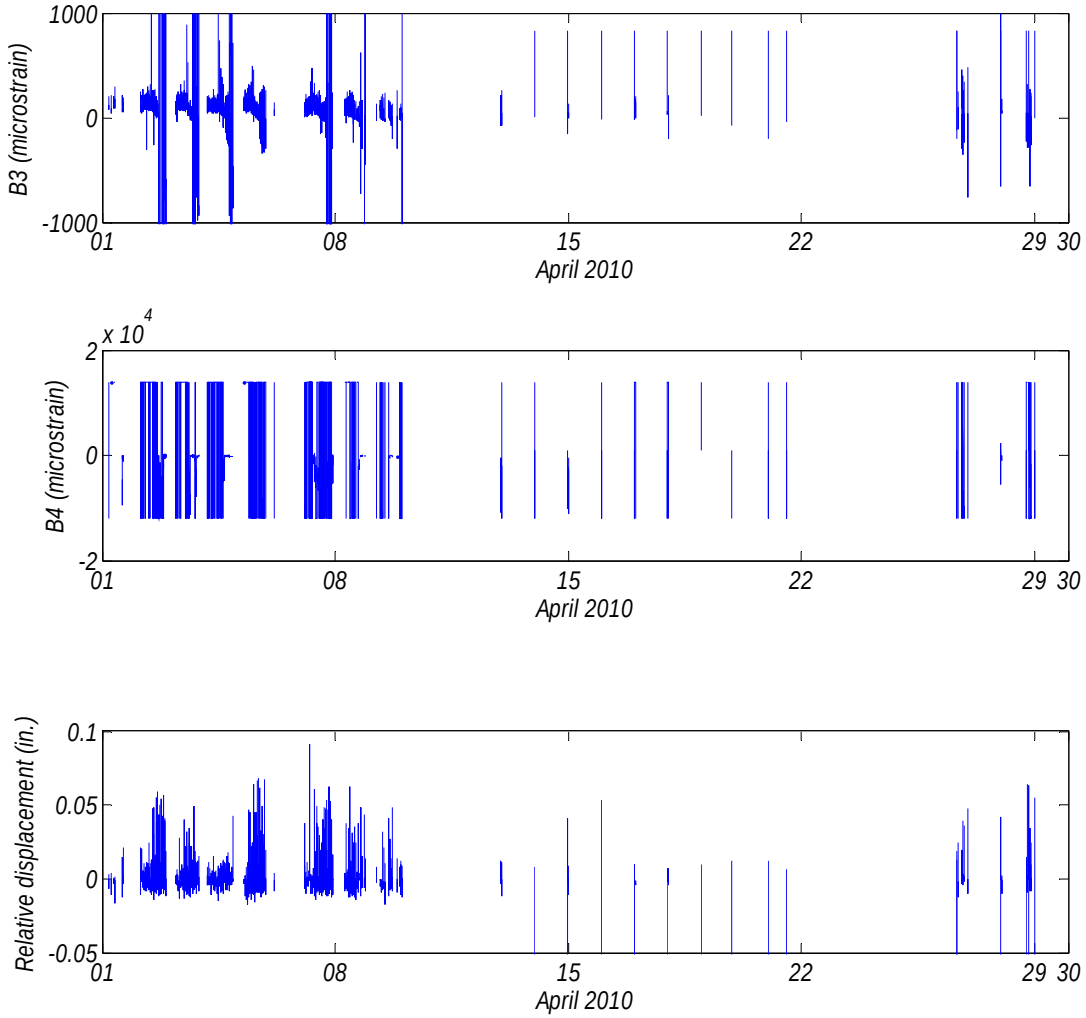
1000
0
-1000
B3 (microstrain)
01
08
15
22
29 30
April 2010
x 10^4
2
0
-2
B4 (microstrain)
01
08
15
22
29 30
April 2010
0.1
0.05
0
-0.05
Relative displacement (in.)
01
08
15
22
29 30
April 2010

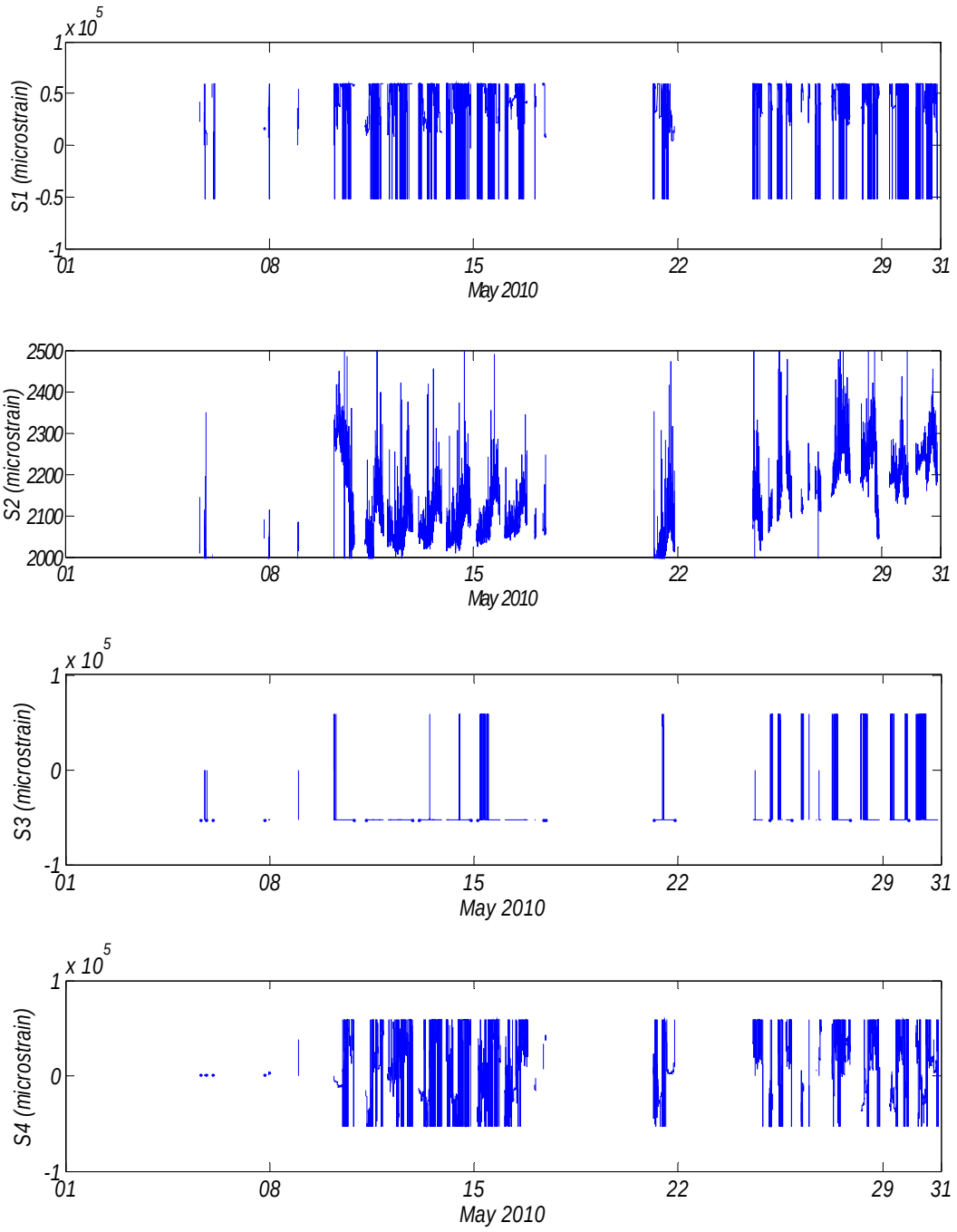
x 10^5
S1 (microstrain)
1
0.5
0
-0.5
-1
01
08
15
22
29
31
May 2010
S2 (microstrain)
2500
2400
2300
2200
2100
2000
S3 (microstrain)
S4 (microstrain)

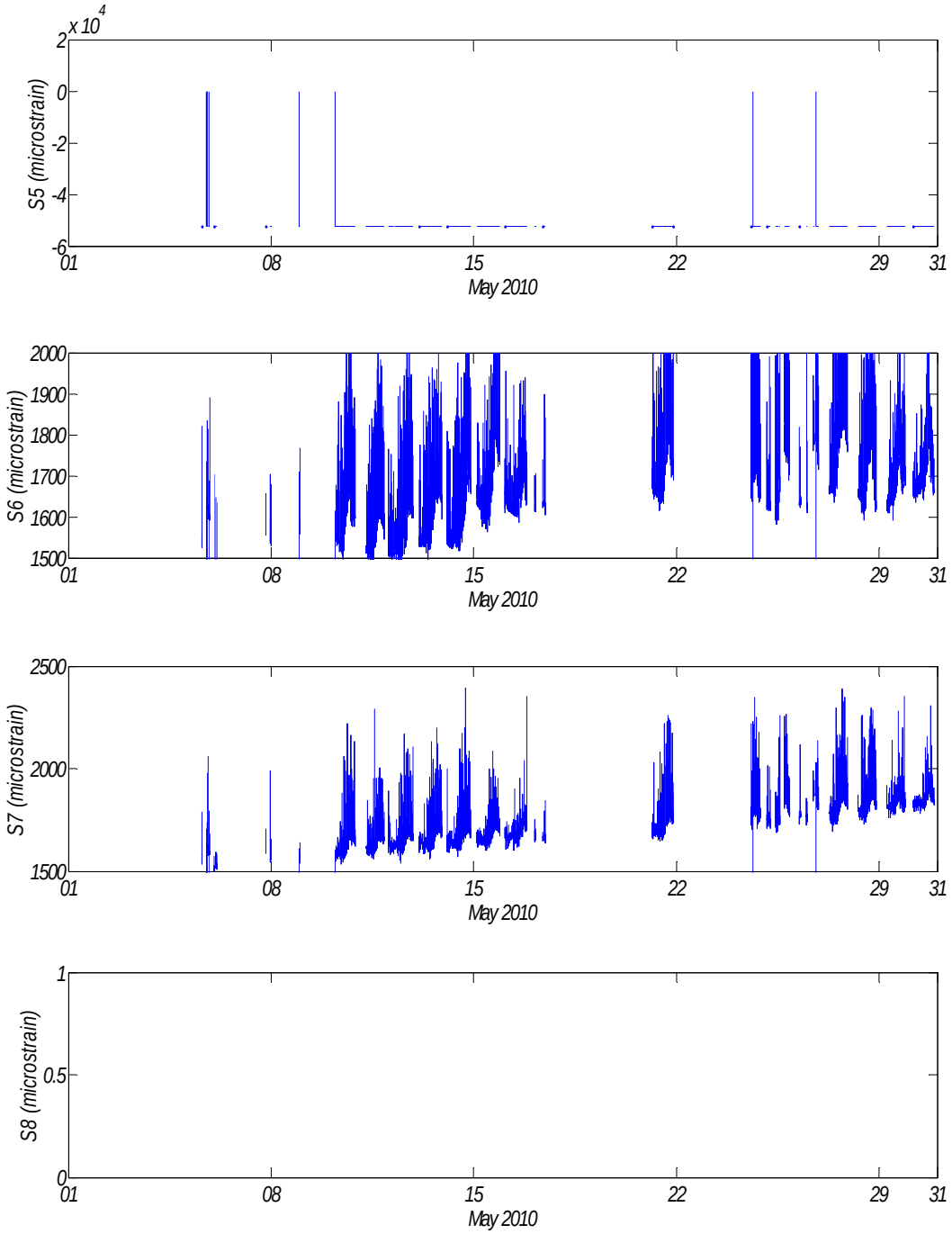
x 10^4
2
0
-2
-4
-6
S5 (microstrain)
01
08
15
22
29
31
May 2010
2000
1900
1800
1700
1600
1500
S6 (microstrain)
May 2010
2500
2000
1500
S7 (microstrain)
May 2010
1
0.5
0
S8 (microstrain)
May 2010

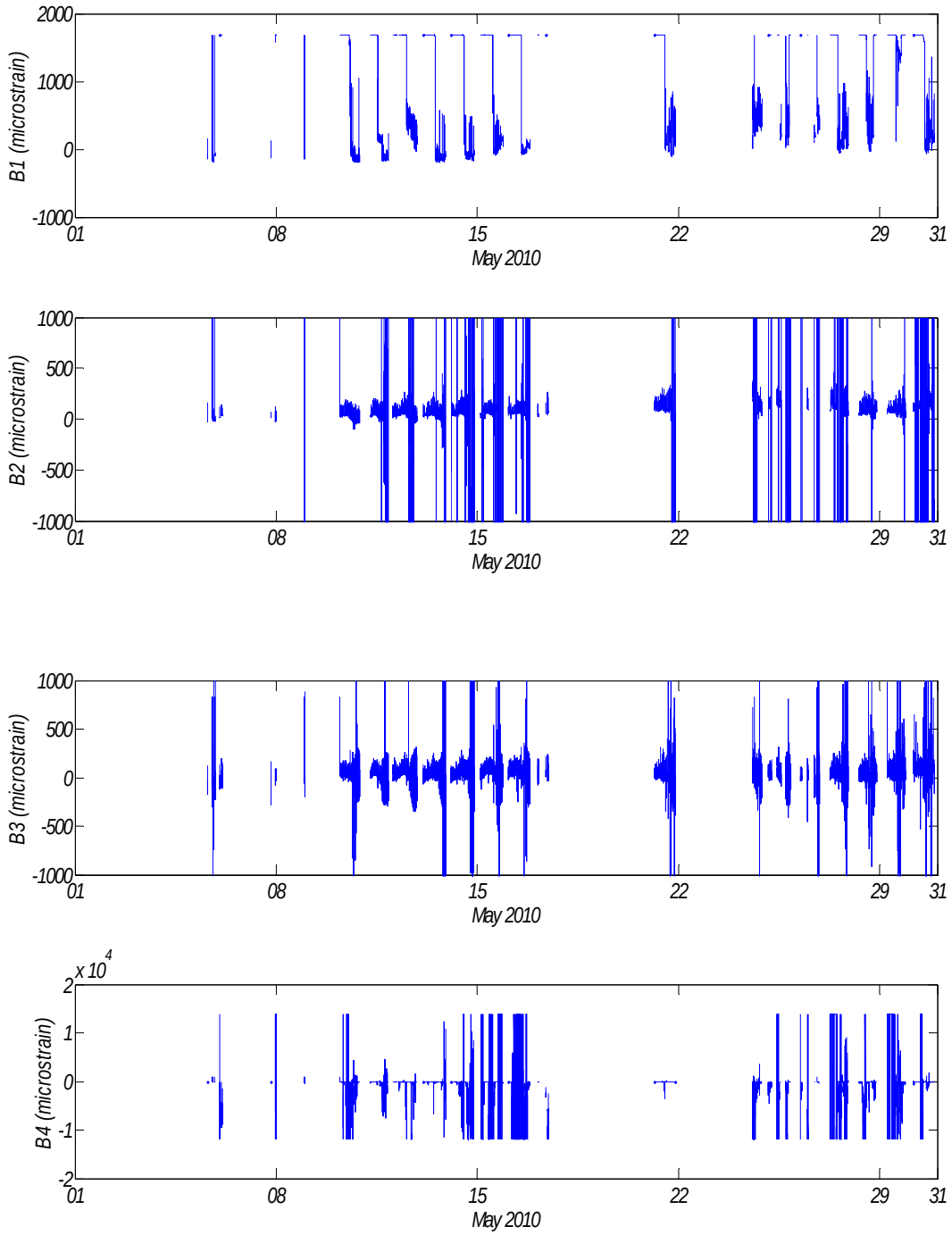
B1 (microstrain)
2000
1000
0
-1000
01
08
15
22
29
31
May 2010
B2 (microstrain)
1000
500
0
-500
-1000
01
08
15
22
29
31
May 2010
B3 (microstrain)
1000
500
0
-500
-1000
01
08
15
22
29
31
May 2010
x 10^4
B4 (microstrain)
2
1
0
-1
-2
01
08
15
22
29
31
May 2010

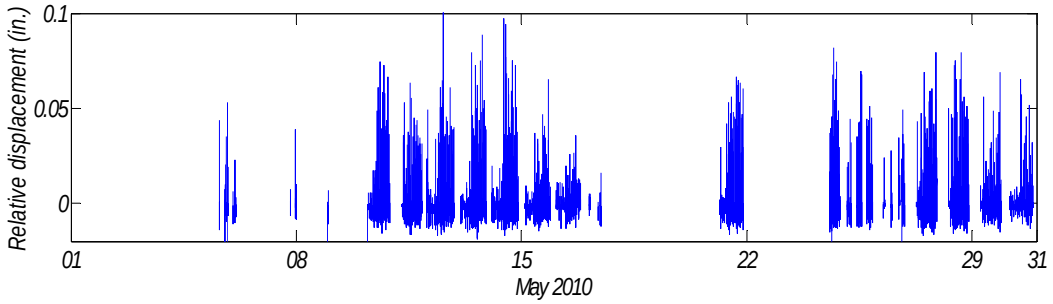
Relative displacement (in.)
0.1
0.05
0
01
08
15
22
29
31
May 2010

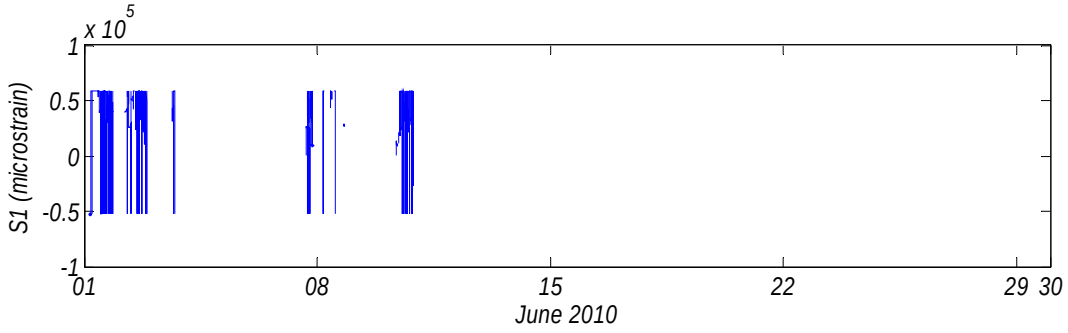
x 10^5
S1 (microstrain)
1
0.5
0
-0.5
-1
01
08
15
22
29
30
June 2010

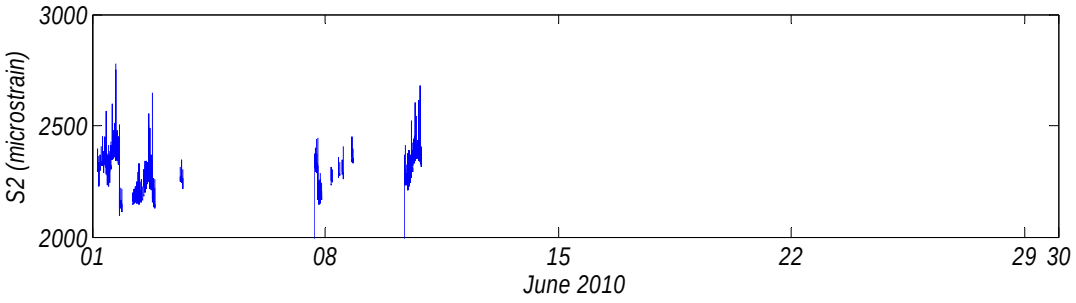
S2 (microstrain)
3000
2500
2000
01
08
15
22
29
30
June 2010

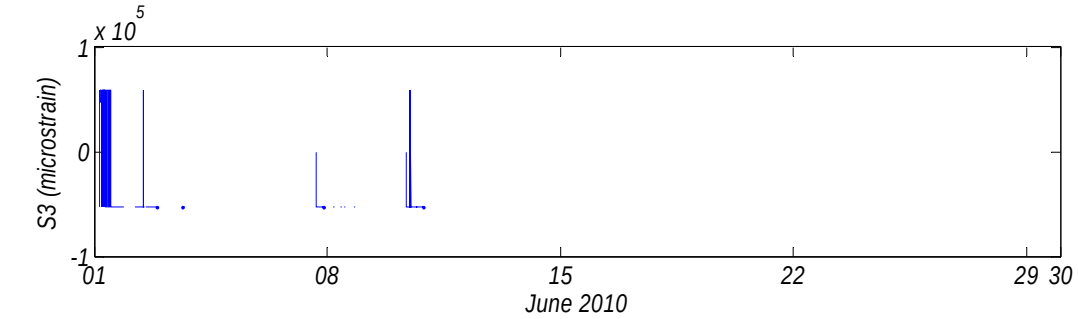
x 10^5
1
0
-1
S3 (microstrain)
01
08
15
22
29
30
June 2010

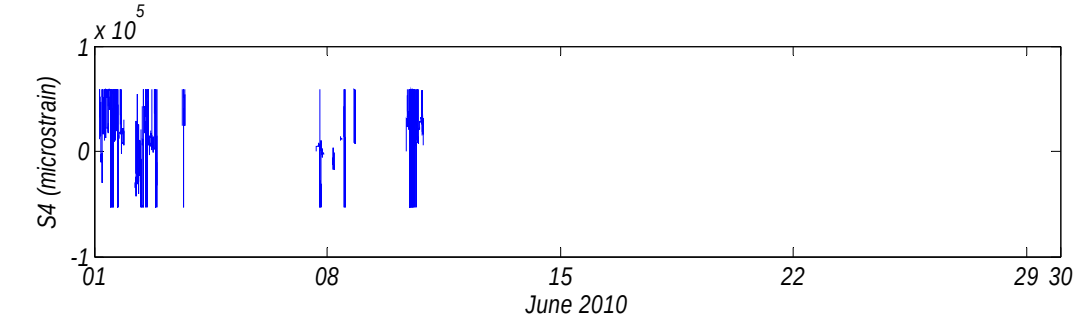
x 10^5
1
0
-1
S4 (microstrain)
01
08
15
22
29
30
June 2010

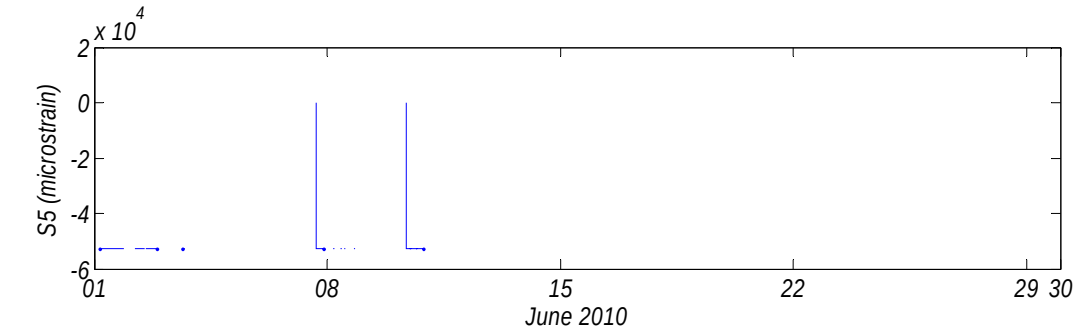
x 10^4
2
0
-2
-4
-6
S5 (microstrain)
01
08
15
22
29
30
June 2010

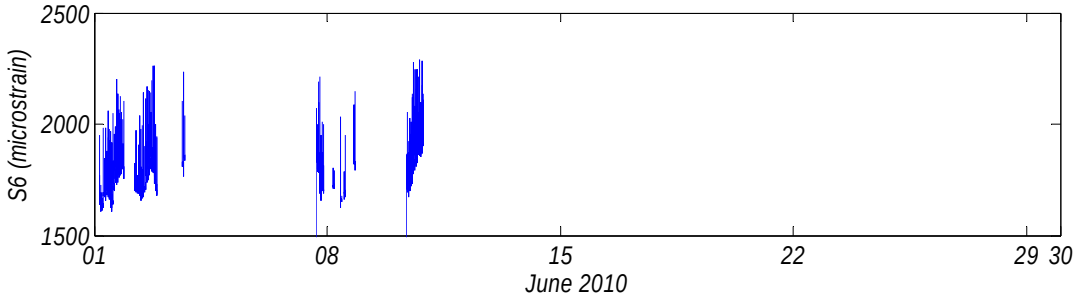
2500
2000
1500
S6 (microstrain)
01
08
15
22
29
30
June 2010

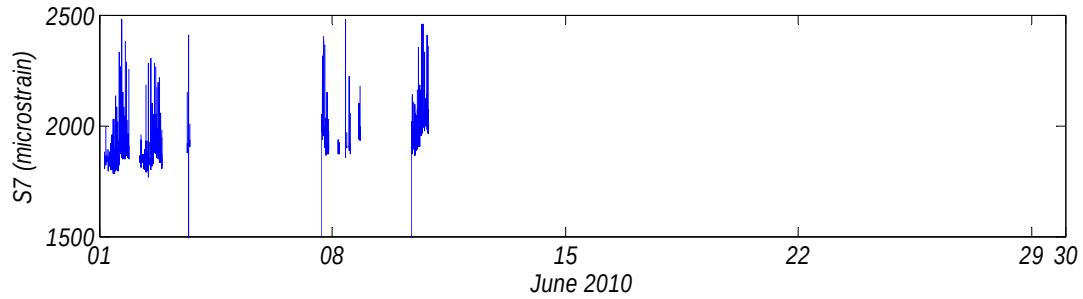
2500
2000
1500
S7 (microstrain)
01
08
15
22
29 30
June 2010

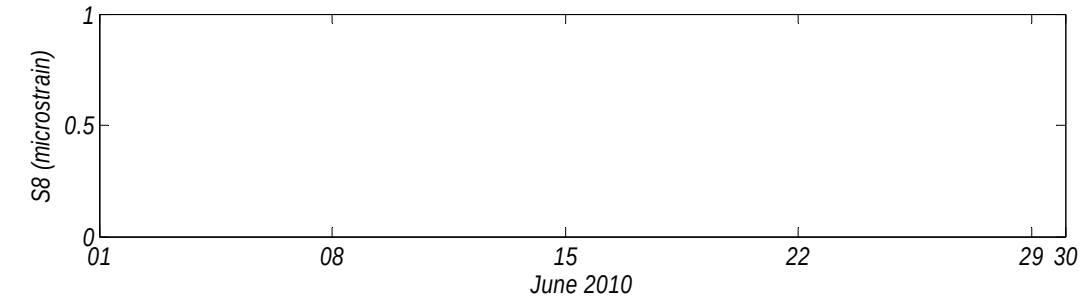
1
0.5
0
S8 (microstrain)
01
08
15
22
29 30
June 2010

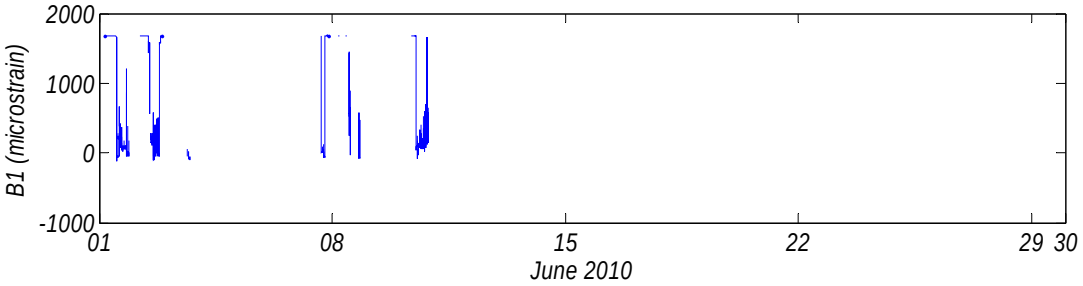
2000
1000
0
-1000
B1 (microstrain)
01
08
15
22
29 30
June 2010

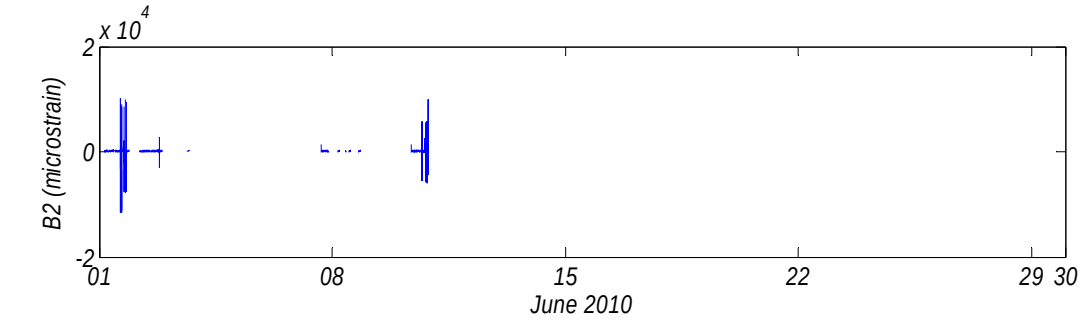
x 10^4
2
0
-2
B2 (microstrain)
01
08
15
22
29 30
June 2010

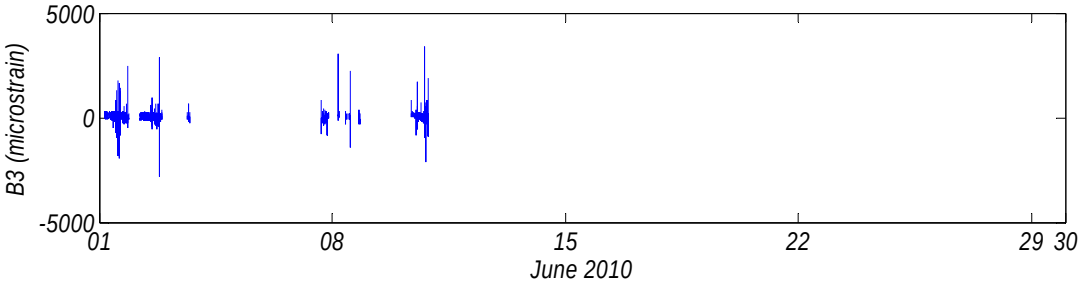
5000
0
-5000
B3 (microstrain)
01
08
15
22
29 30
June 2010

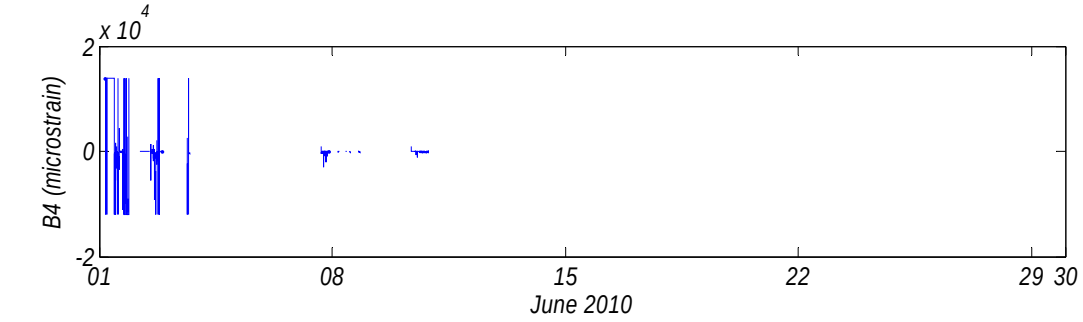
x 10^4
2
0
-2
B4 (microstrain)
01
08
15
22
29 30
June 2010

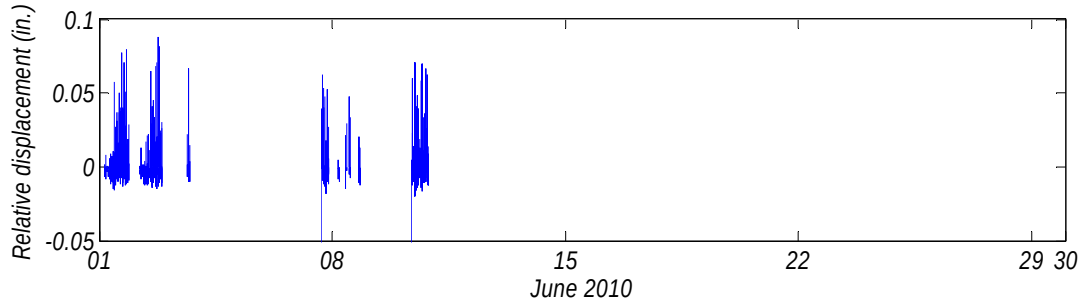
0.1
0.05
0
-0.05
Relative displacement (in.)
01
08
15
22
29 30
June 2010

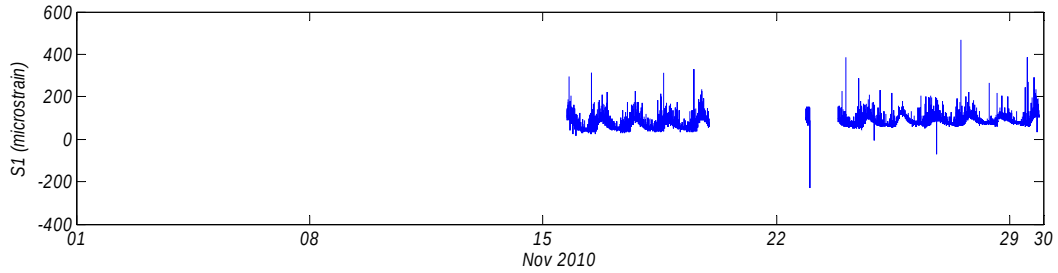
600
400
200
0
-200
-400
S1 (microstrain)
01
08
15
22
29
30
Nov 2010

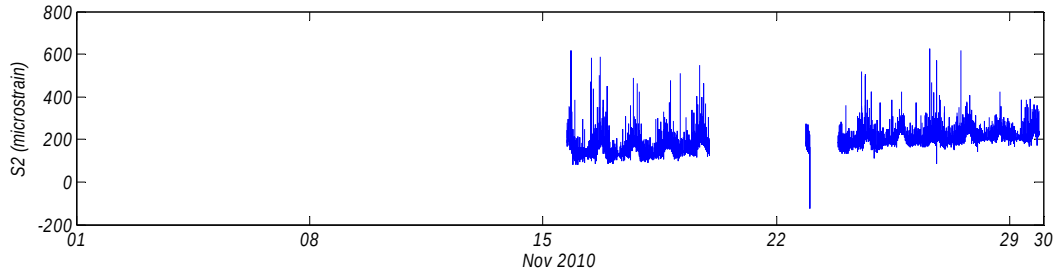
800
600
400
200
0
-200
S2 (microstrain)
01
08
15
22
29
30
Nov 2010

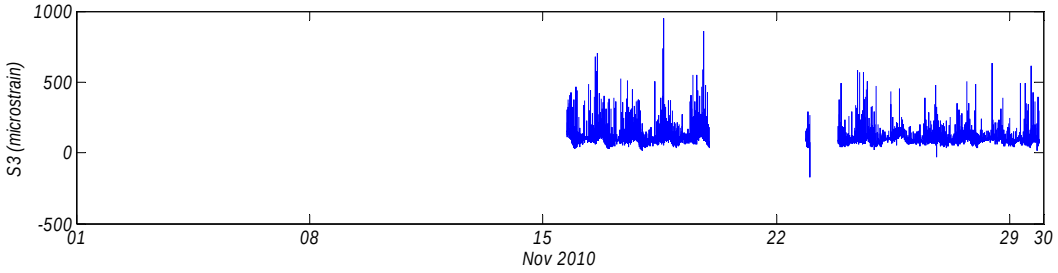
1000
500
0
-500
S3 (microstrain)
01
08
15
22
29
30
Nov 2010

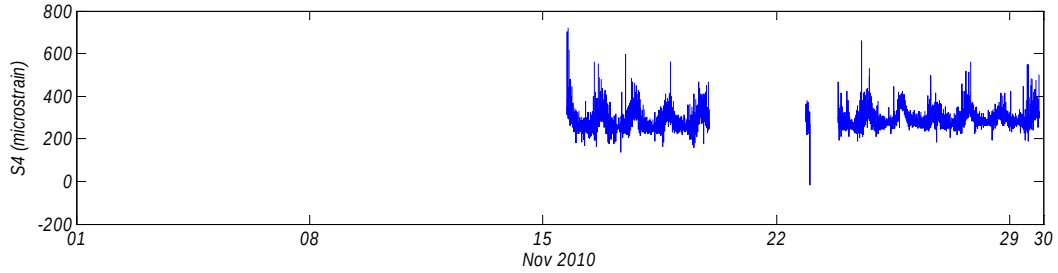
800
600
400
200
0
-200
S4 (microstrain)
01
08
15
22
29
30
Nov 2010

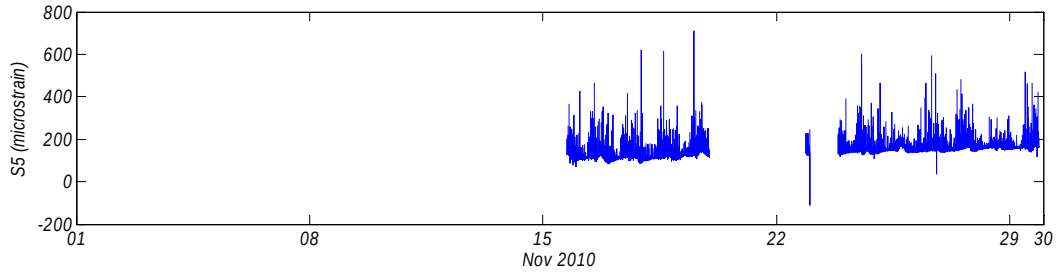
S5 (microstrain)
800
600
400
200
0
-200
01
08
15
22
29
30
Nov 2010

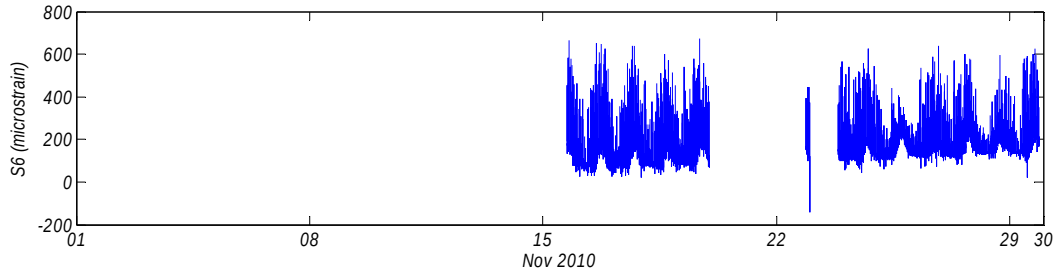
S6 (microstrain)
800
600
400
200
0
-200
01
08
15
22
29
30
Nov 2010

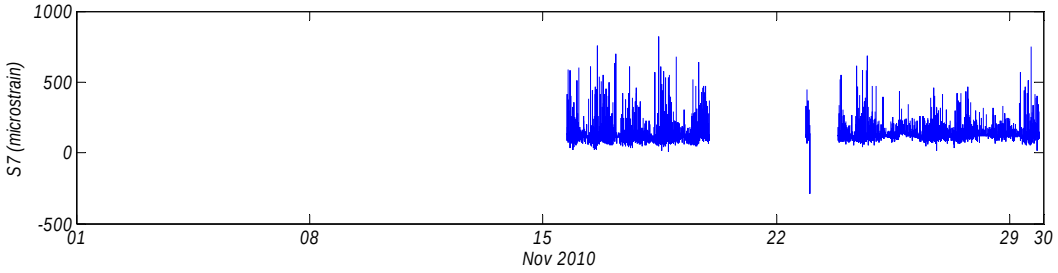
S7 (microstrain)
1000
500
0
-500
01
08
15
22
29
30
Nov 2010

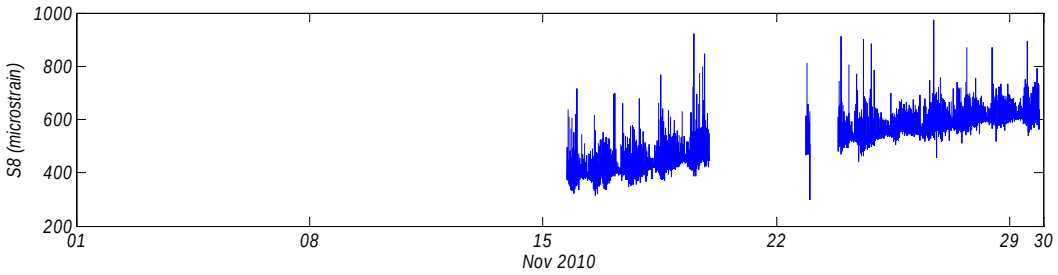
S8 (microstrain)
1000
800
600
400
200
01
08
15
22
29
30
Nov 2010

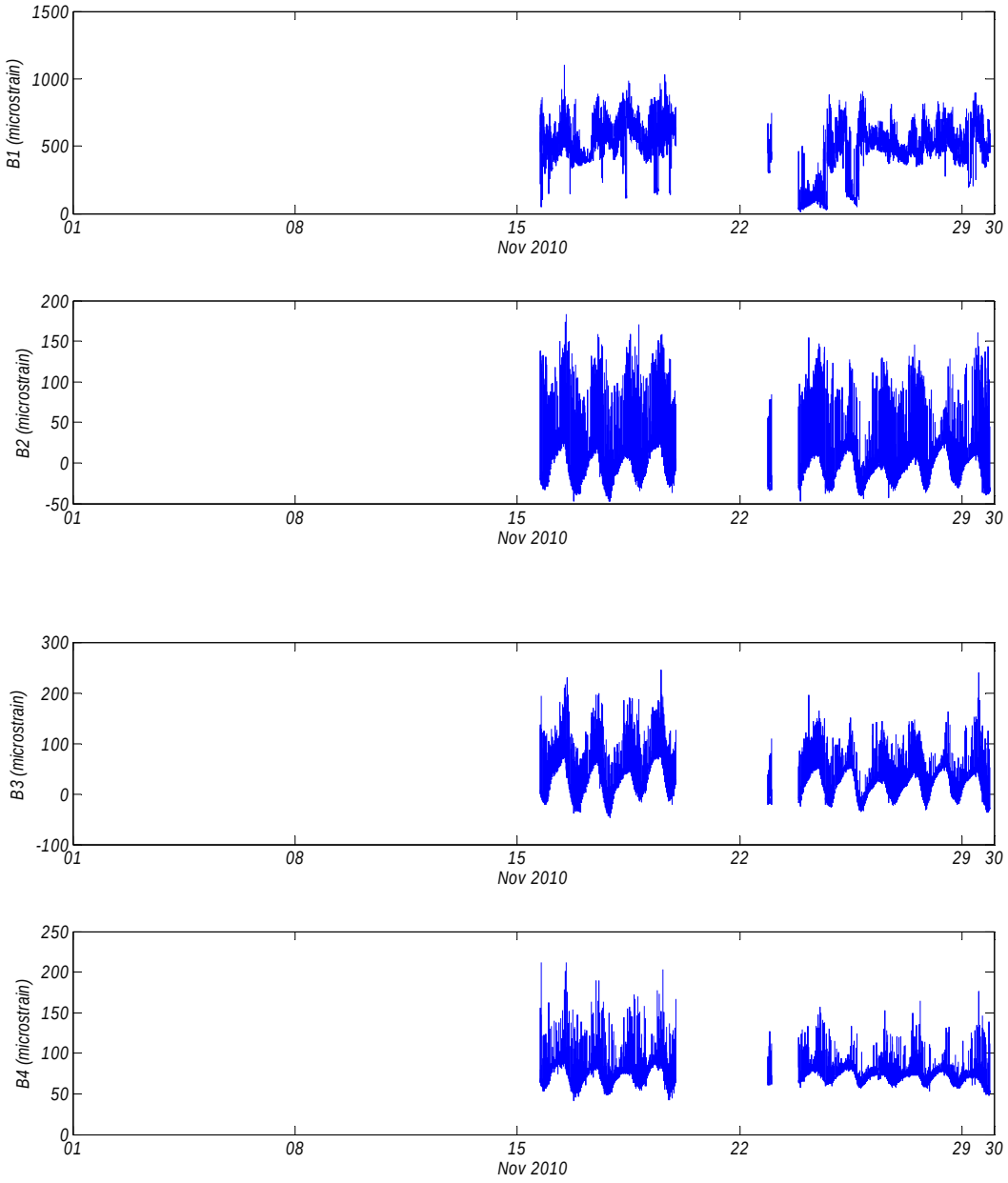
B1 (microstrain)
1500
1000
500
0
01
08
15
22
29
30
Nov 2010
B2 (microstrain)
200
150
100
50
0
-50
01
08
15
22
29
30
Nov 2010
B3 (microstrain)
300
200
100
0
-100
01
08
15
22
29
30
Nov 2010
B4 (microstrain)
250
200
150
100
50
0
01
08
15
22
29
30
Nov 2010

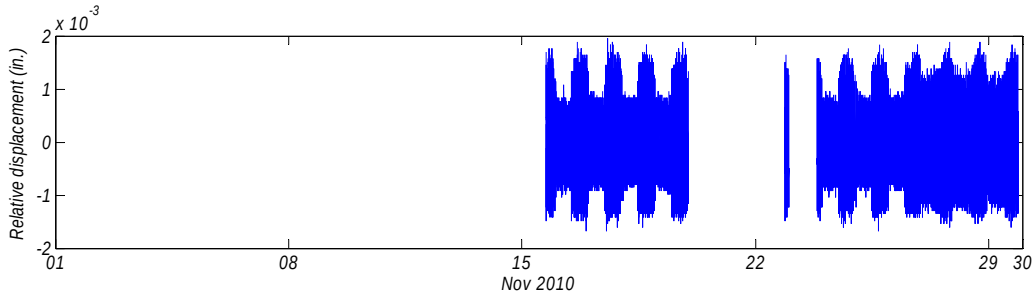
x 10^-3
Relative displacement (in.)
2
1
0
-1
-2
01
08
15
22
29
30
Nov 2010

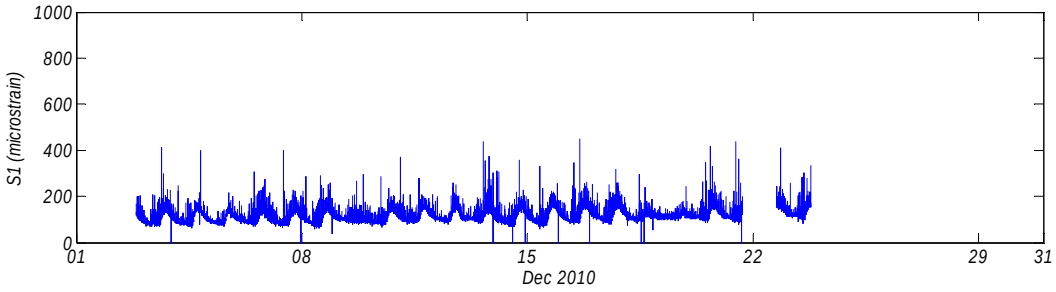
S1 (microstrain)
1000
800
600
400
200
0
01
08
15
22
29
31
Dec 2010

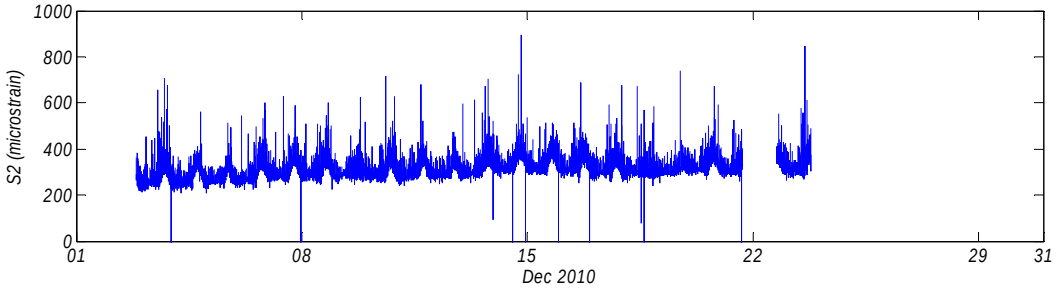
S2 (microstrain)
1000
800
600
400
200
0
01
08
15
22
29
31
Dec 2010

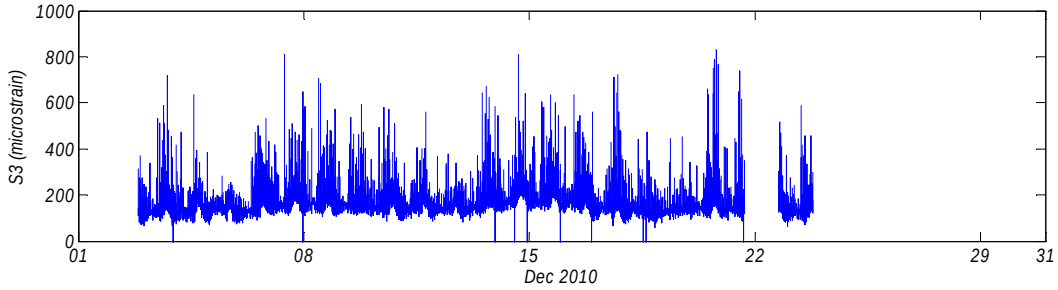
1000
800
600
400
200
0
S3 (microstrain)
01
08
15
22
29
31
Dec 2010

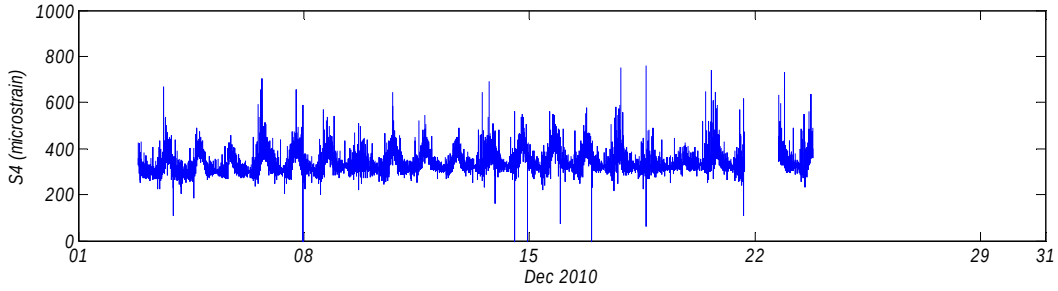
1000
800
600
400
200
0
S4 (microstrain)
01
08
15
22
29
31
Dec 2010

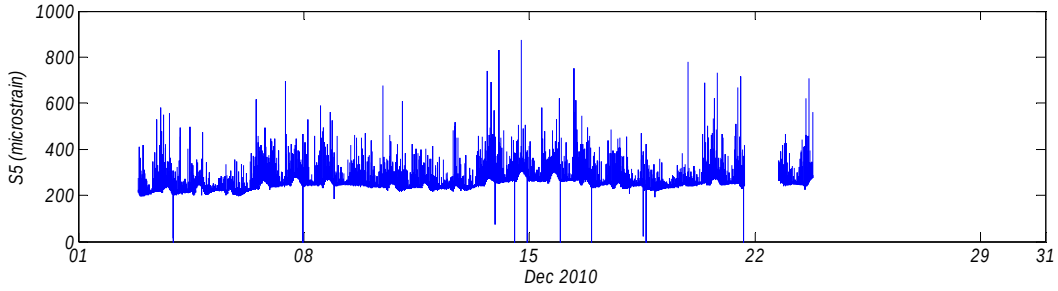
1000
800
600
400
200
0
S5 (microstrain)
01
08
15
22
29
31
Dec 2010

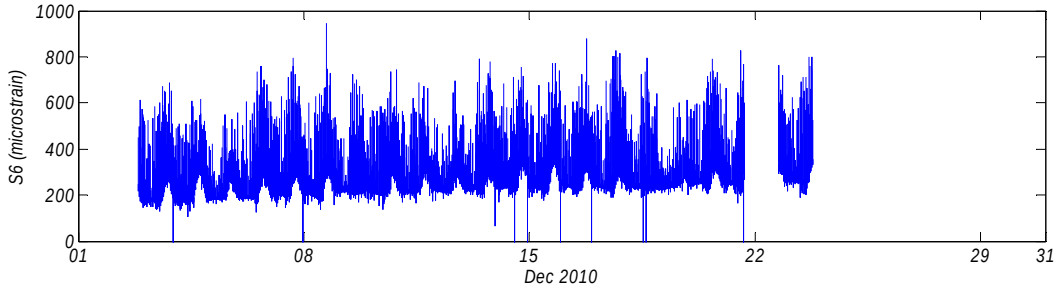
1000
800
600
400
200
0
S6 (microstrain)
01
08
15
22
29
31
Dec 2010

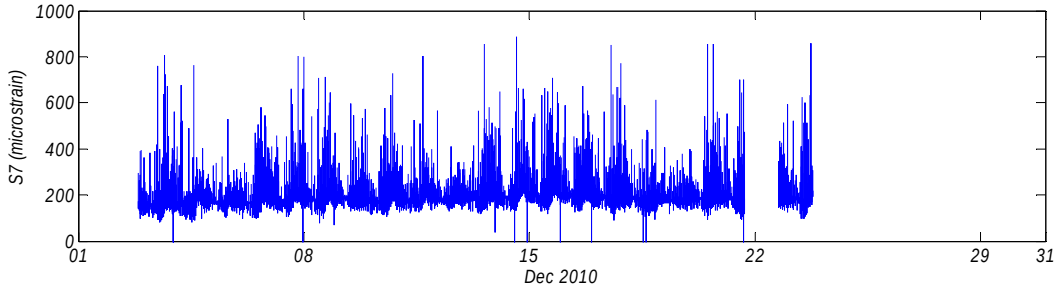
S7 (microstrain)
1000
800
600
400
200
0
01
08
15
22
29
31
Dec 2010

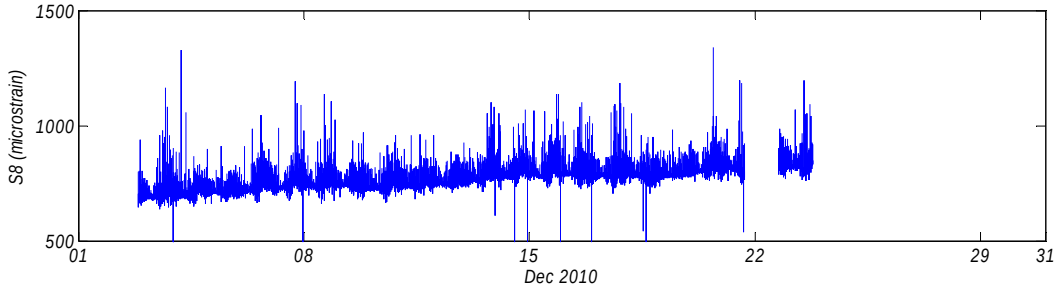
S8 (microstrain)
1500
1000
500
01
08
15
22
29
31
Dec 2010

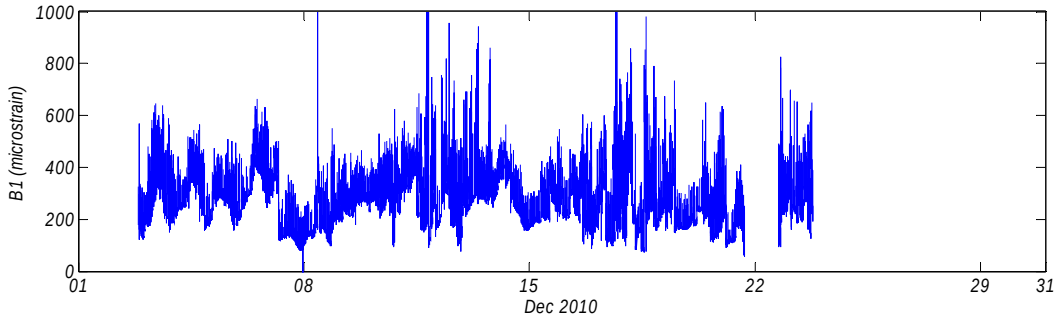
B1 (microstrain)
1000
800
600
400
200
0
01
08
15
22
29
31
Dec 2010

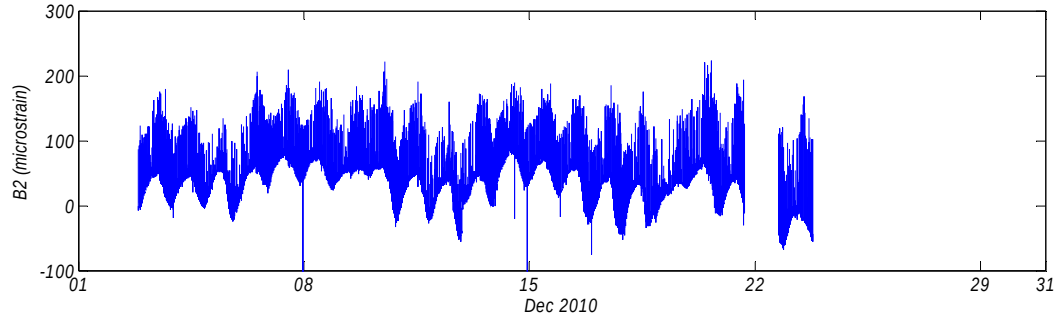
B2 (microstrain)
300
200
100
0
-100
01
08
15
22
29
31
Dec 2010

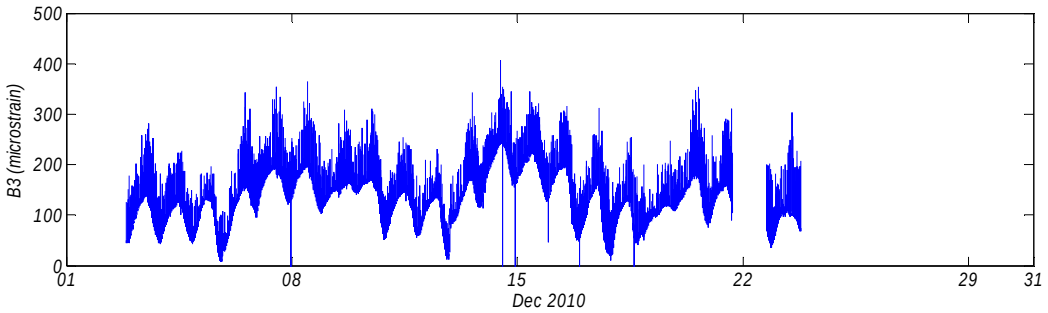
B3 (microstrain)
500
400
300
200
100
0
01
08
15
22
29
31
Dec 2010

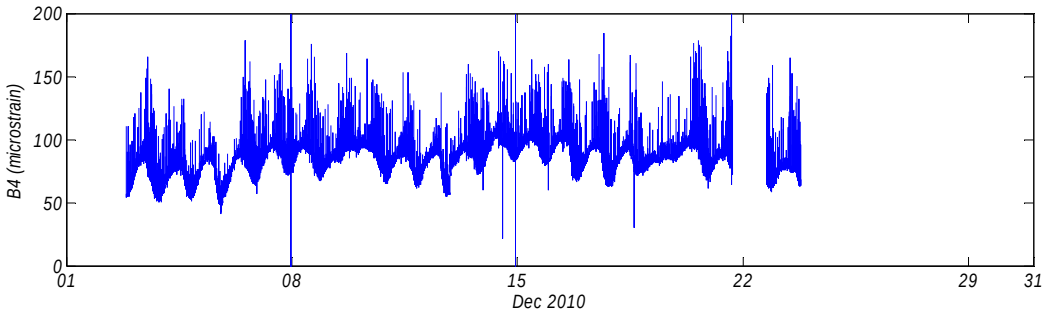
B4 (microstrain)
200
150
100
50
0
01
08
15
22
29
31
Dec 2010

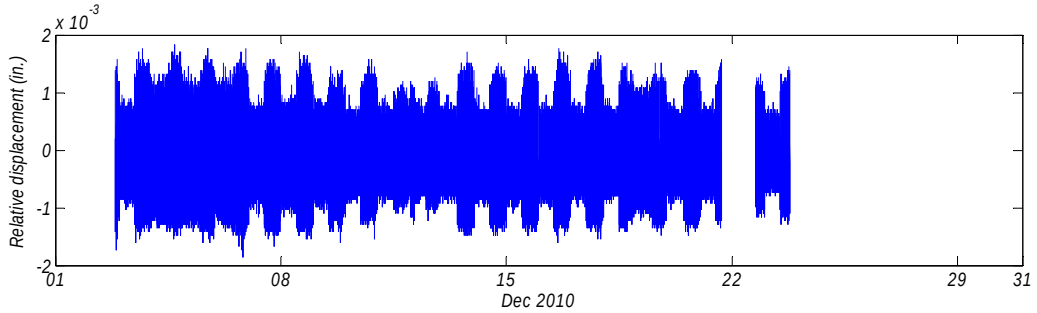
x 10-3
Relative displacement (in.)
2
1
0
-1
-2
01
08
15
22
29
31
Dec 2010

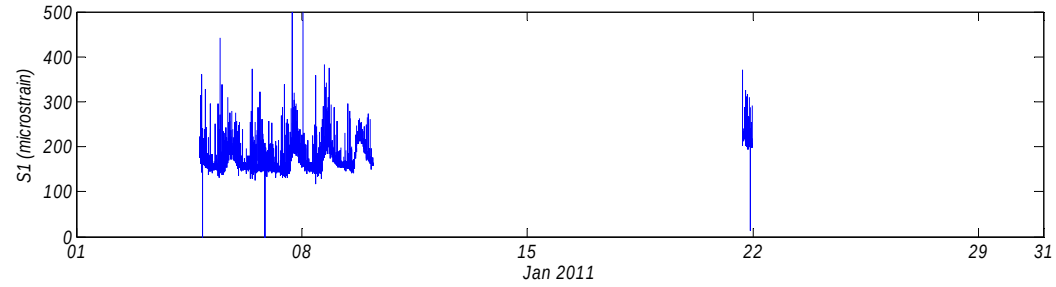
S1 (microstrain)
500
400
300
200
100
0
01
08
15
22
29
31
Jan 2011

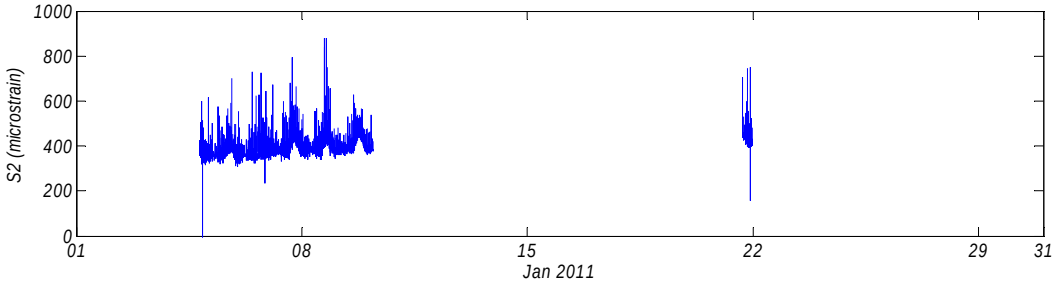
S2 (microstrain)
1000
800
600
400
200
0
01
08
15
22
29
31
Jan 2011

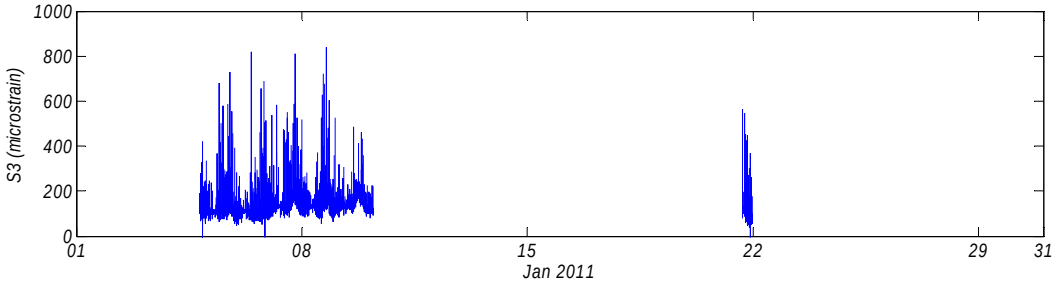
S3 (microstrain)
1000
800
600
400
200
0
01
08
15
22
29
31
Jan 2011

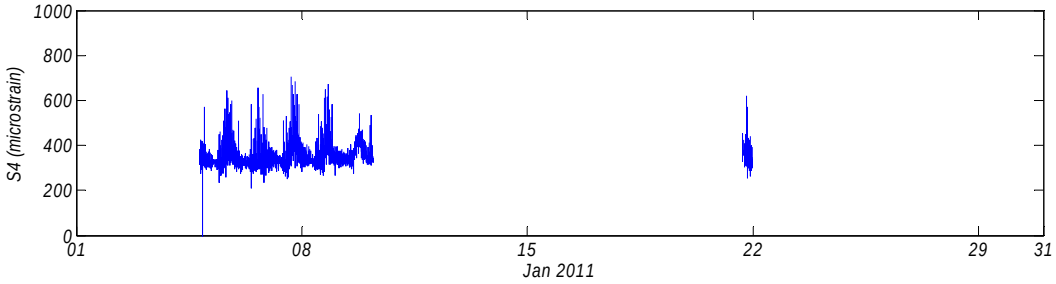
S4 (microstrain)
1000
800
600
400
200
0
01
08
15
22
29
31
Jan 2011

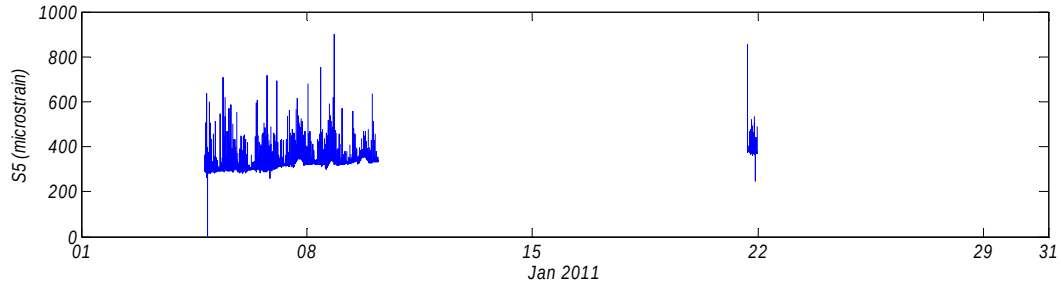
S5 (microstrain)
1000
800
600
400
200
0
01
08
15
22
29
31
Jan 2011

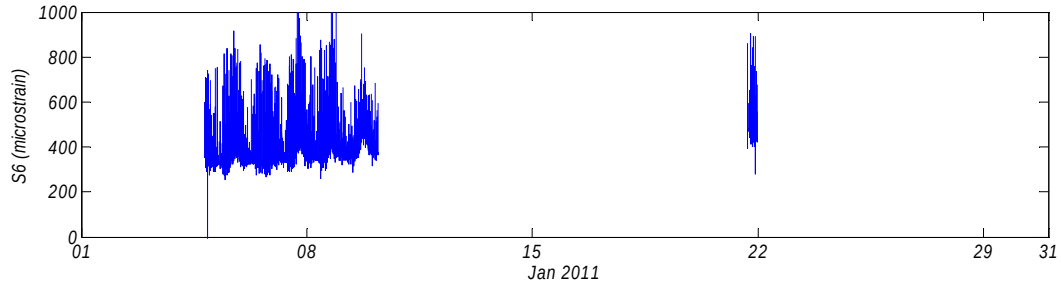
S6 (microstrain)
1000
800
600
400
200
0
01
08
15
22
29
31
Jan 2011

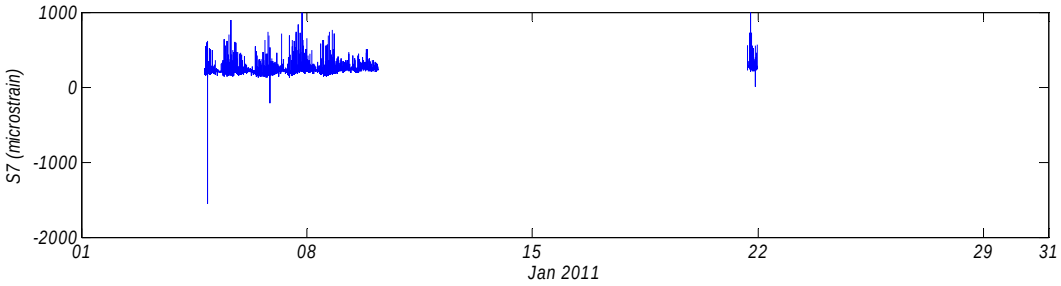
S7 (microstrain)
1000
0
-1000
-2000
01
08
15
22
29
31
Jan 2011

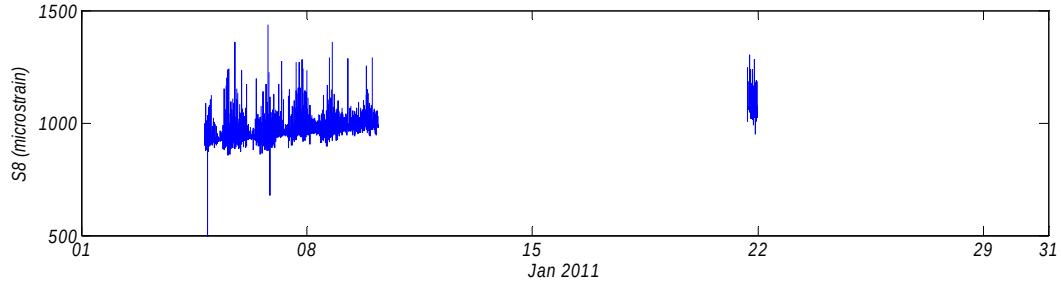
S8 (microstrain)
1500
1000
500
01
08
15
22
29
31
Jan 2011

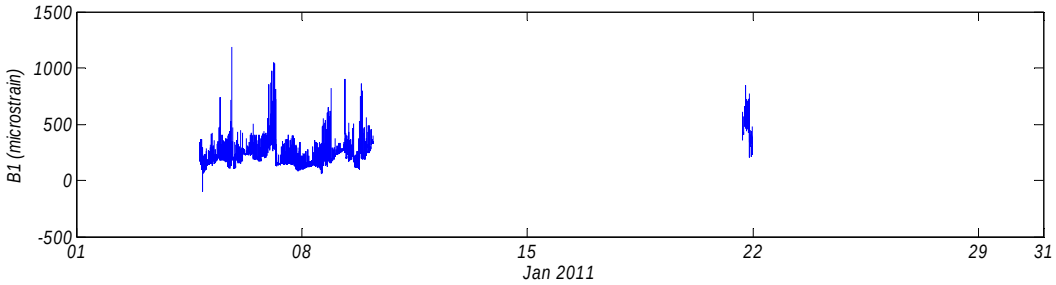
1500
1000
500
0
-500
B1 (microstrain)
01
08
15
22
29
31
Jan 2011

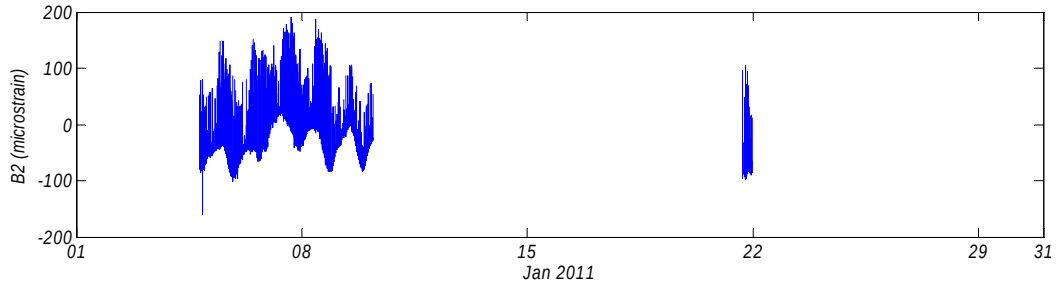
200
100
0
-100
-200
B2 (microstrain)
01
08
15
22
29
31
Jan 2011

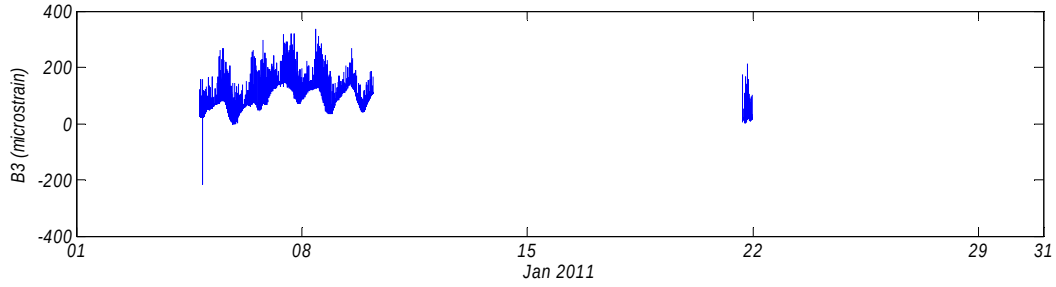
400
200
0
-200
-400
B3 (microstrain)
01
08
15
22
29
31
Jan 2011

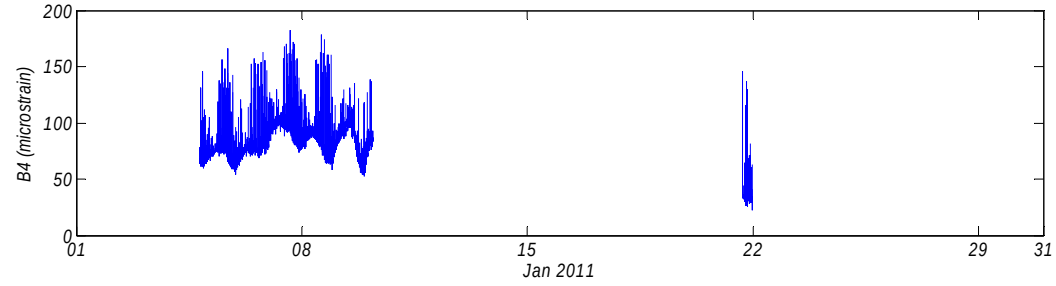
200
150
100
50
0
B4 (microstrain)
01
08
15
22
29
31
Jan 2011

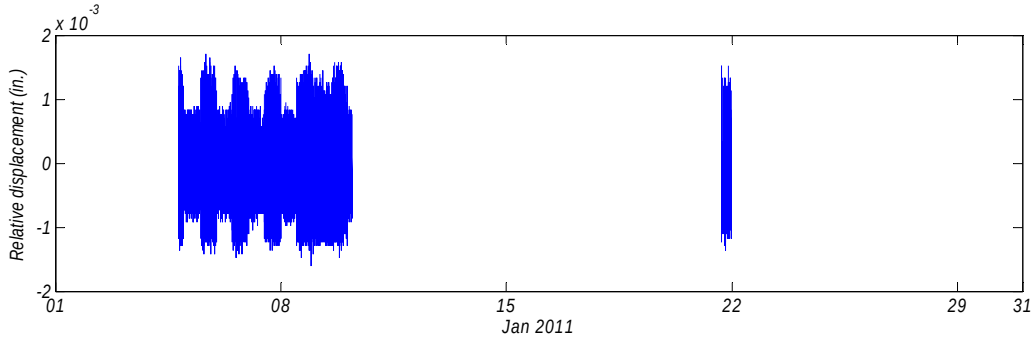
x 10^-3
2
1
0
-1
-2
Relative displacement (in.)
01
08
15
22
29
31
Jan 2011

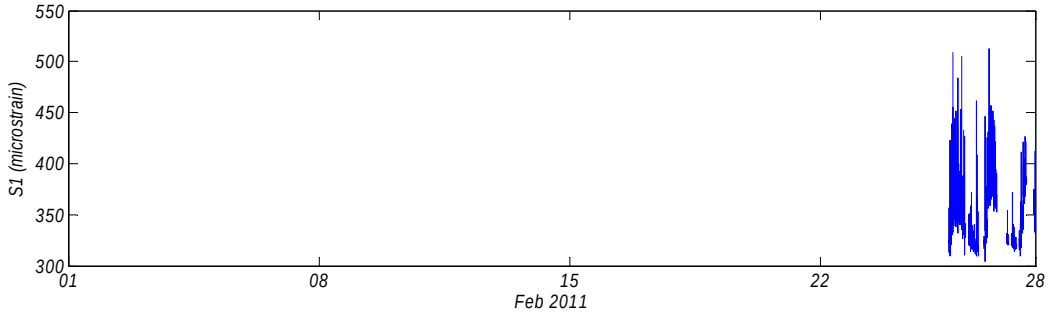
550
500
450
400
350
300
S1 (microstrain)
01
08
15
22
28
Feb 2011

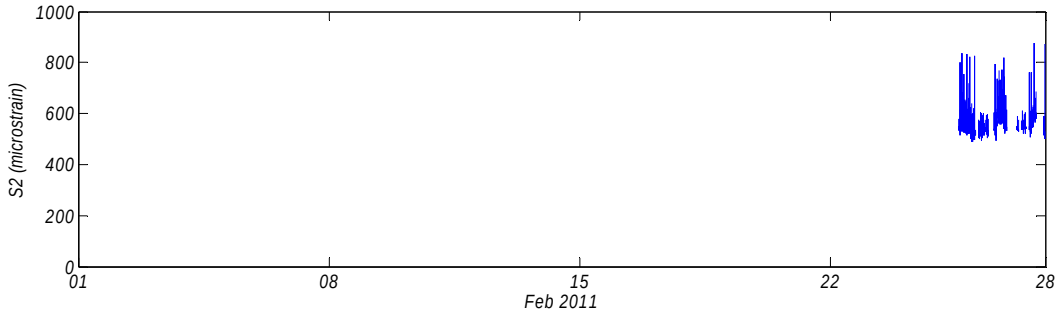
1000
800
600
400
200
0
S2 (microstrain)
01
08
15
22
28
Feb 2011

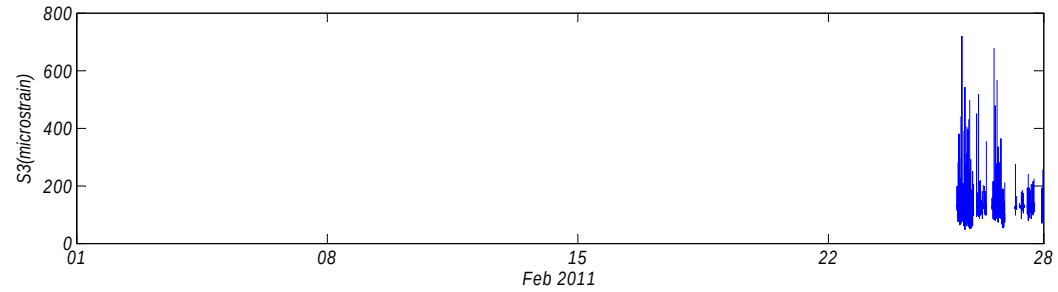
800
600
400
200
0
S3(microstrain)
01
08
15
22
28
Feb 2011

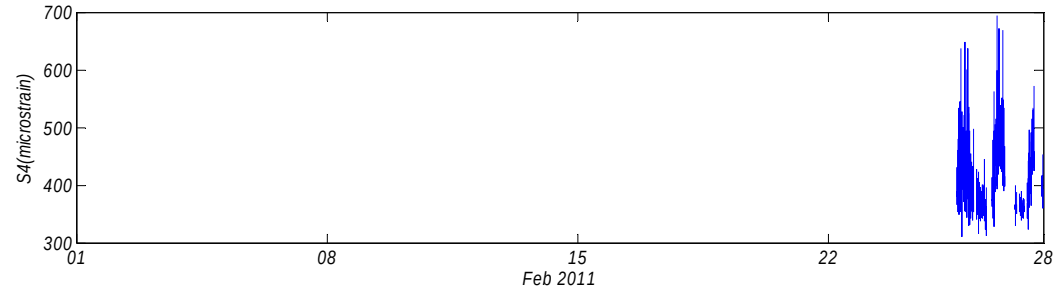
700
600
500
400
300
S4(microstrain)
01
08
15
22
28
Feb 2011

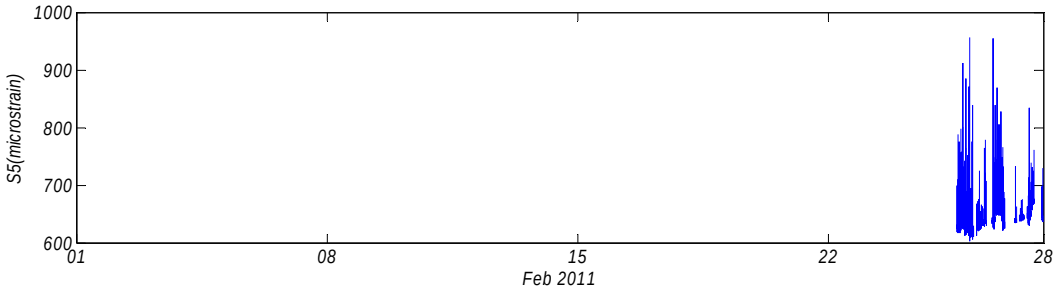
1000
900
800
700
600
S5(microstrain)
01
08
15
22
28
Feb 2011

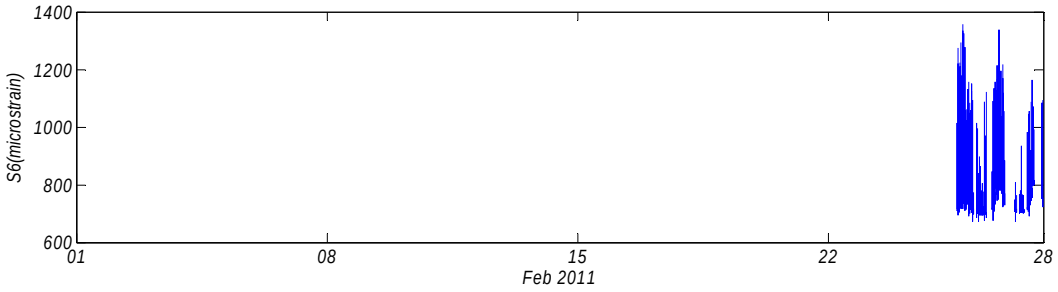
1400
1200
1000
800
600
S6(microstrain)
01
08
15
22
28
Feb 2011

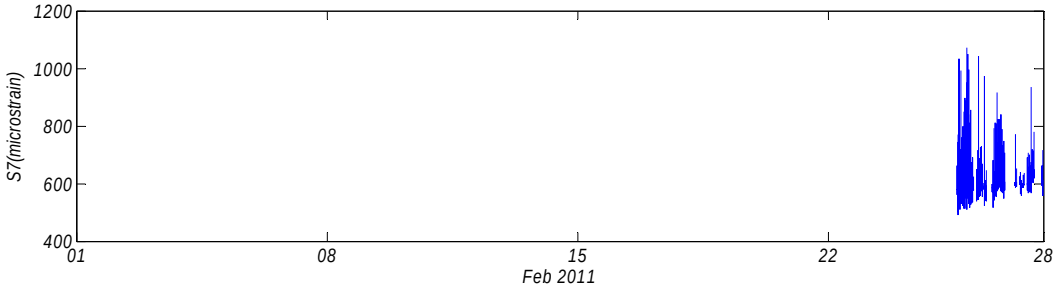
1200
1000
800
600
400
S7(microstrain)
01
08
15
22
28
Feb 2011

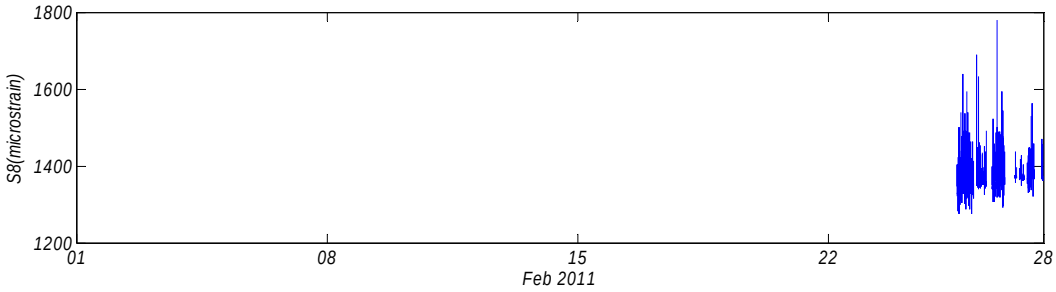
1800
1600
1400
1200
S8(microstrain)
01
08
15
22
28
Feb 2011

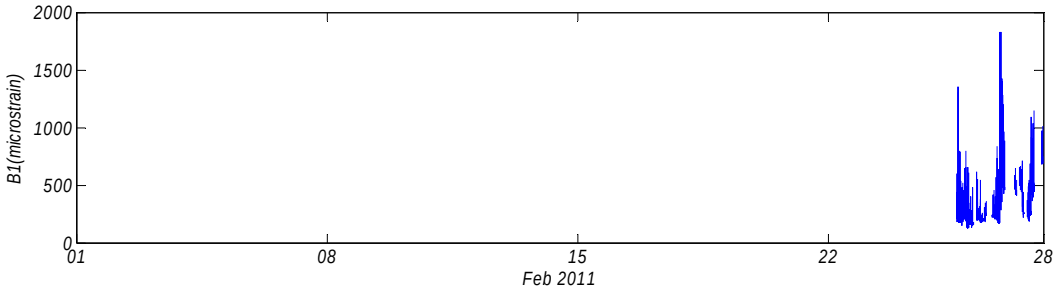
2000
1500
1000
500
0
B1(microstrain)
01
08
15
22
28
Feb 2011

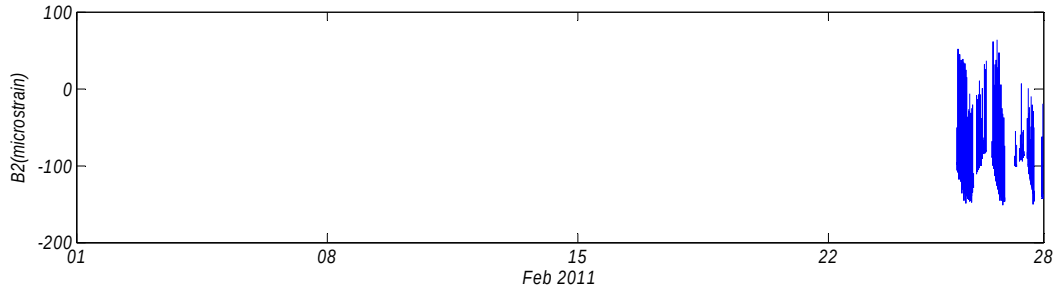
100
0
-100
-200
B2(microstrain)
01
08
15
22
28
Feb 2011

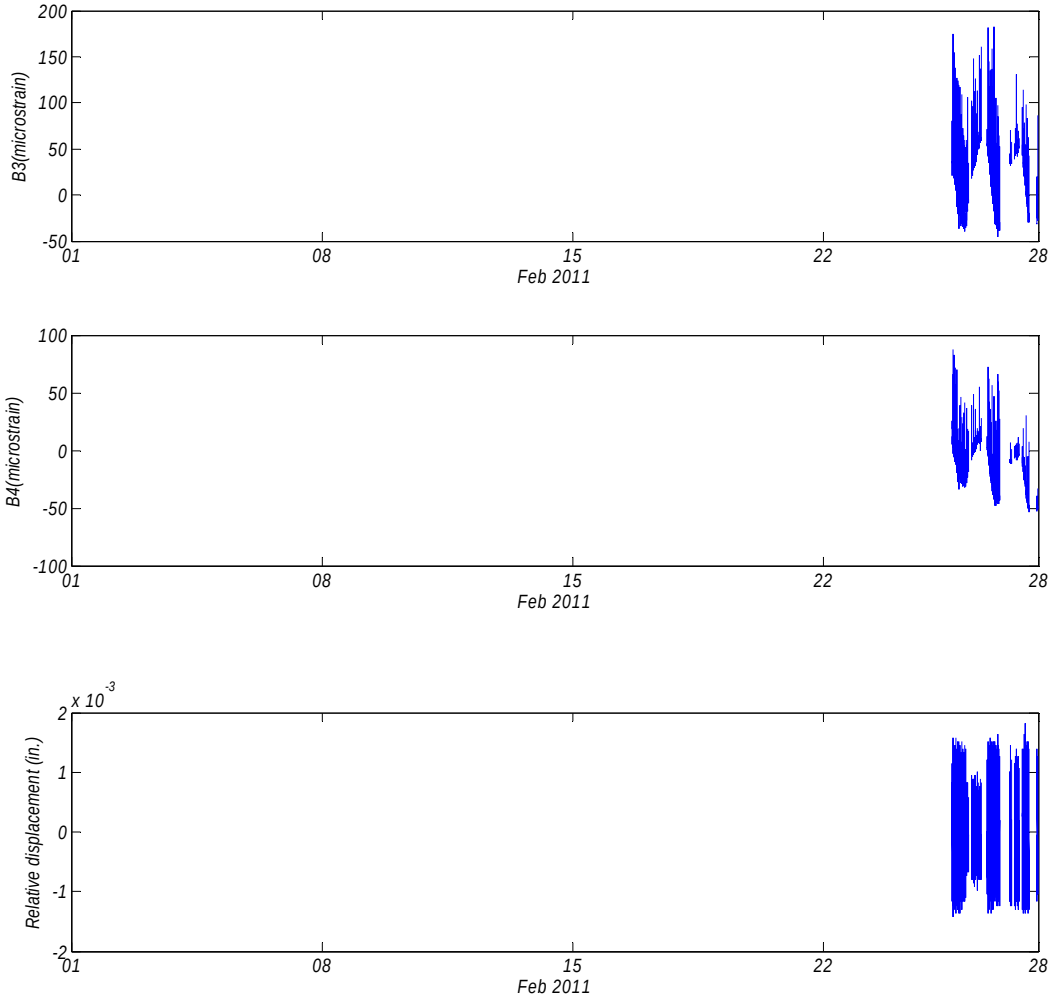
B3(microstrain)
200
150
100
50
0
-50
01
08
15
22
28
Feb 2011
B4(microstrain)
100
50
0
-50
-100
01
08
15
22
28
Feb 2011
x 10^-3
Relative displacement (in.)
2
1
0
-1
-2
01
08
15
22
28
Feb 2011

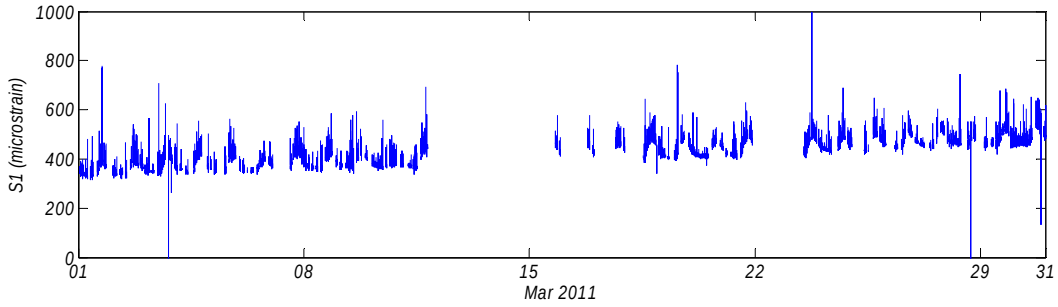
S1 (microstrain)
1000
800
600
400
200
0
01
08
15
22
29
31
Mar 2011

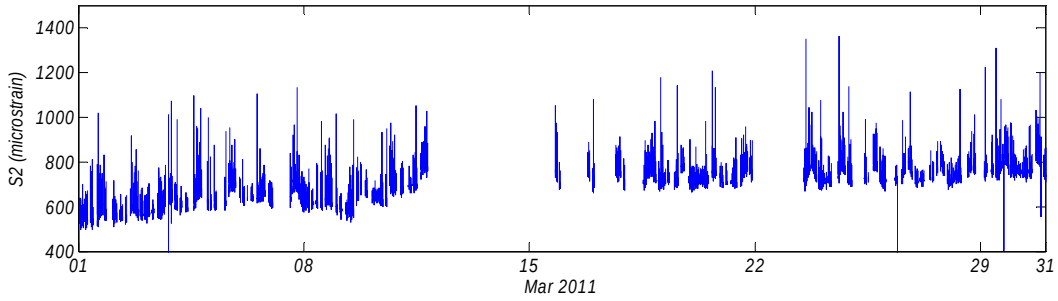
S2 (microstrain)
1400
1200
1000
800
600
400
01
08
15
22
29
31
Mar 2011

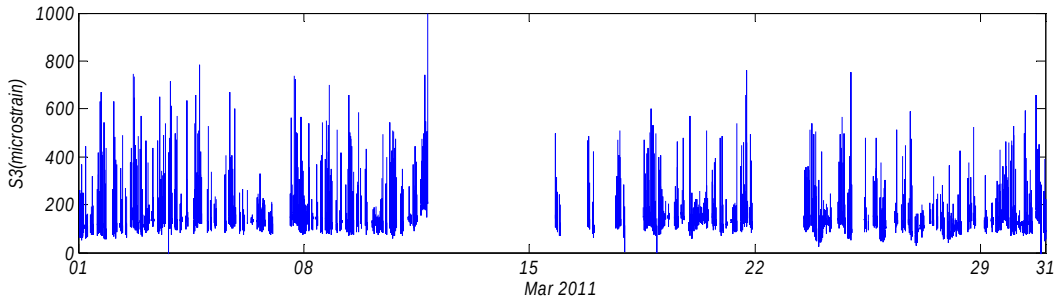
S3(microstrain)
1000
800
600
400
200
0
01
08
15
22
29
31
Mar 2011

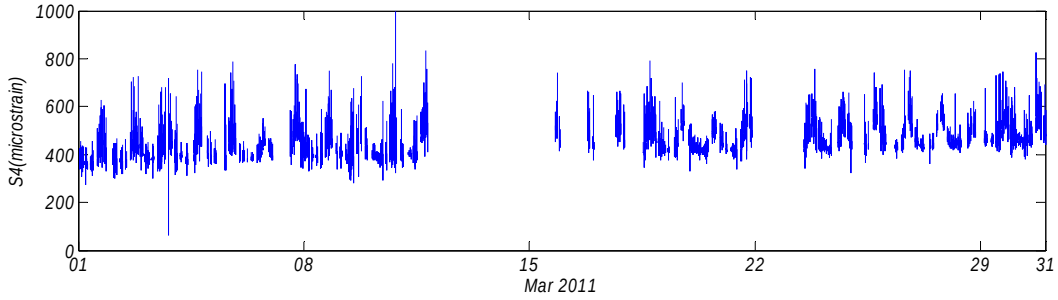
S4(microstrain)
1000
800
600
400
200
0
01
08
15
22
29
31
Mar 2011

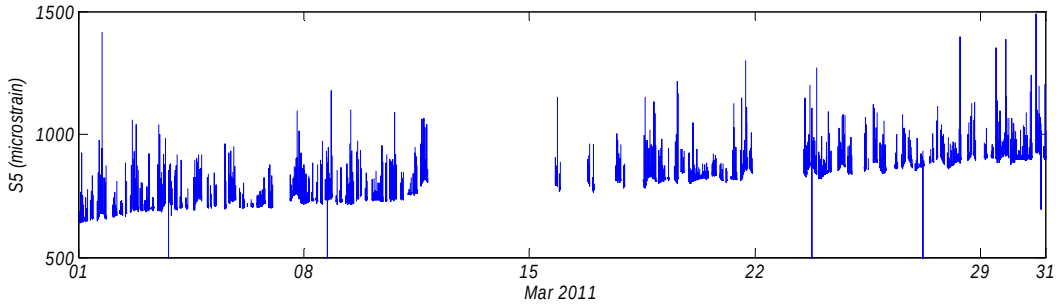
S5 (microstrain)
1500
1000
500
01
08
15
22
29
31
Mar 2011

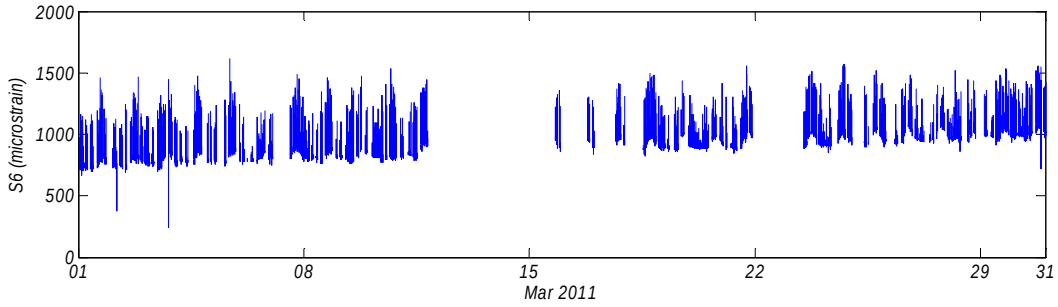
S6 (microstrain)
2000
1500
1000
500
0
01
08
15
22
29
31
Mar 2011

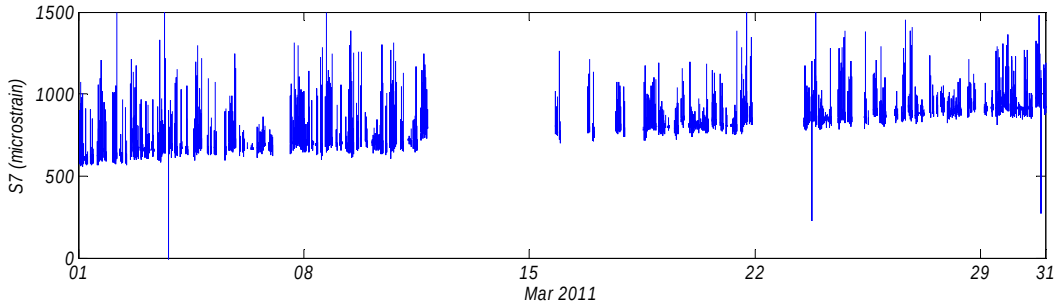
S7 (microstrain)
1500
1000
500
0
01
08
15
22
29
31
Mar 2011

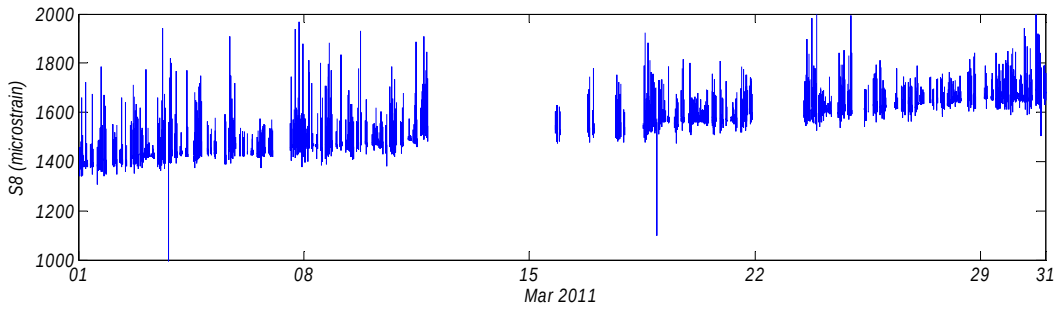
S8 (microstrain)
2000
1800
1600
1400
1200
1000
01
08
15
22
29
31
Mar 2011

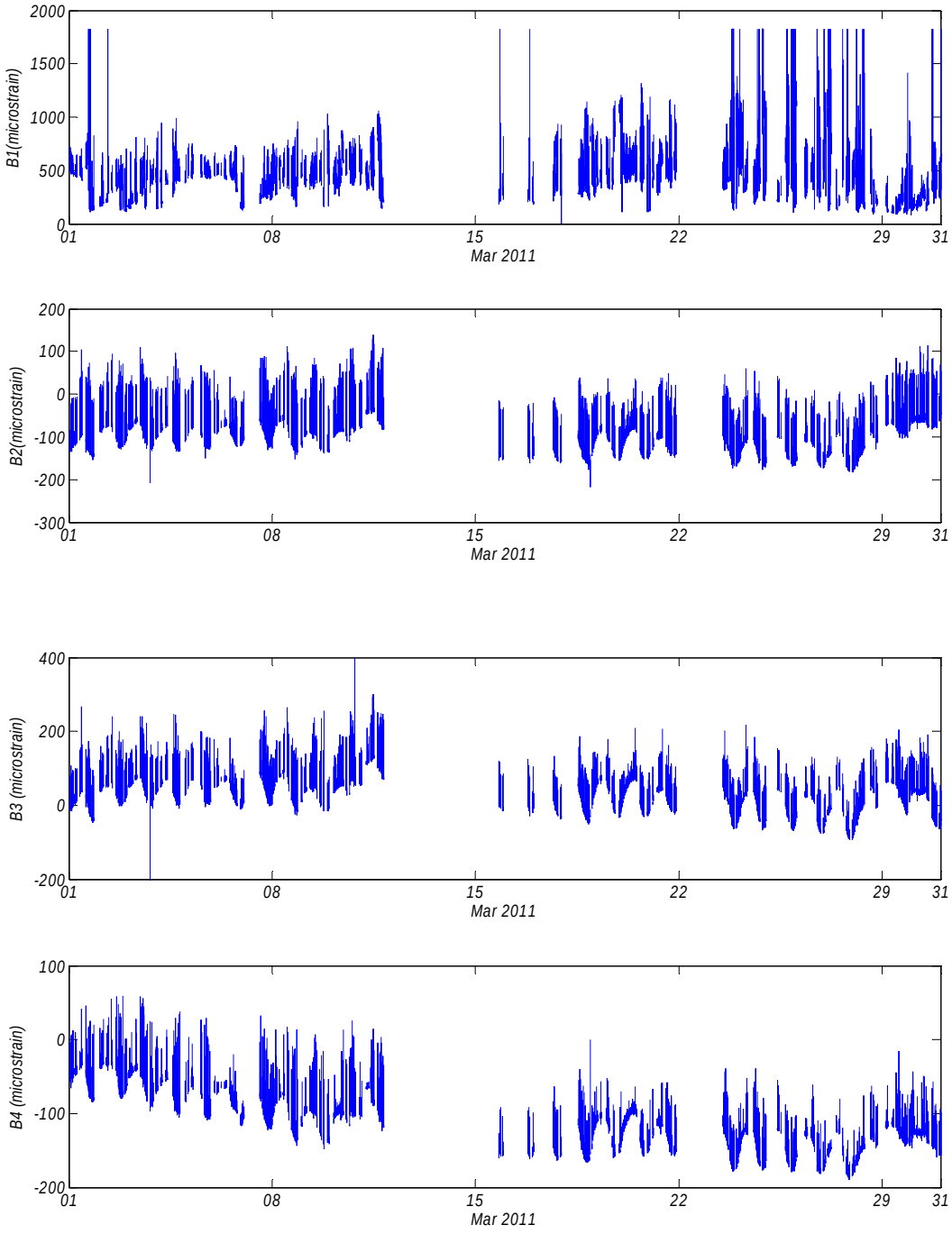
B1(microstrain)
2000
1500
1000
500
0
01
08
15
22
29
31
Mar 2011
B2(microstrain)
200
100
0
-100
-200
-300
01
08
15
22
29
31
Mar 2011
B3 (microstrain)
400
200
0
-200
01
08
15
22
29
31
Mar 2011
B4 (microstrain)
100
0
-100
-200
01
08
15
22
29
31
Mar 2011

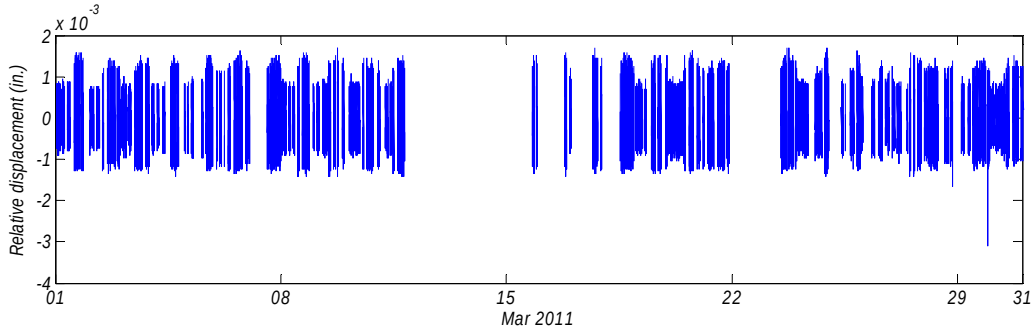
x 10^-3
Relative displacement (in.)
2
1
0
-1
-2
-3
-4
01
08
15
22
29
31
Mar 2011

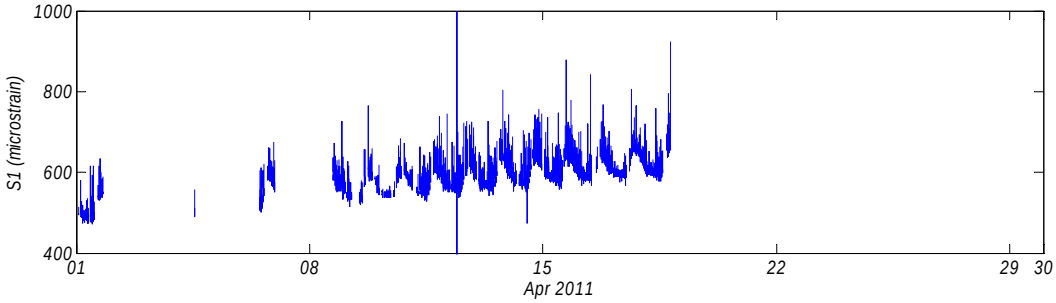
S1 (microstrain)
1000
800
600
400
01
08
15
22
29
30
Apr 2011

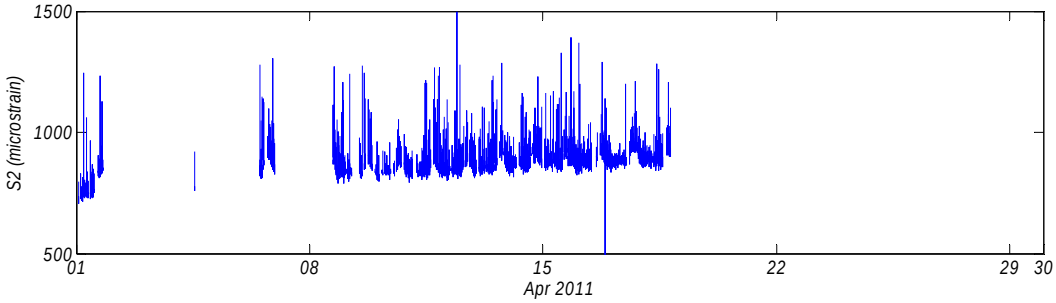
S2 (microstrain)
1500
1000
500
01
08
15
22
29
30
Apr 2011

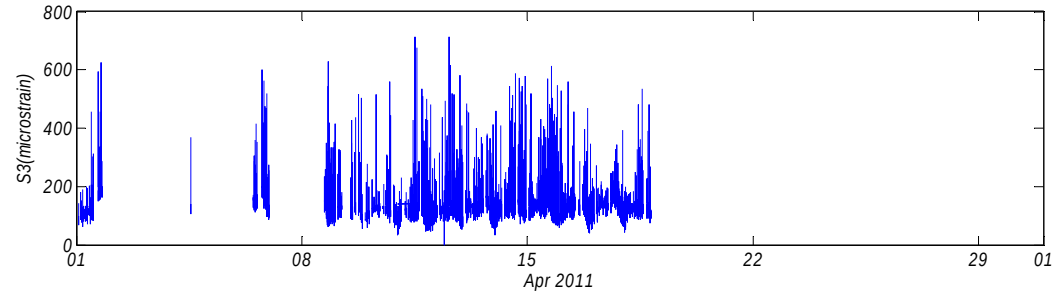
S3(microstrain)
800
600
400
200
0
01
08
15
22
29
01
Apr 2011

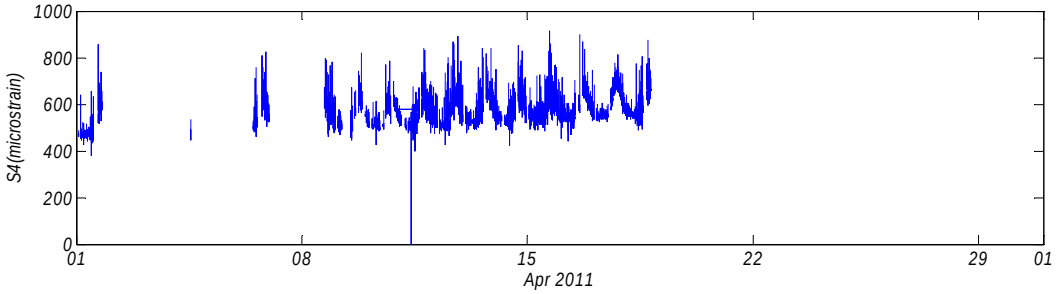
S4(microstrain)
1000
800
600
400
200
0
01
08
15
22
29
01
Apr 2011

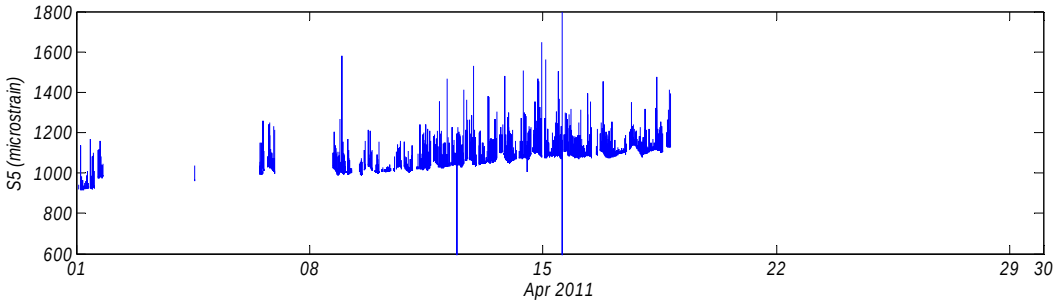
S5 (microstrain)
1800
1600
1400
1200
1000
800
600
01
08
15
22
29
30
Apr 2011

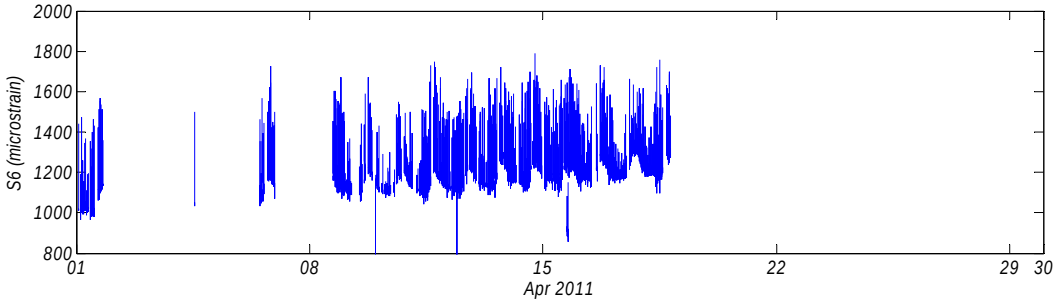
S6 (microstrain)
2000
1800
1600
1400
1200
1000
800
01
08
15
22
29
30
Apr 2011

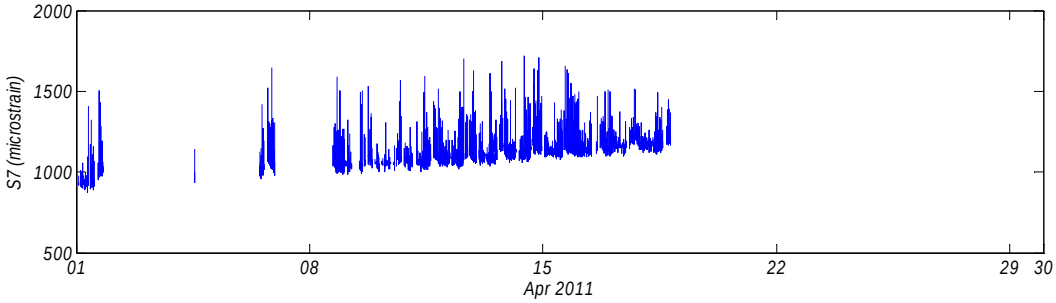
2000
1500
1000
500
S7 (microstrain)
01
08
15
22
29
30
Apr 2011

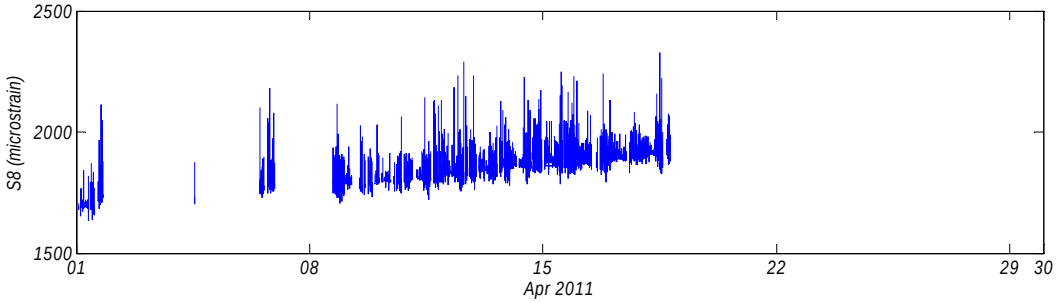
2500
2000
1500
S8 (microstrain)
01
08
15
22
29
30
Apr 2011

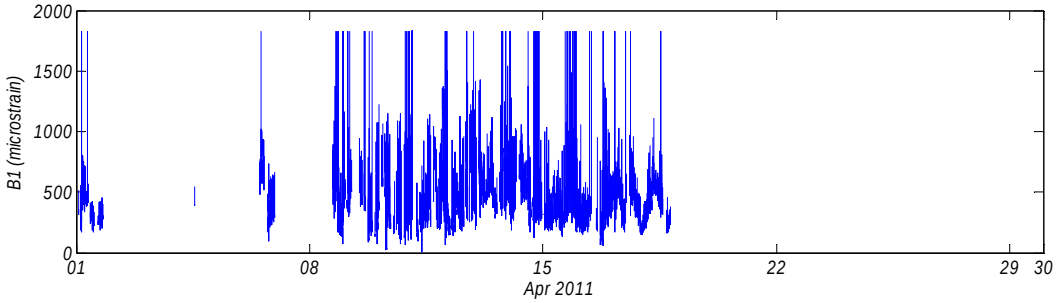
2000
1500
1000
500
0
B1 (microstrain)
01
08
15
22
29
30
Apr 2011

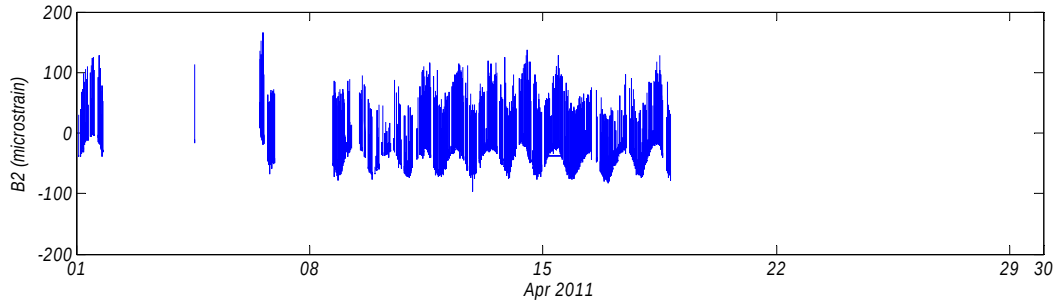
200
100
0
-100
-200
B2 (microstrain)
01
08
15
22
29
30
Apr 2011

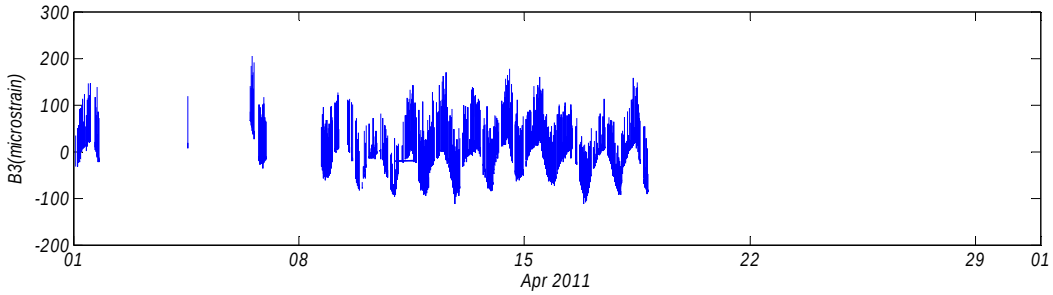
300
200
100
0
-100
-200
B3(microstrain)
01
08
15
22
29
01
Apr 2011

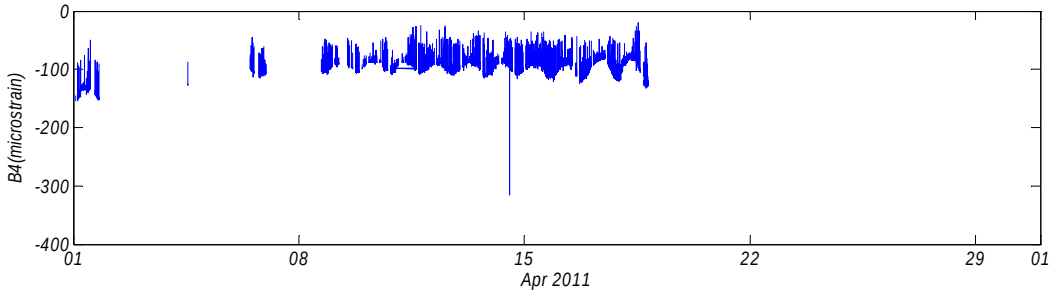
0
-100
-200
-300
-400
B4(microstrain)
01
08
15
22
29
01
Apr 2011

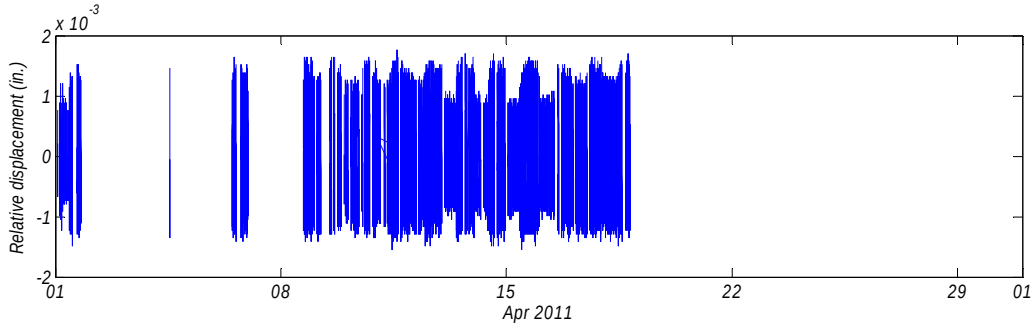
x 10^-3
2
1
0
-1
-2
Relative displacement (in.)
01
08
15
22
29
01
Apr 2011

Appendix E – Soffit Gage Histograms

The following tables give the number of occurrences of each load range recorded by each of the soffit strain gages during the monitoring period. Data covers 7am through 6pm during typical business hours. Data not included here was incomplete or missing during these hours. OC# represents the total number of occurrences; ELR represents the equivalent load range that would be used in a fatigue analysis of the GFRP deck using Miner's Rule.

Load Occurrences for Gage S1

Date	4~8 kip	8~12 kip	12~16 kip	16~20 kip	20~24 kip	24~28 kip	>28kip	OC#	ELR (kip)
2009.10.17	0	0	0	0	0	0	0	0	
2009.10.29	16	5	2	20	0	0	0	43	14
2009.10.31	6	4	2	9	0	0	0	20	14
2009.11.03	8	3	4	2	0	0	0	16	12
2009.11.04	16	2	2	2	0	0	0	22	10
2009.11.05	7	2	1	3	0	0	0	12	12
2009.11.11	599	121	31	13	0	0	0	763	8
2009.11.12	23	3	3	1	0	0	0	29	9
2009.11.13	14	2	0	0	0	0	0	15	7
2009.11.20	5665	2017	1218	3511	0	0	0	12411	13
2009.11.21	22162	3544	1170	4522	0	0	0	31397	11
2009.11.22	14294	1472	255	523	0	0	0	16543	8
2009.11.23	7960	1464	574	1578	0	0	0	11575	11
2009.11.26	6654	261	49	88	0	0	0	7052	7
2009.11.29	6	2	1	1	0	0	0	9	10
2009.11.30	20	9	2	6	0	0	0	37	11
2009.12.08	11028	1075	200	714	0	0	0	13016	9
2009.12.09	3392	382	103	213	0	0	0	4090	9
2009.12.10	33264	2961	508	513	0	0	0	37245	7
2009.12.12	6442	730	158	464	0	0	0	7794	9
2009.12.13	34112	2931	503	802	0	0	0	38346	8
2009.12.14	34374	2747	422	652	0	0	0	38195	7
2009.12.19	3	0	1	1	0	0	0	4	11
2009.12.20	1	0	0	0	0	0	0	1	6
2009.12.21	5	0	0	0	0	0	0	5	6
2010.01.08	16	3	1	2	0	0	0	22	9
2010.01.09	3	0	0	0	0	0	0	3	6

2010.01.13	15	4	2	0	0	0	0	21	8
2010.01.14	9	2	1	0	0	0	0	12	8
2010.01.15	29	9	3	4	0	0	0	44	10
2010.01.16	22	11	5	13	0	0	0	51	13
2010.01.18	47	17	4	30	0	0	0	97	13
2010.01.19	36	11	6	8	0	0	0	61	11
2010.01.20	1339	209	72	322	0	0	0	1942	11
2010.01.21	12223	957	167	729	0	0	0	14075	8
2010.01.23	1785	165	54	1720	0	0	0	3722	14
2010.01.24	25341	2765	562	620	0	0	0	29288	8
2010.01.25	11288	1306	280	1056	0	0	0	13929	9
2010.02.04	32254	2260	284	1299	0	0	0	36097	8
2010.02.05	39411	3127	533	2111	0	0	0	45182	8
2010.02.06	8689	806	139	561	0	0	0	10194	9
2010.02.11	9	2	1	1	0	0	0	12	9
2010.02.16	29	9	4	21	0	0	0	62	13
2010.02.21	5996	695	162	385	0	0	0	7238	9
2010.02.24	13299	1386	277	870	0	0	0	15832	9
2010.03.10	18688	2193	497	820	0	0	0	22198	8
2010.03.11	8095	871	197	588	0	0	0	9751	9
2010.03.12	26063	1560	197	4271	0	0	0	32091	10
2010.03.13	20885	2354	493	791	0	0	0	24522	8
2010.03.20	8478	694	109	378	0	0	0	9658	8
2010.03.21	20858	1701	363	38661	0	0	0	61582	16
2010.03.26	26244	3347	1182	3939	0	0	0	34712	10
2010.03.27	26832	3141	660	6415	0	0	0	37047	11
2010.03.29	17701	1463	250	577	0	0	0	19989	8
2010.03.30	24839	1898	281	4335	0	0	0	31352	10
2010.03.31	21959	1755	237	3795	0	0	0	27745	10
2010.04.02	33518	3275	584	1635	0	0	0	39012	8
2010.04.03	31069	2680	450	5371	0	0	0	39569	10
2010.04.30	12355	1164	308	37268	0	0	0	51095	16
2010.05.10	62004	5670	867	3190	0	0	0	71729	8
2010.05.11	16260	2092	496	24152	0	0	0	43000	15
2010.05.12	8414	667	136	6699	0	0	0	15916	14
2010.05.13	42326	4707	878	7006	0	0	0	54917	10
2010.05.14	14515	1045	179	27641	0	0	0	43379	16
2010.05.15	11325	1016	401	32351	0	0	0	45092	16
2010.05.21	15072	1268	254	962	0	0	0	17555	9
2010.05.27	21769	1737	299	17188	0	0	0	40992	14
2010.05.28	44333	4465	838	1604	0	0	0	51238	8

2010.05.29	24624	2902	756	15427	0	0	0	43709	13
2010.05.30	46514	4748	890	3692	0	0	0	55844	9
2010.05.31	20966	2273	659	103622	0	0	0	127520	17
2010.11.16	9	0	0	0	0	0	0	9	6
2010.11.17	8	1	0	0	0	0	0	9	7
2010.11.18	8	2	0	0	0	0	0	10	7
2010.11.19	4	1	2	0	0	0	0	7	10
2010.11.24	8	4	2	0	0	0	0	14	9
2010.11.25	0	0	0	0	0	0	0	0	
2010.11.26	5	2	0	0	0	0	0	6	7
2010.11.27	3	1	1	0	0	0	0	5	10
2010.11.28	2	0	0	0	0	0	0	2	6
2010.12.03	13	17	6	0	0	0	0	36	10
2010.12.04	4	1	0	0	0	0	0	5	7
2010.12.05	0	0	0	0	0	0	0	0	
2010.12.06	11	2	0	0	0	0	0	13	7
2010.12.07	1	0	0	0	0	0	0	1	6
2010.12.08	11	1	0	0	0	0	0	12	7
2010.12.09	5	2	0	0	0	0	0	7	8
2010.12.10	1	0	0	0	0	0	0	1	6
2010.12.11	1	0	0	0	0	0	0	1	6
2010.12.12	4	0	0	0	0	0	0	4	6
2010.12.13	61	26	6	1	0	0	0	94	9
2010.12.14	36	26	25	88	0	0	0	175	15
2010.12.15	5	0	0	0	0	0	0	5	6
2010.12.16	29	15	12	58	0	0	0	114	15
2010.12.17	8	0	0	0	0	0	0	8	6
2010.12.18	173	146	42	13	0	0	0	374	10
2010.12.19	4	1	0	0	0	0	0	5	7
2010.12.20	8	2	0	0	0	0	0	10	7
2011.01.05	5	2	0	0	0	0	0	7	8
2011.01.06	25	2	0	0	0	0	0	26	6
2011.01.07	7	2	1	0	0	0	0	10	9
2011.01.08	14	1	0	0	0	0	0	15	6
2011.01.09	0	0	0	0	0	0	0	0	

Load Occurrences for Gage S2

Date	4~8 kip	8~12 kip	12~16 kip	16~20 kip	20~24 kip	24~28 kip	>28kip	OC#	ELR (kip)
2009.10.17	2	0	0	0	0	0	0	2	6
2009.10.29	14	2	1	0	0	0	0	17	8
2009.10.31	5	0	0	0	0	0	0	5	6
2009.11.03	12	2	0	0	0	0	0	14	7
2009.11.04	19	1	0	0	0	0	0	20	6
2009.11.05	7	2	0	0	0	0	0	9	7
2009.11.11	9	0	0	0	0	0	0	9	6
2009.11.12	12	2	0	0	0	0	0	14	7
2009.11.13	16	6	0	0	0	0	0	22	8
2009.11.20	38	12	5	0	0	0	0	54	9
2009.11.21	5	1	0	0	0	0	0	6	7
2009.11.22	2	2	0	0	0	0	0	4	8
2009.11.23	32	5	0	0	0	0	0	37	7
2009.11.26	3	0	0	0	0	0	0	3	6
2009.11.29	4	0	0	0	0	0	0	4	6
2009.11.30	40	8	6	1	0	0	0	54	9
2009.12.08	32	4	1	0	0	0	0	37	7
2009.12.09	1	0	0	0	0	0	0	1	6
2009.12.10	17	2	1	0	0	0	0	20	7
2009.12.12	7	0	0	0	0	0	0	7	6
2009.12.13	7	1	0	0	0	0	0	8	7
2009.12.14	31	7	5	0	0	0	0	43	9
2009.12.19	8	0	0	0	0	0	0	8	6
2009.12.20	3	1	0	0	0	0	0	4	7
2009.12.21	13	2	0	0	0	0	0	15	7
2010.01.08	35	13	1	0	0	0	0	49	8
2010.01.09	7	0	0	0	0	0	0	7	6
2010.01.13	27	7	1	0	0	0	0	34	7
2010.01.14	33	14	2	1	0	0	0	49	9
2010.01.15	18	9	2	0	0	0	0	29	9
2010.01.16	13	3	0	0	0	0	0	16	7
2010.01.18	30	4	2	0	0	0	0	36	8
2010.01.19	19	3	1	0	0	0	0	23	7
2010.01.20	23	6	0	1	0	0	0	29	8
2010.01.21	20	3	0	0	0	0	0	23	7
2010.01.23	14	3	0	0	0	0	0	17	7
2010.01.24	4	1	0	0	0	0	0	5	7

2010.01.25	25	8	1	1	0	0	0	35	9
2010.02.04	23	9	1	0	0	1	0	34	9
2010.02.05	28	8	4	1	0	0	0	41	9
2010.02.06	14	4	1	1	0	0	0	20	9
2010.02.11	16	6	1	1	0	0	0	22	8
2010.02.16	26	4	0	0	0	0	0	30	7
2010.02.21	5	0	0	0	0	0	0	5	6
2010.02.24	17	5	0	0	0	0	0	22	7
2010.03.10	26	4	0	0	0	0	0	29	7
2010.03.11	16	3	2	0	0	0	0	21	8
2010.03.12	32	6	3	0	0	0	0	40	8
2010.03.13	8	1	0	0	0	0	0	9	7
2010.03.20	15	7	1	0	0	0	0	23	8
2010.03.21	7	2	0	0	0	0	0	9	7
2010.03.26	29	7	1	2	0	0	0	37	9
2010.03.27	9	2	2	0	0	0	0	13	9
2010.03.29	18	2	0	0	0	0	0	20	7
2010.03.30	27	10	3	0	0	0	0	39	8
2010.03.31	31	3	0	0	0	0	0	34	7
2010.04.02	20	4	2	0	0	0	0	25	8
2010.04.03	20	5	0	1	0	0	0	26	8
2010.04.30	41	8	0	0	0	0	0	48	7
2010.05.10	32	10	4	1	1	0	0	46	9
2010.05.11	44	8	4	1	0	0	0	56	8
2010.05.12	34	7	1	0	0	0	0	41	7
2010.05.13	44	11	3	0	0	0	0	57	8
2010.05.14	32	10	1	0	0	0	0	42	8
2010.05.15	30	3	0	0	0	0	0	33	7
2010.05.21	45	17	5	2	0	0	0	69	9
2010.05.27	29	7	2	0	0	0	0	37	8
2010.05.28	40	6	1	0	0	0	0	46	7
2010.05.29	20	6	1	0	0	0	0	27	8
2010.05.30	17	3	1	0	0	0	0	20	7
2010.05.31	24	2	1	0	0	0	0	27	7
2010.11.16	52	13	4	0	0	0	0	68	8
2010.11.17	41	8	1	0	0	0	0	50	7
2010.11.18	38	5	0	0	0	0	0	43	7
2010.11.19	40	11	5	0	0	0	0	55	8
2010.11.24	50	11	4	0	0	0	0	65	8
2010.11.25	9	0	0	0	0	0	0	9	6
2010.11.26	35	3	3	1	0	0	0	41	8

2010.11.27	14	4	1	0	0	0	0	19	8
2010.11.28	12	1	0	0	0	0	0	13	7
2010.12.03	63	14	14	10	2	0	0	102	11
2010.12.04	20	4	1	0	0	0	0	25	8
2010.12.05	12	2	2	0	0	0	0	16	9
2010.12.06	50	9	4	0	0	0	0	62	8
2010.12.07	36	9	1	0	0	0	0	46	7
2010.12.08	37	8	2	0	0	0	0	47	8
2010.12.09	43	6	2	1	0	0	0	51	8
2010.12.10	36	5	2	1	0	0	0	44	8
2010.12.11	12	3	1	0	0	0	0	15	8
2010.12.12	19	1	0	0	0	0	0	20	6
2010.12.13	85	38	6	0	1	0	0	129	8
2010.12.14	74	56	22	17	12	31	0	210	16
2010.12.15	33	4	0	0	0	0	0	37	7
2010.12.16	56	18	16	12	10	40	0	151	18
2010.12.17	36	8	4	1	0	0	0	49	9
2010.12.18	171	90	50	32	28	5	0	375	13
2010.12.19	15	3	1	0	0	0	0	19	8
2010.12.20	45	7	1	0	0	0	0	53	7
2011.01.05	35	7	0	0	0	0	0	42	7
2011.01.06	70	12	3	1	2	1	0	88	9
2011.01.07	46	11	1	2	0	0	0	59	8
2011.01.08	52	8	6	1	0	0	0	67	9
2011.01.09	21	2	0	0	0	0	0	23	7

Load Occurrences for Gage S3

Date	4~8 kip	8~12 kip	12~16 kip	16~20 kip	20~24 kip	24~28 kip	>28kip	OC#	ELR (kip)
2009.10.17	13	3	0	0	0	0	0	15	7
2009.10.29	3393	416	96	36	155	0	0	4096	9
2009.10.31	4043	419	133	89	637	0	0	5320	12
2009.11.03	10933	875	209	91	463	0	0	12570	9
2009.11.04	13313	1029	226	94	551	0	0	15213	9
2009.11.05	7583	599	102	39	233	0	0	8555	8
2009.11.11	137	49	24	12	66	0	0	287	15
2009.11.12	4934	1530	679	397	1135	0	0	8673	13
2009.11.13	3863	1248	569	355	1316	0	0	7350	14
2009.11.20	2777	238	103	52	1061	0	0	4231	14
2009.11.21	3920	430	167	111	4647	0	0	9274	18
2009.11.22	694	262	223	209	96507	0	0	97894	22
2009.11.23	2901	576	330	232	39221	0	0	43258	21
2009.11.26	8321	407	56	21	63	0	0	8868	7
2009.11.29	11622	2838	1267	643	29540	0	0	45909	19
2009.11.30	15264	2667	1072	530	3884	0	0	23416	13
2009.12.08	3038	591	299	181	60648	0	0	64757	22
2009.12.09	2015	195	140	120	52435	0	0	54904	22
2009.12.10	988	198	99	95	31104	0	0	32483	22
2009.12.12	1850	267	122	92	18914	0	0	21244	21
2009.12.13	6632	663	288	163	59304	0	0	67049	21
2009.12.14	3655	560	229	148	24240	0	0	28831	21
2009.12.19	1882	229	115	79	13877	0	0	16182	21
2009.12.20	0	0	0	0	0	0	0	0	
2009.12.21	0	0	0	0	0	0	0	0	
2010.01.08	173	156	161	163	75246	0	0	75899	22
2010.01.09	0	0	0	0	0	0	0	0	
2010.01.13	0	0	0	0	0	0	0	0	
2010.01.14	4096	1441	607	232	4859	0	0	11235	17
2010.01.15	47	12	1	2	8	0	0	70	12
2010.01.16	4553	1906	1139	730	52199	0	0	60526	21
2010.01.18	100	82	57	73	20378	0	0	20690	22
2010.01.19	0	0	0	0	322	0	0	322	22
2010.01.20	0	0	0	0	0	0	0	0	
2010.01.21	565	104	61	74	24666	0	0	25470	22
2010.01.23	13525	1404	435	221	39249	0	0	54834	20

2010.01.24	7301	951	401	234	33073	0	0	41959	20
2010.01.25	15800	1666	452	181	3843	0	0	21941	13
2010.02.04	198	142	143	138	54852	0	0	55473	22
2010.02.05	1577	167	68	36	25214	0	0	27062	22
2010.02.06	670	338	318	274	128418	0	0	130018	22
2010.02.11	4202	486	116	55	1936	0	0	6794	15
2010.02.16	24	11	19	21	7810	0	0	7885	22
2010.02.21	4	4	2	2	1524	0	0	1536	22
2010.02.24	55	74	58	47	16400	0	0	16634	22
2010.03.10	473	75	15	9	1262	0	0	1834	20
2010.03.11	0	0	0	0	0	0	0	0	
2010.03.12	896	235	225	183	99267	0	0	100805	22
2010.03.13	67	73	70	62	36891	0	0	37163	22
2010.03.20	0	0	0	0	0	0	0	0	
2010.03.21	35	26	32	27	13927	0	0	14047	22
2010.03.26	21	26	20	18	11277	0	0	11362	22
2010.03.27	169	33	16	16	8812	0	0	9046	22
2010.03.29	97	116	76	82	39317	0	0	39688	22
2010.03.30	671	255	108	81	27806	0	0	28921	22
2010.03.31	321	281	257	226	105097	0	0	106182	22
2010.04.02	0	0	0	0	10	0	0	10	22
2010.04.03	15	18	13	15	8189	0	0	8250	22
2010.04.30	0	0	0	0	0	0	0	0	
2010.05.10	0	0	0	0	0	0	0	0	
2010.05.11	0	0	0	0	0	0	0	0	
2010.05.12	0	0	0	0	0	0	0	0	
2010.05.13	0	0	0	0	0	0	0	0	
2010.05.14	7	4	5	1	1874	0	0	1891	22
2010.05.15	10	12	10	7	3341	0	0	3380	22
2010.05.21	0	0	0	0	0	0	0	0	
2010.05.27	0	0	0	0	0	0	0	0	
2010.05.28	0	0	0	0	0	0	0	0	
2010.05.29	20	26	31	24	14993	0	0	15094	22
2010.05.30	0	0	0	0	0	0	0	0	
2010.05.31	8	2	3	0	1187	0	0	1200	22
2010.11.16	107	23	8	1	0	0	0	137	8
2010.11.17	67	25	7	0	0	0	0	98	8
2010.11.18	76	18	6	2	0	0	0	101	8
2010.11.19	92	33	6	1	0	0	0	131	8
2010.11.24	69	24	5	0	0	0	0	98	8
2010.11.25	11	0	1	0	0	0	0	12	8

2010.11.26	33	11	2	0	0	0	0	46	8
2010.11.27	22	5	1	0	0	0	0	28	8
2010.11.28	12	3	1	0	0	0	0	15	8
2010.12.03	94	41	11	3	2	0	0	150	9
2010.12.04	26	8	2	1	0	0	0	37	9
2010.12.05	6	1	0	0	0	0	0	7	7
2010.12.06	106	18	2	1	0	0	0	126	7
2010.12.07	64	21	5	1	0	0	0	90	8
2010.12.08	76	21	6	2	0	0	0	104	9
2010.12.09	85	18	4	0	0	0	0	106	8
2010.12.10	74	17	4	0	0	0	0	95	8
2010.12.11	35	6	2	0	0	0	0	43	8
2010.12.12	20	2	0	0	0	0	0	22	7
2010.12.13	109	35	6	4	16	0	0	168	12
2010.12.14	104	39	19	11	138	0	0	310	17
2010.12.15	88	35	5	1	1	0	0	129	9
2010.12.16	137	34	8	3	76	0	0	258	15
2010.12.17	107	43	8	3	0	0	0	160	9
2010.12.18	127	51	25	17	121	0	0	341	17
2010.12.19	10	1	0	0	0	0	0	11	7
2010.12.20	93	24	10	5	0	0	0	132	9
2011.01.05	70	27	7	3	0	0	0	105	9
2011.01.06	89	26	7	0	3	0	0	125	9
2011.01.07	123	42	12	2	0	0	0	178	9
2011.01.08	91	29	8	8	0	0	0	135	9
2011.01.09	24	5	0	0	0	0	0	29	7

Load Occurrences for Gage S4

Date	4~8 kip	8~12 kip	12~16 kip	16~20 kip	20~24 kip	24~28 kip	>28kip	OC#	ELR (kip)
2009.10.17	4	0	0	0	0	0	0	4	6
2009.10.29	2089	205	304	0	0	0	0	2597	8
2009.10.31	5081	503	3276	0	0	0	0	8859	11
2009.11.03	5495	612	1657	0	0	0	0	7764	9
2009.11.04	61	1	26	0	0	0	0	88	10
2009.11.05	90	5	10	0	0	0	0	104	8
2009.11.11	3048	246	520	0	0	0	0	3814	8
2009.11.12	13	1	0	0	0	0	0	14	6
2009.11.13	18	5	12	0	0	0	0	35	11
2009.11.20	1577	190	483	0	0	0	0	2250	9
2009.11.21	1011	138	231	0	0	0	0	1380	9
2009.11.22	541	57	213	0	0	0	0	811	10
2009.11.23	3864	359	2789	0	0	0	0	7012	11
2009.11.26	4	1	1	0	0	0	0	5	8
2009.11.29	283	91	202	0	0	0	0	575	11
2009.11.30	5265	704	1396	0	0	0	0	7365	9
2009.12.08	12693	970	2437	0	0	0	0	16100	9
2009.12.09	3621	541	477	0	0	0	0	4638	8
2009.12.10	4418	482	458	0	0	0	0	5358	8
2009.12.12	11515	721	3888	0	0	0	0	16124	10
2009.12.13	10400	905	2113	0	0	0	0	13418	9
2009.12.14	6781	755	2252	0	0	0	0	9788	10
2009.12.19	51	3	5	0	0	0	0	58	8
2009.12.20	9	1	9	0	0	0	0	18	11
2009.12.21	35	4	6	0	0	0	0	45	9
2010.01.08	1831	182	234	0	0	0	0	2247	8
2010.01.09	5	0	0	0	0	0	0	5	6
2010.01.13	5011	283	329	0	0	0	0	5622	7
2010.01.14	287	74	190	0	0	0	0	551	11
2010.01.15	5106	500	277	0	0	0	0	5882	7
2010.01.16	1114	133	426	0	0	0	0	1672	10
2010.01.18	4933	408	2058	0	0	0	0	7399	10
2010.01.19	12942	1786	1643	0	0	0	0	16371	8
2010.01.20	4627	553	1985	0	0	0	0	7164	10
2010.01.21	6565	401	2434	0	0	0	0	9399	10
2010.01.23	3088	175	141	0	0	0	0	3403	7

2010.01.24	14735	1199	6739	0	0	0	0	22673	10
2010.01.25	5423	208	2516	0	0	0	0	8146	10
2010.02.04	105259	23753	36335	0	0	0	0	165347	10
2010.02.05	4902	487	803	0	0	0	0	6192	8
2010.02.06	11174	1725	8174	0	0	0	0	21073	11
2010.02.11	971	85	78	0	0	0	0	1133	8
2010.02.16	8709	816	844	0	0	0	0	10368	8
2010.02.21	15316	1507	5162	0	0	0	0	21985	10
2010.02.24	8462	999	4803	0	0	0	0	14264	10
2010.03.10	9657	847	4256	0	0	0	0	14760	10
2010.03.11	6746	394	6342	0	0	0	0	13482	11
2010.03.12	67349	4856	805	0	0	0	0	73010	7
2010.03.13	5015	390	6390	0	0	0	0	11795	12
2010.03.20	53256	10775	13726	0	0	0	0	77757	9
2010.03.21	34439	6309	8791	0	0	0	0	49538	9
2010.03.26	24249	7302	21825	0	0	0	0	53375	11
2010.03.27	20998	3389	6740	0	0	0	0	31126	9
2010.03.29	5163	471	286	0	0	0	0	5920	7
2010.03.30	9414	1048	2248	0	0	0	0	12709	9
2010.03.31	212967	55091	31172	0	0	0	0	299229	9
2010.04.02	29572	7856	17388	0	0	0	0	54815	10
2010.04.03	17806	3991	31898	0	0	0	0	53695	12
2010.04.30	23557	2366	1936	0	0	0	0	27859	8
2010.05.10	35243	3157	2248	0	0	0	0	40648	7
2010.05.11	14234	1200	1557	0	0	0	0	16990	8
2010.05.12	18521	1852	3901	0	0	0	0	24274	9
2010.05.13	15229	1399	10886	0	0	0	0	27513	11
2010.05.14	7946	962	66260	0	0	0	0	75167	13
2010.05.15	25097	3915	5137	0	0	0	0	34149	9
2010.05.21	17925	2386	2702	0	0	0	0	23013	8
2010.05.27	48580	8235	5987	0	0	0	0	62801	8
2010.05.28	34438	5147	3190	0	0	0	0	42774	8
2010.05.29	83104	22078	11610	0	0	0	0	116792	9
2010.05.30	16391	2473	2063	0	0	0	0	20926	8
2010.05.31	47285	10638	9101	0	0	0	0	67024	9
2010.11.16	34	4	0	0	0	0	0	37	7
2010.11.17	30	3	0	0	0	0	0	33	7
2010.11.18	29	1	0	0	0	0	0	30	6
2010.11.19	30	2	0	0	0	0	0	32	6
2010.11.24	37	6	0	0	0	0	0	43	7
2010.11.25	4	0	0	0	0	0	0	4	6

2010.11.26	16	2	0	0	0	0	0	18	7
2010.11.27	10	2	0	0	0	0	0	12	7
2010.11.28	5	0	0	0	0	0	0	5	6
2010.12.03	45	5	0	0	0	0	0	50	7
2010.12.04	11	1	0	0	0	0	0	12	6
2010.12.05	6	1	0	0	0	0	0	6	7
2010.12.06	37	8	0	0	0	0	0	45	7
2010.12.07	37	1	0	0	0	0	0	38	6
2010.12.08	37	4	0	0	0	0	0	41	7
2010.12.09	36	4	0	0	0	0	0	40	7
2010.12.10	27	2	0	0	0	0	0	29	6
2010.12.11	11	1	0	0	0	0	0	12	6
2010.12.12	3	0	0	0	0	0	0	3	6
2010.12.13	68	5	1	0	0	0	0	73	7
2010.12.14	65	29	25	0	0	0	0	119	10
2010.12.15	24	4	0	0	0	0	0	28	7
2010.12.16	48	22	57	0	0	0	0	127	11
2010.12.17	47	8	1	0	0	0	0	55	7
2010.12.18	173	50	4	0	0	0	0	227	8
2010.12.19	3	0	0	0	0	0	0	3	6
2010.12.20	45	10	2	0	0	0	0	57	8
2011.01.05	32	6	0	0	0	0	0	38	7
2011.01.06	32	7	0	0	0	0	0	39	7
2011.01.07	48	16	0	0	0	0	0	64	7
2011.01.08	44	10	2	0	0	0	0	55	8
2011.01.09	4	0	0	0	0	0	0	4	6

Load Occurrences for Gage S5

Date	4~8 kip	8~12 kip	12~16 kip	16~20 kip	20~24 kip	24~28 kip	>28kip	OC#	ELR (kip)
2009.10.17	0	0	0	0	0	0	0	0	
2009.10.29	0	0	0	0	0	0	0	0	
2009.10.31	0	0	0	0	0	0	0	0	
2009.11.03	0	0	0	0	0	0	0	0	
2009.11.04	0	0	0	0	0	0	0	0	
2009.11.05	0	0	0	0	0	0	0	0	
2009.11.11	0	0	0	0	0	0	0	0	
2009.11.12	0	0	0	0	0	0	0	0	
2009.11.13	0	0	0	0	0	0	0	0	
2009.11.20	0	0	0	0	0	0	0	0	
2009.11.21	0	0	0	0	0	0	0	0	
2009.11.22	0	0	0	0	0	0	0	0	
2009.11.23	0	0	0	0	0	0	0	0	
2009.11.26	0	0	0	0	0	0	0	0	
2009.11.29	0	0	0	0	0	0	0	0	
2009.11.30	0	0	0	0	0	0	0	0	
2009.12.08	0	0	0	0	0	0	0	0	
2009.12.09	0	0	0	0	0	0	0	0	
2009.12.10	0	0	0	0	0	0	0	0	
2009.12.12	0	0	0	0	0	0	0	0	
2009.12.13	0	0	0	0	0	0	0	0	
2009.12.14	0	0	0	0	0	0	0	0	
2009.12.19	0	0	0	0	0	0	0	0	
2009.12.20	0	0	0	0	0	0	0	0	
2009.12.21	0	0	0	0	0	0	0	0	
2010.01.08	0	0	0	0	0	0	0	0	
2010.01.09	0	0	0	0	0	0	0	0	
2010.01.13	0	0	0	0	0	0	0	0	
2010.01.14	0	0	0	0	0	0	0	0	
2010.01.15	0	0	0	0	0	0	0	0	
2010.01.16	0	0	0	0	0	0	0	0	
2010.01.18	0	0	0	0	0	0	0	0	
2010.01.19	0	0	0	0	0	0	0	0	
2010.01.20	0	0	0	0	0	0	0	0	
2010.01.21	0	0	0	0	0	0	0	0	
2010.01.23	0	0	0	0	0	0	0	0	

2010.01.24	0	0	0	0	0	0	0	0	
2010.01.25	0	0	0	0	0	0	0	0	
2010.02.04	0	0	0	0	0	1	0	1	26
2010.02.05	0	0	0	0	0	0	0	0	
2010.02.06	0	0	0	0	0	0	0	0	
2010.02.11	0	0	0	0	0	0	0	0	
2010.02.16	0	0	0	0	0	0	0	0	
2010.02.21	0	0	0	0	0	0	0	0	
2010.02.24	0	0	0	0	0	0	0	0	
2010.03.10	0	0	0	0	0	0	0	0	
2010.03.11	0	0	0	0	0	0	0	0	
2010.03.12	0	0	0	0	0	0	0	0	
2010.03.13	0	0	0	0	0	0	0	0	
2010.03.20	0	0	0	0	0	0	0	0	
2010.03.21	0	0	0	0	0	0	0	0	
2010.03.26	0	0	0	0	0	0	0	0	
2010.03.27	0	0	0	0	0	0	0	0	
2010.03.29	0	0	0	0	0	0	0	0	
2010.03.30	0	0	0	0	0	0	0	0	
2010.03.31	0	0	0	0	0	0	0	0	
2010.04.02	0	0	0	0	0	0	0	0	
2010.04.03	0	0	0	0	0	0	0	0	
2010.04.30	0	0	0	0	0	0	0	0	
2010.05.10	0	0	0	0	0	0	0	0	
2010.05.11	0	0	0	0	0	0	0	0	
2010.05.12	0	0	0	0	0	0	0	0	
2010.05.13	0	0	0	0	0	0	0	0	
2010.05.14	0	0	0	0	0	0	0	0	
2010.05.15	0	0	0	0	0	0	0	0	
2010.05.21	0	0	0	0	0	0	0	0	
2010.05.27	0	0	0	0	0	0	0	0	
2010.05.28	0	0	0	0	0	0	0	0	
2010.05.29	0	0	0	0	0	0	0	0	
2010.05.30	0	0	0	0	0	0	0	0	
2010.05.31	0	0	0	0	0	0	0	0	
2010.11.16	42	4	0	0	0	0	0	46	7
2010.11.17	26	7	1	0	0	0	0	34	8
2010.11.18	23	5	0	2	0	0	0	30	9
2010.11.19	29	4	1	1	0	0	0	35	8
2010.11.24	23	7	2	2	0	0	0	34	9
2010.11.25	1	0	0	0	0	0	0	1	6

2010.11.26	24	4	1	0	0	0	0	29	7
2010.11.27	18	3	1	0	0	0	0	22	8
2010.11.28	5	1	0	0	0	0	0	6	7
2010.12.03	38	23	4	1	0	0	0	65	9
2010.12.04	8	2	2	0	0	0	0	12	9
2010.12.05	3	0	0	0	0	0	0	3	6
2010.12.06	24	5	2	0	0	0	0	31	8
2010.12.07	13	1	0	0	0	0	0	14	6
2010.12.08	33	8	2	0	0	0	0	43	8
2010.12.09	18	2	4	0	0	0	0	24	9
2010.12.10	17	0	0	0	0	0	0	17	6
2010.12.11	15	1	0	0	0	0	0	16	6
2010.12.12	17	3	0	0	0	0	0	20	7
2010.12.13	87	15	5	1	0	0	0	107	8
2010.12.14	74	30	33	26	7	5	0	174	14
2010.12.15	23	2	0	0	0	0	0	25	7
2010.12.16	56	18	18	12	7	24	0	135	17
2010.12.17	37	7	0	0	0	0	0	44	7
2010.12.18	194	67	2	1	0	0	0	263	8
2010.12.19	6	1	1	0	0	0	0	8	9
2010.12.20	29	7	1	0	0	0	0	37	8
2011.01.05	33	6	0	0	0	0	0	38	7
2011.01.06	38	4	1	0	0	0	0	42	7
2011.01.07	27	5	0	1	0	0	0	33	8
2011.01.08	43	7	2	0	0	0	0	51	7
2011.01.09	1	0	0	0	0	0	0	1	6

Load Occurrences for Gage S6

Date	4~8 kip	8~12 kip	12~16 kip	16~20 kip	20~24 kip	24~28 kip	>28kip	OC#	ELR (kip)
2009.10.17	52	8	0	0	0	0	0	60	7
2009.10.29	225	57	11	0	0	0	0	292	8
2009.10.31	82	20	1	0	0	0	0	103	7
2009.11.03	251	51	4	0	0	0	0	305	7
2009.11.04	142	30	5	0	0	0	0	177	7
2009.11.05	266	53	4	0	0	0	0	323	7
2009.11.11	266	61	7	0	0	0	0	333	7
2009.11.12	240	44	1	0	0	0	0	284	7
2009.11.13	264	58	8	0	0	0	0	330	7
2009.11.20	259	64	17	0	0	0	0	340	8
2009.11.21	91	21	1	0	0	0	0	113	7
2009.11.22	51	9	0	0	0	0	0	60	7
2009.11.23	218	67	10	0	0	0	0	294	8
2009.11.26	66	9	1	0	0	0	0	75	7
2009.11.29	81	13	0	0	0	0	0	94	7
2009.11.30	508	117	27	0	0	0	0	651	8
2009.12.08	388	85	16	0	0	0	0	488	8
2009.12.09	32	8	0	0	0	0	0	40	7
2009.12.10	364	70	5	1	0	0	0	439	7
2009.12.12	91	15	1	0	0	0	0	106	7
2009.12.13	96	18	1	0	0	0	0	115	7
2009.12.14	365	88	10	1	0	0	0	463	8
2009.12.19	28	4	0	0	0	0	0	31	7
2009.12.20	50	2	0	0	0	0	0	52	6
2009.12.21	350	66	5	0	0	0	0	420	7
2010.01.08	459	91	6	0	0	0	0	555	7
2010.01.09	152	30	0	0	0	0	0	182	7
2010.01.13	329	85	14	0	0	0	0	428	8
2010.01.14	379	93	20	0	0	0	0	491	8
2010.01.15	360	71	6	1	0	0	0	438	7
2010.01.16	151	31	1	0	0	0	0	183	7
2010.01.18	328	72	5	0	0	0	0	404	7
2010.01.19	197	36	6	0	0	0	0	239	7
2010.01.20	418	80	13	1	0	0	0	511	7
2010.01.21	397	86	11	0	0	0	0	494	7
2010.01.23	183	49	4	0	0	0	0	236	7

2010.01.24	90	15	1	0	0	0	0	106	7
2010.01.25	381	84	15	0	0	0	0	479	8
2010.02.04	453	105	23	0	0	1	0	582	8
2010.02.05	410	103	15	0	0	0	0	528	8
2010.02.06	188	50	3	0	0	0	0	240	7
2010.02.11	329	63	10	0	0	0	0	401	7
2010.02.16	520	87	7	0	0	0	0	614	7
2010.02.21	90	17	1	0	0	0	0	107	7
2010.02.24	348	88	8	0	0	0	0	444	7
2010.03.10	429	101	8	0	0	0	0	538	7
2010.03.11	453	111	11	0	0	0	0	574	7
2010.03.12	462	88	12	0	0	0	0	561	7
2010.03.13	177	31	7	1	0	0	0	215	8
2010.03.20	193	43	2	0	0	0	0	237	7
2010.03.21	150	35	1	0	0	0	0	185	7
2010.03.26	421	107	16	0	0	0	0	543	8
2010.03.27	163	39	2	0	0	0	0	204	7
2010.03.29	366	75	7	0	0	0	0	447	7
2010.03.30	401	94	6	1	0	0	0	501	7
2010.03.31	443	117	12	0	0	0	0	572	8
2010.04.02	325	81	7	0	0	0	0	413	7
2010.04.03	137	39	3	0	0	0	0	178	8
2010.04.30	573	137	33	4	0	0	0	747	8
2010.05.10	405	114	10	1	1	0	0	530	8
2010.05.11	480	147	12	0	0	0	0	638	8
2010.05.12	442	115	13	0	0	0	0	570	8
2010.05.13	520	130	14	2	0	0	0	665	8
2010.05.14	549	129	23	1	0	0	0	702	8
2010.05.15	289	73	7	0	0	0	0	369	7
2010.05.21	516	154	22	3	0	0	0	694	8
2010.05.27	446	144	26	2	0	0	0	617	8
2010.05.28	428	134	17	0	0	0	0	578	8
2010.05.29	175	51	3	0	0	0	0	229	8
2010.05.30	89	23	1	0	0	0	0	112	7
2010.05.31	155	33	6	0	0	0	0	194	8
2010.11.16	616	199	54	12	1	0	0	881	9
2010.11.17	641	198	47	12	1	0	0	899	8
2010.11.18	655	181	50	5	1	0	0	891	8
2010.11.19	609	172	36	5	0	0	0	821	8
2010.11.24	730	200	52	4	0	0	0	986	8
2010.11.25	122	21	6	1	0	0	0	150	8

2010.11.26	432	117	25	1	0	0	0	575	8
2010.11.27	255	75	15	0	0	0	0	345	8
2010.11.28	164	34	5	0	0	0	0	203	7
2010.12.03	828	226	65	6	2	2	0	1127	8
2010.12.04	326	80	22	3	1	0	0	430	8
2010.12.05	157	34	9	0	0	0	0	199	8
2010.12.06	776	216	77	10	1	0	0	1079	8
2010.12.07	637	217	57	8	0	0	0	918	8
2010.12.08	665	188	55	8	1	0	0	916	8
2010.12.09	735	180	51	5	0	0	0	970	8
2010.12.10	527	137	41	3	0	0	0	707	8
2010.12.11	266	60	20	4	1	0	0	349	8
2010.12.12	196	54	12	0	0	0	0	261	8
2010.12.13	670	206	45	8	1	0	0	929	8
2010.12.14	544	178	56	19	28	37	0	861	12
2010.12.15	617	178	58	3	0	0	0	855	8
2010.12.16	668	232	67	16	2	28	0	1013	10
2010.12.17	740	294	77	22	3	0	0	1135	9
2010.12.18	516	176	69	14	9	152	0	935	15
2010.12.19	190	37	13	0	0	0	0	240	8
2010.12.20	667	247	82	23	3	0	0	1021	9
2011.01.05	564	190	65	14	2	0	0	834	9
2011.01.06	747	243	78	26	4	0	0	1096	9
2011.01.07	740	271	93	29	4	0	0	1137	9
2011.01.08	483	212	106	36	8	0	0	844	10
2011.01.09	215	51	14	1	0	0	0	280	8

Load Occurrences for Gage S7

Date	4~8 kip	8~12 kip	12~16 kip	16~20 kip	20~24 kip	24~28 kip	>28kip	OC#	ELR (kip)
2009.10.17	15	3	0	0	0	0	0	17	7
2009.10.29	65	13	4	1	0	0	0	82	8
2009.10.31	17	6	3	0	0	0	0	26	9
2009.11.03	80	25	7	1	0	0	0	112	8
2009.11.04	57	15	2	0	0	0	0	73	8
2009.11.05	79	19	4	1	0	0	0	103	8
2009.11.11	82	15	4	1	0	0	0	101	8
2009.11.12	75	13	1	0	0	0	0	89	7
2009.11.13	110	37	4	0	0	0	0	150	8
2009.11.20	252	82	20	5	0	0	0	358	8
2009.11.21	101	30	6	2	0	0	0	138	8
2009.11.22	49	14	2	0	0	0	0	65	8
2009.11.23	294	109	22	9	1	0	0	434	9
2009.11.26	11	0	0	0	0	0	0	11	6
2009.11.29	24	4	1	0	0	0	0	29	7
2009.11.30	184	63	22	10	2	0	0	279	9
2009.12.08	118	25	7	1	0	0	0	150	8
2009.12.09	105	18	5	0	0	0	0	128	8
2009.12.10	126	31	7	2	0	0	0	165	8
2009.12.12	65	21	6	2	0	0	0	93	9
2009.12.13	20	2	2	0	0	0	0	24	8
2009.12.14	110	35	10	2	0	0	0	156	8
2009.12.19	34	8	2	1	0	0	0	45	8
2009.12.20	17	3	0	0	0	0	0	20	7
2009.12.21	94	14	4	3	0	0	0	114	8
2010.01.08	291	60	18	1	0	0	0	368	8
2010.01.09	42	6	1	0	0	0	0	48	7
2010.01.13	79	19	4	1	0	0	0	103	8
2010.01.14	115	24	6	2	0	0	0	147	8
2010.01.15	107	24	3	3	0	0	0	136	8
2010.01.16	37	7	1	0	0	0	0	45	7
2010.01.18	84	18	5	0	0	0	0	107	8
2010.01.19	21	4	0	0	0	0	0	25	7
2010.01.20	80	18	4	1	0	0	0	103	8
2010.01.21	87	24	4	1	0	0	0	116	8
2010.01.23	32	6	1	0	0	0	0	39	7

2010.01.24	18	1	1	0	0	0	0	19	7
2010.01.25	89	25	7	2	0	0	0	123	8
2010.02.04	116	31	10	6	1	0	0	163	9
2010.02.05	97	24	8	3	0	0	0	132	9
2010.02.06	51	9	4	0	0	0	0	64	8
2010.02.11	70	29	9	2	0	0	0	110	9
2010.02.16	96	17	2	1	0	0	0	115	7
2010.02.21	13	1	0	0	0	0	0	14	6
2010.02.24	114	24	6	1	0	0	0	145	8
2010.03.10	103	18	4	1	0	0	0	126	8
2010.03.11	84	17	1	1	0	0	0	103	8
2010.03.12	170	21	3	1	0	0	0	195	7
2010.03.13	38	11	0	0	0	0	0	49	7
2010.03.20	47	8	0	0	0	0	0	54	7
2010.03.21	36	4	0	0	0	0	0	40	7
2010.03.26	124	36	10	3	1	0	0	173	9
2010.03.27	59	8	1	0	0	0	0	68	7
2010.03.29	97	14	4	1	0	0	0	115	7
2010.03.30	108	20	4	0	0	0	0	132	7
2010.03.31	113	27	6	1	0	0	0	146	8
2010.04.02	96	35	6	2	0	0	0	139	8
2010.04.03	33	7	2	0	0	0	0	42	8
2010.04.30	113	24	8	4	0	0	0	148	8
2010.05.10	145	43	12	3	0	0	0	202	8
2010.05.11	133	36	5	2	0	0	0	175	8
2010.05.12	221	60	14	3	0	0	0	298	8
2010.05.13	196	38	11	5	0	0	0	249	8
2010.05.14	200	47	23	5	1	0	0	275	9
2010.05.15	59	12	3	0	0	0	0	73	8
2010.05.21	220	63	16	1	3	0	0	302	9
2010.05.27	169	37	14	1	0	0	0	220	8
2010.05.28	168	46	20	0	0	0	0	233	8
2010.05.29	54	7	4	1	0	0	0	66	8
2010.05.30	32	6	2	0	0	0	0	39	8
2010.05.31	52	13	4	0	0	0	0	69	8
2010.11.16	175	38	13	5	0	0	0	231	8
2010.11.17	127	30	14	4	0	0	0	173	9
2010.11.18	145	34	5	4	0	0	0	188	8
2010.11.19	150	46	14	4	0	0	0	213	9
2010.11.24	164	34	9	2	0	0	0	208	8
2010.11.25	18	3	1	0	0	0	0	22	8

2010.11.26	78	14	5	1	0	0	0	97	8
2010.11.27	58	8	2	0	0	0	0	67	7
2010.11.28	20	4	3	1	0	0	0	27	9
2010.12.03	210	35	18	22	2	0	0	286	10
2010.12.04	53	10	3	2	0	0	0	68	8
2010.12.05	19	0	2	0	0	0	0	21	8
2010.12.06	165	30	9	1	1	0	0	205	8
2010.12.07	130	24	11	2	0	0	0	167	8
2010.12.08	112	33	14	2	1	0	0	162	9
2010.12.09	116	30	9	1	0	0	0	156	8
2010.12.10	130	28	8	1	0	0	0	167	8
2010.12.11	57	8	4	1	0	0	0	69	8
2010.12.12	40	6	0	0	0	0	0	46	7
2010.12.13	185	53	21	3	2	0	0	263	9
2010.12.14	172	46	27	16	99	0	0	360	15
2010.12.15	169	36	14	4	1	0	0	224	9
2010.12.16	197	60	26	14	58	0	0	354	14
2010.12.17	175	63	20	6	0	0	0	263	9
2010.12.18	203	87	64	67	82	0	0	502	15
2010.12.19	28	0	0	0	0	0	0	28	6
2010.12.20	151	36	15	7	3	0	0	211	9
2011.01.05	139	31	11	6	0	0	0	186	9
2011.01.06	194	44	16	3	3	0	0	259	9
2011.01.07	214	46	23	7	0	0	0	290	9
2011.01.08	140	39	21	8	4	0	0	211	10
2011.01.09	54	5	0	0	0	0	0	59	7
2011.01.06	194	44	16	3	3	0	0	259	9
2011.01.07	214	46	23	7	0	0	0	290	9
2011.01.08	140	39	21	8	4	0	0	211	10
2011.01.09	54	5	0	0	0	0	0	59	7

Load Occurrences for Gage S8

Date	4~8 kip	8~12 kip	12~16 kip	16~20 kip	20~24 kip	24~28 kip	>28kip	OC#	ELR (kip)
2009.10.17	0	0	0	0	0	0	0	0	
2009.10.29	0	0	0	0	0	0	0	0	
2009.10.31	0	0	0	0	0	0	0	0	
2009.11.03	0	0	0	0	0	0	0	0	
2009.11.04	0	0	0	0	0	0	0	0	
2009.11.05	0	0	0	0	0	0	0	0	
2009.11.11	0	0	0	0	0	0	0	0	
2009.11.12	0	0	0	0	0	0	0	0	
2009.11.13	0	0	0	0	0	0	0	0	
2009.11.20	0	0	0	0	0	0	0	0	
2009.11.21	0	0	0	0	0	0	0	0	
2009.11.22	0	0	0	0	0	0	0	0	
2009.11.23	0	0	0	0	0	0	0	0	
2009.11.26	0	0	0	0	0	0	0	0	
2009.11.29	0	0	0	0	0	0	0	0	
2009.11.30	0	0	0	0	0	0	0	0	
2009.12.08	0	0	0	0	0	0	0	0	
2009.12.09	0	0	0	0	0	0	0	0	
2009.12.10	0	0	0	0	0	0	0	0	
2009.12.12	0	0	0	0	0	0	0	0	
2009.12.13	0	0	0	0	0	0	0	0	
2009.12.14	0	0	0	0	0	0	0	0	
2009.12.19	0	0	0	0	0	0	0	0	
2009.12.20	0	0	0	0	0	0	0	0	
2009.12.21	0	0	0	0	0	0	0	0	
2010.01.08	0	0	0	0	0	0	0	0	
2010.01.09	0	0	0	0	0	0	0	0	
2010.01.13	0	0	0	0	0	0	0	0	
2010.01.14	0	0	0	0	0	0	0	0	
2010.01.15	0	0	0	0	0	0	0	0	
2010.01.16	0	0	0	0	0	0	0	0	
2010.01.18	0	0	0	0	0	0	0	0	
2010.01.19	0	0	0	0	0	0	0	0	
2010.01.20	0	0	0	0	0	0	0	0	
2010.01.21	0	0	0	0	0	0	0	0	
2010.01.23	0	0	0	0	0	0	0	0	

2010.01.24	0	0	0	0	0	0	0	0	
2010.01.25	0	0	0	0	0	0	0	0	
2010.02.04	0	0	0	0	0	0	0	0	
2010.02.05	0	0	0	0	0	0	0	0	
2010.02.06	0	0	0	0	0	0	0	0	
2010.02.11	0	0	0	0	0	0	0	0	
2010.02.16	0	0	0	0	0	0	0	0	
2010.02.21	0	0	0	0	0	0	0	0	
2010.02.24	0	0	0	0	0	0	0	0	
2010.03.10	0	0	0	0	0	0	0	0	
2010.03.11	0	0	0	0	0	0	0	0	
2010.03.12	0	0	0	0	0	0	0	0	
2010.03.13	0	0	0	0	0	0	0	0	
2010.03.20	0	0	0	0	0	0	0	0	
2010.03.21	0	0	0	0	0	0	0	0	
2010.03.26	0	0	0	0	0	0	0	0	
2010.03.27	0	0	0	0	0	0	0	0	
2010.03.29	0	0	0	0	0	0	0	0	
2010.03.30	0	0	0	0	0	0	0	0	
2010.03.31	0	0	0	0	0	0	0	0	
2010.04.02	0	0	0	0	0	0	0	0	
2010.04.03	0	0	0	0	0	0	0	0	
2010.04.30	0	0	0	0	0	0	0	0	
2010.05.10	0	0	0	0	0	0	0	0	
2010.05.11	0	0	0	0	0	0	0	0	
2010.05.12	0	0	0	0	0	0	0	0	
2010.05.13	0	0	0	0	0	0	0	0	
2010.05.14	0	0	0	0	0	0	0	0	
2010.05.15	0	0	0	0	0	0	0	0	
2010.05.21	0	0	0	0	0	0	0	0	
2010.05.27	0	0	0	0	0	0	0	0	
2010.05.28	0	0	0	0	0	0	0	0	
2010.05.29	0	0	0	0	0	0	0	0	
2010.05.30	0	0	0	0	0	0	0	0	
2010.05.31	0	0	0	0	0	0	0	0	
2010.11.16	107	12	3	1	0	0	0	122	7
2010.11.17	90	11	1	1	0	0	0	103	7
2010.11.18	94	14	1	1	0	0	0	109	7
2010.11.19	104	25	3	2	0	0	0	134	8
2010.11.24	104	23	3	0	0	0	0	130	7
2010.11.25	25	0	0	0	0	0	0	25	6

2010.11.26	55	4	1	0	0	0	0	60	7
2010.11.27	38	4	0	0	0	0	0	42	7
2010.11.28	24	1	0	1	0	0	0	26	8
2010.12.03	129	26	13	2	0	2	0	171	9
2010.12.04	41	2	2	0	0	0	0	45	7
2010.12.05	23	0	0	1	0	0	0	24	8
2010.12.06	103	7	1	0	0	0	0	111	7
2010.12.07	80	10	3	1	0	0	0	93	8
2010.12.08	70	15	2	1	0	0	0	88	8
2010.12.09	86	13	2	0	0	0	0	100	7
2010.12.10	99	14	3	0	0	0	0	115	7
2010.12.11	49	2	1	0	0	0	0	52	7
2010.12.12	36	1	0	0	0	0	0	37	6
2010.12.13	133	24	3	2	0	0	0	161	8
2010.12.14	125	36	17	25	26	24	0	252	16
2010.12.15	104	22	4	1	0	0	0	131	8
2010.12.16	130	45	22	17	15	13	0	241	14
2010.12.17	123	25	8	1	0	0	0	156	8
2010.12.18	251	91	1	1	0	0	0	343	8
2010.12.19	24	0	0	0	0	0	0	24	6
2010.12.20	106	14	5	2	0	0	0	126	8
2011.01.05	92	14	6	1	0	0	0	113	8
2011.01.06	131	17	7	1	3	0	0	157	8
2011.01.07	139	24	7	1	0	0	0	169	8
2011.01.08	90	19	6	5	0	0	0	119	9
2011.01.09	42	2	0	0	0	0	0	44	6

Appendix F – Steel Girder Gage Histograms

The following tables give the number of occurrences of each stress range recorded by each of the girder strain gages during the monitoring period. Data covers 7am through 6pm during typical business hours. Data not included here was incomplete or missing during these hours. OC# represents the total number of occurrences; ESR represents the equivalent stress range that would be used in a fatigue analysis of the girders using Miner's Rule.

Stress Occurrences for Gage B1

Date	1~2 ksi	2~3 ksi	3~4 ksi	4~5 ksi	5~6 ksi	>6 ksi	OC#	ESR (ksi)
2009.10.17	59	8	7	0	0	0	74	2
2009.10.29	224	46	26	24	2	0	320	2
2009.10.31	82	22	16	4	0	0	123	2
2009.11.03	2109	494	353	356	88	40	3440	3
2009.11.04	219	46	24	19	1	0	308	2
2009.11.05	257	60	30	17	0	0	364	2
2009.11.11	231	51	44	13	0	0	338	2
2009.11.12	252	63	27	10	0	0	351	2
2009.11.13	291	70	31	16	1	0	408	2
2009.11.20	195	49	42	19	0	1	305	3
2009.11.21	223	59	33	35	19	10	378	3
2009.11.22	842	20	18	7	1	5	892	2
2009.11.23	213	36	31	6	1	0	286	2
2009.11.26	68	16	4	0	0	0	87	2
2009.11.29	104	18	6	0	0	0	127	2
2009.11.30	448	103	60	42	7	0	660	3
2009.12.08	346	70	38	31	5	1	491	3
2009.12.09	54	10	3	1	0	0	68	2
2009.12.10	760	166	85	45	14	8	1077	3
2009.12.12	155	17	7	1	2	0	181	2
2009.12.13	117	18	6	1	0	0	141	2
2009.12.14	2313	364	120	49	15	8	2867	2
2009.12.19	5840	814	485	617	289	220	8264	3
2009.12.20	139	15	8	5	1	2	170	2
2009.12.21	354	65	23	8	2	0	450	2
2010.01.08	517	91	37	15	0	0	660	2
2010.01.09	164	37	5	0	0	0	205	2

2010.01.13	367	56	32	16	0	0	471	2
2010.01.14	408	79	53	19	1	0	559	2
2010.01.15	387	79	41	8	0	0	514	2
2010.01.16	160	39	10	2	0	0	209	2
2010.01.18	444	102	16	7	2	3	573	2
2010.01.19	161	43	16	3	2	0	224	2
2010.01.20	589	105	44	19	2	1	759	2
2010.01.21	611	119	40	17	7	4	797	2
2010.01.23	393	33	11	3	1	0	440	2
2010.01.24	125	25	4	0	0	0	153	2
2010.01.25	470	100	44	15	1	1	629	2
2010.02.04	545	103	41	31	2	0	721	2
2010.02.05	514	82	34	17	2	0	648	2
2010.02.06	348	54	21	8	0	1	431	2
2010.02.11	20	1	0	0	0	0	21	2
2010.02.16	1580	178	76	88	77	52	2051	3
2010.02.21	143	9	10	0	0	0	162	2
2010.02.24	948	127	37	15	2	1	1129	2
2010.03.10	1004	173	76	57	24	21	1353	3
2010.03.11	491	94	36	10	0	0	630	2
2010.03.12	383	76	27	7	1	1	492	2
2010.03.13	303	43	11	12	2	0	371	2
2010.03.20	798	85	28	13	7	5	936	2
2010.03.21	592	99	28	12	4	0	735	2
2010.03.26	676	127	44	30	7	3	885	2
2010.03.27	391	69	36	24	10	2	531	2
2010.03.29	1723	230	93	57	9	3	2114	2
2010.03.30	2103	225	82	54	17	6	2486	2
2010.03.31	1402	168	49	27	3	2	1649	2
2010.04.02	565	91	36	21	4	1	716	2
2010.04.03	547	58	31	16	2	5	659	2
2010.04.30	2321	331	102	83	86	79	3001	3
2010.05.10	904	95	23	16	6	4	1047	2
2010.05.11	968	99	32	30	13	9	1150	2
2010.05.12	4151	908	555	478	141	75	6307	3
2010.05.13	1359	223	79	58	11	11	1740	2
2010.05.14	1460	138	47	35	18	14	1710	2
2010.05.15	5247	1113	367	309	68	56	7158	2
2010.05.21	5664	985	632	454	192	133	8059	3
2010.05.27	11404	1463	674	480	136	68	14223	2
2010.05.28	4943	791	452	279	199	98	6761	3

2010.05.29	2485	577	442	725	161	34	4423	3
2010.05.30	3975	663	278	163	40	44	5163	2
2010.05.31	6743	1317	557	364	118	57	9154	2
2010.11.16	5932	760	312	238	81	45	7367	2
2010.11.17	8913	1202	527	232	79	35	10987	2
2010.11.18	4391	460	136	80	23	18	5107	2
2010.11.19	9698	1422	552	288	80	40	12079	2
2010.11.24	7772	1177	603	461	153	95	10259	3
2010.11.25	4948	581	266	202	92	54	6142	2
2010.11.26	2759	446	287	171	24	14	3700	2
2010.11.27	5402	968	443	229	20	8	7069	2
2010.11.28	4115	649	245	116	22	9	5155	2
2010.12.03	7709	1881	763	310	29	14	10705	2
2010.12.04	2158	330	97	41	8	3	2635	2
2010.12.05	2058	215	58	31	7	1	2368	2
2010.12.06	2350	264	115	47	7	4	2785	2
2010.12.07	443	86	40	17	3	0	588	2
2010.12.08	2979	535	308	90	18	6	3934	2
2010.12.09	581	75	24	7	1	0	688	2
2010.12.10	4269	737	266	126	37	14	5447	2
2010.12.11	12029	2344	997	676	189	97	16332	2
2010.12.12	7589	1428	627	370	85	44	10142	2
2010.12.13	5315	971	499	269	77	42	7171	2
2010.12.14	360	51	10	12	1	0	433	2
2010.12.15	1030	106	44	17	6	3	1204	2
2010.12.16	6030	905	372	210	28	12	7556	2
2010.12.17	17058	2693	1079	614	145	76	21664	2
2010.12.18	8387	1295	620	414	154	92	10960	2
2010.12.19	562	170	54	15	6	2	809	2
2010.12.20	4999	891	340	278	63	26	6596	2
2011.01.05	1682	297	108	79	19	11	2196	2
2011.01.06	1036	126	54	47	7	1	1269	2
2011.01.07	533	77	44	56	10	1	719	3
2011.01.08	6411	1418	691	466	85	52	9122	3
2011.01.09	7475	1302	663	423	79	35	9976	2

Stress Occurrences for Gage B2

Date	1~2 ksi	2~3 ksi	3~4 ksi	4~5 ksi	5~6 ksi	>6 ksi	OC#	ESR (ksi)
2009.10.17	18	7	9	1	1	0	35	3
2009.10.29	87	39	33	22	3	4	187	3
2009.10.31	22	16	25	4	0	0	66	3
2009.11.03	93	46	49	9	0	0	196	3
2009.11.04	86	28	39	13	1	1	167	3
2009.11.05	116	36	43	16	0	0	210	3
2009.11.11	93	37	51	12	1	0	194	3
2009.11.12	85	42	41	8	0	0	175	3
2009.11.13	119	48	46	14	1	0	227	3
2009.11.20	106	30	42	40	2	0	219	3
2009.11.21	10679	3468	4392	3184	1178	994	23895	4
2009.11.22	85899	40179	74882	66138	29529	26212	322838	4
2009.11.23	29517	13546	24437	19753	8521	7682	103455	4
2009.11.26	24	8	13	0	0	0	45	3
2009.11.29	37	17	8	0	0	0	61	2
2009.11.30	190	68	71	58	19	11	416	3
2009.12.08	8773	6327	18270	29400	19846	23548	106163	5
2009.12.09	14502	10059	25876	36299	22189	24949	133873	5
2009.12.10	45110	27808	64096	74480	40612	42250	294355	5
2009.12.12	47	14	11	2	0	0	74	2
2009.12.13	24322	11723	22231	20738	9349	8841	97203	4
2009.12.14	44024	22867	47554	49034	25533	26147	215159	4
2009.12.19	11	4	1	1	0	0	16	2
2009.12.20	17	4	2	0	0	0	23	2
2009.12.21	126	49	44	10	2	2	231	3
2010.01.08	201	59	53	20	8	0	340	3
2010.01.09	60	28	15	3	0	0	105	2
2010.01.13	136	31	45	17	6	2	235	3
2010.01.14	161	52	65	26	8	8	318	3
2010.01.15	2985	466	384	178	72	66	4149	3
2010.01.16	2030	513	727	632	286	223	4410	4
2010.01.18	5688	62	66	14	2	0	5832	2
2010.01.19	18899	8787	17775	16796	7797	7300	77352	4
2010.01.20	26111	12662	25794	26053	13373	13279	117271	4
2010.01.21	12759	11712	31506	25337	8546	7081	96940	4
2010.01.23	29015	13378	25504	24060	11835	11252	115044	4
2010.01.24	23167	10503	20124	18830	8942	8384	89949	4

2010.01.25	20427	9238	16895	16253	8038	7914	78764	4
2010.02.04	20908	10555	18740	17218	8437	8269	84126	4
2010.02.05	4114	2176	4428	4509	2312	2479	20017	4
2010.02.06	86649	14006	13907	8485	3534	3374	129954	3
2010.02.11	128	39	36	11	2	1	216	3
2010.02.16	16333	4582	5519	3500	1144	904	31981	3
2010.02.21	2169	1257	3317	4444	2506	2774	16465	5
2010.02.24	5178	670	584	243	86	71	6831	3
2010.03.10	8253	6518	8466	4066	1536	1468	30307	4
2010.03.11	172	61	57	11	3	1	304	3
2010.03.12	125	61	41	5	1	1	232	3
2010.03.13	51	17	10	4	5	1	87	3
2010.03.20	53608	22324	32238	21942	9397	10060	149568	4
2010.03.21	12083	4254	7452	7021	3486	3444	37739	4
2010.03.26	6919	3150	6259	5496	2619	2679	27121	4
2010.03.27	66353	26611	25615	8095	2520	2155	131347	3
2010.03.29	139	69	39	7	1	0	254	2
2010.03.30	42513	14438	24023	28081	14514	12994	136562	4
2010.03.31	37760	11864	19484	13606	6608	5136	94457	4
2010.04.02	38254	16792	30620	27720	12914	12143	138441	4
2010.04.03	24879	9102	15968	13791	6639	6385	76763	4
2010.04.30	13436	3539	5356	5094	2080	1499	31004	4
2010.05.10	1961	337	387	55	12	5	2756	2
2010.05.11	93691	30390	51147	39370	17433	16939	248969	4
2010.05.12	54913	16364	26076	20972	9202	7794	135319	4
2010.05.13	28450	7943	11133	6943	2860	2643	59970	3
2010.05.14	24263	8011	9809	6653	2833	2792	54358	4
2010.05.15	33569	8866	13420	10083	4920	4975	75832	4
2010.05.21	21468	4917	8053	6469	2955	2645	46505	4
2010.05.27	55547	16448	29625	23968	10739	9206	145532	4
2010.05.28	21511	4144	5616	4050	1598	1446	38363	3
2010.05.29	16564	3746	3856	2000	768	671	27604	3
2010.05.30	45553	9346	14274	11213	4978	4493	89855	4
2010.05.31	12679	1524	1699	1119	332	280	17632	3
2010.11.16	186	48	41	13	1	0	288	2
2010.11.17	159	52	36	11	0	0	257	2
2010.11.18	174	37	38	6	1	0	256	2
2010.11.19	170	47	32	5	0	0	253	2
2010.11.24	174	44	48	6	0	0	271	2
2010.11.25	13	8	1	0	0	0	21	2
2010.11.26	123	37	23	2	1	0	185	2

2010.11.27	65	26	15	0	0	0	106	2
2010.11.28	29	12	4	0	0	0	45	2
2010.12.03	177	50	28	2	0	0	257	2
2010.12.04	80	9	7	0	0	0	95	2
2010.12.05	26	8	2	0	0	0	35	2
2010.12.06	161	44	24	1	0	0	229	2
2010.12.07	156	29	11	0	0	0	196	2
2010.12.08	146	27	18	0	0	0	190	2
2010.12.09	138	22	8	0	0	0	168	2
2010.12.10	119	29	16	3	0	0	166	2
2010.12.11	50	17	10	2	0	0	79	2
2010.12.12	55	11	5	0	0	0	70	2
2010.12.13	176	34	24	3	0	0	236	2
2010.12.14	147	45	17	1	1	1	211	2
2010.12.15	125	33	8	0	0	0	166	2
2010.12.16	157	36	21	4	0	0	217	2
2010.12.17	186	57	55	20	2	0	318	3
2010.12.18	77	12	22	4	1	0	116	3
2010.12.19	46	15	3	0	0	0	63	2
2010.12.20	161	48	77	20	2	0	308	3
2011.01.05	129	36	43	25	3	0	234	3
2011.01.06	167	42	49	28	4	0	289	3
2011.01.07	154	44	67	31	3	0	299	3
2011.01.08	121	37	71	58	12	1	299	3
2011.01.09	28	9	5	0	0	0	42	2

Stress Occurrences for Gage B3

Date	1~2 ksi	2~3 ksi	3~4 ksi	4~5 ksi	5~6 ksi	>6 ksi	OC#	ESR (ksi)
2009.10.17	21630	7383	4003	2520	1992	1332	38860	3
2009.10.29	78501	46826	28367	18228	15785	13945	201651	4
2009.10.31	95036	53352	31834	19752	19108	15397	234477	4
2009.11.03	112134	60097	34917	19605	18053	15346	260151	4
2009.11.04	68450	28631	14360	8018	5651	4154	129263	3
2009.11.05	77980	29989	15292	9371	7550	3878	144058	3
2009.11.11	36899	17247	10280	6804	6182	4902	82312	4
2009.11.12	143789	12115	346	15	7	4	156274	2
2009.11.13	132615	67893	36868	26696	22849	21723	308643	4
2009.11.20	125145	62214	31302	14125	13750	11222	257756	3
2009.11.21	166940	90360	37742	18306	16285	13272	342904	3
2009.11.22	127276	55138	23833	13239	11977	8314	239776	3
2009.11.23	161072	88630	35540	15492	15026	11241	326999	3
2009.11.26	2176	34	14	2	1	1	2226	2
2009.11.29	100132	60978	36419	20448	20028	17909	255914	4
2009.11.30	98962	52659	30070	16531	15320	12249	225790	4
2009.12.08	106277	46800	24660	13243	11435	7163	209577	3
2009.12.09	98700	56365	32524	17358	18009	14931	237886	4
2009.12.10	100745	54082	30900	17783	16940	14588	235036	4
2009.12.12	248501	59830	14245	7455	6788	4871	341689	3
2009.12.13	284253	118761	81775	45847	22088	15455	568178	3
2009.12.14	336438	117050	48667	25457	22651	17939	568201	3
2009.12.19	83339	42047	22102	15049	13220	9473	185229	4
2009.12.20	86519	43921	22506	15212	15012	12485	195654	4
2009.12.21	88547	40632	20193	13186	11622	8893	183072	3
2010.01.08	132179	81575	47218	35862	30439	27232	354504	4
2010.01.09	551	57	6	1	0	0	615	2
2010.01.13	150760	72612	38247	25031	23261	17972	327882	4
2010.01.14	113360	59995	29586	20175	16612	12182	251908	3
2010.01.15	391277	119558	51163	19606	14113	9617	605333	3
2010.01.16	430275	186852	52211	2000	440	296	672073	2
2010.01.18	352150	199014	86489	33363	25153	20886	717054	3
2010.01.19	468962	137422	31091	15824	14074	9092	676465	3
2010.01.20	366301	128880	38913	22295	21081	17602	595070	3
2010.01.21	439159	169148	67830	20762	16018	12606	725521	3
2010.01.23	405272	199938	45911	3556	1384	749	656810	2

2010.01.24	451316	130888	14566	5289	4685	3270	610013	2
2010.01.25	441183	286289	58444	14298	11305	8062	819580	3
2010.02.04	529345	151738	110666	50131	14529	9541	865949	3
2010.02.05	638595	154572	88172	68285	49979	3240	1002842	3
2010.02.06	523438	154911	90391	78926	55519	16829	920013	3
2010.02.11	564311	86027	31888	18957	17209	13021	731412	3
2010.02.16	647136	79355	30528	18370	17265	13314	805967	3
2010.02.21	467991	81307	12231	11415	18860	24262	616065	3
2010.02.24	609266	249619	136423	64103	21694	4008	1085111	3
2010.03.10	336207	100110	34042	25846	33213	38999	568416	3
2010.03.11	549520	307229	232947	76171	58307	56154	1280326	3
2010.03.12	638761	592478	262306	70548	204300	319005	2087397	4
2010.03.13	501845	153295	53524	21051	12555	10658	752927	3
2010.03.20	289816	80729	30681	16591	14548	15378	447741	3
2010.03.21	263929	133800	76110	52216	54644	55971	636669	4
2010.03.26	515116	150055	109782	96683	53181	9587	934402	3
2010.03.27	1168220	209705	68686	19283	12206	8931	1487029	2
2010.03.29	566363	330184	94387	45999	92189	87721	1216841	4
2010.03.30	361210	119377	51737	24255	17655	14908	589141	3
2010.03.31	476827	124138	42856	25828	23790	17624	711061	3
2010.04.02	266605	65974	26229	16939	24149	31630	431524	3
2010.04.03	306160	97347	38886	28179	34509	35808	540888	3
2010.04.30	422099	84818	31661	18585	15893	10255	583310	3
2010.05.10	469370	112908	33927	20582	16040	11349	664175	3
2010.05.11	611789	157691	49704	22391	18310	13110	872994	3
2010.05.12	541925	158597	60908	20636	17136	11390	810591	3
2010.05.13	655447	136818	41103	21306	19137	14771	888581	3
2010.05.14	690007	191212	52292	23042	18519	14052	989122	3
2010.05.15	501314	245059	61994	21293	18113	12501	860273	3
2010.05.21	556473	246802	93026	24936	17393	12881	951510	3
2010.05.27	482679	148034	37287	22269	17529	13236	721032	3
2010.05.28	446907	229208	37034	13105	10540	7862	744655	3
2010.05.29	410667	253755	71215	15862	9048	6080	766626	3
2010.05.30	438589	212084	60364	26245	17369	11299	765948	3
2010.05.31	474776	227823	69103	25093	18355	12594	827744	3
2010.11.16	372	78	27	8	1	0	485	2
2010.11.17	337	79	23	5	2	0	445	2
2010.11.18	354	68	15	5	1	0	443	2
2010.11.19	356	73	16	3	1	0	447	2
2010.11.24	387	90	13	0	0	0	490	2
2010.11.25	31	5	0	0	0	0	36	2

2010.11.26	241	53	5	1	0	0	299	2
2010.11.27	135	36	1	0	0	0	172	2
2010.11.28	57	12	2	1	0	0	72	2
2010.12.03	382	82	23	7	1	0	495	2
2010.12.04	141	29	4	1	0	0	174	2
2010.12.05	44	11	0	0	0	0	55	2
2010.12.06	334	77	27	6	0	0	443	2
2010.12.07	293	69	13	3	0	0	377	2
2010.12.08	299	72	19	3	0	0	392	2
2010.12.09	290	43	11	1	0	0	344	2
2010.12.10	263	40	9	1	0	0	311	2
2010.12.11	93	27	4	0	0	0	124	2
2010.12.12	87	16	0	0	0	0	103	2
2010.12.13	337	88	19	4	2	0	449	2
2010.12.14	235	68	25	23	28	23	402	3
2010.12.15	273	65	11	0	0	0	349	2
2010.12.16	340	80	15	2	1	0	438	2
2010.12.17	360	112	38	11	2	0	521	2
2010.12.18	202	76	29	23	0	1	330	3
2010.12.19	73	12	2	0	0	0	87	2
2010.12.20	273	111	48	13	1	0	445	2
2011.01.05	249	71	47	7	2	0	374	2
2011.01.06	329	79	52	13	5	0	477	2
2011.01.07	343	118	57	9	3	0	530	2
2011.01.08	202	115	70	34	3	0	423	3
2011.01.09	77	14	1	0	0	0	92	2

Stress Occurrences for Gage B4

Date	1~2 ksi	2~3 ksi	3~4 ksi	4~5 ksi	5~6 ksi	>6 ksi	OC#	ESR (ksi)
2009.10.17	27	3	0	0	0	0	30	2
2009.10.29	95	6	3	0	0	0	104	2
2009.10.31	5272	419	183	105	44	34	6057	2
2009.11.03	29712	5224	2706	2410	1023	739	41813	3
2009.11.04	14176	3512	2210	1982	928	708	23515	3
2009.11.05	186	11	4	1	0	0	201	2
2009.11.11	96	16	6	3	0	0	120	2
2009.11.12	118	9	1	0	0	0	127	2
2009.11.13	132	15	1	0	0	0	148	2
2009.11.20	269	50	16	2	0	0	336	2
2009.11.21	443	37	5	2	0	0	486	2
2009.11.22	60	11	1	0	0	0	72	2
2009.11.23	273	53	23	2	0	0	351	2
2009.11.26	7	2	0	0	0	0	9	2
2009.11.29	25	3	2	0	0	0	29	2
2009.11.30	147	24	11	9	2	0	193	2
2009.12.08	167	17	4	13	1	0	201	2
2009.12.09	361	58	10	3	0	0	432	2
2009.12.10	2916	387	160	83	29	18	3593	2
2009.12.12	119	20	5	1	0	0	145	2
2009.12.13	127	6	6	2	1	0	141	2
2009.12.14	3064	858	529	515	266	204	5435	3
2009.12.19	116	30	1	1	0	0	147	2
2009.12.20	28	0	0	0	0	0	28	2
2009.12.21	127	16	2	0	0	0	144	2
2010.01.08	379	29	8	0	1	0	416	2
2010.01.09	44	1	0	0	0	0	45	2
2010.01.13	47268	9741	4868	4281	1809	1364	69330	3
2010.01.14	7491	1763	1074	907	422	300	11956	3
2010.01.15	118	8	0	0	0	0	126	2
2010.01.16	332	5	1	1	0	0	338	2
2010.01.18	15059	3163	1820	1562	609	478	22689	3
2010.01.19	74552	19405	12216	11696	5382	4060	127310	3
2010.01.20	37349	10939	6936	7002	3273	2611	68109	3
2010.01.21	15249	3174	1996	1809	866	671	23764	3
2010.01.23	43490	9350	5253	4455	1877	1295	65718	3
2010.01.24	122078	24238	12394	9517	3538	2332	174096	3

2010.01.25	33065	8203	4990	4796	2188	1666	54908	3
2010.02.04	61844	6131	3692	3290	1613	1201	77770	3
2010.02.05	82560	18574	10512	9661	4229	3355	128890	3
2010.02.06	118371	36160	23239	22770	10770	8292	219601	3
2010.02.11	130521	45867	31344	32121	15572	12795	268218	4
2010.02.16	124027	38192	24595	24583	11781	8990	232167	3
2010.02.21	146266	48521	37355	45763	26091	22422	326416	4
2010.02.24	111661	29687	18871	18862	8768	7166	195014	3
2010.03.10	135724	58158	46276	52271	24617	19388	336432	4
2010.03.11	103313	29194	19294	19334	9177	7213	187524	3
2010.03.12	500054	144057	86226	79007	34685	26196	870224	3
2010.03.13	93138	24740	15577	15264	7100	5692	161510	3
2010.03.20	111655	41311	26703	28145	14717	13053	235583	4
2010.03.21	50937	16628	11877	12988	6474	5522	104426	4
2010.03.26	200484	49894	28757	26024	11315	8368	324841	3
2010.03.27	173477	42615	25534	23691	10455	7928	283698	3
2010.03.29	305007	32993	10373	5488	1616	890	356366	2
2010.03.30	271933	69503	40725	35111	14880	10635	442785	3
2010.03.31	39044	11075	7226	7183	3359	2809	70695	3
2010.04.02	126967	52410	37544	43894	25637	23569	310019	4
2010.04.03	84447	27245	19579	21351	11012	9094	172726	4
2010.04.30	299730	93274	59834	58090	26506	20730	558163	3
2010.05.10	187265	37755	21897	19762	8888	7018	282584	3
2010.05.11	278412	59166	31709	26152	10883	8048	414369	3
2010.05.12	135404	31380	16942	14013	5513	4031	207281	3
2010.05.13	78713	11065	5028	2857	1179	914	99755	2
2010.05.14	229507	63617	39535	37880	17518	14024	402079	3
2010.05.15	106312	26156	15351	14041	6070	4555	172484	3
2010.05.21	2324	413	227	219	96	63	3340	3
2010.05.27	204233	48477	28403	26016	11654	8766	327547	3
2010.05.28	48221	10288	5798	5122	2137	1600	73164	3
2010.05.29	138983	32089	18236	16262	7048	5468	218085	3
2010.05.30	30518	3457	1650	1244	548	364	37778	2
2010.05.31	137475	30742	17317	14889	6502	4795	211719	3
2010.11.16	70	9	0	0	0	0	79	2
2010.11.17	66	12	0	0	0	0	78	2
2010.11.18	53	8	1	0	0	0	61	2
2010.11.19	67	4	0	0	0	0	71	2
2010.11.24	57	0	0	0	0	0	57	2
2010.11.25	8	0	0	0	0	0	8	2
2010.11.26	24	0	0	0	0	0	24	2

2010.11.27	21	1	0	0	0	0	22	2
2010.11.28	5	0	0	0	0	0	5	2
2010.12.03	64	1	0	0	0	0	65	2
2010.12.04	19	0	0	0	0	0	19	2
2010.12.05	3	0	0	0	0	0	3	2
2010.12.06	67	1	0	0	0	0	67	2
2010.12.07	52	1	0	0	0	0	53	2
2010.12.08	55	1	0	0	0	0	56	2
2010.12.09	47	0	0	0	0	0	47	2
2010.12.10	38	0	0	0	0	0	38	2
2010.12.11	17	0	0	0	0	0	17	2
2010.12.12	4	0	0	0	0	0	4	2
2010.12.13	55	1	0	0	0	0	56	2
2010.12.14	100	10	7	5	1	0	122	2
2010.12.15	46	0	0	0	0	0	46	2
2010.12.16	55	6	3	1	0	0	63	2
2010.12.17	55	1	0	0	0	0	56	2
2010.12.18	41	2	0	0	0	0	43	2
2010.12.19	4	0	0	0	0	0	4	2
2010.12.20	82	4	0	0	0	0	86	2
2011.01.05	55	1	0	0	0	0	56	2
2011.01.06	42	1	0	0	0	0	43	2
2011.01.07	79	2	0	0	0	0	81	2
2011.01.08	59	11	0	0	0	0	70	2
2011.01.09	8	0	0	0	0	0	8	2